

For Reference

NOT TO BE TAKEN FROM THIS ROOM

Ex LIBRIS
UNIVERSITATIS
ALBERTAEASIS





Digitized by the Internet Archive
in 2023 with funding from
University of Alberta Library

<https://archive.org/details/Dawe1980>

THE UNIVERSITY OF ALBERTA

RELEASE FORM

NAME OF AUTHOR John L. Dawe

TITLE OF THESIS "LOCAL BUCKLING OF W SHAPES USED AS
COLUMNS, BEAMS, AND BEAM-COLUMNS."

.....
DEGREE FOR WHICH THESIS WAS PRESENTED PhD

YEAR THIS DEGREE GRANTED 1980

Permission is hereby granted to THE UNIVERSITY OF
ALBERTA LIBRARY to reproduce single copies of this
thesis and to lend or sell such copies for private,
scholarly or scientific research purposes only.

The author reserves other publication rights, and
neither the thesis nor extensive extracts from it may
be printed or otherwise reproduced without the author's
written permission.

THE UNIVERSITY OF ALBERTA

LOCAL BUCKLING
OF W SHAPES USED AS
COLUMNS, BEAMS, AND BEAM-COLUMNS

by



JOHN L. DAWE

A THESIS

SUBMITTED TO THE FACULTY OF GRADUATE STUDIES AND RESEARCH
IN PARTIAL FULFILMENT OF THE REQUIREMENTS FOR THE DEGREE
OF DOCTOR OF PHILOSOPHY
IN CIVIL ENGINEERING

EDMONTON, ALBERTA

FALL, 1980

THE UNIVERSITY OF ALBERTA
FACULTY OF GRADUATE STUDIES AND RESEARCH

The undersigned certify that they have read, and
recommend to the Faculty of Graduate Studies and Research,
for acceptance, a thesis entitled "LOCAL BUCKLING OF W SHAPES
USED AS COLUMNS, BEAMS, AND BEAM-COLUMNS" submitted by
JOHN L. DAWE in partial fulfilment of the requirements for
the degree of Doctor of Philosophy in CIVIL ENGINEERING.

ABSTRACT

An analytical model, based on an extended Rayleigh-Ritz technique, has been developed for the purpose of predicting local buckling behaviour of columns, beams, or beam-columns composed of W shape sections. A tangent modulus buckling theory is used and a tri-linear stress - strain curve for an elastic - plastic - strain-hardening material is assumed. The effects of residual stresses as well as the interactive effects of web - flange restraints are included directly in the formulation. The flexibility of the analytical model allows for the possibility of separate flange or web buckling as well as simultaneous buckling of the web and flanges. An elaborate formulation of plate component stiffness matrices permits the use of varying material properties for longitudinal strips of a member as yielding and strain-hardening progress during loading.

A computer program based on the analytical model was verified by an extensive comparison of results with available classical results for elastic local buckling of plates. The validity of the local buckling analysis beyond the elastic range was well-established by comparison of computer results with the results of 57 tests conducted by various investigators using column, beam, and beam-column specimens.

Having thus been verified, the computer program was used to conduct an exhaustive study of the effect of various parameters

which were expected to have an important effect on local buckling behaviour. As a result of this study, various modifications to existing web and flange slenderness limitations for columns, beams and beam-columns are indicated. Further research in the form of full-size laboratory specimen tests is recommended and various suggestions are made with regard to future testing.

ACKNOWLEDGEMENTS

This study was carried out under the supervision of Dr. G.L. Kulak of the Department of Civil Engineering at the University of Alberta. It forms part of a continuing research investigation into the local buckling behaviour of W shape sections. The project is funded by the Canadian Steel Industries Construction Council.

The author also wishes to thank Dr. T.M. Hrudey and Dr. D.W. Murray for their helpful suggestions during the early stages of the theoretical development. The many words of encouragement from my friend and fellow student, Dr. Michael Hatzinikolas, are also greatly appreciated. I am especially grateful to Mrs. Gladys Stephens who so painstakingly prepared the final typewritten manuscript.

TABLE OF CONTENTS

	Page
Abstract	iv
Acknowledgements	vi
Table of Contents	vii
List of Tables	xii
List of Figures	xiv
List of Symbols	xvii
CHAPTER 1 - INTRODUCTION	1
1.1 General	1
1.2 Local Buckling	1
1.3 Design Considerations	2
1.3.1 Current Requirements for Flanges and Webs	3
1.3.2 Previous Requirements for Flanges and Webs	3
1.4 Objectives	4
1.5 Scope	5
CHAPTER 2 - LITERATURE SURVEY	7
CHAPTER 3 - GENERAL ANALYTICAL METHOD	14
3.1 Introduction	14
3.2 Idealized Cross-section	15
3.3 Material Properties	16
3.4 Analytical Technique	17
3.5 Effects of Initial Imperfections	24

	Page
3.6 Coordinate Systems	26
3.7 Flange Shape Functions	27
3.8 Web Shape Functions	28
3.9 Longitudinal Shape Functions	29
3.10 Integration of Cross-sectional Shape Functions	30
3.11 Integration of Longitudinal Shape Functions	33
3.12 General Procedure for W Shapes	34
3.13 Iteration on the Number of Wavelengths	37
3.14 Effect of Residual Stresses	37
CHAPTER 4 - ANALYSIS FOR COMBINED AXIAL COMPRESSION AND BENDING.....	49
4.1 Introduction	49
4.2 Assumptions	49
4.3 Stiffness Matrix Formulations	51
4.3.1 Introduction	51
4.3.2 Application of Incremental Bending Strains	52
4.3.3 Stiffness Submatrices	53
4.3.3.1 Compression Flange	54
4.3.3.2 Tension Flange	56
4.3.3.3 Web - Tension Zone	58
4.3.3.4 Web - Compression Zone	59
4.4 Iterative Technique	62
CHAPTER 5 - COMPARISON OF THEORETICAL PREDICTIONS WITH TEST RESULTS	81

	Page
5.1 Introduction	81
5.2 Prediction of Buckling Loads	81
5.3 Column Local Buckling Tests	82
5.3.1 Discussion of Column Test Results	83
5.4 Beam Local Buckling Tests	84
5.4.1 Discussion of Beam Test Results	86
5.5 Beam-Column Local Buckling Test	87
5.5.1 Discussion of Beam-Column Test Results	88
5.6 Sources of Error	89
5.7 Summary of Test Results	93
5.8 Summary	93
CHAPTER 6 - THEORETICAL STUDY AND EVALUATION OF PARAMETERS ..	99
6.1 Introduction	99
6.2 Columns	99
6.2.1 Effects of Residual Stresses	102
6.2.2 Effects of Strain-Hardening Modulus	103
6.3 Beams	104
6.3.1 Class 3 Beams	104
6.3.2 Class 2 Beams	105
6.3.3 Class 1 Beams	105
6.3.4 Effects of Residual Stresses	106
6.3.5 Effects of Strain-Hardening Modulus	107
6.4 Beam-Columns	108

	Page
6.4.1 Class 3 Beam-Columns	109
6.4.1.1 Current Specifications	109
6.4.1.2 Theoretical Limitations as Determined Herein	110
6.4.2 Class 2 Beam-Columns	112
6.4.2.1 Current Specifications	113
6.4.2.2 Theoretical Limitations as Determined Herein	114
6.4.3 Class 1 Beam-Columns	116
6.4.3.1 Current Specifications	118
6.4.3.2 Theoretical Limitations as Determined Herein	119
6.4.4 Effects of Residual Stresses	122
6.4.5 Effects of Strain-hardening Stresses.....	123
6.4.6 Effects of Specimen Length	124
CHAPTER 7 - SUMMARY AND CONCLUSIONS	144
7.1 Introduction	144
7.2 Summary of the Theoretical Method	145
7.3 Summary of Findings	145
7.4 Recommendations for Design	146
7.4.1 Class 1 Sections	147
7.4.2 Class 2 Sections	147
7.4.3 Class 3 Sections	148
7.5 Further Recommendations	149
7.6 Conclusions	151
LIST OF REFERENCES	154

APPENDIX A - Derivation of a Plate Buckling Condition	160
APPENDIX B - Material Properties	174
APPENDIX C - Computer Program	187
APPENDIX D - Sample Problems	256

LIST OF TABLES

Table		Page
4.1(a)	Strains for a Compression Flange	65
4.1(b)	Stresses for a Compression Flange	65
4.2(a)	Strains for a Tension Flange	66
4.2(b)	Stresses for a Tension Flange	66
4.3(a)	Strains Adjacent to Lower Edge of Web	67
4.3(b)	Strains Adjacent to Middle of Web	67
4.3(c)	Stresses for the Tension Zone of a Web	67
4.4(a)	Strains for the Compression Zone of a Web (Case I - Center of Web Elastic)	69
4.4(b)	Stresses for the Compression Zone of a Web (Case I - Center of Web Elastic)	69
4.5(a)	Strains for the Compression Zone of a Web (Case II - Center of Web Yielded)	70
4.5(b)	Stresses for the Compression Zone of a Web (Case II - Center of Web Yielded)	70
4.6(a)	Strains for the Compression Zone of a Web (Case III - Center of Web Strain-hardened)	71
4.6(b)	Stresses for the Compression Zone of a Web (Case III - Center of Web Strain-hardened)	71
5.1(a)	Comparison of Experimental and Predicted Values for Columns. (Results of Haaijer and Thurlimann) ...	95
5.1(b)	Comparison of Experimental and Predicted Values for Columns. (Results of Kulak)	95
5.2(a)	Comparison of Experimental and Predicted Values for Beams. (Results of Haaijer and Thurlimann)	96

Table		Page
5.2(b)	Comparison of Experimental and Predicted Values for Beams. (Results of Holtz and Kulak)	96
5.2(c)	Comparison of Experimental and Predicted Values for Beams. (Results of Lukey and Adams)	96
5.3(a)	Comparison of Experimental and Predicted Values for Beam-Columns. (Results of Perlynn and Kulak for Compact Sections)	98
5.3(b)	Comparison of Experimental and Predicted Values for Beam-Columns. (Results of Nash and Kulak for Non-Compact Sections)	98

LIST OF FIGURES

Figure	Page
3.1 Idealized Cross-section	40
3.2 Idealized Tri-linear Stress-Strain Curve	40
3.3 Relationship between Cartesian and Natural Coordinates	41
3.4 Local Coordinates and Numbering System	41
3.5 Shape Functions for Flanges	42
3.6 Shape Functions for Webs	43
3.7 Longitudinal Shape Functions	44
3.8 Natural Coordinate Systems for a W Shape	45
3.9 Node Numbering and Coordinate Displacements	46
3.10 Schematic Stiffness Assembly	47
3.11 Residual Strain Distribution	48
4.1 Superposition of Beam-Column Strains	72
4.2 Flexural Strain on an Inelastic Section	73
4.3 Strain and Stress Distributions for a Flange in Compression	74
4.4 Strain and Stress Distributions for a Flange in Tension	75
4.5 Strain and Stress Distributions for Tension Zone of a Web	76
4.6 Strain and Stress Distributions for Compression Zone of a Web (Case I - Center of Web Elastic)	77
4.7 Strain and Stress Distributions for Compression Zone of a Web (Case II - Center of Web Yielded)	78

Figure	Page
4.8 Strain and Stress Distributions for Compression Zone of a Web (Case III - Center of Web Strain-hardened	79
4.9 Iterative Technique for Critical Buckling Strain	80
6.1 Effect of $h\sqrt{F_y}/w$ on P_{cr}/P_y for Various Values of $b\sqrt{F_y}/2t$	127
6.2 Effect of $h\sqrt{F_y}/w$ on P_{cr}/P_y for $b\sqrt{F_y}/2t$ Values of 54, 64, and 72	128
6.3 P_{cr}/P_y vs. $h\sqrt{F_y}/w$ for Values of $E_{st} = 700, 800,$ and 900 ksi.	129
6.4 Effect of $h\sqrt{F_y}/w$ on M_{cr}/M_y for Various Values of $b\sqrt{F_y}/2t$	130
6.5 Effect of $h\sqrt{F_y}/w$ on M_{cr}/M_p for Values of $b\sqrt{F_y}/2t$ of 54 and 64	131
6.6 M_{cr}/M_y vs. $h\sqrt{F_y}/w$ for Values of $E_{st} = 700, 800,$ and 900 ksi.	132
6.7 M_{cr}/M_p vs. $h\sqrt{F_y}/w$ for Values of $E_{st} = 700, 800,$ and 900 ksi.	133
6.8 Effect of P/P_y on M_{cr}/M_y for Various Values of $h\sqrt{F_y}/w$	134
6.9 $h\sqrt{F_y}/w$ vs. P/P_y for a Class 3 Section	135
6.10 Effect of P/P_y on M_{cr}/M_p for Various Values of $h\sqrt{F_y}/w$	136
6.11 $h\sqrt{F_y}/w$ vs. P/P_y for a Class 2 Section	137
6.12 Effect of P/P_y on M_{cr}/M_p for Various Values of $h\sqrt{F_y}/w$	138
6.13 $h\sqrt{F_y}/w$ vs. P/P_y for a Class 1 Section	139
6.14 P/P_y vs. M_{cr}/M_p for Various Values of $h\sqrt{F_y}/w$ and $\sigma_{rc} = 0$	140

Figure	Page
6.15 Effect of E_{st} on the Interaction of P/P_y and M_{cr}/M_y	141
6.16 Effect of Length on Critical Load Prediction	142
6.17 Effect of Length on the Interaction of P/P_y and M_{cr}/M_p	1-3
7.1 Summary of Indicated Modifications	153
A-1 Rectangular Plate Subjected to Plane Stress	173
A-2 Plate Buckling in the x-z Plane	173
B-1 Effective Stress - Effective Strain Relationships	186

LIST OF SYMBOLS

The following is a list of the more commonly used symbols which are presented here for ease of reference. The meanings of all symbols used in the text are defined where they first appear. The meanings of symbolic names used in the computer program are explained within the program listing presented in Appendix C.

Dimensions and Displacements

α_t , α'_t	= Locations of material boundaries (Compression flange)
α_b , α'_b	= Locations of material boundaries (Tension flange)
β_1 , β_2 , β'_2 , β_3 , β'_3	= Locations of material boundaries (Web)
b	= Flange width
h	= Web height
L	= Length of a specimen
t_1	= Tension flange thickness
t_u	= Compression flange thickness
t_w	= Web thickness
y_1	= Distance to neutral axis from mid-height of web
u , v , w	= x-, y-, and z- Components of displacement
u_i , u_j , u_k	= Subscript notation for displacements

w_0 = Displacement due to initial imperfection

w_1 = Displacement beyond w_0

Forces and Moments

M = Applied end moment

M_{cr} = Critical local buckling moment

M_p = Plastic moment

M_{pc} = Plastic moment reduced for compressive load

M_y = Yield moment

M_{yc} = Yield moment reduced for compressive load

M_x, M_{xy}, M_y = Plate bending moments per unit width

N_x, N_{xy}, N_y = In-plane plate forces per unit width

P = Compressive axial force

P_{cr} = Critical local buckling axial force

P_y = Column yield load

Geometric Properties

A_u = Area of compression flange

A_l = Area of tension flange

A_w = Area of web

$b\sqrt{F_y}/2t$ = Flange slenderness term

f = A general function

F_i = Buckling factors based on longitudinal shapes

$h\sqrt{F_y}/w$	= Web slenderness term
I	= Moment of inertia of a unit strip of plate
m	= Number of longitudinal half sinewaves
π	= Ratio of circumference to diameter of a circle
$s(\zeta)$	= Flange shape function at a cross-section
x, y, z	= Rectangular coordinates in three dimensions
η, ζ, ξ	= Natural coordinates
$P_o(\zeta)$	= Longitudinal shape envelope

Material Properties

D_x, D_y, D_{xy}, D_{yx}	= Plate bending rigidity factors
E	= Modulus of elasticity
E_o	= Slope of yield plateau of stress - strain curve
E_{st}	= Strain-hardening modulus
E_t	= Tangent modulus
E_x, E_y, E_z	= Material moduli of anisotropic materials
G	= Shear modulus
G_t	= Tangent shear modulus
ν	= Poisson's ratio

Matrices and Vectors

[C]	= Matrix of shape function coefficients
{ F_o }	= Equivalent lateral load vector

$\{H\}$	= Vector of polynomial terms
$[I]$	= Identity matrix
$[K]$	= Bending stiffness matrix
$[K_G]$	= Geometric stiffness matrix
$[K_{G_o}]$	= Intermediate geometric stiffness matrix
$[K_t]$	= Stiffness matrix of tension flange
$[K_u]$	= Stiffness matrix of compression flange
$[K_w]$	= Stiffness matrix of web
$[S]$	= Sweeping matrix
$[\Phi_i]$	= Component stiffness matrices
$\langle \phi \rangle$	= Transpose of shape function vector
$\{\phi\}_i$	= Eigenvectors
$\{\theta\}$	= Vector of coordinate displacements
$\{\theta_0\}$	= Vector of initial coordinate imperfections

Strains

ϵ_a	= Applied axial strain
ϵ_b	= Applied bending strain in compression
ϵ'_b	= Applied bending strain in tension
ϵ_c	= Strain at mid-height of web
ϵ_{rc}	= Residual compressive strain
ϵ_i ($i = 1, 2, 3, 4, 5$)	= Residual strains on a W shape section
$\epsilon_{b_{cr}}$	= Critical compressive bending strain
ϵ_y	= Yield strain

$\bar{\varepsilon}^{(P)}$	= Effective plastic strain
ε_{st}	= Strain at onset of strain-hardening
e_x, e_y, e_z	= Strains in the x-, y-, and z - coordinate directions
$\gamma_{xy}, \gamma_{yz}, \gamma_{zx}$	= Shear Strains

Stresses

F_y	= Specified minimum yield stress
$s_i (i = 1,2,3,4,5,6)$	= Piecewise linear stress components
$\sigma_i (i = 1,2,3,4,5)$	= Residual stresses on a W shape section
σ_y	= Yield stress
σ_{rc}	= Residual compressive stress
$\sigma_x, \sigma_y, \sigma_z$	= Stress in the x-, y-, and z- coordinate directions
$\tau_{xy}, \tau_{yz}, \tau_{zx}$	= Shear stresses

Tensors

c_{ijkl}	= Fourth-order tensor of material constants
e_{ij}	= Strain tensor
$e_{ij}^{(P)}$	= Plastic strain tensor
S_{ij}	= Stress deviator tensor
δ_{ij}	= Kronecker delta
σ_{ij}	= Stress tensor

Miscellaneous

d	= Differential operator (eg. dS)
δ	= Variational operator (eg. δw)

- H' = Slope of effective stress - strain curve
 k^2 = Constant defining a von Mise's yield surface
 J_2 = Loading function used in von Mise's criterion
 λ = An eigenvalue
 λ_o = An intermediate eigenvalue
 λ' = An eigenvalue strain
 λ'' = An eigenvalue difference ($= \lambda_o - \lambda'$)
 μ = Eigenvalue shift
 ω = Smallest eigenvalue of a system ($= 1/\lambda$)
 ω_s = Eigenvalue after shift applied

Chapter 1

INTRODUCTION

1.1 General

A large proportion of the members used in present-day steel structures are uniform throughout their lengths and have I-shaped cross-sections¹. Such members are referred to as W shapes and are particularly efficient when used as beams for transferring bending moments within a structure. W shapes are also used as columns for transferring pure axial compression and as beam-columns for transferring combined axial compression and bending. Depending on the width-to-thickness ratios of their flanges, W shapes are classified as Class 1, Class 2, Class 3, and Class 4 sections¹. Because of their thin-walled characteristics these members are particularly susceptible to local buckling^{1,2,3} of their component plates and this local instability limits the load-carrying capacity of the members. Thus, in limit states design^{1,4} local buckling of component plates of W shapes is one limit which must be met.

1.2 Local Buckling

In the present study the limit state of local buckling is isolated from other limit states such as those related to overall instability, material strength and excessive deflections¹. This

procedure coincides with present design philosophies which require that local buckling be prevented prior to the attainment of the maximum strength of a member^{1,3,5}. Since local buckling is isolated, a fundamental assumption is that all members are fully braced against overall instability. Local buckling of W shapes may be defined as a bifurcation phenomenon⁵ whereby a component plate subjected to in-plane stresses may be in equilibrium in its original planar configuration or in a neighboring deflected configuration. This critical state can occur in the elastic or inelastic regions of material response depending on the level of yield stress, the plate width-to-thickness ratio, and plate boundary conditions^{2,3,6,7}. Because of the nature of buckling, it is more precisely defined by a mathematical formulation. In the present study such a formulation is based on the principle of virtual work⁸ and is presented in Appendix A.

1.3 Design Considerations

As already established by previous investigators^{2,3,6,7}, a significant parameter affecting the stability of a plate is its width-to-thickness ratio. Therefore, a designer must consider the width-to-thickness ratios of flanges and webs when determining the local buckling resistance of W shapes. Other factors which affect plate stability in W shapes are the type of plate edge supports at the ends of a member, the type of stress distribution on a member cross-section, and the material properties of the steel^{2,7}. Because of the significant effect that the yield stress level has on plate buckling⁷, the present design code⁴ specifies limitations on the width-to-thickness ratios of webs and flanges multiplied by the square root of the yield stress.

1.3.1 Current Requirements for Flanges and Webs

The current Canadian design standard used for steel⁴, specifies width-to-thickness terms for four classes of W shape beam-columns. It is required that Class 1 sections permit the attainment of the reduced plastic moment and also allow for sufficient rotation capacity for subsequent redistribution of load before local buckling occurs. A Class 2 section is required to permit the attainment of the reduced plastic moment capacity with no provision for the requirement of subsequent load redistribution. A Class 3 section must permit the attainment of the reduced yield moment and for a Class 4 section the limit state of structural capacity is local buckling of elements in compression. Class 4 sections are light-gauge cold-formed sections and their behaviour does not form a part of this study. The present design limitations for Class 1, 2, and 3 sections are presented in detail in Chapter 6. These limitations are such that for a given class of section, local buckling of the component plates must not occur until the section has satisfied the minimum requirements for its classification. Since columns are not designed according to a required bending moment capacity, they are not classified as above. However, it is usual to use the same limitation for column flanges as that specified for Class 3 sections, while column webs are limited by a maximum width-to-thickness term⁴.

1.3.2 Previous Requirements for Flanges and Webs

Previous design codes⁹ have presented width-to-thickness ratios for flanges and webs of W shapes subjected to axial compression, bending, and axial compression and bending combined. As will be examined further in Chapter 2, these values are based on the results of an investigation

by Haaijer and Thurlimann⁷. Recently, however, studies performed at the University of Alberta by Kulak et al^{10,11,12,13} have shown that previously specified width-to-thickness limitations were overly conservative. As a result of these studies, the present code⁴ uses values that supersede previously specified width-to-thickness limitations for component plates of columns, beams, and beam-columns.

1.4 Objectives

The investigations conducted at the University of Alberta have been largely experimental and empirical in nature. The work has resulted in new design equations and graphs which are presently in use⁴. The present study is a continuation of this work with emphasis on the theoretical nature of plate buckling as it relates to W shapes subjected to axial compression, bending, and axial compression and bending combined.

The objectives of the present study are as follows:

1. to establish an idealized mathematical model to study local buckling of W shapes subjected to axial compression, bending, or to axial compression and bending combined.
2. to establish the validity of the mathematical technique by comparing analytical results with test results.
3. to present design equations and graphs for a broad spectrum of practical cases for which test results are not available.
4. to suggest, where appropriate, additional revisions

to presently specified width-to-thickness limitations for component plates of W shapes.

1.5 Scope

The mathematical formulation presented herein permits an analysis for local buckling of W shapes of various cross-sectional dimensions and material properties. The analysis is performed for axial compression, bending, and combined axial compression and bending applied at the member ends. The effects of residual stresses are included and web, flange, or combined web and flange buckling is predicted in the elastic or inelastic ranges. The restraint interaction of flanges and web is also accounted for by the mathematical model.

In Chapter 2 a review of the available literature that relates to the present study is outlined. In Chapter 3 the general mathematical formulation technique is discussed in detail and the application of this technique to the general case of combined axial compression and bending is presented in Chapter 4. In Chapter 5 the analytical technique is applied to the investigation of local buckling of 57 specimens that have been tested by various investigators. Theoretical and test results are compared. Analytical results for a wide range of Class 1, 2, and 3 columns, beams, and beam-columns are presented in Chapter 6, and in addition these theoretical results are interpreted for application to design. Also presented in Chapter 6 is a study of the parameters considered important in the analysis. The conclusions of the present study and the resulting design recommendations are presented in Chapter 7.

The mathematical formulation of plate buckling based on the

principle of virtual work⁸ is presented in Appendix A and the material properties are discussed in Appendix B. Because of the nature of the mathematical formulation which employs the use of matrix algebra as well as the use of iterative techniques for the inelastic cases, hand computation is highly impractical. Therefore, a computer program coded in Fortran IV and suitable for use with an Amdahl 470V/6 or an IBM 3032 computer was used for the computations. A listing of the program with explanations of the subroutines and typical input data and corresponding output are presented in Appendices C and D.

Chapter 2

LITERATURE SURVEY

A review of the available literature indicates that the problem of elastic plate buckling has been thoroughly investigated since the publication in 1891 of the original work done in this area¹⁴. The theoretical investigations include the closed-form solutions of single plates having regular geometric shapes and various stress and displacement boundary conditions. These solutions have been well-documented and are readily available in the literature^{2, 3, 6, 15, 16}.

It was not until the 1920's that the problem of inelastic plate buckling first began to receive some attention. In much the same way as for columns, inelastic buckling of rectangular plates was first treated by replacing the elastic modulus by a reduced modulus or a tangent modulus above the proportional limit. Bleich⁶, for example, assumed that above the proportional limit, the reduced modulus would be effective in the direction of uniaxial stress while the elastic modulus remained effective in the transverse direction. It was further assumed that an effective shear modulus equal to the geometric average of the elastic and reduced moduli would be applicable. Alternatively, Ros and Eichinger¹⁷, assuming isotropy in the inelastic range, suggested using the reduced modulus in all directions. Of the two, it was found that Bleich's assumptions led to values in closer agreement with test results.

Other investigators have attempted to improve upon the

existing knowledge in this area by including the total elastic-plastic stress-strain relationships in the plate buckling analysis. Prominent among those investigators were Bijlaard¹⁸, Ilyushin¹⁹, and Stowell²⁰ who used the deformation theory of plasticity⁸ while Onat and Drucker²¹ and Handelman and Prager²² promoted the use of the incremental theory⁸ in the plastic analysis of plate buckling. While the former method showed much better agreement with test results, it has been recognized that the latter method is the mathematically correct one^{7,21,23,24}. The main reason for this paradox appears to be the prediction by the incremental theory of a value of the shear modulus in the inelastic range equal to its value in the elastic range^{7,21,23,25}. It has been shown that a reduction in this value leads to much better correlation between theory and test results^{7,25}.

Early investigations of web and flange stability for W shape members were based on several simplifying assumptions. For both elastic and inelastic buckling it was assumed that the plate components at web-to-flange junctions were either rigidly supported or simply supported and the effects of residual stresses were neglected. Using these assumptions as well as Bleich's assumption of anisotropy in the inelastic range it was possible to arrive at closed-form solutions for several types of in-plane loadings^{2,6,26}.

In the late 1950's Haaijer and Thurlimann published the results of an investigation of inelastic local buckling in steel⁷. The main purpose of this investigation was to determine maximum plate width-to-thickness ratios for W shapes suitable for plastic design. An incremental theory²² was used in the analysis and the inelastic value of the shear modulus was reduced by 80 per cent. (The investigators

attributed this reduction to the effects of initial imperfections. However, in a more recent investigation²⁵, Lay discounted this effect of initial imperfections and arrived at a similar reduction in the shear modulus by applying slip-line field theory).

In their investigations, Haaijer and Thurlimann presented analytical solutions for single web or flange plates assuming either simple support or fully rigid support at the web-to-flange junctions. The effects of residual stresses were not included directly in the analysis. However, for the buckling strength of columns and plates in uniaxial compression, an empirical transition curve was suggested for use above the proportional limit. The experimental investigation of W shapes included six axial specimens and six flexural specimens. The present code limitations for flanges and webs of Class 1 W shapes are based on the results of these tests⁴.

Although Haaijer and Thurlimann did not test any specimens subjected to axial and flexural loadings combined, they used the results of a semi-empirical method to suggest plate width-to-thickness values for such members. In this method it was assumed that values obtained for axial specimens failing by web buckling would be applicable to an average strain in the compression zone of the webs of beam-columns. The present code limitations for plate components of Class 1 W shape beam-columns are based on the results of this semi-empirical method⁴.

In the years following the work of Haaijer and Thurlimann many investigators published results of research concerning the elastic and inelastic buckling strength of single plates. With the aid of discretization techniques and computer methods it has been possible to investigate many different cases^{27,28,29,30,31,32}. However, although

useful, none of these works is concerned directly with the understanding of local buckling behaviour in W shape members. More to the point, other studies have been directed towards local buckling in W shape beams. The studies of Lay³³, Culver³⁴, and McDermott³⁵, for example, have all indicated a flange width-to-thickness limitation of $b\sqrt{F_y}/2t = 54$ for sections required to reach the strain-hardening strain. Results of tests performed by Lukey and Adams³⁶ have indicated that a flange width-to-thickness term of 64 can be used for sections required to develop the full plastic moment capacity. A study by Basler and Thurlimann³⁷ has indicated that webs of girders required to reach M_y can have a value of $h\sqrt{F_y}/w$ as high as 980. More recent research by Croce³⁸ has indicated that $h\sqrt{F_y}/w$ can have a value as high as 750 for beams used in plastic design.

In 1973 a study of coupled local buckling in beam-columns was presented by Rajasekaran and Murray³⁹. The method of analysis was based on finite element techniques and could accommodate a large variety of boundary conditions. The method assumed linear elastic material response and did not include the effects of residual stresses. It was found that the analysis gave good results for flange local buckling but web buckling could not be accurately predicted.

In 1977, Akay, Johnson, and Will presented a study of lateral and local buckling of beams and frames⁴⁰. A finite element technique using plate elements for webs and line elements for flanges was used. The buckling modes were restricted by the assumption that straight lines across the flanges and normal to the web remain straight during buckling. Although the method is quite general with regard to

plate geometry and boundary conditions it assumes linear elastic response and neglects the effects of residual stresses.

In 1978, a study of local, distortional, and lateral buckling of W shape beams was presented by Hancock⁴¹. A finite strip technique was used in the analysis and an elastic, linear material response was assumed. The effects of residual stresses were not included in the analysis. Other studies using finite strip techniques were presented in 1964 by Plank and Wittrick⁴² and in 1974 by Goldberg, Bogdanoff, and Glauz⁴³, who extended the work of Przemieniecki³². Plank and Wittrick suggested a method for analysing thin-walled sections for lateral-torsional buckling. Presumably local buckling could be predicted by iterating on the length parameter. Plate thickness as well as geometry, material properties, and loading could be varied for a given member. However the effects of residual stresses were not included and apparently the method was not suitable for local buckling of W shapes since it was neither used, nor recommended, for this purpose.

As mentioned above, Goldberg, Bogdanoff, and Glauz⁴³ extended the work of Przemieniecki³² to include lateral buckling modes as well as more complicated states of stress. An elastic material response was assumed and the effects of residual stresses were not included in the analysis. Again, the method was neither applied to, nor recommended for, the analysis of local buckling of W shapes.

None of the above-mentioned techniques has been applied to an in-depth study of local buckling of Class 1, Class 2, and Class 3 W shape sections. In 1973, Kulak initiated such a study on an experimental basis¹⁰. A total of ten beams (eight Class 2 and two

Class 1 sections) were tested under equal third-point loadings. Based on the results of these tests it was concluded that the existing web width-to-thickness limitations for Class 2 sections were conservative and a need for additional tests on beams and beam-columns was indicated. Other tests followed, and in 1975 two Class 3 beams were tested and an increase in the existing web limitations for Class 3 beams was indicated¹¹.

In 1974 Kulak and Perlynn published the results of a study in which nine Class 2 W shape beam-columns were tested under various amounts of axial load¹². Again it was determined that the existing web limitations were too conservative for Class 2 beam-columns and a need for additional tests on Class 3 beam-columns were indicated. In 1976, the results of such a study were reported by Kulak and Nash¹³. It was indicated that web limitations for Class 3 beam-columns could also be somewhat relaxed. As a result of the work carried out by Kulak, et al. at the University of Alberta, significant changes in the web limitation requirements for W shapes have been implemented for Class 2 and Class 3 sections⁴.

The investigations carried out by Kulak, et al. were largely experimental although two semi-empirical methods for determining critical web width-to-thickness ratios were presented¹². Method I was based directly on test results and Method II combined test results with a variation of the method used by Haaijer and Thurlimann⁷. Because of the limited number of test results used, the methods were valid only for sections that were similar to those tested. Furthermore, the methods did not allow for variations in flange sizes, lengths of specimens, residual stresses, and material properties. For the types of

specimens tested, the methods were valid only between the limits of P/P_y equal to 0.15 and 0.80 since these were the lower and upper limits used in the tests. A purely analytical method was not developed.

Chapter 3

GENERAL ANALYTICAL METHOD

3.1 Introduction

The problem of plate buckling in the elastic range has been thoroughly investigated and solutions are available for many cases including various plate shapes and stress and displacement boundary conditions^{2,3,16,44}. Solutions for the analysis of orthotropic plates and for buckling capacities of plates in the inelastic range have also been published^{2,6,18,44}. The technique for obtaining a mathematical formulation for such problems is based on either an equilibrium method or an energy method².

In the equilibrium method^{2,6}, the equations of equilibrium are formulated on a deformed configuration of the plate. This configuration is compatible with the expected mode of buckling. Once the equations of equilibrium are solved simultaneously, the problem reduces to that of the solution of a biharmonic differential equation. This method makes use of the fact that, during buckling, a plate may be in equilibrium in its original planar configuration as well as in a neighboring buckled configuration; that is, the plate is at a point of bifurcation.

Two commonly used energy techniques for formulating plate buckling problems are the principle of minimum potential energy and the principle of virtual work⁸. Of these two methods, the principle of virtual work is a more general statement of the principle of the

conservation of energy. It does not require the assumption of the existence of a strain energy function and it can be applied to an elastic or an inelastic material^{8,45}. In the present analysis the principle of virtual work is used for the formulation of a plate buckling condition. In applying this method, a buckled configuration is first assumed. Then, a virtual displacement⁴⁶ from a buckled configuration is postulated. By equating the internal work done by the equilibrium stress field existing in a plate during this virtual displacement to the work done by the external forces acting on the plate during the same displacement, an integral differential equation is obtained. Using a Rayleigh-Ritz technique^{5,46,47} and a displacement field defined in terms of a set of nodal displacement coordinates, a matrix buckling condition is obtained and a standard eigenvalue problem results^{48,49,50}. This technique is developed in detail in Appendix A.

3.2 Idealized Cross-section

The technique outlined above is applied to W shapes having idealized cross-sections such as that illustrated in Figure 3.1. All subsequent mathematical formulations are referred to the mid-planes of the component plates of a W shape. Thus, the assumed height of web extends into each flange by a distance equal to one-half the flange thickness. Consequently, the area corresponding to each projection is twice included in the calculations of axial loads and bending moments. The purpose of this is to recognize that fillets at web-to-flange junctions do exist and that these additional areas of projection do, to some extent, account for them.

The width-to-thickness ratio for a flange is obtained by dividing one half the flange width by the flange thickness. In determining the width-to-thickness ratio of a web it is assumed that web-to-flange fillets have leg lengths equal to one-half the flange thickness. Therefore, the length of the web is taken as the clear distance between flanges minus the fillet leg lengths. The purpose of this is to take into account, to some extent, the effects of the fillets in decreasing the effective buckling height of a web.

As shown in Figure 3.1, variations in flange dimensions are permitted by using different flange widths and thicknesses. In subsequent discussions, in addition to the notations shown in Figure 3.1, A_l represents the area of a lower flange, A_w represents the area of a web, and A_u represents the area of an upper flange. Furthermore, for clearness of discussion, it is assumed that an upper flange is one that will normally be in compression and a lower flange will normally be in tension under an applied bending moment. The subscripts, l and u, are used to refer to the lower and upper flanges respectively.

3.3. Material Properties

In applying any mathematical technique to the prediction of plate buckling capacities it is necessary to have an accurate evaluation of the material properties to be used. In the method presented herein, a uniaxially stressed longitudinal fibre of a W shape section is assumed to have an idealized tri-linear tensile stress - strain response such as that shown in Figure 3.2. It is further assumed that this stress - strain response also applies to a fibre in compression. At the point where yielding occurs in a fibre, the strain

is designated by ϵ_y and the corresponding yield stress is designated by σ_y . For values of strain less than the yield strain, the fibre has an elastic modulus (also called Young's modulus) designated by E . At the point where strain-hardening of a fibre begins, the strain is represented by ϵ_{st} . For strains larger than this, the fibre displays an increased resistance to further straining. This fibre stiffness is evaluated as the strain-hardening modulus, E_{st} .

In the intermediate range of strain between ϵ_y and ϵ_{st} , the fibre yields and a yield modulus, E_0 , represents the slope of this portion of the curve. If the value of E_0 is zero there exists no explicit and definable relationship between stress and strain. That is, at the yield stress level, a fibre can assume an arbitrary value of strain and, if the direction of loading is such that strains tend to increase, it is likely that the strain-hardening modulus will govern the behaviour of a fibre that has yielded. The assumption that strain-hardening material properties govern buckling behaviour for strains above the yield strain has been successfully used by several investigators^{25,34,51,52,53,54} and this assumption is also made in the present investigation.

3.4 Analytical Technique

As explained in section 3.1 a plate buckling condition is derived using the principle of virtual work. This derivation is presented in detail in Appendix A and it results in an integral differential equation for the buckling condition. For a uniaxially stressed orthotropic plate, the buckling condition is as follows:

$$\int_x \int_y (D_{xx} w_{xx}, D_{yy} w_{yy}, D_{xy} w_{xy}, D_{yx} w_{yx}) dx dy + 4G_t I w_{xy} dx dy - \int_x \int_y N_x w_{xx}, N_y w_{yy} dx dy = 0$$

(A-35)

where D_x , D_y , D_{xy} , and D_{yx} are plate bending rigidities, G_t is the tangent shear modulus, and I is the moment of inertia per unit length of plate. These properties are further discussed in Appendix B. Also in Equation A-35, w represents the deflection of a point normal to the middle plane of the plate, δw represents a virtual deflection in this direction, x and y represent Cartesian coordinate directions, and differentiation is indicated using comma notation⁴⁷.

In Equation A-35 the first integral represents the virtual work resulting from the strain energy of plate bending while the second integral represents the virtual work done by the in-plane stresses which act during buckling.

Once a plate buckling condition has been formulated into a mathematical expression using an energy method, one may try to obtain an exact mathematical solution or an approximate solution. Because of the complexity of the present formulation, solutions are obtained using the Rayleigh-Ritz technique⁴⁸. This method has also been applied quite successfully by other investigators^{4,47,48,49,50}.

A basic assumption of this technique is that the displacement field describing a buckled shape can be expressed in terms of a set of assumed shape functions and corresponding coordinate displacements⁵⁵.

Together these must form a set of kinematically admissible generalized coordinate displacements which requires that the assumed displacement function satisfy the boundary conditions of the physical problem. The development of appropriate shape functions is discussed in a later section. However, it is appropriate here to state that a displacement function can be defined as follows:

$$w = f\langle\phi\rangle\{\theta\} \quad (3.1)$$

where $\{\theta\}$ is a vector of displacement coordinates defined at distinct nodal points in a cross-section (Figure 3.4) and $\langle\phi\rangle$ is a set of shape functions which interpolate the coordinate displacements over a cross-section. The function, f , is a shape function which interpolates a set of cross-sectional displacements over the length of a member. By substituting this assumed displacement function into Equation A-35, the problem is reduced from a continuum problem, with an infinite number of degrees of freedom, to a problem with a finite number of degrees of freedom equal to the total number of coordinate displacements defined at the nodes. As a result, a system of algebraic equations, rather than a partial differential equation, must be solved. This procedure is carried out in detail in Appendix A where it is shown that the problem of local buckling reduces to the form:

$$\left[[K] - \lambda [K_G] \right] \{ \theta \} = \{ 0 \} \quad (A-51)$$

where $[K]$ is a bending stiffness matrix depending on material properties and plate dimensions, $[K_G]$ is a geometric stiffness matrix depending on the distribution and magnitude of applied in-plane stresses, and λ is a

multiple of the applied loading which causes buckling.

The expression in brackets represents the reduced stiffness of a plate which buckles when, depending upon the value of λ , the determinant of the reduced stiffness matrix becomes zero. The corresponding values of λ and $\{\theta\}$ are referred to as the eigenvalue and eigenvector, respectively. The eigenvalue in this case is the critical stress at which a plate buckles and the eigenvector defines the critical buckled shape.

The solution to the buckling problem as presented herein reduces to the problem of extracting the lowest eigenvalue from the system of equations expressed by Equation A-51. If, in this equation, $[K]$ and $[k_G]$ are each of dimension $n \times n$, then the characteristic equation⁵⁰ of the reduced stiffness matrix will have n roots, each one corresponding to an eigenvalue of the system. However, in problems concerning statical stability only the lowest of these roots is of interest. A method that is commonly used to find the smallest eigenvalue of a system, and also one that is readily adaptable to electronic computation, is that of inverse matrix iteration⁵⁰.

Using this technique, Equation A-51 is first rewritten as:

$$[K]\{\theta\} = \lambda[k_G]\{\theta\} \quad (3.2)$$

Multiplying both sides of Equation 3.2 by the inverse of $[K]$ and dividing by λ result in:

$$[K]^{-1}[k_G]\{\theta\} = \frac{1}{\lambda}\{\theta\} \quad (3.3)$$

or:

$$[E]\{\theta\} = \omega\{\theta\} \quad (3.4)$$

where,

$$[E] = [K]^{-1}[K_G] \quad (3.5)$$

and,

$$\omega = \frac{1}{\lambda}. \quad (3.6)$$

In the solution of Equation 3.4, an initial shape vector, $\{\theta\}_0$, is assumed and this vector is multiplied by matrix $[E]$. The resulting vector, $\{\theta\}_1$, is then normalized by dividing by the highest-valued element of the vector. The process is then repeated with this new normalized vector. It has been shown⁵⁰ that, after several cycles of iteration, ω converges to the highest eigenvalue of the system. As a result, the lowest critical value of $\lambda = 1/\omega$ is obtained for the original system, Equation 3.2, and the corresponding eigenvector gives the critical buckled shape.

In certain eigensystems the smallest eigenvalue may appear as a positive value or a negative value. For example, the bending stress required to cause local buckling in a doubly-symmetric W shape may occur as a positive or negative eigenvalue of the associated eigensystem. This result is due solely to the symmetry of the system and the positivity or negativity of the eigenvalue has no physical significance. It does however result in considerable mathematical difficulty in achieving convergence during matrix iteration. This is because the rate of convergence is proportional to the ratio of the

lowest eigenvalue to the next higher value⁵⁰, and for values of this ratio approaching 1.0 the rate of convergence is very slow. For problems of the type described above, the first two eigenvalues of the system are equal but of opposite sign; that is, $\omega_1 = -\omega_2$. Therefore, the rate of convergence is $\omega_1/\omega_2 = -1.0$ and the technique will not converge.

To avoid this problem, a constant shift, μ , is applied to all of the eigenvalues of the system, in which case the rate of convergence is proportional to $(\omega_1 - \mu)/(\omega_1 + \mu) < 1.0$ and the method will converge.

Applying a shift, μ , to the system, Equation 3.4 becomes:

$$[E]\{\theta\} - \mu\{\theta\} = \omega\{\theta\} - \mu\{\theta\} \quad (3.7)$$

or,

$$[[E] - \mu[I]]\{\theta\} = \omega_s\{\theta\} \quad (3.8)$$

where $\omega_s = \omega - \mu$ and $[I]$ is an identity matrix of the same dimension as $[E]$. It has been shown⁵⁰ that the eigensystem defined by Equation 3.8 has the same eigenvectors as those defined by the original system described by Equation 3.4. The relationship between the eigenvalues of the two systems is given by:

$$\omega - \mu = \omega_s \quad (3.9)$$

or,

$$\omega = \frac{1}{\lambda} = \omega_s + \mu \quad (3.10)$$

In subsequent sections, the eigenvalue problem is formulated in such a way that only the smallest positive eigenvalue is

required. Although the eigenvalue shift technique increases the rate of convergence in most cases, it does not guarantee the convergence will be to the lowest positive root. In some cases it is found that the process converges to the lowest negative root. It is desirable therefore to have a method for eliminating certain eigenpairs from the system so that inverse iteration can be repeated to determine the lowest positive root. The method used to do this in the present analysis is referred to as a sweeping technique^{48,50}.

Since the eigenvectors, $\{\phi\}_i$, of an eigensystem are linearly independent⁵⁰, they provide a vector basis for the system, and any starting vector, $\{\theta\}$, may be expressed as a linear combination of these eigenvectors, that is:

$$\{\theta\} = \sum_{i=1}^n c_i \{\phi\}_i \quad (3.11)$$

If it is desired to remove the k th eigenmode from the system, a starting vector should be selected as follows:

$$\{\theta\}_o = \{\theta\} - c_k \{\phi\}_k \quad (3.12)$$

The value of c_k is found by pre-multiplying Equation 3.11 by $\langle \phi \rangle [K_G]$ and using the orthogonality properties⁵⁰ of eigenvectors. Doing so, results in:

$$c_k = \frac{\langle \phi \rangle_k [K_G] \{\theta\}}{\langle \phi \rangle_k [K_G] \{\phi\}_k} \quad (3.13)$$

Substituting this value into Equation 3.12 gives:

$$\{\theta\}_o = \left[[I] - \frac{\{\phi\}_k \langle \phi \rangle_k [K_G]}{\langle \phi \rangle_k [K_G] \{\phi\}_k} \right] \{\theta\}$$

$$= [S]_k \{\theta\} \quad (3.14)$$

where $[S]_k$ is the desired sweeping matrix. Using this value of $\{\theta\}_o$ as a starting value, Equation 3.8 becomes:

$$[[E] - \mu[I]] [S]_k \{\theta\} = \omega_s \{\theta\} \quad (3.15)$$

which represents an eigensystem with the k^{th} mode removed. In the analytical technique presented herein this method is used to remove negative eigenvalues and corresponding eigenvectors from a system. It has been found that only one application of a sweeping matrix is required for the majority of cases where the first eigenvalue calculated is negative.

3.5 Effects of Initial Imperfections

As described previously, the present analysis uses a precise mathematical formulation to describe the local buckling condition. This implies that the maximum strength of a plate or system of plates is limited only by critical local buckling and this is the basis on which the formulation is made. The assessment of the effects of initial imperfections on the buckling strength of plates is also based on this type of formulation.

It is assumed for this purpose that $\{\theta\}_o$ is a set of initial

coordinate displacements defined at the nodes of a plate system.

Using the same interpolation functions as those in Equation 3.1, initial deflections may be described by:

$$w_o = f<\phi>\{\theta_o\} \quad (3.16)$$

and additional deflections due to applied in-plane loads are given by:

$$w_1 = f<\phi>\{\theta\} \quad (3.17)$$

Therefore, the total out-of-plane deflection at any point is given by:

$$\begin{aligned} w &= w_o + w_1 \\ &= f<\phi>\{\theta_o\} + f<\phi>\{\theta\} \end{aligned} \quad (3.18)$$

To evaluate the effects of initial imperfections, the appropriate values of deflection are substituted into the buckling condition, Equation A-35. Since the first integral in Equation A-35 represents the work done by bending of a plate from its initially deflected position to its buckled shape, the net deflection, $w - w_o$, must be used to evaluate this integral². The second integral in Equation A-35 represents the work done by the in-plane forces during buckling of a plate. It can be evaluated by calculating the work done by the in-plane forces acting through displacements caused by initial imperfections only. The net work is then obtained by subtracting this value from the work done by the in-plane forces acting through displacements caused by the total deflection of a plate. By proceeding in this manner, and using the concepts of bending and geometric stiffness matrices, as used in Section 3.4, Equation A-35 results in the following set of equations:

$$[K] - \lambda [K_G] \{ \theta \} = \lambda [K_G] \{ \theta_0 \} \quad (3.19)$$

From this relationship it can be seen that the effect of initial imperfections is to simulate an equivalent lateral load of:

$$\{ F_0 \} = \lambda [K_G] \{ \theta_0 \} \quad (3.20)$$

The effect of this equivalent lateral load is to cause deflections to increase gradually as the in-plane loads are increased. However, the mathematical definition of buckling can be expressed by setting the determinant of the reduced stiffness matrix equal to zero. Since the reduced stiffness matrix formulated with initial imperfections included is identical to that for the case of a perfectly straight plate, initial imperfections do not affect the value of the critical buckling load as defined herein. As the in-plane loads increase, lateral deflections increase gradually and as the critical buckling load is approached the lateral deflections become asymptotic to the critical buckled shape.

3.6 Coordinate Systems

In the formulation of the theory for local buckling, the shape functions are referred to a system of natural coordinates^{50,55}. Figure 3.3. illustrates the relationship between a natural coordinate system for a plate of length ℓ , and a Cartesian coordinate system. Points 1, 2, and 3 in this figure are referred to as nodes at which the coordinate displacements comprising the vector, $\{ \theta \}$, are defined. At these nodes the elements of $\{ \theta \}$ may represent translations,

rotations, curvatures, and higher order derivatives. Using these coordinates and an appropriate set of interpolating polynomials it is possible to define a set of shape functions at a cross-section for the flanges and web of a W shape section.

Local natural coordinate systems for the flanges and web of a W shape cross-section as well as the corresponding node numbering system are shown in Figure 3.4. Each coordinate displacement defined at a given node is interpolated by a polynomial function over the cross-sectional edge of a flange or a web. The order of each such interpolating polynomial is equal to the number of coordinate displacements that must be interpolated for a flange or web. Thus, for example, if a translation and a rotation are defined for each of three nodes of a flange, a quintic polynomial interpolating function is used for each nodal displacement.

3.7 Flange Shape Functions

Polynomial functions used to interpolate coordinate displacements along a plate edge at a cross-section may be obtained by a matrix technique⁵⁵ or by inspection. Since the latter method is used herein it is described in detail below. Quintic polynomials are used to interpolate the nodal displacements for flanges at a cross-section. At each of three nodes on a flange, a translation and a rotation are interpolated. These interpolation functions and their shapes are shown in Figure 3.5.

The method of inspection for obtaining shape functions is presented as an illustration for the particular case of interpolating a translation at node number one of Figure 3.4. Since a total of six

coordinate displacements are defined (a translation and a rotation at each of three nodes) a fifth order polynomial is first assumed as follows:

$$S(\zeta) = \zeta^2(\zeta-1)^2(a_o\zeta+b_o) \quad (3.21)$$

A shape function evaluated at the coordinate displacement being interpolated must have a value of 1.0 and must have a zero value when evaluated at all other coordinate displacements. The first factor of the above function ensures that the translation and rotation at $\zeta=0$ are both zero. The second factor ensures that the translation and rotation at $\zeta=1$ are zero. The third factor is chosen so that the function will be a fifth order polynomial. Also, the constants, a_o and b_o , can be determined so that at $\zeta=-1$, the rotation is zero and the translation is positive and unity. Evaluating a_o and b_o for these two conditions results in the function:

$$S(\zeta) = \frac{1}{4}\zeta^2(\zeta-1)^2(3\zeta+4) \quad (3.22)$$

The value of this expression is positive unity at the coordinate displacement being interpolated while at all other coordinate displacements its value is zero.

3.8 Web Shape Functions

Octic polynomials are used to interpolate nodal displacements for webs at a cross-section. For the purpose of studying local buckling of W shapes, it is assumed that the line of intersection of two plates at a flange-to-web junction does not translate during buckling. This line appears as a nodal point on a cross-section of a W shape and the

corresponding translations are not interpolated for the flange or web since they have zero value. Therefore, octic polynomials are used to interpolate rotations and curvatures of a web at its extremities and translation, rotation, and curvature at its center for a given cross-section. The interpolating polynomials for webs are obtained by the method of inspection as described previously for flanges. The polynomials and their corresponding shapes for coordinate displacements of a web at a cross-section are shown in Figure 3.6.

3.9 Longitudinal Shape Functions

A buckled shape which has been established at a cross-section of a W shape member must be interpolated over the length of the member. For plates simply supported at the loaded edges and subjected to uniaxial stresses, it has been determined^{2,6} that the buckled shape in the direction of applied stress occurs in the form of a sine wave. This result is inherent in the nature of the solution to a partial differential equation which defines the plate buckling of a simply supported rectangular plate subjected to uniaxial stresses.

For this reason, and because the Rayleigh-Ritz solution is not very sensitive to the actual shapes used^{4,47,48,50}, a sine shape is included as a principle component of longitudinal shape functions used in this study. As shown in Figure 3.7, the effect of various boundary conditions can be accounted for by multiplying a sine function by a polynomial function which adequately describes the boundary conditions. Essentially, this technique applies an envelope to a sine function.

The general form of a longitudinal shape function is $P_o(\xi) \sin m\pi\xi$. In this form $P_o(\xi)$ represents a polynomial envelope of a

sine function where m is the number of half sinewaves that occurs along the length of a plate during buckling. The complete buckled shape of a plate component of a W shape is given by:

$$w = P_o(\xi) \sin m\pi\xi\phi\{\theta\} \quad (3.23)$$

As described previously, $\phi\{\theta\}$ describes the buckled shape of a flange or a web at a cross-section. Each polynomial of ϕ is a function of ζ when referring to a flange, and a function of η when referring to a web. ξ is the natural coordinate in the longitudinal direction of a member. The natural coordinates, ξ , ζ , and η and the corresponding natural coordinate systems are defined in Figure 3.8 for a W shape.

3.10 Integration of Cross-Sectional Shape Functions

As is evident from the formulation presented in Appendix A, extensive use of integration and differentiation of shape functions is required. Furthermore, shape functions expressed in terms of natural coordinates must be integrated and differentiated with respect to Cartesian coordinates. The function in Equation 3.22, for example, may be integrated as follows:

$$\int_0^{b/2} s(\zeta) dy = \frac{b}{2} \int_0^1 s(\zeta) d\zeta \quad (3.24)$$

In this operation, the limits of integration and the differential element dy in the Cartesian coordinate system were transformed to a natural coordinate system using the relationship,

$$\zeta = \frac{2y}{b} \quad (3.25)$$

as defined in Figure 3.5. Differentiation of the function in Equation 3.22 proceeds as follows:

$$\frac{\partial S(\zeta)}{\partial y} = \frac{\partial S}{\partial \zeta} \cdot \frac{\partial \zeta}{\partial y} = \frac{2}{b} \frac{\partial S}{\partial \zeta} \quad (3.26)$$

where the chain rule of differentiation⁵⁶ and the relationship of Equation 3.25 were used.

As indicated by Equations A-42 to A-51, it is necessary to integrate many different functions and products of functions in order to obtain a solution for a given problem. These operations are best performed by computer if they are first expressed in terms of matrices. As an illustration of the technique, the following integral from Equation A-48 will be considered:

$$[\Phi_2] = \int_y \{\phi_{yy}\} \langle \phi_{yy} \rangle dy \quad A-48$$

A set of shape functions, $\{\phi\}$, may be expressed by:

$$\{\phi\} = [C]\{H\} \quad (3-27)$$

where $[C]$ is a matrix of constant coefficients of shape functions and,

$$\{H\} = \begin{Bmatrix} 1 \\ \zeta \\ \zeta^2 \\ \zeta^3 \\ \zeta^4 \\ \zeta^5 \end{Bmatrix} \quad (3.28)$$

for a quintic polynomial. Differentiating Equation 3.27 twice with

respect to y gives:

$$\{\phi_{yy}\} = [C]\{H_{yy}\}$$

$$= \frac{4}{b^2} [C] \begin{Bmatrix} 0 \\ 0 \\ 2 \\ 6\zeta \\ 12\zeta^2 \\ 20\zeta^3 \end{Bmatrix} \quad (3.29)$$

where the relationship given by Equation 3.25 was used.

Using the relationships of Equation 3.29, the integrand of Equation A-48 may be written as follows:

$$\{\phi_{yy}\} \langle \phi_{yy} \rangle = [C]\{H_{yy}\} \langle H_{yy} \rangle [C]^T$$

$$= \frac{16}{b^2} [C] \begin{Bmatrix} 0 \\ 0 \\ 2 \\ 6\zeta \\ 12\zeta^2 \\ 20\zeta^3 \end{Bmatrix} \langle 0 \ 0 \ 2 \ 6\zeta \ 12\zeta^2 \ 20\zeta^3 \rangle [C]^T$$

$$= \frac{16}{b^2} [C] \begin{bmatrix} 0 & 0 & 0 & 0 & 0 & 0 \\ 0 & 0 & 0 & 0 & 0 & 0 \\ 0 & 0 & 4 & 12\zeta & 24\zeta^2 & 40\zeta^3 \\ 0 & 0 & 12\zeta & 36\zeta^2 & 72\zeta^3 & 120\zeta^4 \\ 0 & 0 & 24\zeta^2 & 72\zeta^3 & 144\zeta^4 & 240\zeta^5 \\ 0 & 0 & 40\zeta^3 & 120\zeta^4 & 240\zeta^5 & 400\zeta^6 \end{bmatrix} [C]^T \quad (3.30)$$

The integral of Equation A-48 may now be evaluated by integrating each term in the matrix of variables in Equation 3.30, to obtain the following:

$$\int_y \{\phi,_{yy}\} \langle \phi,_{yy} \rangle dy =$$

$$\frac{16}{b^2} [C] \begin{bmatrix} 0 & 0 & 0 & 0 & 0 & 0 \\ 0 & 0 & 0 & 0 & 0 & 0 \\ 0 & 0 & 4\zeta & 6\zeta^2 & 8\zeta^3 & 10\zeta^4 \\ 0 & 0 & 6\zeta^2 & 12\zeta^3 & 18\zeta^4 & 24\zeta^5 \\ 0 & 0 & 8\zeta^3 & 18\zeta^4 & 24\zeta^5 & 40\zeta^6 \\ 0 & 0 & 10\zeta^4 & 24\zeta^5 & 40\zeta^6 & (400/7)\zeta^7 \end{bmatrix}_{l_1}^{l_2} [C]^T$$

(3.31)

where the elements of the matrix of variables are to be evaluated for the integration limits, l_1 and l_2 . This method permits the use of computer techniques to obtain the integral of functions between any limits of integration. This is important because, depending on the level of stress and the stress distribution, longitudinal strips of a flange or a web may be elastic, yielded, or strain-hardened. Therefore the integration over a cross-section of a plate component is performed in a piecewise fashion between the limits of these zones so that the differing material properties may be included in the evaluation of a stiffness matrix. In this way also, abrupt changes in stress distribution may be accommodated in evaluating a geometric stiffness matrix.

3.11 Integration of Longitudinal Shape Functions

As shown in the formulation of the analytical technique in

Appendix A, extensive integration is also required for longitudinal shape functions. For example, factor F_1 in Equation A-42 is expressed as:

$$F_1 = \int_x f_{xx}^2 dx \quad (A-42)$$

As discussed in Section 3.9, the function, $f(\xi)$, may be of the form,

$$f(\xi) = P_o(\xi) \sin(m\pi\xi) \quad (3.32)$$

where $P_o(\xi)$ is a polynomial function. As a result, the functions to be integrated over the length of a member may be quite complicated expressions depending on the order of the polynomial, $P_o(\xi)$, and therefore a numerical integration technique is used. The length of a member is divided into a number of equal intervals over which Gaussian quadrature⁵⁰ is used to integrate a function. The total integral over a length is obtained by adding together these sub-integrals. The number of intervals used for a given length is equal to the number of half sine wavelengths along a member and a 6-point Gauss integration⁵⁰ technique is performed for each interval.

3.12 General Procedure for W shapes

The procedure described in Section 3.4 is used to develop a bending stiffness matrix and a geometric stiffness matrix for the web and each flange of a W shape. These represent stiffness submatrices that must be assembled into overall stiffness matrices for an entire member. In assembling the matrices, compatibility between the flanges and web at a cross-section is maintained by enforcing zero

relative rotation between the plate components at a web-to-flange junction.

Figure 3.9 illustrates the node numbering and coordinate displacements for a typical W shape cross-section. The notations of this figure will be used in describing the assembly of a stiffness matrix. Since a bending stiffness matrix and a geometric stiffness matrix are both assembled in exactly the same manner the procedure is illustrated for a bending stiffness matrix assembly only. In Section 3.4 it was shown that a plate buckling problem reduced to an eigenvalue form as shown by Equation A-52 which can be rewritten as follows:

$$[K]\{\theta\} = \lambda [K_G]\{\theta\} \quad (3.33)$$

The bending strain energy of a component plate during buckling results in the term on the left hand side of this equation. Therefore, assembling the stiffness submatrices of the two flanges and the web of a W shape section to obtain the assembled stiffness matrix is, in effect, equivalent to adding together the plate bending strain energies of the individual component plates. Using the notation given in Figure 3.9, the left hand side of Equation 3.33 may be written as;

$$[K]\{\theta\} = [K_1] \begin{Bmatrix} u_1 \\ u'_1 \\ u_2 \\ u'_2 \\ u'_3 \end{Bmatrix} \quad (3.34)$$

for a lower flange;

$$[K]\{\theta\} = [K_w] \begin{Bmatrix} u'_3 \\ u'''_3 \\ u'''_4 \\ u'_4 \\ u'''_5 \\ u'_5 \end{Bmatrix} \quad (3.35)$$

for a web; and

$$[K]\{\theta\} = [K_u] \begin{Bmatrix} u'_5 \\ u_6 \\ u'_6 \\ u_7 \\ u'_7 \end{Bmatrix} \quad (3.36)$$

for an upper flange. The slopes u'_3 and u'_5 represent the rotations of the flanges and web at the web-to-flange junctions of a W shape cross-section. The fact that u'_3 is common to Equations 3.34 and 3.35 and u'_5 is common to Equations 3.35 and 3.36 ensures compatibility (in this case, rigidity of attachment) between the flanges and web. Therefore in assembling the stiffness submatrices, $[K_1]$, $[K_w]$, and $[K_u]$, to obtain the total stiffness matrix of a W shape, stiffness elements of the submatrices corresponding to u'_3 and u'_5 must be added directly. This procedure is illustrated schematically in Figure 3.10.

3.13 Iteration on the Number of Wavelengths

The vector of coordinate displacements, $\{\theta\}$, represents the amplitudes of the shape functions defining the buckled shape of a cross-section. This vector is automatically obtained as a natural part of the process of matrix iteration⁵⁰ for each assumed value of m , where m is the number of half sine wavelengths of buckling along the length of a member. The correct value of m is that value for which the energy of a system is a minimum since this represents the lowest energy state of the buckled configuration².

In an actual solution, a starting value of $m = 1$ is assumed. This value is successively incremented in steps of unity and at each increment a matrix iteration is performed to determine an eigenvalue and the corresponding critical buckled shape of a cross-section. As m is incremented, the critical eigenvalue continues to decrease until a point of minimum potential energy of a system is reached. Thereafter, increases in m cause an increase in the potential energy. The correct value of m is that value for which the potential energy of the system is a minimum and the corresponding eigenpair gives the critical stress and the buckled shape of a cross-section.

3.14 Effect of Residual Stresses

Residual stresses acting on a W shape section alter the characteristics of a geometric stiffness matrix and therefore influence the value of a critical stress. In order to include this effect in the analysis, a residual strain pattern, as shown in Figure 3.11, is assumed. Such a pattern allows for a fairly general representation and has been used successfully by other investigators^{37, 51, 57, 58, 59} in

assessing the effects of residual stresses. At the outset of a problem, values must be specified for ε_2 , the residual tension strain at the lower edge of a web, ε_3 , the residual compressive strain at mid-depth of a web, and ε_4 , the residual tension strain at the upper edge of a web. The values of ε_1 and ε_5 , the residual strains at the lower and upper flange tips respectively, are then determined using the following conditions of equilibrium for a cross-section subjected to residual stresses:

$$\Sigma F = 0 \quad (3.37)$$

$$\Sigma M = 0 \quad (3.38)$$

Equation 3.37 is an expression of translational equilibrium of a cross-section in the longitudinal direction of a member, and Equation 3.38 expresses equilibrium of a cross-section with respect to rotation about an axis perpendicular to the web.

The residual strain pattern of Figure 3.11 may be transformed into a stress pattern using a simple stress - strain relationship as shown in Figure 3.2. The forces and moments due to the residual stresses are obtained by integrating the effects of the stresses over the web and each flange of a W shape. Performing this integration, Equations 3.37 and 3.38 may be written as follows:

$$\Sigma F = 2A_u(\sigma_5 - \sigma_4) + 2A_1(\sigma_1 - \sigma_2) + A_w(2\sigma_3 - \sigma_4 - \sigma_1) = 0 \quad (3.39)$$

and,

$$\Sigma M = \frac{A_w h}{24} (6\sigma_3 - 5\sigma_4 - \sigma_2) + \frac{h}{A_2} (\sigma_5 - \sigma_4) = 0 \quad (3.40)$$

where, σ_i ($i=1,2,3,4,5$) are stresses corresponding to the strains ϵ_i ($i=1,2,3,4,5$), A_1 is the area of a lower flange, A_u is the area of an upper flange, A_w is the web area, and h is the web height.

Solving Equations 3.39 and 3.40 simultaneously and using Figure 3.2 to transform from stress to strains, results in the following values:

$$\epsilon_1 = \epsilon_4 - \frac{A_w}{12A_u} (\epsilon_2 - 6\epsilon_3 + 5\epsilon_4) \quad (3.41)$$

$$\epsilon_5 = \epsilon_2 - \frac{A_w}{12A_1} (5\epsilon_2 - 6\epsilon_3 + \epsilon_4) \quad (3.42)$$

In subsequent formulations, residual strains are added to applied strains so that their effects on yielding and strain-hardening as well as their effects on decreasing a geometric stiffness matrix are included directly in the analytical technique.

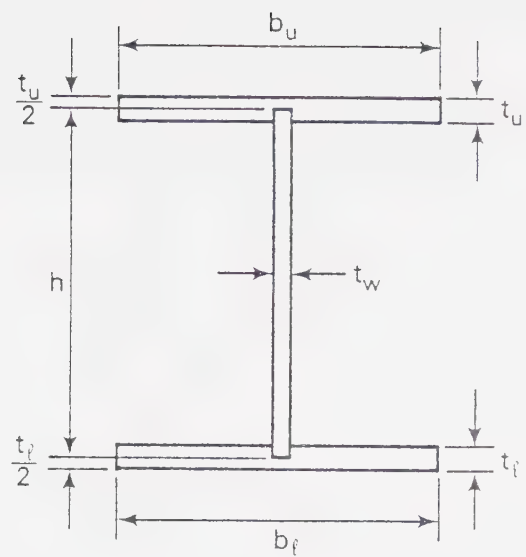


Figure 3.1 Idealized Cross-section

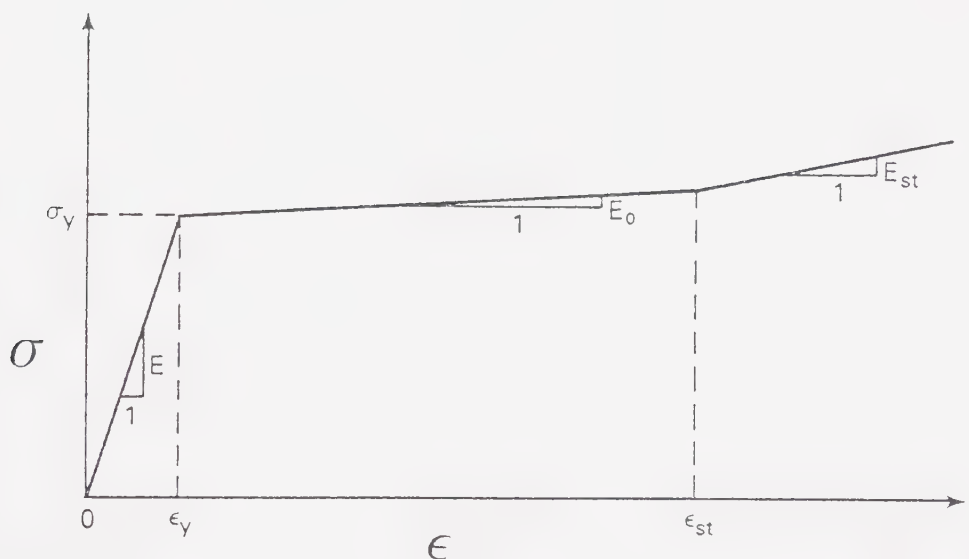


Figure 3.2 Idealized Tri-linear Stress-Strain Curve

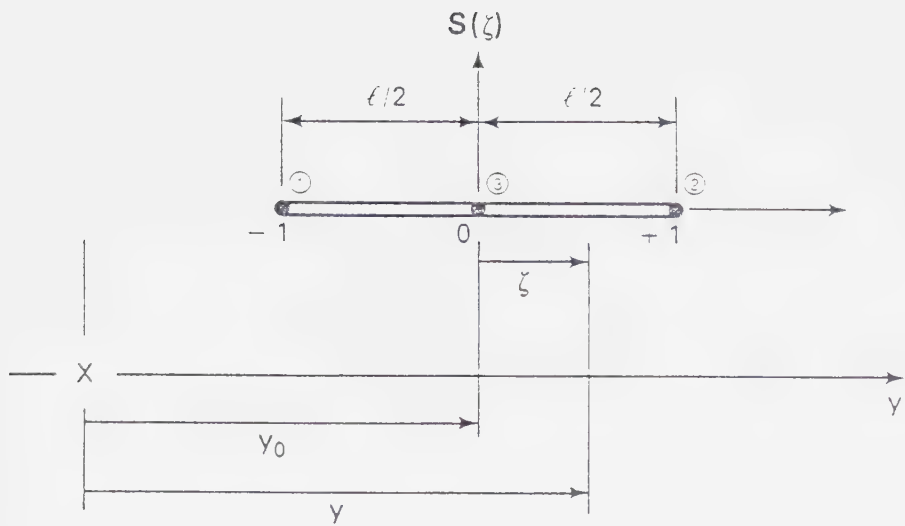


Figure 3.3 Relationship Between Cartesian and Natural Coordinates

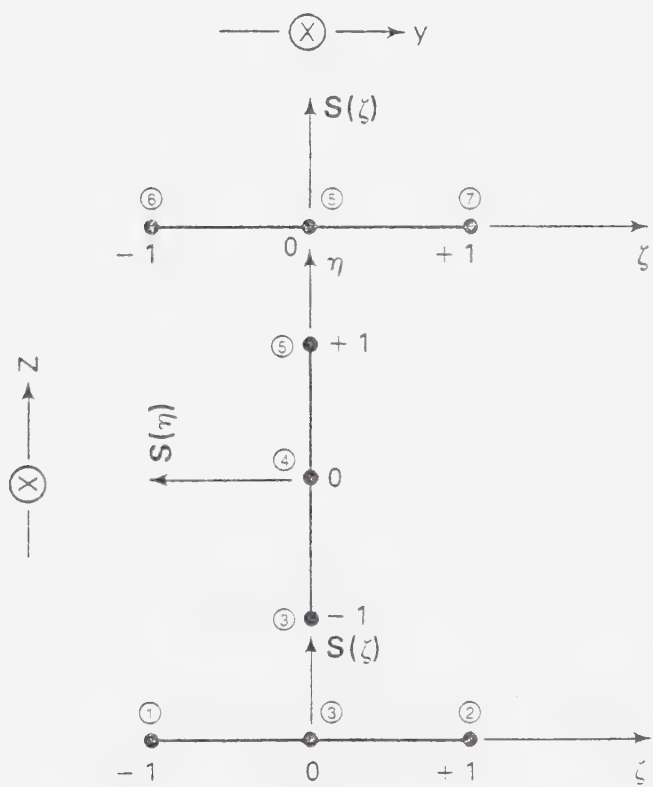


Figure 3.4 Local Coordinates and Numbering System

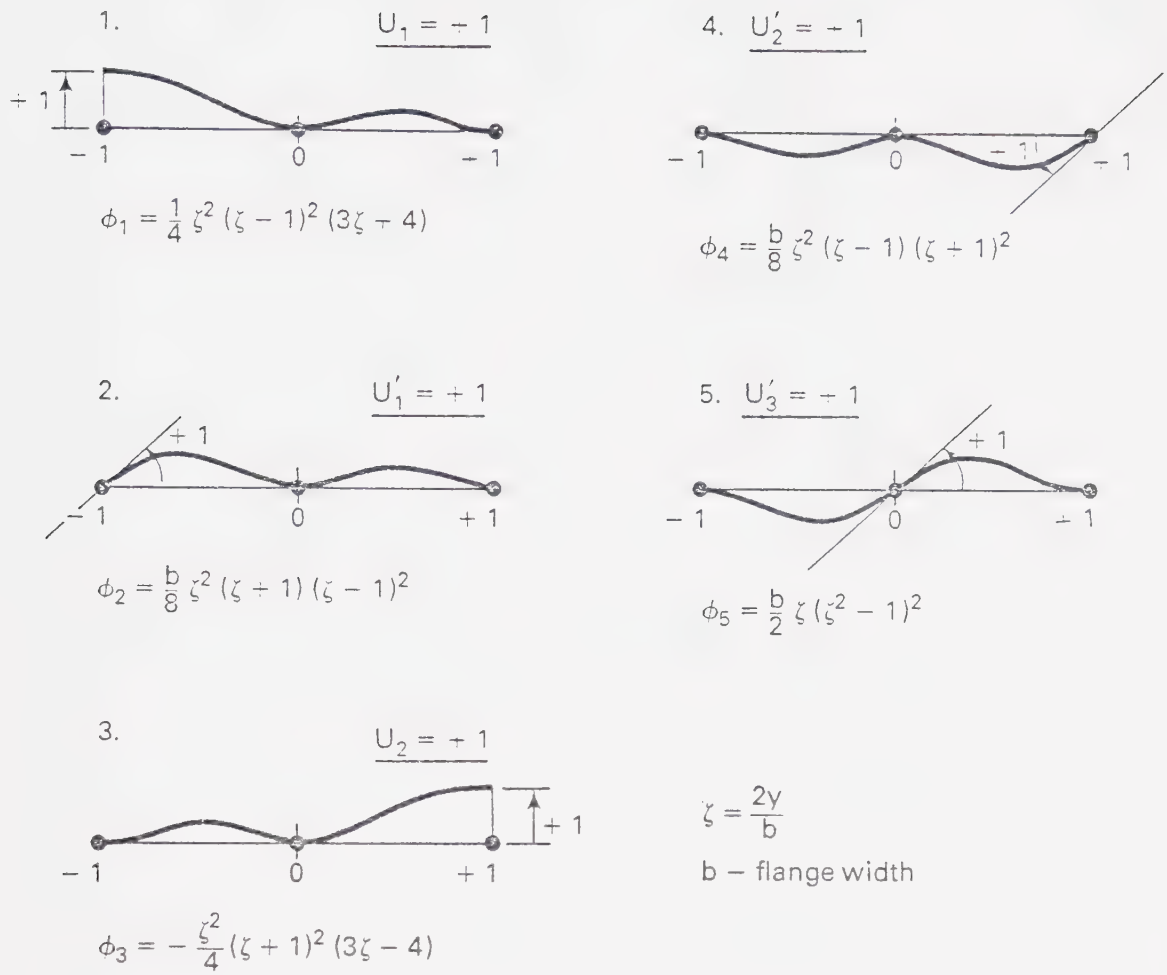


Figure 3.5 Shape Functions for Flanges

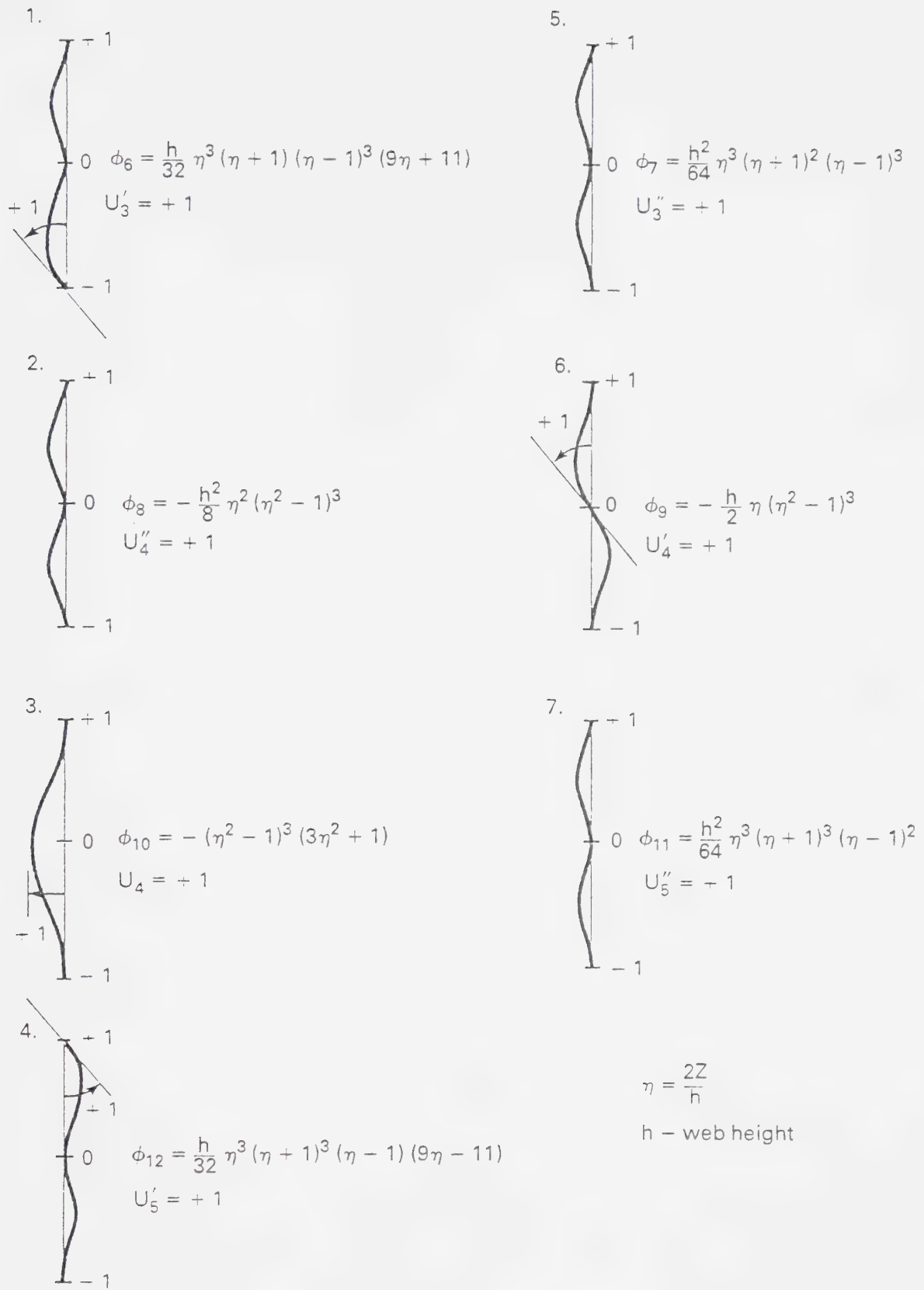


Figure 3.6 Shape Functions for Webs

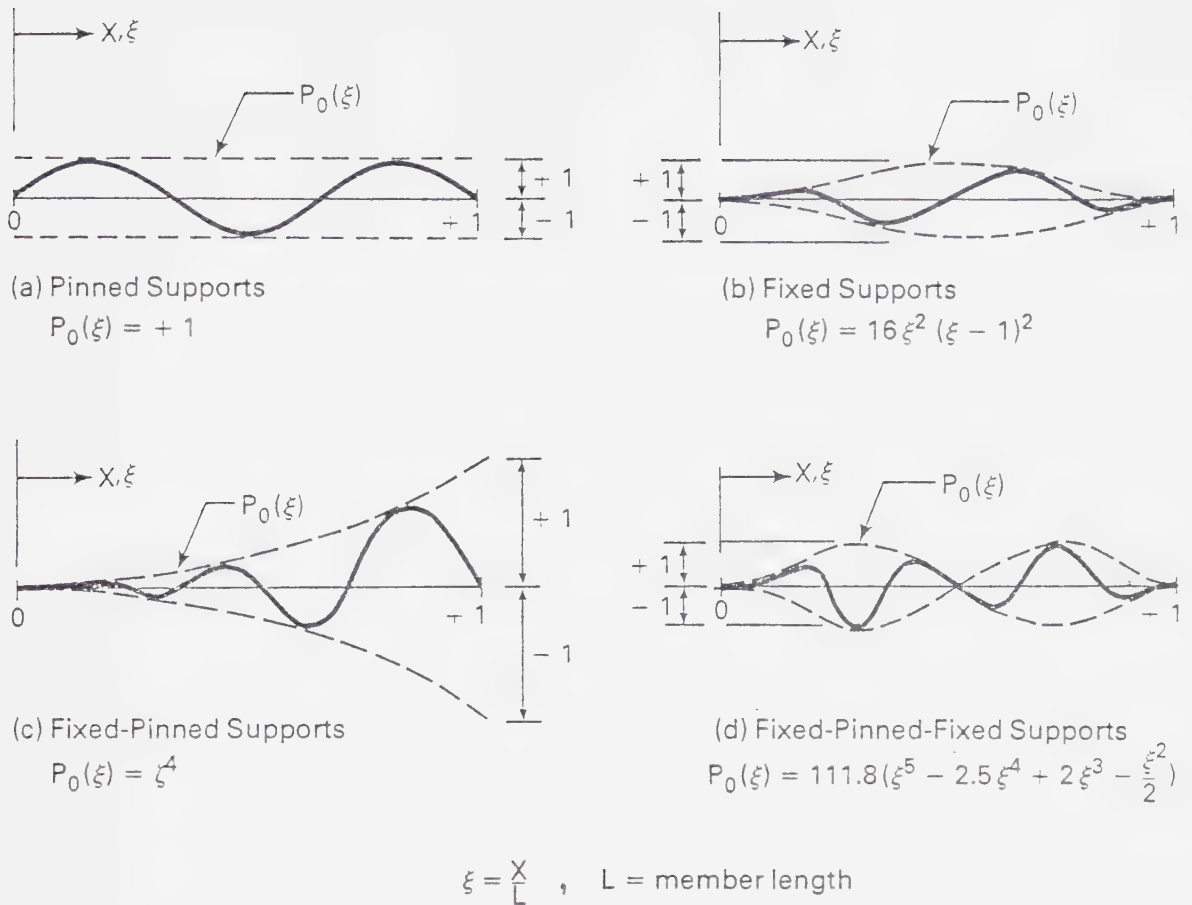


Figure 3.7 Longitudinal Shape Functions

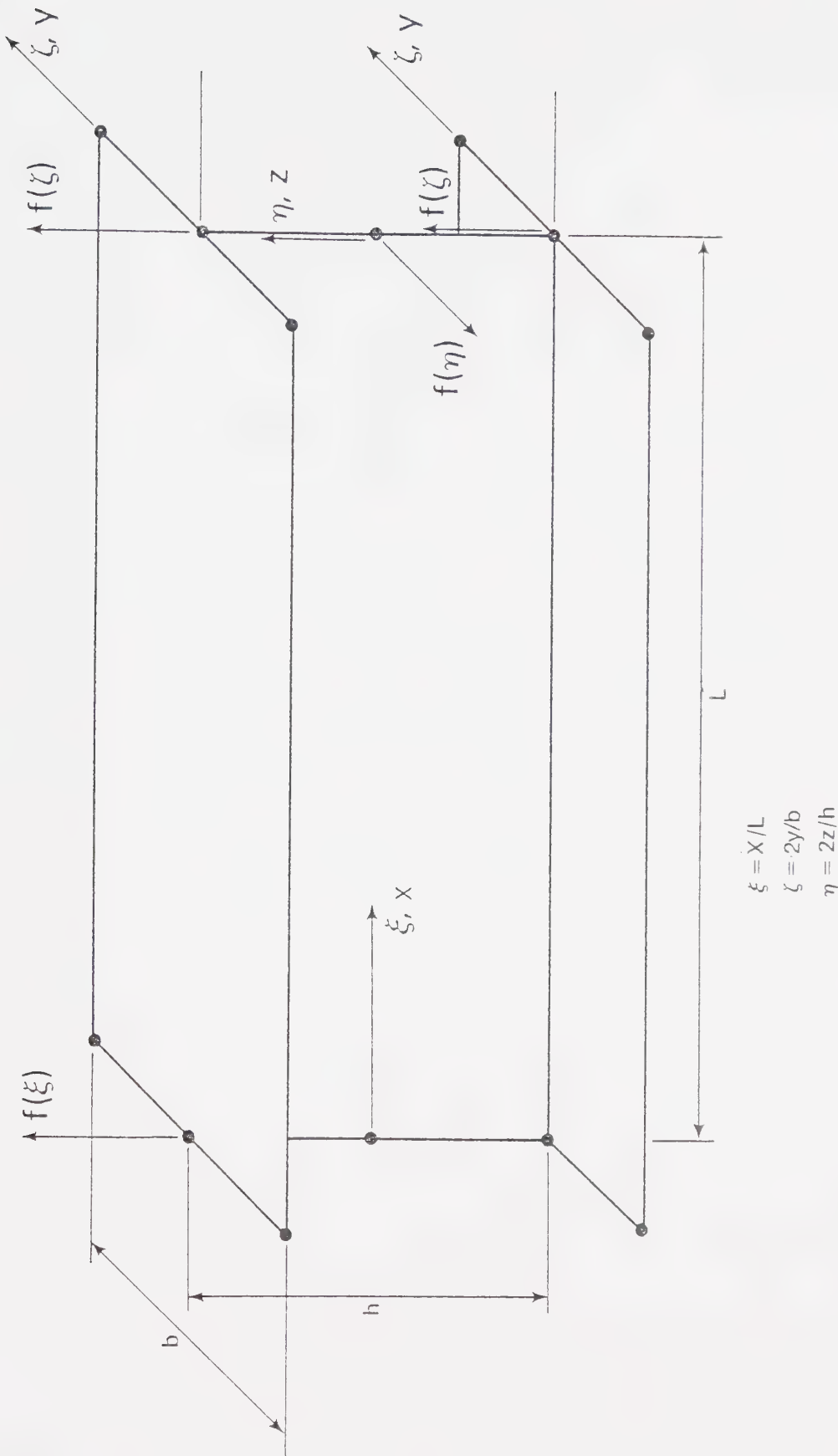


Figure 3.8 Natural Coordinate Systems for a W shape

$$\xi = X/L$$

$$\zeta = 2y/b$$

$$\eta = 2z/h$$

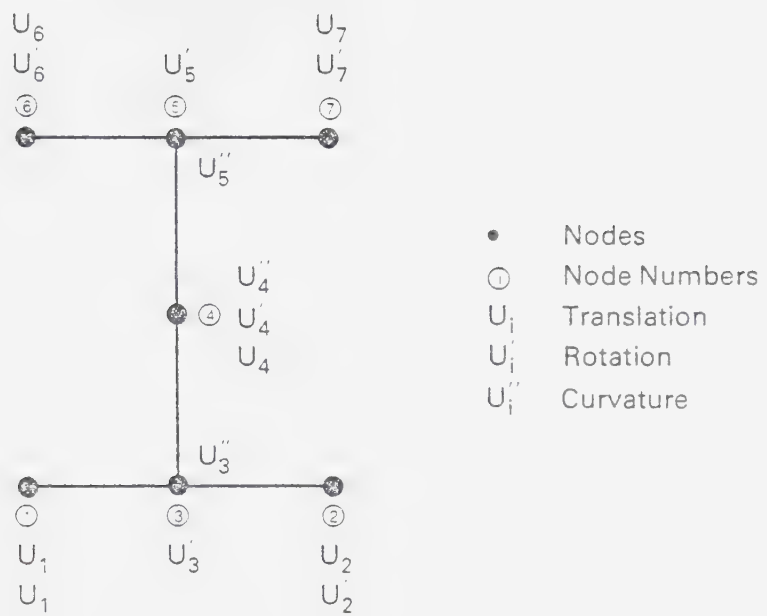


Figure 3.9 Node Numbering and Coordinate Displacements

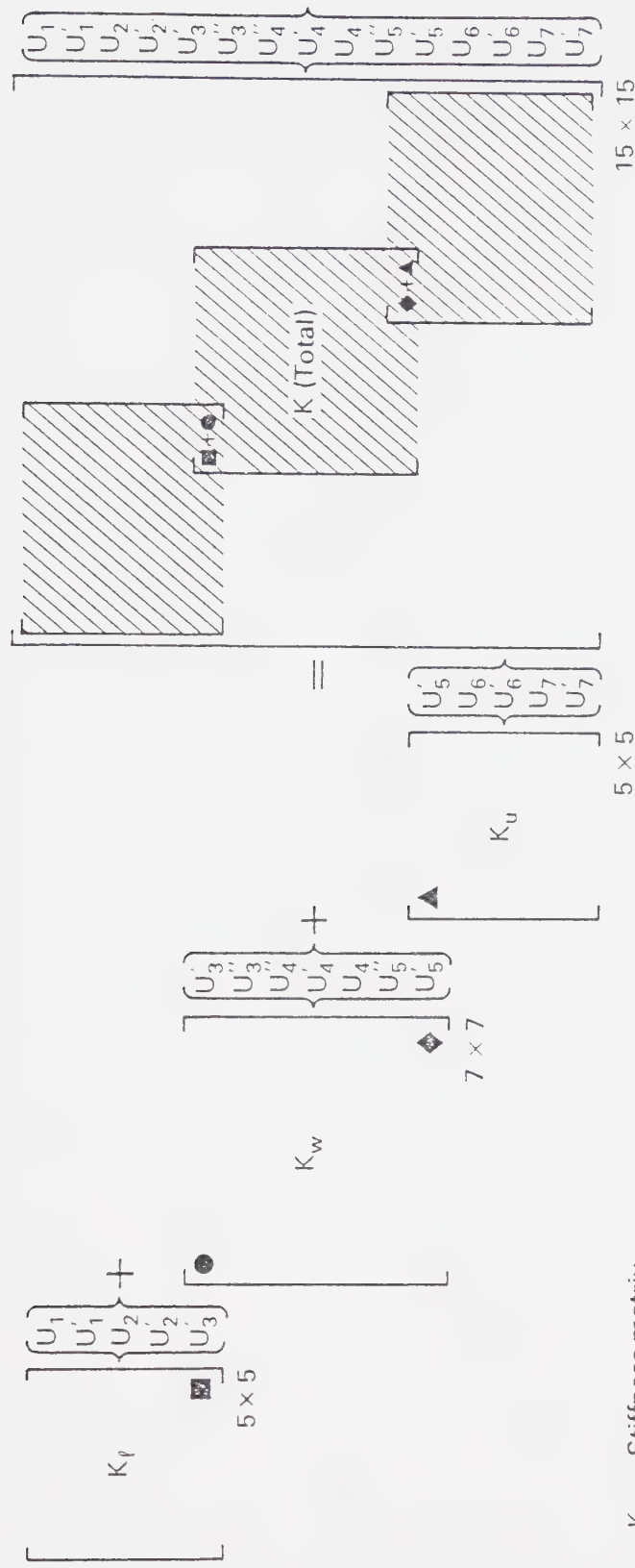


Figure 3.10 Schematic Stiffness Assembly

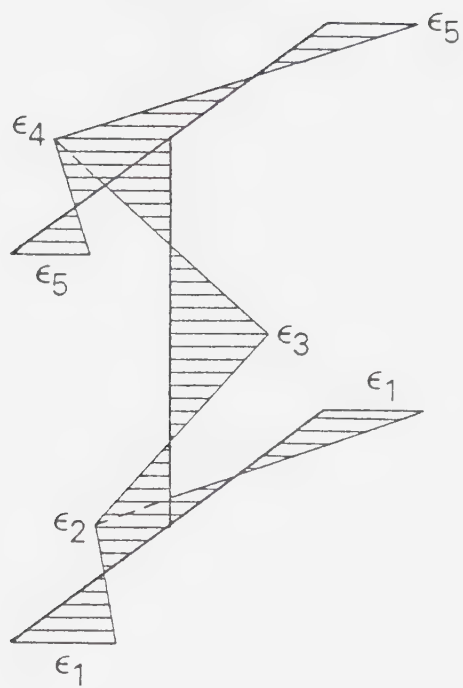


Figure 3.11 Residual Strain Distribution

Chapter 4

ANALYSIS FOR COMBINED AXIAL COMPRESSION AND BENDING

4.1 Introduction

In Chapter 3 a general formulation was presented for the analysis of buckling of plates subjected to piecewise linearly varying uniaxial stresses. The inclusion of residual stresses was also discussed and it was stated that the method could be applied to buckling in the elastic as well as the inelastic range. A W shape subjected to combined axial compression and strong-axis bending is composed of three uniaxially stressed plates (two flanges and a web). Because of the presence of residual stresses, uniaxial stresses on a component plate are piecewise linear at a section. The problem of local buckling of a W shape section is formulated by combining the effects of the individual component plates to obtain the total stiffness matrices for a member. In this chapter the procedure is explained in detail for the general loading case of a W shape section subjected to axial compression and strong axis bending combined. The formulation for the general case may be applied to a particular case of pure axial load or pure bending by setting the applied bending moment or the applied axial load equal to zero, respectively.

4.2 Assumptions

In Appendix A, a plate buckling condition is developed for a single uniaxially stressed rectangular plate. This buckling condition

is derived using the principle of virtual work and it is applicable to the elastic and inelastic ranges of stress. In addition to the usual assumptions of plate buckling presented in Appendix A, the following assumptions applicable to local buckling of a structural steel W shape section are made:

1. The member is loaded in such a way that all longitudinal fibres are subjected only to uniaxial stresses.
2. The idealized stress - strain response shown in Figure 3.2 applies for each longitudinal fibre in a cross-section.
3. The buckling condition expressed by Equation A-35 is applicable to material which is elastic, yielded, or strain-hardened.
4. Shape functions for a cross-section are continuous across boundaries between elastic and yielded material and between yielded and strain-hardened material.
5. Local buckling of component plates may occur when a cross-section is in any one of the following strain ranges:
 - (a) fully elastic range
 - (b) partly elastic and partly yielded range
 - (c) fully yielded range
 - (d) partly yielded and partly strain-hardened range
 - (e) fully strain-hardened range
6. Member failure occurs when a plate component of a cross-section buckles locally.

4.3 Stiffness Matrix Formulations

4.3.1 Introduction

In the following sections, stiffness submatrices are formulated for individual plate components of a W shape. An applied uniform axial strain is superimposed on a general residual strain distribution such as that shown in Figure 4.1 where ε_i ($i=1, 2, 3, 4, 5$) are residual strains, and ε_a is an axial strain. A bending moment strain, ε_b , is then added. The resulting total strain distribution is used to determine the stresses on each component plate as well as the extent of yielded and strain-hardened regions within a plate. Stiffness submatrices are formulated for each plate component for a general case of material being partly elastic, partly yielded, and partly strain-hardened. The component plate stiffness submatrices are then combined as described in Chapter 3.

As previously mentioned, it is assumed for the purpose of clarity, that a section is oriented with its web in a vertical plane. Furthermore, it is assumed that the direction of an applied moment is such that it tends to place the upper flange in compression and the lower flange in tension. As a result of this assumption, the upper flange will always be in compression under the actions of the applied axial compression and bending loads combined. The lower flange, however, may be in tension when the axial load is low compared to the flexural load or in compression when the flexural load is low compared to the axial load. In the latter case, the general analysis of a lower flange is identical to that of an upper flange in compression.

4.3.2 Application of Incremental Bending Strains

In this analysis of local buckling of beam-columns, it is necessary to apply additional increments of bending strains to a cross-section. Before an increment is applied, a cross-section may be partially yielded or strain-hardened as a result of previously applied strains. Before additional bending strain increments can be applied it is therefore necessary to update the location of the neutral axis.

Figure 4.2(a) shows a cross-section which is partially elastic and partially yielded as a result of a total strain distribution such as that shown in Figure 4.1. The neutral axis is located at a distance, y_1 , from the mid-depth of a web. This location is determined from the requirement that a cross-section must be in equilibrium under the action of applied loads. Once the neutral axis has been located the bending strains, ε_c , at mid-depth of a web, and ε'_b , at the lower edge of a web may be determined from the strain geometry.

Referring to Figure 4.2(b), the following expressions for ε_c and ε'_b may be obtained:

$$\varepsilon_c = \left(\frac{2y_1}{2y_1 - h} \right) \varepsilon_b \quad (4.1)$$

where h is the web depth and ε_b is the applied compressive bending strain, and

$$\varepsilon'_b = \left(\frac{h+2y_1}{h-2y_1} \right) \varepsilon_b. \quad (4.2)$$

In these relationships ε_c and ε'_b are given as functions of the applied compressive bending strain, ε_b . Thus the distribution of incremental bending strains is completely specified when a value of the applied strain, ε_b , is specified. In subsequent formulations an analytical technique is set up so that ε_b is an eigenvalue which corresponds to a critical buckling strain.

4.3.3 Stiffness Submatrices

In this section, bending and geometric stiffness submatrices are formulated for individual plate components of a W shape. The stiffness matrices, $[K]$ and $[K_G]$, are formulated separately for a compression flange, a tension flange, and a web. For the purpose of analysis only, a web is considered to consist of two parts; the lower half of a web between nodes 3 and 4, and the upper half between nodes 4 and 5 as shown in Figure 3.9, Chapter 3. Because the origin of local coordinates is at node 4 of a web, this particular division simplifies the analysis somewhat with regard to integration of piecewise continuous functions along its height.

Equations A-53 and A-54 are expressions for bending and geometric plate stiffness matrices, respectively. These expressions are repeated below for ease of reference:

$$[K] = F_i [\Phi_i] \quad (A-53)$$

$$[K_G] = F_5 [\Phi_5] \quad (A-54)$$

where $i = 1, 2, 3, 4$ and repeated subscripts indicate summation in Equation A-53. In this expression, $[\Phi_i]$ are integral matrices as

defined by Equations A-47 to A-50, and F_i are material constants as defined by Equations A-42 to A-45. The values of F_i depend on whether the material is elastic, yielded, or strain-hardened. In Equation A-54, F_5 is a constant depending on the material thickness and is given by Equation A-46, and $[\Phi_5]$ is an integral matrix as defined by Equation A-51.

Partial yielding or strain-hardening of a cross-section results in non-uniform material properties and stresses defined piecewise over a section. Therefore, the integral expressions of Equations A-53 and A-54 are also defined piecewise over a section. The limits of integration correspond to the locations of material boundaries between elastic and yielded material and between yielded and strain-hardened material within a plate cross-section. Therefore, in order to carry out the integration required to determine $[K]$, it is necessary to locate boundaries corresponding to material discontinuities within a plate cross-section. The evaluation of $[K_G]$ can be made once the stress discontinuities and stress distributions are determined for a plate cross-section. In the following sections these quantities are evaluated and explicit values of $[K]$ and $[K_G]$ are determined for each plate component of a W shape.

4.3.3.1 Compression Flange

The distributions of strain and stress for a compression flange subjected to combined residual, axial, and flexural stresses are shown in Figure 4.3. In Figure 4.3(a), ϵ_a is an axial strain, ϵ_b is a bending strain, ϵ_4 is a residual tensile strain, ϵ_5 is a residual compressive strain, ϵ_y is a yield strain, and ϵ_{st} is a strain-hardening

strain. The corresponding stresses shown in Figure 4.3(b) are derived from the strain diagram according to the stress - strain relationship defined in Figure 3.2. In Figure 4.3(b), s_i ($i = 1, 2, 3, 4, 5, 6$) are stress components and α_t and α'_t , in natural coordinates, are the locations of the material boundaries between elastic and yielded and between yielded and strain-hardened material.

The values of α_t and α'_t are listed in Table 4.1(a) for various levels of strain. The second column of this table indicates the material condition for the corresponding range of strain indicated in the first column. For example, for the second strain range indicated the material is partially elastic (e) and partially yielded (y), and for the fifth strain range indicated the material is fully strain-hardened (s). The stresses defined piecewise for the various stress regions of Figure 4.3(b) are defined in Table 4.1(b). In this table, ζ is a natural coordinate as indicated in Figure 4.3, E is the elastic modulus, E_0 is the slope of the yield portion of a stress - strain curve, and E_{st} is the strain-hardening modulus.

Using the limits of integration, α_t and α'_t , as given in Table 4.1(a), and expanding the expression in Equation A-53 over the non-uniform material regions, the stiffness matrix for a flange in compression is given as:

$$\begin{aligned}
 [K] = & F_{ie} [\phi_i]_{-\alpha_t}^{\alpha_t} + F_{iy} \left[[\phi_i]_{-\alpha'_t}^{-\alpha_t} + [\dot{\phi}_i]_{\alpha_t}^{\alpha'_t} \right] \\
 & + F_{is} \left[[\dot{\phi}_i]_{-1}^{-\alpha'_t} + [\dot{\epsilon}_i]_{\alpha'_t}^1 \right]
 \end{aligned} \tag{4.4}$$

where subscripts, e, y, and s, indicate that material constants, F_i , have elastic, yielded, and strain-hardened values, respectively. The limits of integration are shown as subscripts and superscripts on each integral matrix, and double subscripts, i, indicate summation.

The geometric stiffness matrix for a compression flange is obtained by substituting the stresses, s_i , from Table 4.1(b) into Equation A-54 and integrating between the appropriate limits defined in column one of Table 4.1(b). The following expression is obtained:

$$\begin{aligned}
 [K_G] = & F_5 \left\{ s_1 \left[[\Phi_5]_{-1}^{-\alpha'_t} + [\Phi_5]_{\alpha'_t}^1 \right] - s_2 \left[[\zeta\Phi_5]_{-1}^{-\alpha'_t} - [\zeta\Phi_5]_{\alpha'_t}^1 \right] \right. \\
 & + s_3 \left[[\Phi_5]_{-\alpha'_t}^{-\alpha'_t} + [\Phi_5]_{\alpha'_t}^{\alpha'_t} \right] - s_4 \left[[\zeta\Phi_5]_{-\alpha'_t}^{-\alpha'_t} - [\zeta\Phi_5]_{\alpha'_t}^{\alpha'_t} \right] \\
 & \left. + s_5 [\Phi_5]_{-\alpha'_t}^{\alpha'_t} - s_6 \left[[\zeta\Phi_5]_{-\alpha'_t}^0 - [\zeta\Phi_5]_{0}^{\alpha'_t} \right] \right\} \quad (4.5)
 \end{aligned}$$

where $[\zeta\Phi_5]$ is used to indicate that matrix, $[\Phi_5]$, is multiplied by natural coordinate, ζ , before integration is performed. This accounts for linearly varying stresses on a portion of a plate cross-section.

4.3.3.2 Tension Flange

The strain and stress distributions for a flange in tension are shown in Figure 4.4. In addition to the previously explained symbols, ϵ_1 is the residual compressive stress at the flange tips and

ε_2 is the residual tensile stress at the flange-to-web junction. The strain ranges and limits of integration corresponding to Figure 4.4(a) are listed in Table 4.2(a) and the corresponding stresses and stress regions illustrated in Figure 4.4(b) are listed in Table 4.2(b).

The stiffness matrix for a tension flange may now be obtained by performing the integration in Equation A-53 over the limits indicated by Figure 4.4 and Table 4.2(a) and using the appropriate material constants, F_i . The resulting expression is as follows:

$$[K] = F_{ie} \left[\left[\Phi_i \right]_{-1}^{-\alpha_b} + \left[\Phi_i \right]_{\alpha_b}^1 \right] + F_{iy} \left[\left[\Phi_i \right]_{-\alpha_b}^{-\alpha'_b} + \left[\Phi_i \right]_{\alpha'_b}^{\alpha_b} \right] \\ + F_{is} \left[\Phi_i \right]_{-\alpha'_b}^{\alpha'_b} \quad (4.6)$$

The geometric stiffness matrix is obtained from Equation A-54 by substituting the stresses given in Table 4.2(b) and integrating over the appropriate limits as indicated in Figure 4.4 and Table 4.2(b). The resulting expression is as follows:

$$[K_G] = F_5 \left\{ s_1 \left[\left[\Phi_5 \right]_{-1}^{-\alpha_b} + \left[\Phi_5 \right]_{\alpha_b}^1 \right] - s_2 \left[\left[\zeta \Phi_5 \right]_{-1}^{-\alpha_b} - \left[\zeta \Phi_5 \right]_{\alpha_b}^1 \right] \right. \\ \left. + s_3 \left[\left[\Phi_5 \right]_{-\alpha_b}^{-\alpha'_b} + \left[\Phi_5 \right]_{\alpha'_b}^{\alpha_b} \right] - s_4 \left[\left[\zeta \Phi_5 \right]_{-\alpha_b}^{-\alpha'_b} - \left[\zeta \Phi_5 \right]_{\alpha'_b}^{\alpha_b} \right] \right. \\ \left. + s_5 \left[\Phi_5 \right]_{-\alpha'_b}^{\alpha'_b} - s_6 \left[\left[\zeta \Phi_5 \right]_{-\alpha'_b}^0 - \left[\zeta \Phi_5 \right]_0^{\alpha'_b} \right] \right\} \quad (4.7)$$

4.3.3.3 Web - Tension Zone

The general strain and stress distributions for the lower half of a web (loaded in the orientation described previously) are shown in Figure 4.5. In this Figure, β_1 , β'_1 , β_3 , and β'_3 , in natural coordinates, locate the boundaries between elastic and yielded material and between yielded and strain-hardened material. These values are defined in Tables 4.3(a) and 4.3(b) for the various ranges of strain indicated. The stresses corresponding to the stress regions indicated, are listed in Table 4.3(c).

Referring to Figure 4.5 and Table 4.3 and proceeding in the manner described previously for the flanges, the bending stiffness and geometric stiffness matrices for the tension zone of a web are obtained as follows:

$$\begin{aligned}
 [K] = & F_{ie} [\Phi_i]_{-\beta_1}^{-\beta_3} + F_{iy} \left[[\Phi_i]_{-\beta'_1}^{-\beta_1} + [\Phi_i]_{-\beta'_3}^{\beta'_3} \right] \\
 & + F_{is} \left[[\Phi_i]_{-1}^{-\beta'_1} + [\Phi_i]_{-\beta'_3}^0 \right]
 \end{aligned} \tag{4.8}$$

and,

$$\begin{aligned}
 [K_G] = & F_5 \left\{ s_1 [\Phi_5]_{-1}^{\beta'_1} + s_2 \left[[\eta\Phi_5]_{-1}^{-\beta'_1} + [\eta\Phi_5]_{-\beta'_3}^0 \right] \right. \\
 & \left. + s_3 [\Phi_5]_{-\beta'_1}^{-\beta_1} + s_4 \left[[\eta\Phi_5]_{-\beta'_1}^{-\beta_1} + [\eta\Phi_5]_{-\beta'_3}^{\beta'_3} \right] \right\}
 \end{aligned}$$

... continued

$$\begin{aligned}
 & + s_5 [\phi_5]_{-\beta_1}^{-\beta_3} + s_6 [\eta\phi_5]_{-\beta_1}^{-\beta_3} + s_7 [\phi_5]_{-\beta_3}^{-\beta_3} \\
 & + s_8 [\phi_5]_{-\beta_3}^0 \Big\} \quad (4.9)
 \end{aligned}$$

4.3.3.4 Web - Compression Zone

Because of the complex yield pattern possible under the actions of residual, axial, and flexural stresses combined, three cases must be considered for the compression zone of a web. These three cases correspond to the material condition at the center of the web which may be elastic, yielded, or strain-hardened at the time the incremental bending strains are applied. Each of the three cases is considered separately.

The strain and stress distributions for the compression zone of a web when the center of the web is elastic are shown in Figure 4.6. In this case the total strain at a web center must not be greater than the yield strain, and therefore,

$$\epsilon_a + \epsilon_c + \epsilon_3 \leq \epsilon_y \quad (4.10)$$

The material boundaries corresponding to the various ranges of strain possible are given in Table 4.4(a) and the stresses corresponding to the material zones indicated in Figure 4.6(b) are listed in Table 4.4(b). Referring to Figure 4.6 and Table 4.4, and proceeding as described for the previous cases, the bending and

geometric stiffness matrices may be written as follows:

$$[K] = F_{ie} [\Phi_i]_0^{\beta_2} + F_{iy} [\Phi_i]_0^{\beta'_2} + F_{is} [\Phi_i]_{\beta_2}^1, \quad (4.11)$$

and,

$$\begin{aligned} [K_G] = & F_5 \left\{ s_1 [\Phi_5]_0^{\beta_2} + s_2 [\eta \Phi_5]_0^{\beta_2} + s_3 [\Phi_5]_{\beta_2}^{\beta'_2} \right. \\ & \left. + s_4 [\Phi_5]_{\beta_2}^{\beta'_2} + s_5 [\Phi_5]_{\beta'_2}^1 + s_6 [\Phi_5]_{\beta_2}^1 \right\} \end{aligned} \quad (4.12)$$

The center of a web is yielded when,

$$\varepsilon_y < \varepsilon_a + \varepsilon_c + \varepsilon_3 \leq \varepsilon_{st} \quad (4.13)$$

and the corresponding strain and stress distributions as well as the limits of integration and various material zones are described in Figure 4.7 and Table 4.5. Using the appropriate values obtained therefrom, the bending and geometric stiffness matrices for this case may be written as follows:

$$[K] = F_{ie} [\Phi_i]_{\beta_2}^{\beta'_2} + F_{iy} [\Phi_i]_0^{\beta_2} + F_{is} [\Phi_i]_{\beta_2}^1, \quad (4.14)$$

and,

$$\begin{aligned}
 [K_G] = & F_5 \left\{ s_1 [\Phi_5]_0^{\beta_2} + s_2 [n\Phi_5]_0^{\beta_2} + s_3 [\Phi_5]_{\beta_2}^{\beta'_2} \right. \\
 & \left. + s_4 [n\Phi_5]_{\beta_2}^{\beta'_2} + s_5 [\Phi_5]_{\beta_2}^1 + s_6 [n\Phi_5]_{\beta_2}^1 \right\}
 \end{aligned} \tag{4.15}$$

The third and final case which must be considered for the compression zone of a web is that corresponding to the center of the web being in the strain-hardened condition. In this case,

$$\varepsilon_{st} < \varepsilon_a + \varepsilon_c + \varepsilon_3 \tag{4.16}$$

The corresponding distributions of strain and stress are shown in Figure 4.8 and the material boundaries and stress components for each region are given in Table 4.6. The resulting expressions for the bending and geometric stiffness matrices are as follows:

$$[K] = F_{ie} [\Phi_i]_{\beta_2}^1 + F_{iy} [\Phi_i]_{\beta_2}^{\beta_2} + F_{is} [\Phi_i]_0^{\beta'_2} \tag{4.17}$$

and,

$$\begin{aligned}
 [K_G] = F_5 & \left\{ s_1 [\Phi_5]_0^{\beta'_2} + s_2 [\eta\Phi_5]_0^{\beta'_2} + s_3 [\Phi_5]_{\beta'_2}^{\beta_2} \right. \\
 & \left. + s_4 [\eta\Phi_5]_{\beta'_2}^{\beta_2} + s_5 [\Phi_5]_{\beta_2}^1 + s_6 [\eta\Phi_5]_{\beta_2}^1 \right\}
 \end{aligned} \tag{4.18}$$

4.4 Iterative Technique

In the solution of a particular problem, bending stiffness and geometric stiffness submatrices for each flange and a web are formulated as described in the previous sections. The global stiffness matrices are then assembled as explained in Chapter 3. In any problem of axial, bending, or combined loading, the required eigenvalue will be either ϵ_b , the bending strain, or ϵ_a the axial strain. However, because of material and stress non-linearities over a cross-section, the bending stiffness matrix, $[K]$, and the geometric stiffness matrix, $[K_G]$, are implicit functions of the eigenvalue strain. Therefore at each successive value of an eigenvalue strain, it is necessary to reformulate $[K]$ and $[K_G]$ for that particular value of strain. Thus an iterative technique is required.

As described in Chapter 3, an eigenvalue problem reduces to the form:

$$[K] - [K_G]\{\theta\} = \{0\} \tag{4.19}$$

As stated previously, $[K]$ and $[K_G]$ are implicit functions of $(\epsilon_b + \epsilon_a)$ when a material is non-linear. Equation 4.19 may be re-written as

follows:

$$\left[[K] - \lambda_o [K_{G_o}] \right] \{ \theta \} = \{ 0 \} \quad (4.20)$$

where,

$$[K_{G_o}] = \frac{1}{\varepsilon_b + \varepsilon_a} [K_G] \quad (4.21)$$

In the solution of Equation 4.20, a value of $(\varepsilon_b + \varepsilon_a)$ is assumed. Knowing this value, the elastic, yield, and strain-hardening material zones in a cross-section as well as the discontinuous stress distributions are fully defined. Therefore, $[K]$ and $[K_{G_o}]$ are completely determinable and matrix iteration may be performed to determine λ_o . The solution to Equation 4.19 will be obtained when,

$$\frac{\lambda_o}{\varepsilon_b + \varepsilon_a} = 1.0 \quad (4.22)$$

In general, this will require the determination of several values of λ_o by matrix iteration. An exact solution is obtained when the eigenvalue, λ_o , is equal to the assumed value of $\varepsilon_b + \varepsilon_a$. In general, however, this will not be true, and,

$$\lambda_o = \lambda' + \lambda'' \quad (4.23)$$

where,

$$\lambda' = \varepsilon_b + \varepsilon_a \quad (4.24)$$

and λ'' is a residue which represents the amount by which λ_o deviates

from the exact value of $(\varepsilon_b + \varepsilon_a)$. Thus, the problem reduces to that of finding a value of λ_o such that,

$$|\lambda''| = |\lambda_o - \lambda'| \leq e \quad (4.25)$$

where e , is a small positive value which reflects the required precision of a solution.

For the purpose of illustration, Figure 4.9 shows a graph of $(\lambda_o - \lambda')$ vs. $(\varepsilon_b + \varepsilon_a)$. In the iteration technique, an initial value of $(\varepsilon_b + \varepsilon_a)$ is chosen so that $(\lambda_o - \lambda')$ is positive. Another value of $(\varepsilon_b + \varepsilon_a)$ is found so that the corresponding value of $(\lambda_o - \lambda')$ is negative. Once these two starting values have been found (by trial and error, if necessary) the method of bisection³¹ is used to determine a value of $(\varepsilon_b + \varepsilon_a)$ for which $|\lambda_o - \lambda'| \leq e$. Once the convergence criterion is satisfied, the critical bending strain is given by:

$$\varepsilon_{b_{cr}} = \lambda_o - \varepsilon_a \quad (4.26)$$

This general technique may be used for pure bending when $\varepsilon_a = 0$, or for pure axial load when $\varepsilon_b = 0$. In the case of axial compression and bending combined, ε_a is a constant value of axial strain depending on the magnitude of applied axial load.

Strain Range	Material Condition	Location of Material Boundaries	
		α_t	α'_t
$\varepsilon_b + \varepsilon_a \leq \varepsilon_y - \varepsilon_5$	(e)	1.0	1.0
$\varepsilon_y - \varepsilon_5 < \varepsilon_b + \varepsilon_a \leq \varepsilon_y + \varepsilon_4$	(e,y)	$\frac{\varepsilon_y + \varepsilon_4 - \varepsilon_b - \varepsilon_a}{\varepsilon_4 + \varepsilon_5}$	1.0
$\varepsilon_y + \varepsilon_4 < \varepsilon_b + \varepsilon_a \leq \varepsilon_{st} - \varepsilon_5$	(y)	0.0	1.0
$\varepsilon_{st} - \varepsilon_5 < \varepsilon_b + \varepsilon_a \leq \varepsilon_{st} + \varepsilon_4$	(y,s)	0.0	$\frac{\varepsilon_{st} + \varepsilon_4 - \varepsilon_b - \varepsilon_a}{\varepsilon_4 + \varepsilon_5}$
$\varepsilon_{st} + \varepsilon_4 < \varepsilon_b + \varepsilon_a$	(s)	0.0	0.0

(a) Strains

Stress Region	Stress	Stress Components
$-1.0 \leq \zeta \leq -\alpha'_t$ (s)	$s_1 - s_2 \zeta$	$s_1 = \sigma_y + (\varepsilon_{st} - \varepsilon_y)E_0 + (\varepsilon_b + \varepsilon_a - \varepsilon_{st} - \varepsilon_4)E_{st}$
$-\alpha'_t \leq \zeta \leq -\alpha_t$ (y)	$s_3 - s_4 \zeta$	$s_2 = (\varepsilon_4 + \varepsilon_5)E_{st}$
$-\alpha_t \leq \zeta \leq 0.0$ (e)	$s_5 - s_6 \zeta$	$s_3 = \sigma_y + (\varepsilon_b + \varepsilon_a - \varepsilon_y - \varepsilon_4)E_0$
$0.0 \leq \zeta \leq \alpha_t$ (e)	$s_5 + s_6 \zeta$	$s_4 = (\varepsilon_4 + \varepsilon_5)E_0$
$\alpha_t \leq \zeta \leq \alpha'_t$ (y)	$s_3 + s_4 \zeta$	$s_5 = (\varepsilon_b + \varepsilon_a - \varepsilon_4)E$
$\alpha'_t \leq \zeta \leq 1.0$ (s)	$s_1 + s_2 \zeta$	$s_6 = (\varepsilon_4 + \varepsilon_5)E$

(b) Stresses

Table 4.1 Stresses and Strains for a Compression Flange

Strain Range	Material Condition	Location of Material Boundaries	
		α_b	α'_b
$\varepsilon'_b - \varepsilon_a \leq \varepsilon_y - \varepsilon_2$	(e)	0.0	0.0
$\varepsilon_y - \varepsilon_2 < \varepsilon'_b - \varepsilon_a \leq \varepsilon_y + \varepsilon_1$	(e,y)	$\frac{\varepsilon'_b - \varepsilon_a - \varepsilon_y + \varepsilon_2}{\varepsilon_1 + \varepsilon_2}$	0.0
$\varepsilon_y + \varepsilon_1 < \varepsilon'_b - \varepsilon_a \leq \varepsilon_{st} - \varepsilon_2$	(y)	1.0	0.0
$\varepsilon_{st} - \varepsilon_2 < \varepsilon'_b - \varepsilon_a \leq \varepsilon_{st} + \varepsilon_1$	(y,s)	1.0	$\frac{\varepsilon'_b - \varepsilon_a - \varepsilon_{st} + \varepsilon_2}{\varepsilon_1 + \varepsilon_2}$
$\varepsilon_{st} + \varepsilon_1 < \varepsilon'_b - \varepsilon_a$	(s)	1.0	1.0

(a) Strains

Stress Region	Stresses	Stress Components
$-1.0 \leq \zeta \leq -\alpha_b$	$s_1 - s_2 \zeta$	$s_1 = (\varepsilon_a - \varepsilon'_b - \varepsilon_2) E$
$-\alpha_b \leq \zeta \leq -\alpha'_b$	$s_3 - s_4 \zeta$	$s_2 = (\varepsilon_1 + \varepsilon_2) E$
$-\alpha'_b \leq \zeta \leq 0.0$	$s_5 - s_6 \zeta$	$s_3 = -\sigma_y + (\varepsilon_y - \varepsilon_2 + \varepsilon_a - \varepsilon'_b) E_o$
$0.0 \leq \zeta \leq \alpha'_b$	$s_5 + s_6 \zeta$	$s_4 = (\varepsilon_1 + \varepsilon_2) E_o$
$\alpha'_b \leq \zeta \leq \alpha_b$	$s_3 + s_4 \zeta$	$s_5 = -\sigma_y - (\varepsilon_{st} - \varepsilon_y) E_o + (\varepsilon_{st} + \varepsilon_a - \varepsilon'_b - \varepsilon_2) E_{st}$
$\alpha_b \leq \zeta \leq 1.0$	$s_1 + s_2 \zeta$	$s_6 = (\varepsilon_1 + \varepsilon_2) E_{st}$

(b) Stresses

Table 4.2 Stresses and Strains for a Tension Flange.

Strain Range	Material Condition	Location of Material Boundaries	
		β_1	β'_1
$\varepsilon_b' - \varepsilon_a \leq \varepsilon_y - \varepsilon_2$	(e)	1.0	1.0
$\varepsilon_y - \varepsilon_2 < \varepsilon_b' - \varepsilon_a \leq \varepsilon_{st} - \varepsilon_2$	(e,y)	$\frac{\varepsilon_a + \varepsilon_c + \varepsilon_y + \varepsilon_3}{\varepsilon_b' + \varepsilon_c + \varepsilon_2 + \varepsilon_3}$	1.0
$\varepsilon_{st} - \varepsilon_2 < \varepsilon_b' - \varepsilon_a$	(e,y,s)	$\frac{\varepsilon_a + \varepsilon_c + \varepsilon_y + \varepsilon_3}{\varepsilon_b' + \varepsilon_c + \varepsilon_2 + \varepsilon_3}$	$\frac{\varepsilon_a + \varepsilon_c + \varepsilon_{st} + \varepsilon_3}{\varepsilon_b' + \varepsilon_c + \varepsilon_2 + \varepsilon_3}$

(a) Strains Adjacent to Lower Edge of Web

Strain Range	Material Condition	Location of Material Boundaries	
		β_3	β'_3
$\varepsilon_a + \varepsilon_c + \varepsilon_3 \leq \varepsilon_y$	(e)	0.0	0.0
$\varepsilon_y < \varepsilon_a + \varepsilon_c + \varepsilon_3 \leq \varepsilon_{st}$	(e,y)	$\frac{\varepsilon_a + \varepsilon_c + \varepsilon_3 - \varepsilon_y}{\varepsilon_b' + \varepsilon_c + \varepsilon_2 + \varepsilon_3}$	0.0
$\varepsilon_{st} < \varepsilon_a + \varepsilon_c + \varepsilon_3$	(e,y,s)	$\frac{\varepsilon_a + \varepsilon_c + \varepsilon_3 - \varepsilon_y}{\varepsilon_b' + \varepsilon_c + \varepsilon_2 + \varepsilon_3}$	$\frac{\varepsilon_a + \varepsilon_c + \varepsilon_3 - \varepsilon_{st}}{\varepsilon_b' + \varepsilon_c + \varepsilon_2 + \varepsilon_3}$

(b) Strains Adjacent to Middle of Web

Table 4.3 Stresses and Strains for the Tension Zone of a Web -

... cont'd.

Table 4.3 - continued

Stress Region		Stress	Stress Components
$-1 \leq \eta \leq -\beta'_1$	(s)	$s_1 + s_2 \eta$	$s_1 = -\sigma_y - (\varepsilon_{st} - \varepsilon_y) E_o + (\varepsilon_a + \varepsilon_c + \varepsilon_3) E_{st}$
$-\beta'_1 \leq \eta \leq -\beta_1$	(y)	$s_3 + s_4 \eta$	$s_2 = (\varepsilon'_b + \varepsilon_c + \varepsilon_2 + \varepsilon_3) E_{st}$
$-\beta_1 \leq \eta \leq -\beta_3$	(e)	$s_5 + s_6 \eta$	$s_3 = -\sigma_y + (\varepsilon_a + \varepsilon_c + \varepsilon_y + \varepsilon_3) E_o$
$-\beta_3 \leq \eta \leq -\beta'_3$	(y)	$s_7 + s_4 \eta$	$s_4 = (\varepsilon'_b + \varepsilon_c + \varepsilon_2 + \varepsilon_3) E_o$
$-\beta'_3 \leq \eta \leq 0$	(s)	$s_8 + s_2 \eta$	$s_5 = (\varepsilon_a + \varepsilon_c + \varepsilon_3) E$
			$s_6 = (\varepsilon'_b + \varepsilon_c + \varepsilon_2 + \varepsilon_3) E$
			$s_7 = \sigma_y + (\varepsilon_a + \varepsilon_c + \varepsilon_3 - \varepsilon_y) E_o$
			$s_8 = \sigma_y + (\varepsilon_{st} - \varepsilon_y) E_o + (\varepsilon_a + \varepsilon_c + \varepsilon_{st} + \varepsilon_3) E_{st}$

(c) Stresses

Table 4.3 Stresses and Strains for the Tension Zone of a Web

Strain Range	Material Condition	Location of Material Boundaries	
		β_2	β'_2
$\varepsilon_b + \varepsilon_a \leq \varepsilon_y + \varepsilon_4$	(e)	1.0	1.0
$\varepsilon_y + \varepsilon_4 < \varepsilon_b + \varepsilon_a \leq \varepsilon_{st} + \varepsilon_4$	(e,y)	$\frac{\varepsilon_y - \varepsilon_3 - \varepsilon_c - \varepsilon_a}{\varepsilon_b - \varepsilon_c - \varepsilon_3 - \varepsilon_4}$	1.0
$\varepsilon_{st} + \varepsilon_4 < \varepsilon_b + \varepsilon_a$	(e,y,s)	$\frac{\varepsilon_y - \varepsilon_3 - \varepsilon_c - \varepsilon_a}{\varepsilon_b - \varepsilon_c - \varepsilon_3 - \varepsilon_4}$	$\frac{\varepsilon_{st} - \varepsilon_3 - \varepsilon_c - \varepsilon_a}{\varepsilon_b - \varepsilon_c - \varepsilon_3 - \varepsilon_4}$

(a) Strains

Stress Region	Stresses	Stress Components
$0.0 \leq \eta \leq \beta_2$	(e) $s_1 + s_2 \eta$	$s_1 = (\varepsilon_a + \varepsilon_c + \varepsilon_3) E$
		$s_2 = \varepsilon_b - \varepsilon_c - \varepsilon_3 - \varepsilon_4$
$\beta_2 \leq \eta \leq \beta'_2$	(y) $s_3 + s_4 \eta$	$s_3 = \sigma_y + (\varepsilon_a + \varepsilon_c - \varepsilon_y + \varepsilon_3) E_o$
		$s_4 = (\varepsilon_b - \varepsilon_c - \varepsilon_3 - \varepsilon_4) E_o$
$\beta'_2 \leq \eta \leq 1.0$	(s) $s_5 + s_6 \eta$	$s_5 = \sigma_y + (\varepsilon_{st} - \varepsilon_y) E_o + (\varepsilon_a + \varepsilon_c - \varepsilon_{st} + \varepsilon_3) E_{st}$
		$s_6 = (\varepsilon_b - \varepsilon_c - \varepsilon_3 - \varepsilon_4) E_{st}$

(b) Stresses

Table 4.4 Stresses and Strains in the Compression Zone of a Web (Case I - Center of Web Elastic)

Strain Range	Material Condition	Location of Material Boundaries	
		β_2	β'_2
$\varepsilon_b + \varepsilon_a \leq \varepsilon_y + \varepsilon_4$	(e)	$\frac{\varepsilon_y - \varepsilon_3 - \varepsilon_a - \varepsilon_c}{\varepsilon_b - \varepsilon_c - \varepsilon_3 - \varepsilon_4}$	1.0
$\varepsilon_y + \varepsilon_4 < \varepsilon_b + \varepsilon_a \leq \varepsilon_{st} + \varepsilon_4$	(e,y)	1.0	1.0
$\varepsilon_{st} + \varepsilon_4 < \varepsilon_b + \varepsilon_a$	(y,s)	$\frac{\varepsilon_{st} - \varepsilon_3 - \varepsilon_a - \varepsilon_c}{\varepsilon_b - \varepsilon_c - \varepsilon_3 - \varepsilon_4}$	$\frac{\varepsilon_{st} - \varepsilon_3 - \varepsilon_a - \varepsilon_c}{\varepsilon_b - \varepsilon_c - \varepsilon_3 - \varepsilon_4}$

(a) Strains

Stress Region	Stress	Stress Components
$0.0 \leq \eta \leq \beta_2$	(y) $s_1 + s_2 \eta$	$s_1 = \sigma_y + (\varepsilon_a + \varepsilon_c - \varepsilon_y + \varepsilon_3) E_o$
		$s_2 = (\varepsilon_b - \varepsilon_c - \varepsilon_3 - \varepsilon_4) E_o$
		$s_3 = (\varepsilon_a + \varepsilon_c + \varepsilon_3) E$
$\beta_2 \leq \eta \leq \beta'_2$	(e) $s_3 + s_4 \eta$	$s_4 = (\varepsilon_b + \varepsilon_c - \varepsilon_3 - \varepsilon_4) E$
		$s_5 = \sigma_y + (\varepsilon_s - \varepsilon_y) E_o + (\varepsilon_a + \varepsilon_c - \varepsilon_{st} + \varepsilon_3) E_{st}$
$\beta'_2 \leq \eta \leq 1.0$	(s) $s_5 + s_6 \eta$	$s_6 = (\varepsilon_b - \varepsilon_c - \varepsilon_3 - \varepsilon_4) E_{st}$

(b) Stresses

Table 4.5 Stresses and Strains for the Compression Zone of a Web
(Case II - Center of Web Yielded)

Strain Range	Material Condition	Location of Material Boundaries	
		β_2	β'_2
$\varepsilon_b + \varepsilon_a \leq \varepsilon_y + \varepsilon_4$	(e, y, s)	$\frac{\varepsilon_y - \varepsilon_3 - \varepsilon_a - \varepsilon_c}{\varepsilon_b - \varepsilon_c - \varepsilon_3 - \varepsilon_4}$	$\frac{\varepsilon_{st} - \varepsilon_3 - \varepsilon_a - \varepsilon_c}{\varepsilon_b - \varepsilon_c - \varepsilon_3 - \varepsilon_4}$
$\varepsilon_y + \varepsilon_4 < \varepsilon_b + \varepsilon_a \leq \varepsilon_{st} + \varepsilon_4$	(y, s)	1.0	$\frac{\varepsilon_{st} - \varepsilon_3 - \varepsilon_a - \varepsilon_c}{\varepsilon_b - \varepsilon_c - \varepsilon_3 - \varepsilon_4}$
$\varepsilon_{st} - \varepsilon_4 < \varepsilon_b + \varepsilon_a$	(s)	1.0	1.0

(a) Strains

Stress Region	Stress	Stress Components
$0.0 \leq \eta < \beta$	(s) $s_1 + s_2 \eta$	$s_1 = \sigma_y + (\varepsilon_{st} - \varepsilon_y) E_o + (\varepsilon_a + \varepsilon_c - \varepsilon_{st} + \varepsilon_3) E_{st}$
		$s_2 = (\varepsilon_b - \varepsilon_c - \varepsilon_3 - \varepsilon_4) E_{st}$
$\beta'_2 \leq \eta \leq \beta_2$	(y) $s_3 + s_4 \eta$	$s_3 = \sigma_y + (\varepsilon_a + \varepsilon_c - \varepsilon_y + \varepsilon_3) E_o$
		$s_4 = (\varepsilon_b - \varepsilon_c - \varepsilon_3 - \varepsilon_4) E_o$
$\beta_2 \leq \eta \leq 1.0$	(e) $s_5 + s_6 \eta$	$s_5 = (\varepsilon_a + \varepsilon_c + \varepsilon_3) E$
		$s_6 = (\varepsilon_b - \varepsilon_c - \varepsilon_3 - \varepsilon_4) E$

(b) Stresses

Table 4.6 Stresses and Strains for the Compression Zone of a Web
(Case III - Center of Web Strain-hardened)

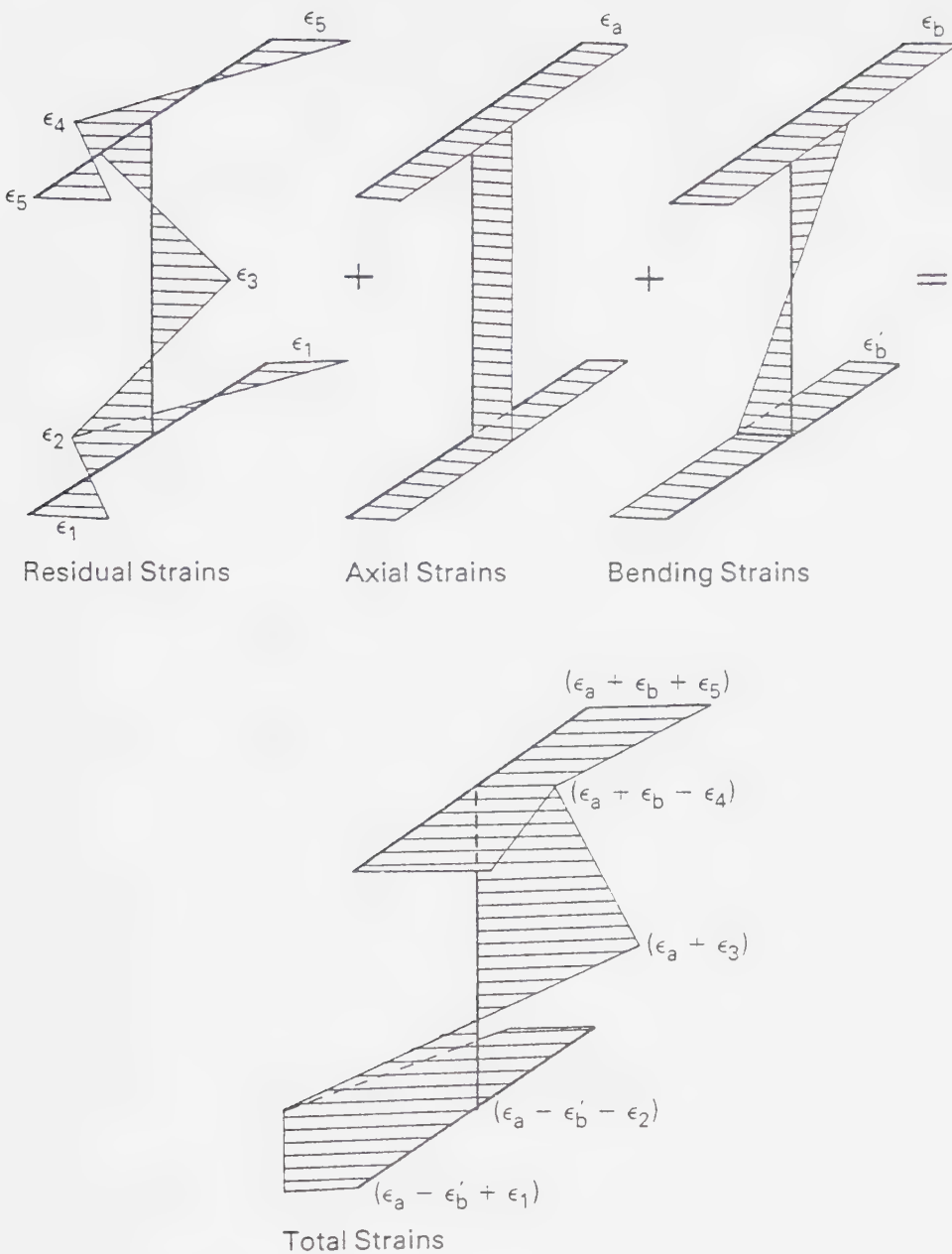


Figure 4.1 Superposition of Beam-Column Strains

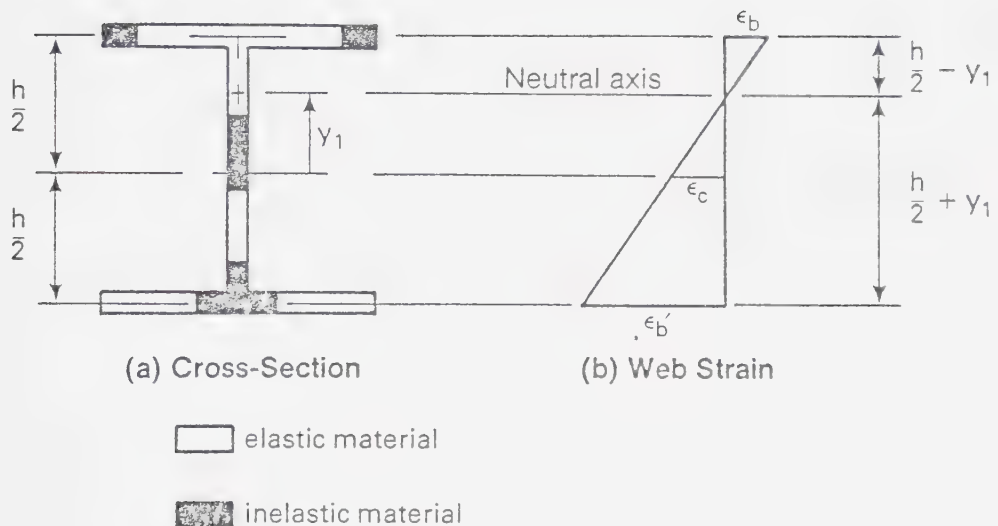
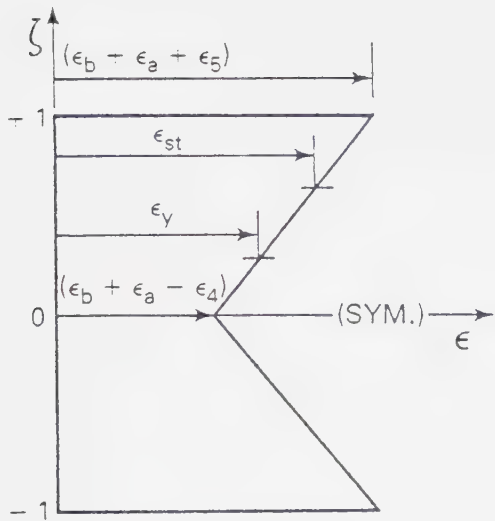
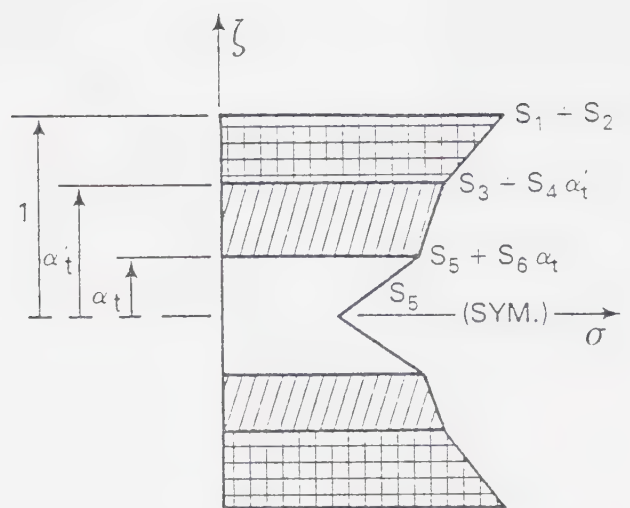


Figure 4.2 Flexural Strain on an Inelastic Section



(a) Strain Distribution



(b) Stress Distribution

$$0 \leq \zeta \leq +1$$

$$\epsilon = \epsilon_b + \epsilon_a - \epsilon_4 + (\epsilon_4 + \epsilon_5) \zeta$$

$$-1 \leq \zeta \leq 0$$

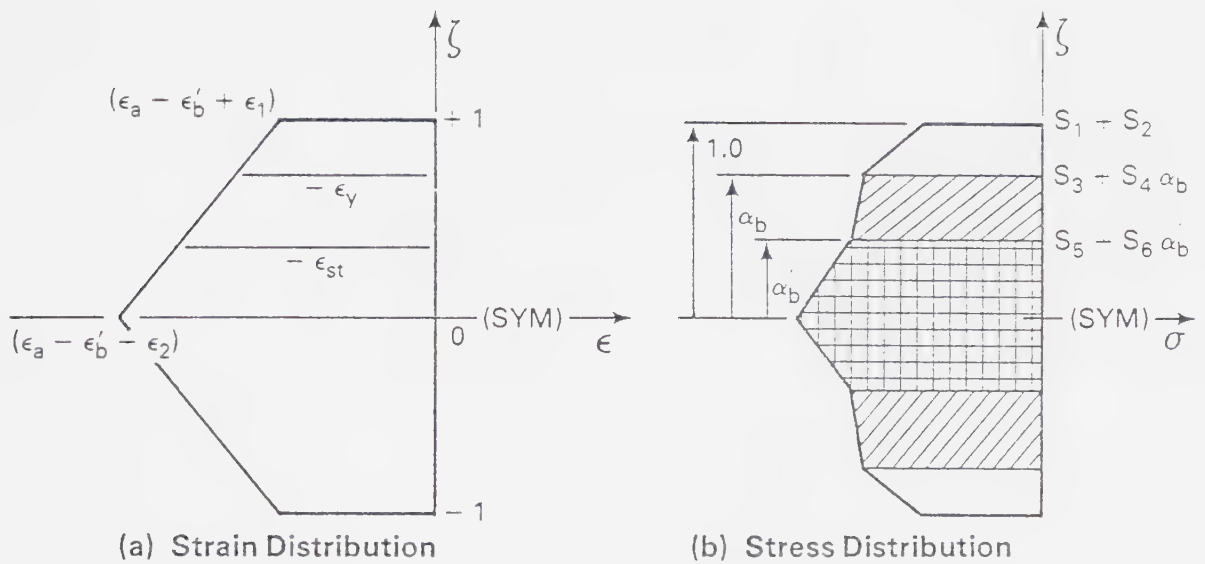
$$\epsilon = \epsilon_b + \epsilon_a - \epsilon_4 - (\epsilon_4 + \epsilon_5) \zeta$$

Elastic (e)

Yielding (y)

Strain Hardened (s)

Figure 4.3 Strain and Stress Distributions for a Flange in Compression.



$$-1 \leq \zeta \leq 0$$

$$\epsilon = -\epsilon'_b + \epsilon_a - \epsilon_2 - (\epsilon_1 + \epsilon_2) \zeta$$

$$0 \leq \zeta \leq 1$$

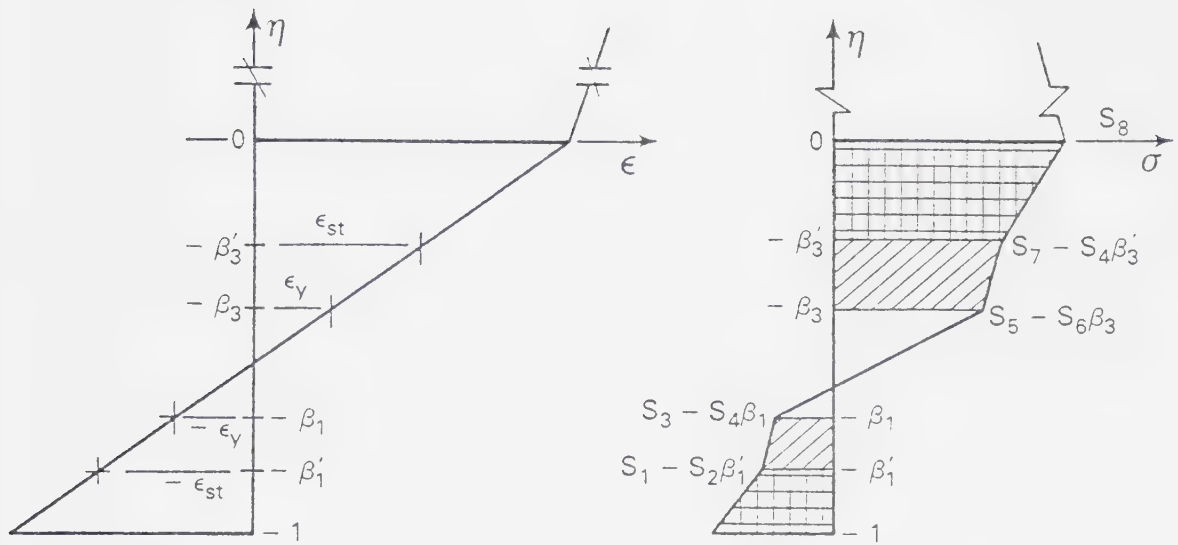
$$\epsilon = -\epsilon_b + \epsilon_a - \epsilon_2 + (\epsilon_1 + \epsilon_2) \zeta$$

Elastic (e)

Yielding (y)

Strain Hardened (s)

Figure 4.4 Strain and Stress Distributions for a Flange in Tension.



(a) Strain Distribution

(b) Stress Distribution

$$-1 \leq \eta \leq 0$$

$$\epsilon = \epsilon_a + \epsilon_c + \epsilon_3 + (\epsilon'_b + \epsilon'_c + \epsilon_2 + \epsilon_3) \eta$$

$$\eta = -1$$

$$\epsilon = \epsilon_a - \epsilon'_b - \epsilon_2$$

$$\eta = 0$$

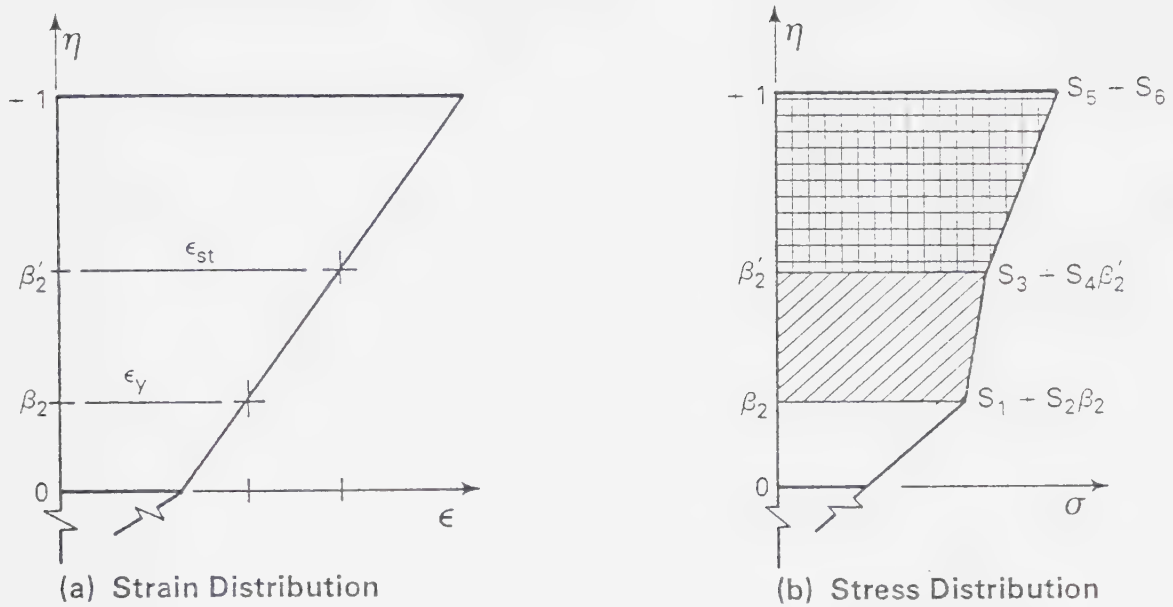
$$\epsilon = \epsilon_a + \epsilon_c + \epsilon_3$$

Elastic (e)

Yielding (y)

Strain Hardened (s)

Figure 4.5 Strain and Stress Distributions for Tension Zone of a Web.



$$0 \leq \eta \leq +1$$

$$\epsilon = \epsilon_a + \epsilon_c + \epsilon_3 + (\epsilon_b - \epsilon_c - \epsilon_3 - \epsilon_4)\eta$$

$$\eta = 0$$

$$\epsilon = \epsilon_a + \epsilon_c + \epsilon_3$$

$$\eta = +1$$

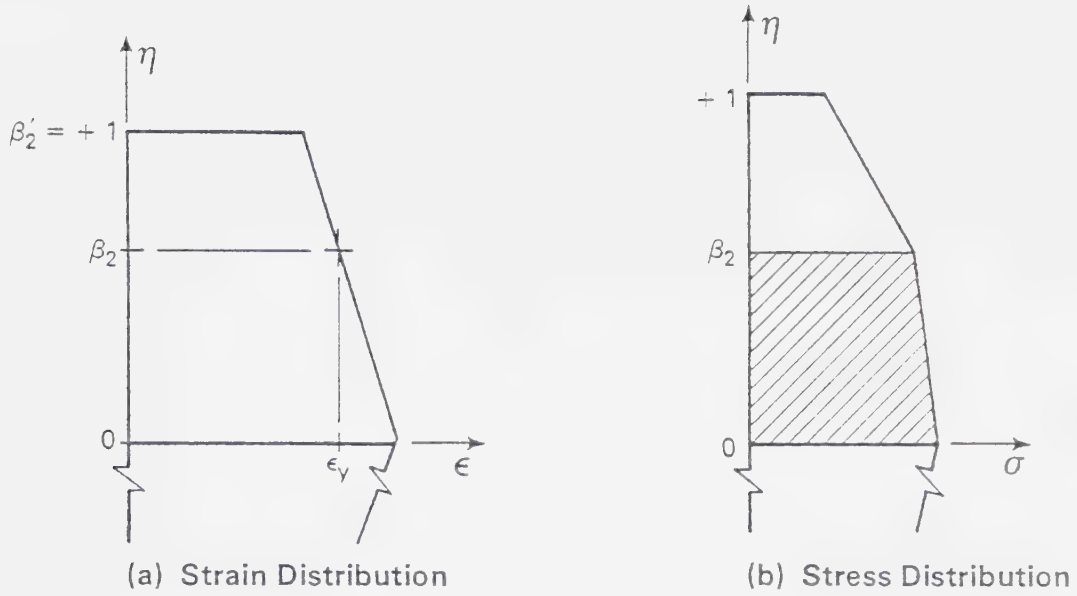
$$\epsilon = \epsilon_b + \epsilon_a - \epsilon_4$$

 Elastic (e)

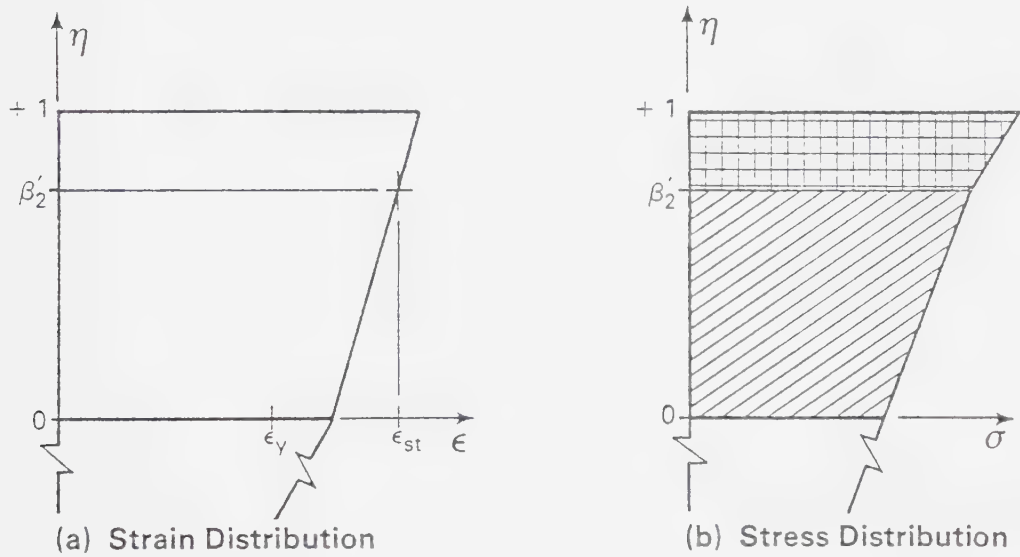
 Yielding (y)

 Strain Hardened (s)

Figure 4.6 Strain and Stress Distributions for Compression Zone of Web —
(Case I - Center of Web Elastic)



Case (i) Strain at $\eta = +1 \leq$ Strain at $\eta = 0$



Case (ii) Strain at $\eta = 1 >$ Strain at $\eta = 0$

$$0 \leq \eta \leq 1$$

$$\epsilon = \epsilon_a + \epsilon_c + \epsilon_3 + (\epsilon_b - \epsilon_c - \epsilon_4 - \epsilon_3)\eta$$

$$\eta = 0$$

$$\epsilon = \epsilon_a + \epsilon_c + \epsilon_3$$

$$\eta = 1$$

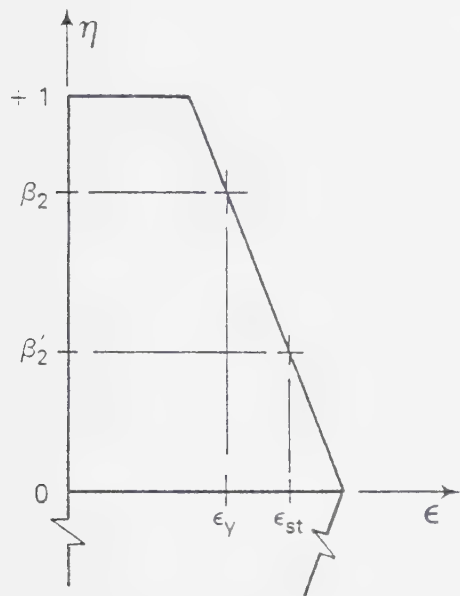
$$\epsilon = \epsilon_b + \epsilon_a - \epsilon_4$$

Elastic (e)

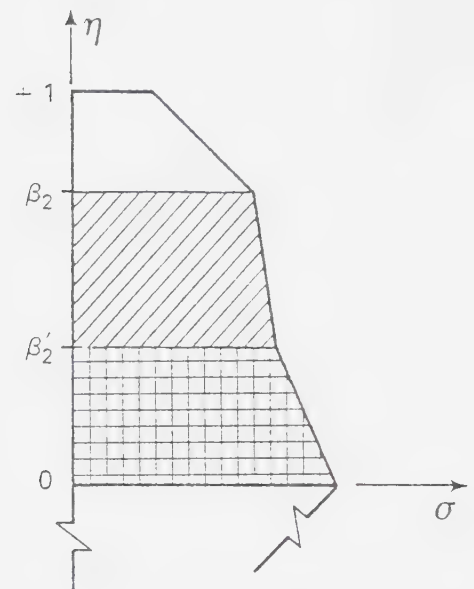
Yielding (y)

Strain Hardened (s)

Figure 4.7 . Strain and Stress Distributions for Compression Zone of Web — (Case II - Center of Web Yielded)



(a) Strain Distribution



(b) Stress Distribution

$$0 \leq \eta \leq 1$$

$$\epsilon = \epsilon_a + \epsilon_c + \epsilon_3 + (\epsilon_b - \epsilon_c - \epsilon_4 - \epsilon_3)\eta$$

$$\eta = 0$$

$$\epsilon = \epsilon_a + \epsilon_c + \epsilon_3$$

$$\eta = 1$$

$$\epsilon = \epsilon_b + \epsilon_a - \epsilon_4$$

Elastic (e)

Yielding (y)

Strain Hardened (s)

Figure 4.8 Strain and Stress Distributions for Compression Zone of Web — (Case III - Center of Web Strain-hardened)

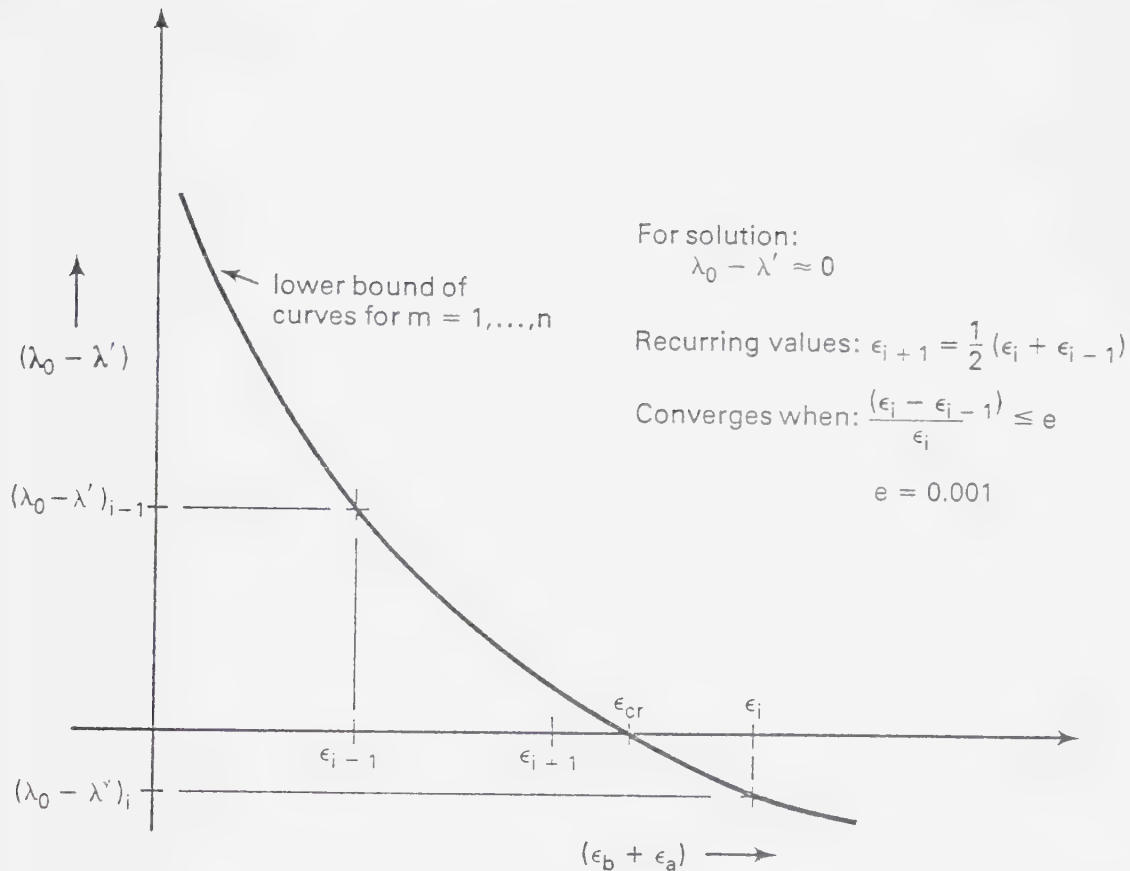


Figure 4.9 Iterative Technique for Critical Buckling Strain.

Chapter 5

COMPARISON OF THEORETICAL PREDICTIONS WITH TEST RESULTS

5.1 Introduction

An analytical procedure for the calculation of critical loads causing local buckling of plate components of W shapes has been presented in Chapters 3 and 4. This procedure uses matrix techniques to predict critical local buckling loads which may occur either in the elastic or inelastic load region. Because of the large number of iterative calculations required it was necessary to use a computer program which was written for this purpose. In this chapter, theoretical results are compared with the results of laboratory tests performed on 57 specimens. These tests include six column specimens and six beam specimens tested by Haaijer and Thurlimann¹⁰. Of the remaining 45 specimens, 4 were column specimens, 26 were beam specimens, and 15 were beam-column specimens all tested at the University of Alberta^{11,12,13,36}. In all cases, local buckling of plate components of W shapes was the principal point of interest during testing.

5.2 Prediction of Buckling Loads

In the analysis of local plate buckling as presented herein, it is assumed that portions of a cross-section having strains higher than the yield strain, have effective material properties corresponding to those in the strain-hardening region. As mentioned previously, this assumption has also been used successfully by other investigators in

this area^{25,34,51,53,54}. These material properties are presented in Appendix B and have values dependent on the elastic modulus, E, the strain-hardening modulus, E_{st} , and Poisson's ratio, ν . Where these values are not reported for a given laboratory specimen, values of $E = 29,600$ ksi., $E_{st} = 800$ ksi., and $\nu = 0.3$ are assumed. In the case where a residual stress is not available, a value of $0.3 \sigma_y$ is assumed^{3,5} as a maximum value of compressive and tensile residual stresses and the distribution configuration shown in Figure 3.11 is used. For the specimens tested by Haaijer and Thurlimann, specific values of D_x , D_y , D_{xy} and G_t were reported for a value of $E_{st} = 900$ ksi. Consequently these values are used in the prediction of local buckling capacities for the specimens tested by Haaijer and Thurlimann.

5.3 Column Local Buckling Tests

Results of six column tests were published in 1958 by Haaijer and Thurlimann⁷. The specimens were designed to study the behaviour of W shape columns susceptible to local buckling beyond the elastic range. Each specimen was placed flat-ended between fixed plates in a testing machine and subjected to axial compression. During the tests, observations were made at each load increment to determine axial strains, web and flange deflections, and lateral movement. Column lengths varied between 23 and 32 inches while $b\sqrt{F_y}/2t$ varied between 40 and 56 for the flanges and $h\sqrt{F_y}/w$ varied between 147 and 265 for the webs.

The resulting critical column loads at the point of local buckling for these tests are shown in Table 5.1(a). The predicted loads as determined from the analytical procedure presented herein as

well as the ratios of the predicted to the experimentally determined loads are also shown in this table. The letters, F and W in brackets, indicate the plate component (flange or web) which initiated local buckling in each case.

In 1979 at the University of Alberta, G.L. Kulak tested four W shape column specimens for local buckling capacities. The end edges of the flanges and web of each specimen were rounded and fitted into grooved platens before being placed in a testing machine and subjected to axial compression. During the tests, local strains and plate deflections were recorded at various load levels so that a continuous monitoring of local, lateral and axial deflections was possible. The webs of all four specimens were proportioned to have a value of $h\sqrt{F_y}/w = 200$. Specimen numbers 1 to 3 were 36 inches long and had a value of $b\sqrt{F_y}/2t = 72$ for the flanges. Specimen number four was 24 inches long and the value of $b\sqrt{F_y}/2t$ for the flanges was set at 100 by milling the flanges to the required thickness. The results of these tests are presented in Table 5.1(b) where the values predicted by the analysis presented herein as well as the ratios of predicted to experimental values are also shown.

5.3.1 Discussion of Column Test Results

The ratios of predicted to experimental values of buckling loads presented in Table 5.1 vary between 0.97 and 1.08. It appears that there is better correlation of predicted and experimental values for Kulak's specimens than for those tested by Haaijer and Thurlimann. This difference in correlation for the two sets of test specimens is attributed to the fact that the test values for the specimens tested by

Haaijer and Thurlimann were scaled from published graphs whereas the measured values for the specimens tested by Kulak were directly available. Although this is considered to be the main source of error, other sources of error that are considered to be applicable to all test results presented herein are discussed in Section 5.6.

5.4 Beam Local Buckling Tests

Theoretical values of critical moments causing local buckling in W shapes are compared with corresponding test results for 32 beam specimens. Six beam specimen test results were obtained from the work of Haaijer and Thurlimann¹⁰ and twelve results were obtained from tests carried out by Holtz and Kulak^{11,12}. The remaining 14 test results were obtained from experiments carried out by Lukey and Adams³⁶.

The six beam sections tested by Haaijer and Thurlimann were identical to those tested in the column test series mentioned above. All beams were simply supported at the ends and loaded symmetrically by two concentrated loads so that local buckling could be expected to occur within the uniform moment region. Although the specimens were laterally braced failure was initiated by flange local buckling followed by some lateral movement between bracing points. It is to be expected that this combined failure mode affects the results predicted by the method presented herein although the extent of this effect is difficult to estimate.

In table 5.2(a) bending moments at failure for each of the six specimens tested by Haaijer and Thurlimann are compared with those predicted by the analysis presented herein. As before, the letter, F, in brackets indicates flange local buckling and in this case also, the

letter, L indicates the presence of lateral buckling. The ratios of experimental to predicted moment values are also shown.

In 1973, Holtz and Kulak¹¹ reported test results for a series of ten compact beam specimens. During testing, all specimens were simply supported and loaded symmetrically with equal concentrated loads so that a uniform moment region existed between load points. All specimens were laterally braced at the load and reaction points so that the possibility of lateral buckling was precluded. Similar tests were performed on a series of two non-compact beams in 1975¹².

Table 5.2(b) shows the critical buckling moments obtained for the bending tests performed by Holtz and Kulak. The corresponding moments as determined by the analysis presented herein are shown as well as the ratios of predicted to experimental values. The letters, F and W, indicate which element (either flange or web) precipitated the local failure.

The beam specimen tests performed by Lukey and Adams³⁶ were designed for the purpose of studying the relationship between flange slenderness ratios and rotation capacities of W shape beams subjected to a moment gradient. All specimens were simply supported and loaded with a concentrated load placed at mid-span with lateral bracing placed at reaction and load points. The analytical method presented herein was not developed to predict local buckling capacities of beams subjected to moment gradients. It was assumed, however, that a buckle would normally occur in a localized region at the location of maximum moment and that adjacent moment gradient regions would not significantly affect the critical buckling moment. For this reason it was decided to include the results of the beams tested under a moment gradient as

described above.

The critical buckling moments for the specimens tested by Lukey and Adams are presented in Table 5.2(c). The critical element initiating local failure and the ratio of experimental to predicted buckling moment values are also indicated for each specimen.

5.4.1 Discussion of Test Results

For the beam specimens tested by Haaijer and Thurlimann, the ratios of predicted to experimental values of the buckling moment vary between 0.97 to 1.13 as shown in Table 5.2(a). For five of the six specimens tested, the predicted values are within five per cent of the actual test values and for specimen number one the predicted value is slightly high. This slightly high value is not unacceptable, however, in view of the possible sources of error outlined in the next section.

The correlation between experimental and predicted buckling moments for the specimens tested by Holtz and Kulak is generally quite good as can be seen from Table 5.2(b). The ratios of experimental to predicted values vary between 0.89 and 1.12. For ten of the twelve specimens tested, the predicted values of buckling moment are within six per cent of the test values. For specimen numbers 5 and 9 the error is +12 per cent and -11 per cent respectively. Again, in view of the possible sources of error, as discussed in the next section for all test series, these values are considered to be acceptable.

For the specimens tested by Lukey and Adams, the ratios of predicted to experimental values of buckling moment vary between 0.87 and 1.08 for eleven of the fourteen specimens tested. For specimen numbers 2, 4, and 13, the ratios of predicted to experimental values

vary between 1.18 and 1.46 which must be considered as unacceptable correlation between test and theory for these three specimens. In attempting to explain this discrepancy between predicted and test values, it must be pointed out that all of the beam specimens tested eventually failed by a combination of local and lateral buckling. The laterally buckled shape, in plan view, was an S-shaped buckle symmetrically formed about the mid-span lateral brace. As a result, the final buckling mode was that of a combined local and lateral buckle. It is possible, therefore, that for specimen numbers 2, 4, and 13, additional lateral bracing placed at the quarter-points may have prevented lateral buckling thus permitting a failure by pure local buckling. Under such circumstances a higher test load would be obtained and a better correlation between test and theory would result. For the eleven remaining specimens, for which good correlation was obtained, it is assumed that this effect was not as significant presumably because the moment required to cause pure local buckling failure was either less than or equal to that required to cause a pure lateral buckling failure.

5.5 Beam-Column Local Buckling Tests

Local buckling tests on nine beam-columns using compact⁴ sections were carried out by Perlynn and Kulak¹². An additional series of tests consisting of six non-compact⁴ beam-column specimens was carried out by Nash and Kulak¹³. Each specimen for both test series was aligned in a universal testing machine which was used to apply the principal concentric load through steel rockers at the top and bottom of a specimen. A moment was superimposed by using a center-hole jack acting between loading arms rigidly connected to the ends of a specimen.

As the eccentric load was increased to provide an increment of moment the principal load was decreased so that the total axial load remained constant and equal to a prescribed value. At each increment of moment, web and flange deflections were monitored locally at various points along the specimen, and overall rotations and deflections were also recorded. Each specimen was laterally braced at mid-span and adequate torsional restraint was provided at the ends by means of the rigidly connected loading arms.

The critical buckling moments for the compact beam-columns tested by Perlynn and Kulak are presented in Table 5.3(a). The ratio of the applied axial load to the yield load is also shown for each specimen. As mentioned previously, the critical element (either flange or web) which precipitates a local failure is indicated by the letter F or W. The predicted value of the local buckling moment as well as the ratio of predicted to experimental moment is also shown for each specimen. In a similar manner the results of the non-compact beam-columns tested by Nash and Kulak are presented in Table 5.3(b).

5.5.1 Discussion of Beam-Column Test Results

For the specimens tested by Perlynn and Kulak the predicted values of buckling moment are within 7 per cent of the test moment for seven of the nine specimens as shown in Table 5.3(a). For the remaining two specimens, the errors are +12 per cent and +13 per cent. In view of the possible sources of error as discussed in the next section, these values are considered to be acceptable.

As shown in Table 5.3(b), for the specimens tested by Nash and Kulak, the predicted values of buckling moment are in error with

respect to the test values by less than 5 per cent for three specimens and by +11 and -13 per cent for two of the remaining three specimens. These errors are considered to be acceptable in view of the possible sources of error as discussed in the next section. For specimen number six the predicted load was only 64 per cent of the maximum load recorded during the test. The validity of this test result is in doubt when compared to that obtained for specimen number five. This specimen was identical except for a 25 per cent increase in the $h\sqrt{F_y}/w$ term which is unlikely to result in a 40 per cent decrease in moment as is apparent from Table 5.3(b). Additional doubt is cast upon the validity of this test result since difficulty of specimen alignment at high axial loads ($P/P_y = 0.7$) was apparently evident during the testing procedure⁶⁰.

5.6 Sources of Error

In addition to the sources of error discussed in the previous sections for specific test series, the following sources of error are applicable as noted:

(a) Material Properties

This area is probably the most significant source of error as well as the least determinable. No investigator has as yet come up with an unquestionable evaluation of plate buckling properties that can be applied over the entire inelastic plate buckling range. Apparently, the most reliable guidance presently available for these values in the strain-hardening range is based on the works of Handelman and Prager²², Haaijer and Thurlimann⁷, and Lay³³. In all cases these values are apparently closely related to the strain-hardening modulus, E_{st} , of a

simple tension coupon test and any error involved in determining E_{st} would doubtlessly be reflected in the theoretical values predicted.

No estimate in the error involved in determining E_{st} values is available.

Because the specimens tested by Haaijer and Thurlimann and Lukey and Adams were proportioned so that failure in the plastic range was expected, an evaluation of E_{st} was made for each specimen. The specimens tested by Kulak et al on the other hand, were not proportioned as plastic design sections and therefore the effect of E_{st} was not expected to be as significant. In these cases the value of E_{st} was not available for each specimen. However, a value of $E_{st} = 800$ ksi. has been estimated from the available stress - strain curves.

Assuming that various material properties have been accurately determined from a simple tension test, it is generally accepted that these properties also apply to larger specimens of different shape subjected to compression. It is further assumed that the material is uniform throughout the test specimens. Local material discontinuities due to welding and forming specimens may contribute to error in this respect. No estimate of the error arising from the use of tension coupon material properties is available.

(b) Residual Stresses

The actual magnitudes and distributions of residual stresses were not available for the specimens tested by Haaijer and Thurlimann, and of the tests carried out by Kulak et al, residual stresses were available only for the column specimens. In these cases the residual stress distribution shown in Figure 3.11 with a maximum value of

residual stress of $0.3\sigma_y$ was assumed. Residual stresses vary in magnitude and distribution from specimen to specimen³² and affect the local buckling capacity. The effect of changing residual stress values is studied parametrically in Chapter 6.

(c) End Conditions

The end conditions existing at the longitudinal extremities of a local buckle depend largely upon the method of testing and usually they will lie between the pinned and fixed end conditions. In the analysis presented herein, after careful consideration of the methods of testing used in each test series, it was decided that pinned end conditions best represent the end support conditions of the column specimens. Because of the elastic moment gradient region adjacent to either end of a local buckle developing in the beam specimens tested, fixed-end support conditions were assumed. The very rigid attachment of the loading arms to the beam-columns tested resulted also in the assumption of fixed ends for these specimens. The effects of end conditions vary with the length of a specimen² and therefore any resulting errors will be more significant for shorter members. With the reduction in plate bending stiffnesses due to inelastic action, it is expected that the affects of end conditions would be lessened. For these reasons it is felt that the effects of estimating degrees of end fixity are not likely to contribute significantly to error.

(d) Iterative Technique

All specimens buckled beyond the elastic range and therefore a considerable amount of iteration involving matrices was required to arrive at a solution for each specimen. Although tolerances were set at 0.1 per cent in the computer program, round-off error is expected to

contribute to the total error.

(e) Analytical Technique

The buckled shapes of the webs and flanges of specimens are approximated using polynomials which result in the least energy shapes for a given specimen. It has been shown^{6,18} that this technique results in over-estimation of buckling loads when theoretical shapes do not exactly fit the true buckled shapes. The present technique and associated computer program were checked for this source of error by comparing elastic critical values of plates with values presented by Timoshenko¹⁸ and Bleich¹⁹. It was found for rectangular plates with various boundary conditions and loadings that this error varied from zero per cent for simply supported plates to about 3.0 per cent for fixed boundary conditions. Since neither web plates nor flange plates of these specimens are fully fixed, it is expected this source of error would be below 2.0 per cent in the majority of cases.

(f) Scaling from graphs

The values reported by Haaijer and Thurlimann⁷ and by Lukey and Adams³⁶ were presented in graphical form and the critical loads were scaled from these graphs. It is estimated that the error involved in this procedure would be about ± 1.0 per cent.

(g) Test Measurements

No test difficulties, other than those mentioned above, were reported by the investigators. There are no other significant errors attributable to this source, although, as in all tests, some error, either human-related or machine-related, or both, is probable.

(h) Mode of Failure

It is apparent that in several tests, local buckling was

closely followed by, or in fact coupled with lateral buckling. Since the analytical method presented herein specifically excludes the occurrence of lateral buckling, such effects have not been evaluated. In any case, the degree to which lateral buckling was involved in the actual failure mechanism is not clearly known, and no estimate of the error involved is available.

5.7 Summary of Test Results

As explained previously, four of the 57 test results included herein, are not considered to be valid for the purpose of verifying a theoretical method which does not include the effects of lateral buckling. For the 53 specimens remaining, the predicted results were within 5 per cent of the test results for 60 per cent of the specimens, and within 10 per cent of the test values for 85 per cent of the specimens. The error was between ± 10 percent and an overall maximum of ± 13 per cent for only 15 per cent of the specimens. Overall, the ratio of theoretical to test values (of either critical load or critical moment) varies from -0.87 to +1.13 with a mean value of 1.00 and a standard deviation of 0.065. In all but four cases, the prediction of the critical component (either flange or web) which initiated the local buckling failure agreed with buckling observations made during the tests.

5.8 Summary

As outlined above, a comprehensive survey of available test data was used to substantiate the validity of the theoretical analysis presented herein as well as the associated computer program.

The comparison between predicted and experimental results has indicated satisfactory agreement between test and theory. In Chapter 6 this same technique is used to evaluate the effects of various parameters which are considered to be of some significance in affecting theoretical predictions.

Load at Buckling

Specimen Number	Experimental L_E -(kips)	Predicted L_T -(kips)	Ratio (L_T/L_E)
1	330 (F)	357 (F)	1.08
2	232 (F,W)	253 (F)	1.09
3	442 (F)	429 (F)	0.97
4	514 (F,W)	548 (F,W)	1.07
5	380 (F)	374 (F)	0.98
6	207 (W)	221 (W)	1.07

1 kip = 4.448 kN

(a) Results of G. Haaijer and B. Thurlimann

Load at Buckling

Specimen Number	Experimental L_E -(kips)	Predicted L_T -(kips)	Ratio (L_T/L_E)
1	1010 (F)	1015 (F)	1.01
2	1010 (F)	1018 (F)	1.01
3	1000 (F)	1019 (F)	1.02
4	680 (F)	693 (F)	1.02

1 kip = 4.448 kN

(b) Results of G.L.Kulak

5.1 Comparison of Experimental and Predicted Values for Columns.

Moment at Buckling

Specimen Number	Experimental M_E -(in.-kips)	Predicted M_T -(in.-kips)	Ratio (M_T/M_E)
1	1325 (F)	1491 (F)	1.13
2	812 (F,L)	842 (F)	1.04
3	1825 (F,L)	1797 (F)	0.98
4	2951 (L)	2848 (F)	0.97
5	1280 (F,L)	1295 (F)	1.01
6	819 (F,L)	847 (F)	1.03

1 in.-kip = 112.98 N·M

(a) Results of Haaijer and Thurlimann

Moment at Buckling

Specimen Number	Experimental M_E -(in.-kips)	Predicted M_T -(in.-kips)	Ratio (M_T/M_E)
1	3840 (F)	3851 (F)	1.00
2	4910 (F)	4893 (F)	1.00
3	5740 (W)	6091 (F,W)	1.06
4	6820 (W)	6796 (W)	1.00
5	3940 (W)	4400 (W)	1.12
6	3380 (F)	3571 (F,W)	1.06
7	3770 (W)	4005 (W)	1.06
8	3910 (F)	3790 (F)	0.97
9	4580 (F)	4092 (F)	0.89
10	4780 (F)	4588 (F)	0.96
11	5367 (W)	5452 (W)	1.02
12	5696 (W)	5939 (W)	1.04

1 in.-kip = 112.98 N·M

(b) Results of Holtz and Kulak

5.2 Comparison of Experimental and Predicted Values for Beams.

....cont'd

Moment at Buckling

Specimen Number	Experimental M_E -(in.-kips)	Predicted M_T -(in.-kips)	Ratio (M_T/M_E)
1	2251 (F)	2324 (F)	1.03
2	1845 (F)	2698 (F)	1.46
3	549 (F)	476 (F)	0.87
4	463 (F)	548 (F)	1.18
5	487 (F)	491 (F)	1.01
6	488 (F)	463 (F)	0.95
7	390 (F)	423 (F)	1.08
8	701 (F)	628 (F)	0.90
9	656 (F)	643 (F)	0.98
10	659 (F)	645 (F)	0.98
11	698 (F)	639 (F)	0.92
12	679 (F)	647 (F)	0.95
13	391 (F)	525 (F)	1.34
14	440 (F)	403 (F)	0.92

1 in.-kip = 112.98 N·M

(c) Results of Lukey and Adams

5.2 Comparison of Experimental and Predicted Values for Beams.

Moment at Buckling

Specimen Number	P/P _y	Experimental M _E -(in.-kips)	Predicted M _T -(in.kips)	Ratio (M _T /M _E)
1	0.2	2370 (F)	2376 (F)	1.00
2	0.2	2732 (F)	2534 (F)	0.93
3	0.2	2887 (W)	2796 (W)	0.97
4	0.4	1606 (F)	1808 (F)	1.13
5	0.4	1829 (F)	1781 (F)	0.97
6	0.4	2303 (F,W)	2157 (F,W)	0.94
7	0.8	738 (F)	825 (F)	1.12
8	0.8	694 (W)	660 (W)	0.95
9	0.8	582 (W)	588 (W)	1.01

1 in.-kip = 112.98 N·M

(a) Results of Perlynn and Kulak for Compact Sections

Moment at Buckling

Specimen Number	P/P _y	Experimental M _E -(in.-kips)	Predicted M _T -(in.kips)	Ratio (M _T /M _E)
1	0.15	3704 (F)	3698 (F)	1.00
2	0.15	2622 (F)	2923 (F)	1.11
3	0.30	2827 (W,F)	2712 (W,F)	0.96
4	0.30	2488 (F)	2171 (F)	0.87
5	0.70	668 (W,F)	682 (W,F)	1.02
6	0.70	1095 (F)	705 (F)	0.64

1 in.-kip = 112.98 N·M

(b) Results of Nash and Kulak for Non-Compact Sections

5.3 Comparison of Experimental and Predicted Values for Beam-Columns.

Chapter 6

THEORETICAL STUDY AND EVALUATION OF PARAMETERS

6.1 Introduction

As presented in Chapter 5, test results are available for a limited number of local plate buckling specimens subjected to axial, flexural, and combined axial and flexural loadings. The number and variation of dimensions of these specimens are not sufficient in themselves to be able to establish general design parameters. Furthermore, the critical buckling loads may be significantly influenced by certain parameters which have not been specifically studied in the tests. In this chapter, analytical results in the form of critical plate buckling curves are presented and discussed for a wide variety of columns, beams, and beam-columns. Additionally, the effects of important parameters on local plate buckling capacities are evaluated and discussed. Unless specifically varied the following basic values are used in the parametric study: $E = 29,600 \text{ ksi.}$, $\sigma_y = 44 \text{ ksi.}$, $\epsilon_y = \sigma_y/E$, $\epsilon_{rc} = 0.3\epsilon_y$, $E_{st} = 800 \text{ ksi.}$, flange aspect ratio = 4, and web aspect ratio = 2.

6.2 Columns

Figure 6.1 shows the variation of the critical load ratio (P_{cr}/P_y) with respect to the web width-to-thickness term ($h\sqrt{F_y}/w$) for various values of the flange width-to-thickness term ($b\sqrt{F_y}/2t$). The knee portion of each curve results from the presence of unavoidable

residual stresses. For the sake of comparison a curve corresponding to a theoretical value of zero residual stress is also shown. By this comparison it can be seen that the effects of residual stresses are most pronounced in the elastic and partially elastic regions. Assuming a residual compressive stress $\sigma_{rc} = 0.3\sigma_y$, yielding begins at $P_{cr}/P_y = 0.7$ and $h\sqrt{F_y}/w = 475$. As $h\sqrt{F_y}/w$ decreases, flange buckling becomes predominant as the yield load is approached, and at lower values strain-hardening occurs. The dashed curve represents the elastic buckling solution.

The CSA S16.1-1975 Standard⁴ specifies a flange slenderness value for column flanges of 100. As illustrated in Figure 6.1, the analysis presented herein predicts that this value is slightly conservative. At the currently specified limitations⁴ of $b\sqrt{F_y}/2t = 100$ and $h\sqrt{F_y}/w = 255$ for columns, the analysis presented herein predicts a value of $P_{cr}/P_y = 0.9$. Also, the figure shows that P_{cr}/P_y does not reach a value of 1.0 until $b\sqrt{F_y}/2t$ has been reduced to 72 and values of $h\sqrt{F_y}/w$ are less than 300.

This theoretical result for columns has been substantiated by the results of four column specimens tested by Kulak at the University of Alberta. As discussed in Section 5.3, three of the specimens had flange slenderness values of 72, and the fourth specimen had a flange slenderness value of 100. The value of web slenderness was 200 for all four specimens. The flanges of the three specimens having $b\sqrt{F_y}/2t = 72$ buckled at or slightly above $P_{cr}/P_y = 1.0$, while the flanges of the specimen having $b\sqrt{F_y}/2t = 100$ buckled at $P_{cr}/P_y = 0.9$. These test results as well as the theoretical analysis presented herein indicate that a value of $b\sqrt{F_y}/2t = 72$ (as opposed to the current

limitation⁴ of $b\sqrt{F_y}/2t = 100$) should be used for columns. For this reason, subsequent parametric studies presented herein are based on a value of flange slenderness of 72 for columns.

In order to be able to later tie in column local buckling behaviour as one limiting case of beam-columns, the local buckling strength curves for axially loaded Class 1, Class 2, and Class 3 sections are shown in Figure 6.2. The rounded portion of each curve between values of $h\sqrt{F_y}/w$ of about 300 and 475 is due to gradual yielding in the presence of residual stresses. A curve corresponding to zero residual stresses as mentioned previously is also shown in Figure 6.2. For web slenderness values greater than 475, elastic buckling of the web occurs and for values between 475 and 300, web buckling occurs in the inelastic range. For values of web slenderness less than about 300, flange buckling in the yielded and strain-hardening ranges occurs at values of P_{cr}/P_y equal to or greater than 1.0.

A column local buckling curve is shown in Figure 6.2 for a value of $b\sqrt{F_y}/2t = 64$ corresponding to the present CSA-S16.1 specification⁴ for a Class 2 section. For a Class 1 section with $b\sqrt{F_y}/2t = 54$, a similar column curve is shown in Figure 6.2. Although these two sections are not explicitly designated for use as columns, the corresponding column curves are presented here so that the effect of the $b\sqrt{F_y}/2t$ term for columns may be evaluated. Also, these sections subjected to column action, represent a limit of the corresponding beam-columns when bending moments are negligible.

The effect of the flange slenderness values can be seen by comparing the curves in Figure 6.2. For values of $h\sqrt{F_y}/w$ greater than

300, where web buckling is predominant, varying $b\sqrt{F_y}/2t$ from 54 to 72 has virtually no effect on the web buckling capacity. The effect of this term is most significant for values of $h\sqrt{F_y}/w$ less than 300 since that is the region wherein flange buckling is predominant. For $b\sqrt{F_y}/2t = 72$ strain-hardening of the section begins at a value of $h\sqrt{F_y}/w = 220$. As $b\sqrt{F_y}/2t$ is decreased, strain-hardening begins at progressively higher values of $h\sqrt{F_y}/w$, the upper limit being $h\sqrt{F_y}/w = 325$ for a Class 1 section with a flange slenderness value of 54.

6.2.1 Effects of Residual Stresses

The effects of residual stresses on the local buckling loads of columns is shown in Figure 6.1 for $b\sqrt{F_y}/2t$ ratios of 72, 80, 90, and 100, and in Figure 6.2 for $b\sqrt{F_y}/2t$ ratios of 54, 64, and 72. In these figures, column local buckling curves for a theoretical value of $\sigma_{rc} = 0$ are compared with those corresponding to a more practical value of $\sigma_{rc} = 0.3\sigma_y$ and a residual stress distribution as shown in Figure 3.11. The value of $\sigma_{rc} = 0.3\sigma_y$ is representative of values used by other investigators^{3,5,61,62} for the purpose of including the effects of residual stresses when exact values are unknown.

By comparing the curves corresponding to $\sigma_{rc} = 0$ with those corresponding to $\sigma_{rc} = 0.3\sigma_y$, it can be seen that, in the range where elastic web buckling occurs (at values of $h\sqrt{F_y}/w$ greater than about 475), a residual stress of $0.3\sigma_y$ reduces the critical buckling load ratio by about 25 per cent. The influence of residual stresses diminishes as the value of P_{cr}/P_y approaches 1.0, and completely disappears as strain-hardening becomes imminent at lower values of $h\sqrt{F_y}/w$.

According to the theoretical method presented herein, the

values of $b\sqrt{F_y}/2t = 100$ as presently specified for W shape columns⁴ appears to be too liberal when a residual stress of $\sigma_{rc} = 0.3\sigma_y$ is assumed. In Figure 6.1, the curve corresponding to $b\sqrt{F_y}/2t = 100$ and $\sigma_{rc} = 0.3\sigma_y$ reaches a value of $P_{cr}/P_y = 0.9$ at the presently specified⁴ web slenderness ratio of 255. The curve corresponding to $b\sqrt{F_y}/2t = 100$ and the theoretical value of $\sigma_{rc} = 0$ on the other hand, reaches a value of $P_{cr}/P_y = 1.0$ for values of web slenderness as high as 475. For this reason therefore, the analytical method presented herein suggests that the presently specified value of $b\sqrt{F_y}/2t = 100$ is too liberal because of the effects of residual stresses. The analytical method presented herein predicts that when a W shape column is proportioned so that $b\sqrt{F_y}/2t \leq 72$ and $h\sqrt{F_y}/w \leq 300$ a value of $P_{cr}/P_y \geq 1.0$ can be reached for an assumed residual stress of $\sigma_{rc} = 0.3\sigma_y$.

6.2.2 Effects of Strain-hardening Modulus

Figure 6.3 shows the effects of strain-hardening modulus values of 700, 800, and 900 ksi. on the local buckling capacity of columns. These values of strain-hardening moduli were chosen because they are representative of values that have been determined by several investigators in this area^{5, 7, 36, 54, 59, 61, 62}. For columns proportioned so that $b\sqrt{F_y}/2t = 72$, variations in the values of the strain-hardening modulus are influential for values of $h\sqrt{F_y}/w$ less than about 200. In this region the curve separates into three branches corresponding to the three different values of the strain-hardening modulus investigated. As would be expected in this region, for a given value of web slenderness, the value of P_{cr}/P_y increases as the strain-hardening modulus increases. As can be seen from Figure 6.3, in the practical ranges of plate

proportions for W shape columns ($b\sqrt{F_y}/2t = 72$ and $h\sqrt{F_y}/w = 300$), the value of the strain-hardening modulus has negligible effect on column local buckling strength.

6.3 Beams

Figure 6.4 shows values of the ratio of critical local buckling moment to the yield moment plotted against the web width-to-thickness term ($h\sqrt{F_y}/w$), for various values of the flange width-to-thickness term ($b\sqrt{F_y}/2t$). Again, the effects of residual stresses are included as is evident from the rounded knee portions of these curves. For values of $h\sqrt{F_y}/w$ greater than about 1100, local buckling of the slender web occurs in the form of warping due to the presence of residual stresses.

6.3.1 Class 3 Beams

According to the CSA S16.1-1975 Standard⁴, the flange width-to-thickness term for a Class 3 beam is set at 100 and is the same as that for a column. The currently specified web width-to-thickness ratio is 690. For these values, Figure 6.4 shows that $M_{cr}/M_y = 0.9$.

Comparing similar curves for various values of $b\sqrt{F_y}/2t$ in Figure 6.4, it is seen that M_{cr}/M_y attains a value of 1.04 at $b\sqrt{F_y}/2t = 72$ over a large range of web slenderness (up to about $h\sqrt{F_y}/w = 800$). Although M_{cr} slightly exceeds M_y (by only 4 per cent) for $b\sqrt{F_y}/2t = 72$, this value seems to be appropriate for a Class 3 beam in that it corresponds with the value suggested for columns. In this way, the same value may be used throughout for a Class 3 beam-column which has as its limits, pure axial load at one end of the loading spectrum, and pure flexure at the other. For $b\sqrt{F_y}/2t = 72$, Figure 6.4 shows that for curves

of web slenderness greater than 975 the web buckles elastically. For values of web slenderness between 800 and 975 the web buckles in the inelastic range as a consequence of the influence of residual stresses. The mode of failure changes from web buckling at a value of 800 to flange buckling for values less than 800. At a web slenderness value of 260 the curve begins to increase rapidly as strain-hardening becomes influential.

6.3.2 Class 2 Beams

The Standard⁴ specifies that Class 2 beams have a flange slenderness value not exceeding 64 and a web slenderness value not exceeding 520. In Figure 6.5 values of the ratio of critical moment, M_{cr} , to the plastic moment, M_p , are plotted against the web width-to-thickness term, $h\sqrt{F_y}/w$, for a flange width-to-thickness value of 64. For values of $h\sqrt{F_y}/w$ greater than 1100, local buckling occurs in the form of warping of the slender web subjected to residual stresses. Referring to the curve corresponding to a value of $b\sqrt{F_y}/2t = 64$, local buckling of the web occurs in the inelastic range between values of $h\sqrt{F_y}/w$ of about 800 and 975. For values of $h\sqrt{F_y}/w$ less than 800, flange buckling occurs at a value of $M_{cr}/M_y = 1.0$, and at $h\sqrt{F_y}/w = 300$ strain-hardening of the section begins and strength increases rapidly as $h\sqrt{F_y}/w$ decreases further.

6.3.3 Class 1 Beams

For Class 1 beams the Standard⁴ specifies a flange slenderness of 54 and a web slenderness limit of 420. Values of M_{cr}/M_p are plotted against $h\sqrt{F_y}/w$ for a value of $b\sqrt{F_y}/2t = 54$ as shown in Figure 6.5. For $h\sqrt{F_y}/w$ greater than 800, the behaviour of these beams is similar to

that described previously for Class 2 sections. Because of the increased sturdiness of the flanges however, web buckling continues to be the mode of failure for values of $h\sqrt{F_y}/w$ as low as 600. Below this value, flange buckling occurs. For values less than 800, M_{cr}/M_p is greater than 1.0 and this implies that the strain in the flanges can reach the strain-hardening range before local buckling occurs. Therefore, these sections can undergo sufficient rotation to permit redistribution of stresses while sustaining the plastic moment value, as required of Class 1 sections^{2,3,4}.

6.3.4 Effects of Residual Stresses

The critical buckling moment ratio is plotted against values of web slenderness for values of flange slenderness of 72, 80, 90, and 100 in Figure 6.4 and for values of flange slenderness of 54 and 64 in Figure 6.5. Again, the assumed residual stress value is $\sigma_{rc} = 0.3\sigma_y$ and the assumed residual stress distribution is similar to that shown in Figure 3.11. For the purpose of comparison, these curves are also plotted for the theoretical value of $\sigma_{rc} = 0.0$. In the range where web buckling is critical ($P_{cr}/P_y < 1.0$ and $h\sqrt{F_y}/w > 800$) residual stresses have their greatest effect in reducing the critical buckling moment capacity. For values of $h\sqrt{F_y}/w$ greater than about 1100, the residual stress causes web buckling in the form of warping of the very slender webs. As values of $h\sqrt{F_y}/w$ decrease below 800, the significance of residual stresses diminishes and as strain-hardening is approached their effects become negligible.

As discussed for columns, it appears here also that the presently specified flange slenderness⁴ of 100 is too liberal for

Class 3 beams when a value of $\sigma_{rc} = 0.3\sigma_y$ is assumed. Referring to Figure 6.4, for a value of flange slenderness of 100 and $\sigma_{rc} = 0.3\sigma_y$, the critical local buckling moment is 90 per cent of the yield moment at the presently specified web slenderness⁴ of 690. The theoretical curve for which $b\sqrt{F_y}/2t = 100$ and $\sigma_{rc} = 0$, on the other hand, shows that the critical local buckling moment reaches the yield moment for values of web slenderness as high as 800. This suggests, therefore, that the value of $b\sqrt{F_y}/2t = 100$ for Class 3 beams is too liberal because of the effects of residual stresses.

6.3.5 Effects of Strain-hardening Modulus

The effect of varying the strain-hardening modulus upon the local buckling behaviour of beams is shown in Figure 6.6 for a value of $b\sqrt{F_y}/2t = 72$ and in Figure 6.7 for a value of $b\sqrt{F_y}/2t = 54$. As for columns, the same three values of strain-hardening modulus are used here for beams. Figure 6.6 shows that for sections with $b\sqrt{F_y}/2t = 72$, the effect of strain-hardening is evident only for values of $h\sqrt{F_y}/w$ less than about 280. Although not explicitly shown herein, it has been determined that these same observations apply to compact sections⁴ with a value of $b\sqrt{F_y}/2t = 64$. For plastic design sections⁴, Figure 6.7 shows that the effect of strain-hardening is influential for values of $h\sqrt{F_y}/w$ less than 800. This is because the very sturdy flanges ($b\sqrt{F_y}/2t = 54$) enable these sections to reach strain-hardening strains at relatively high web slenderness values.

For the values of E_{st} examined, there are no significant differences in local buckling strength for beams having flange slenderness values of 72 and 64 when practical values of web slenderness

are used. The local buckling strength of plastic design sections, on the other hand, are significantly affected by changes in the strain-hardening modulus for all values of web slenderness less than about 800. As would be expected, this effect increases as web slenderness values decrease.

6.4 Beam-Columns

The previous section has indicated that suitable flange slenderness values for flexural members are $b\sqrt{F_y}/2t = 54, 64,$ and 72 for Class 1, 2, and 3 respectively. Further, a suitable value for axially loaded members is $b\sqrt{F_y}/2t = 72.$ These will therefore be the values principally investigated for beam-columns. The analysis will be based on the assumption that an axial strain less than the critical one will be applied first. A flexural strain is then superimposed and gradually increased until local buckling occurs.

At each increment of flexural strain, equilibrium of a cross-section is satisfied and the position of the neutral axis is updated to account for yielding of a section. For a given flange width-to-thickness term, values of the ratio of applied load to yield load can then be plotted against values of the ratio of critical moment to yield moment or plastic moment for various web width-to-thickness terms. The web width-to-thickness term is varied from 300 to 800, corresponding to the limits determined previously for a pure column (zero flexural strain) and a pure beam (zero axial strain). In this way, for a given $b\sqrt{F_y}/2t$ value, a set of interaction curves is generated for various $h\sqrt{F_y}/w$ values.

6.4.1 Class 3 Beam-Columns

As discussed in Section 6.3.1, the present code value of $b\sqrt{F_y}/2t = 100$ for a Class 3 section appears to be too high according to the theory presented herein. Furthermore, a value of $b\sqrt{F_y}/2t = 72$ was found to be adequate for local buckling requirements of columns and for beams required to reach the yield moment, M_y , before local buckling occurs. In this section, therefore, interaction curves are generated for beam-columns corresponding to a $b\sqrt{F_y}/2t$ value of 72 and various values of $h\sqrt{F_y}/w$.

Ratios of applied load to yield load are plotted against the ratios of critical moment to yield moment for various $h\sqrt{F_y}/w$ values in Figure 6.8. Values along the vertical axis represent pure column behaviour and those along the horizontal axis represent pure beam behaviour. For each curve corresponding to a fixed $h\sqrt{F_y}/w$ value, as M_{cr}/M_y increases above zero, a point of tangency is approached on the line joining the points $P/P_y = 1.0$ and $M_{cr}/M_y = 1.04$. At the point of tangency the mode of failure changes from web local buckling to flange buckling and beyond this point each curve remains tangent to the line. The sloping dashed line, $M_{yc} = M_y (1-P/P_y)$, represents the strength interaction equation for a Class 3 beam-column.

6.4.1.1 Current Specifications

For Class 3 beam-columns the web limitations are currently specified as follows:

$$h\sqrt{F_y}/w = 690 (1 - 2.60 P/P_y) \quad 0 \leq P/P_y \leq 0.15 \quad (6.1)$$

$$h\sqrt{F_y}/w = 450 \left(1 - 0.43 \frac{P}{P_y}\right) \quad 0.15 \leq \frac{P}{P_y} \leq 1.0 \quad (6.2)$$

These web limitations are based on test results obtained by Kulak and Nash¹³. Since the time of publication of these limitations, additional work in this area by Kulak and Nash¹³ has indicated the following increases:

$$h\sqrt{F_y}/w = 690 \left(1 - 1.69 \frac{P}{P_y}\right) \quad 0 \leq \frac{P}{P_y} \leq 0.15 \quad (6.3)$$

$$h\sqrt{F_y}/w = 535 \left(1 - 0.28 \frac{P}{P_y}\right) \quad 0.15 \leq \frac{P}{P_y} \leq 1.0 \quad (6.4)$$

Although the theory presented herein indicates that a $b\sqrt{F_y}/2t$ value of 72 should be used for Class 3 sections, the specimens tested by Kulak and Nash were designed on the basis of the existing code value of $b\sqrt{F_y}/2t = 100$. Furthermore, the specimens were able to reach, and in some cases exceed the value of M_y reduced in the presence of axial load. The theory presented herein also predicts values in good agreement with these test results when the effects of the rigid plate boundary constraints (necessitated by the attachment of the loading arms to the test specimens) are included in the analysis. In practice, however, the effects of these rigid supports for longer members are negligible. Omitting the effects of these supports, the present method predicts that a value of $b\sqrt{F_y}/2t = 72$ is indicated for Class 3 sections. For this value, the web limitations as predicted by the theory presented herein are discussed in the following section.

6.4.1.2 Theoretical Limitations as Determined Herein

For a Class 3 section the beam-column interaction curves are

plotted in Figure 6.8 for various values of $h\sqrt{F_y}/w$. At various values of P/P_y each curve intersects the line described by:

$$M = M_y (1 - P/P_y). \quad (6.5)$$

In Figure 6.9 these values of P/P_y are plotted against the corresponding values of $h\sqrt{F_y}/w$. For pure beam action at $P/P_y = 0$, the predicted web limitation is $h\sqrt{F_y}/w = 850$. As P/P_y increases, the slope of the curve decreases rapidly and becomes constant in the region of P/P_y between 0.42 and 0.75. As P/P_y further increases the slope decreases slightly as pure axial strains are approached at $P/P_y = 1.0$ and a minimum value of $h\sqrt{F_y}/w = 300$ is reached.

A linear approximation to the curve described above is also shown in Figure 6.9 and it is given by the following relationship:

$$h\sqrt{F_y}/w = 725 (1.0 - 0.59(P/P_y)) \quad 0 \leq P/P_y \leq 1.0 \quad (6.6)$$

This approximation deviates markedly on the conservative side from the theoretical curve for low values of P/P_y . In this region however, a conservative limitation is desirable in order to account for small residual axial loads occurring in service and as well to avoid the sensitivity of the steep theoretical gradient in this region. The relationship of Equation 6.6 as well as the limitations described by Equations 6.1 and 6.2 are also shown in Figure 6.9.

Referring to Figure 6.9, the theoretical method presented herein indicates a web limitation of $h\sqrt{F_y}/w = 725$ at $P/P_y = 0.0$ for beams. As P/P_y increases, a linear decrease in $h\sqrt{F_y}/w$ as a result of decreasing web flexural tension, is indicated. For pure column action, at $P/P_y = 1.0$, a minimum value of $h\sqrt{F_y}/w$ of 300 is reached. This theoretical

limitation differs from that presently specified by Equations 6.1 and 6.4 in the region of pure beam action ($P/P_y = 0.0$) by about +5 per cent. As P/P_y increases this difference reaches a maximum of about +60 per cent at $P/P_y = 0.15$ and from there it decreases to +18 per cent at $P/P_y = 1.0$. This comparison should be considered in light of the fact that the theoretical web limitations are based on the assumption of a flange slenderness ratio of $b\sqrt{F_y}/2t = 72$ (as previously explained), whereas the present limitations are based on the results of test specimens whose flange slenderness ratios were $b\sqrt{F_y}/2t = 100$.

6.4.2 Class 2 Beam-Columns

As already indicated, it will be assumed that a Class 2 beam-column is proportioned so that the flange width-to-thickness term is $b\sqrt{F_y}/2t = 64$. According to the theory presented herein, this value was found to be adequate for compact beam sections as illustrated in Figure 6.5. At the other extreme of beam-column action, namely pure axial load, these sections can reach a P_{cr}/P_y value of 1.0 for a value of $h\sqrt{F_y}/w = 300$, as shown in Figure 6.2. Accordingly, these beam-column sections were investigated for a range of P_{cr}/P_y ratios between zero and one, with the $h\sqrt{F_y}/w$ values varying from 300 to 800. The results of this investigation are presented in Figure 6.10.

In this figure, values of the ratio of applied load to yield load are plotted against ratios of critical moment to plastic moment for various values of $h\sqrt{F_y}/w$. The flange width-to-thickness term for all curves has a constant value of 64. For these curves, the same discussion as presented for Class 3 beam-columns in Section 6.4.1, is valid here for Class 2 beam-columns.

6.4.2.1 Current Specifications

The present limitations specified for web width-to-thickness terms for Class 2 beam-columns are as follows⁴:

$$\frac{h\sqrt{F_y}}{w} = 520 \left(1 - 1.28 \frac{P}{P_y}\right) \quad 0 \leq \frac{P}{P_y} \leq 0.15 \quad (6.7)$$

$$\frac{h\sqrt{F_y}}{w} = 450 \left(1 - 0.43 \frac{P}{P_y}\right) \quad 0.15 \leq \frac{P}{P_y} \leq 1.0 \quad (6.8)$$

These web limitations are based on test results from a series of nine compact beam-columns tested by Perlynn and Kulak¹². As presented in Chapter 5, the analytical method presented herein substantiates these results when the effects of rigid supports necessary for testing purposes are included in the analysis. Conservatively omitting the effects of these rigid supports however, the analysis presented herein shows that the conventional value of plastic moment reduced for the presence of axial load^{63,64},

$$M_{pc} = M_p \quad 0 \leq \frac{P}{P_y} \leq 0.15 \quad (6.9(a))$$

and,

$$M_{pc} = 1.18 M_p \left(1 - \frac{P}{P_y}\right) \quad 0.15 \leq \frac{P}{P_y} \leq 1.0 \quad (6.9(b))$$

cannot be attained by compact sections when $\frac{h\sqrt{F_y}}{w}$ is greater than 250. Such a limitation however would severely restrict the choice of web sizes available for use in compact sections. As shown in Figure 6.10, the analytical method presented herein predicts a maximum local buckling strength for compact sections of:

$$M_{pc} = M_p \left(1 - \frac{P}{P_y}\right), \quad (6.10)$$

when the web slenderness ratio varies between 300 and 800. Therefore, in accordance with the analytical results presented in Figure 6.10, Equation 6.10 is suggested for use with compact sections and, in this way, all values of $h\sqrt{F_y}/w$ up to 800 can be utilized for Class 2 sections.

6.4.2.2 Theoretical Limitations as Determined Herein

As shown in Figure 6.10 the curves corresponding to various values of $h\sqrt{F_y}/w$ become tangent to the line described by Equation 6.10 at various values of P/P_y . In Figure 6.11 these values of $h\sqrt{F_y}/w$ are plotted against the corresponding values of P/P_y . The resulting curve has a value of $h\sqrt{F_y}/w = 800$ for pure beam action ($P/P_y = 0.0$). As P/P_y increases, the slope of the curve rapidly increases to a constant value in the region of P/P_y between 0.42 and 0.75. As P/P_y further increases, the slope decreases slightly as pure axial strains are approached at $P/P_y = 1.0$. At this value of P/P_y a minimum value of $h\sqrt{F_y}/w = 300$ is reached.

The curve described above may be approximated by a linear relationship given by:

$$h\sqrt{F_y}/w = 660 (1 - 0.55 (P/P_y)) \quad 0 \leq P/P_y \leq 1.0 \quad (6.11)$$

This relationship as well as the relationships defined by Equations 6.7 and 6.8 as established by Kulak and Perlynn¹² are shown in Figure 6.11.

In establishing the above linear approximation a line was drawn from point A at the end of the curve at $P/P_y = 1.0$ to the point of tangency at B and extended to intersect the vertical axis at

$h\sqrt{F_y}/w = 660$. This approximation results in conservative limitations of $h\sqrt{F_y}/w$ for low values of P/P_y . This is desirable however in order to avoid the sensitivity of the steep theoretical gradient in this region as well as to recognize the possibility of small unavoidable axial loads that may occur in service.

As can be seen from Figure 6.11, the theoretical method presented herein predicts more liberal web limitations than those presently required for Class 2 sections. However, implicit in these limitations is the use of M_{pc} as defined by Equation 6.10 based on local buckling considerations rather than the use of M_{pc} as defined on a strength basis by Equations 6.9. Referring to Figure 6.11, the web limitation for pure beam action at $P/P_y = 0.0$ is $h\sqrt{F_y}/w = 660$. As P/P_y increases, the web is subjected to decreasing amounts of flexural tension. As a result, the $h\sqrt{F_y}/w$ limitation decreases linearly to a minimum value of 300 for pure column action at $P/P_y = 1.0$. In the region of pure bending ($P/P_y = 0.0$), this theoretical limitation differs by about +27 per cent from that presently specified by Equations 6.7 and 6.8. As P/P_y increases this difference increases to a maximum of about 45 per cent at $P/P_y = 0.15$ and decreases to a minimum of +18 per cent for pure column action at $P/P_y = 1.0$. As explained previously, the theoretical limitations are based on the assumption that the maximum moment in the presence of axial load is that given by Equation 6.10. The presently specified limitations, on the other hand, are based on the results of test specimens whose moment capacities equalled or exceeded that given by Equations 6.9. In addition to the above theoretical limitations, the analytical method presented herein also gives results in good agreement with these test

results when the effects of the rigid plate boundary constraints necessary for testing are included. The marked difference between the theoretical limitations and the presently specified limitations is therefore largely attributable to the effects of necessary constraints used during testing.

6.4.3 Class 1 Beam-Columns

A Class 1 beam-column is proportioned so that the flange width-to-thickness term $b\sqrt{F_y}/2t = 54$. As discussed in Sections 6.2 and 6.3.3, this value was found to be adequate at the two extremes of beam-column action, namely pure axial strain and pure flexural strain. The behaviour of Class 1 beam-columns was investigated for a range of values of P/P_y between zero and one, and for values of $h\sqrt{F_y}/w$ between 325 and 800. The results of this investigation are presented in the form of interaction curves in Figure 6.12, where values of P/P_y are plotted against values of M_{cr}/M_p for various values of $h\sqrt{F_y}/w$.

Unlike those for Class 2 and Class 3 sections, the interaction curves for Class 1 sections do not become tangential to a line joining the points at $P/P_y = 1.0$ and $M_{cr}/M_p = 1.0$. For Class 2 and Class 3 sections it was found that at a given value of P/P_y , the maximum critical moment value is determined by flange local buckling capacity. However, in the present case, local buckling is controlled by the web for values of M_{cr}/M_p less than about 1.05. Since web buckling controls, for a given value of P/P_y an increase in the sturdiness of the web (corresponding to a reduced $h\sqrt{F_y}/w$ value) will result in an increase in the value of M_{cr}/M_p . Thus the curves in Figure 6.12 do not become tangential but rather, they are separated to

the right of one another as $h\sqrt{F_y}/w$ decreases.

In the region of pure flexural strains, an upward sweep of the curves is evident for values of $h\sqrt{F_y}/w$ less than or equal to 600. This is apparently due to two factors. Firstly, as the region of pure flexural strain is approached in the vicinity of $M_{cr}/M_p = 1.05$, the mode of failure changes from web buckling to flange buckling. The second factor which contributes to this upward sweep is the effect of strain-hardening on the flange. (It is shown in Figure 6.15 that a reduction in the value of E_{st} reduces this upward sweep).

Referring again to Figure 6.12, the equation of the line joining the points, $P/P_y = 1.0$ and $M_{cr}/M_p = 1.0$ is given by Equation 6.10 and is restated here as follows:

$$\frac{M_{cr}}{M_p} = \left(1 - \frac{P}{P_y}\right) \quad (6.10)$$

For all values of $h\sqrt{F_y}/w$ corresponding to the curves shown in the figure, the moment ratio given by Equation 6.10 is either equalled or exceeded for certain values of P/P_y . This implies that the strain-hardening strain may be reached or exceeded for these values and therefore the hinge rotation necessary for plastic design sections is attainable. For values of $h\sqrt{F_y}/w$ equal to 325 and 350, the effect of strain-hardening is more pronounced as indicated by the increased slopes of the corresponding curves.

The cross-sectional strength interaction equation commonly used for plastic design sections^{63,64} is also shown in Figure 6.12. This is described by Equations 6.9 as stated previously and repeated here for convenience as follows:

$$M_{pc} = M_p \quad 0 \leq P/P_y \leq 0.15 \quad (6.9(a))$$

$$M_{pc} = 1.18 M_p (1 - P/P_y) \quad 0.15 \leq P/P_y \leq 1.0 \quad (6.9(b))$$

These values are applicable as long as local and overall instability do not occur. The validity of Equations 6.9 has been verified experimentally using W12 x 36, W8 x 31, W4 x 13, and W14 x 78 sections^{5,63,64,66} with values of $b\sqrt{F_y}/2t$ of 38, 60, 39 and 53, and values of $h\sqrt{F_y}/w$ of 206, 153, 84 and 186, respectively. For these plate width-to-thickness terms the theory presented herein verifies that local buckling indeed is not critical in these sections and therefore does not interfere with the strength limitation as given by Equations 6.9. However, it should be noted that the specimens used for the experimental verification of the strength limitation are considerably sturdier than those presently designated as Class 1 sections.

6.4.3.1 Current Specifications

As mentioned previously, Class 1 sections are those for which the flange width-to-thickness term is presently limited to 54. Under pure axial loading the web width-to-thickness term for all W shapes is presently limited to 255 and for pure beam action the limit⁴ is set at 420. In the intermediate range where beam-column action is required, a bi-linear curve is applicable. This bi-linear relationship is presently expressed as follows⁴:

$$h\sqrt{F_y}/w = 255 \quad 0.28 \leq P/P_y \leq 1.0 \quad (6.12)$$

$$h\sqrt{F_y}/w = 420 (1 - 1.4 P/P_y) \quad 0 \leq P/P_y \leq 0.28 \quad (6.13)$$

The current code width-to-thickness limitation for column webs is set at $h\sqrt{F_y}/w = 255$. This value is based upon the results of specimen D6, one of six tested by Haaijer and Thurlimann⁷. The current web limitations for Class 1 beam-columns are based on semi-empirical values obtained by Haaijer and Thurlimann. Although no beam-columns were tested, they used the test results of specimens D2, D4, and D6 in which the webs were uniformly compressed. It was then assumed that values obtained at the level of critical strain for these specimens could be applied at the level of mean strain in the compression zone of a beam-column. Although the analysis did not directly incorporate the effects of residual stresses, in the region of critical stress between the proportional limit and complete yield, a transition curve was fitted on the basis of geometric considerations.

According to the present theory, the current value of $b\sqrt{F_y}/2t = 54$ is an adequate limitation for Class 1 sections and no reduction or increase is indicated. It is apparent, however, that the present web width-to-thickness limitations for these sections are conservative. The present theory predicts that the value of $h\sqrt{F_y}/w$ can be increased for all values of P/P_y .

6.4.3.2 Theoretical Limitations as Determined Herein

Class 1 beam-columns are required to reach and sustain the reduced plastic moment capacity through a hinge rotation sufficient for the redistribution of stresses within a structure prior to collapse^{4,33,63}. Because of the stricter requirements, these sections

should be expected to satisfy the strength limitations of Equations 6.9. In fact, the theoretical method presented herein predicts that this is so and that the present web limitations are somewhat conservative for Class 1 sections.

Values of P/P_y versus M_{cr}/M_p are plotted for various values of $h\sqrt{F_y}/w$ for Class 1 sections as shown in Figure 6.12. The strength relationship given by Equations 6.9 is also plotted in this figure. As shown in Figure 6.12 the local buckling capacity equals or exceeds the strength capacity of Equations 6.9 for some values of $h\sqrt{F_y}/w$. Values of P/P_y may be determined at the points of intersection of the local buckling curves with the strength curve of Equations 6.9. The corresponding values of $h\sqrt{F_y}/w$ are plotted against P/P_y values in Figure 6.13.

The resulting curve has a value of $h\sqrt{F_y}/w = 800$ for pure beam action ($P/P_y = 0.0$). For a relatively small increase of P/P_y from zero to about 0.08 the $h\sqrt{F_y}/w$ values decrease rapidly to a value of 430. As P/P_y increases, a sharp knee portion of the curve occurs and at $P/P_y = 0.23$ and $h\sqrt{F_y}/w = 370$ the curve becomes linear with a slight drop in $h\sqrt{F_y}/w$ to about 360 as P/P_y increases to 0.75. As P/P_y increases further, a slightly rounded portion of the curve occurs with a gradual decrease in slope. The $h\sqrt{F_y}/w$ term reaches a value of 325 for pure column action ($P/P_y = 1.0$). (This value of $h\sqrt{F_y}/w$ is in contrast to a value of 300 for Class 2 and 3 sections. The slightly higher value for Class 1 sections is due to the effect of the sturdier flanges).

The curve described above may be approximated by a bilinear relationship given by:

$$h\sqrt{F_y}/w = 430 (1 - 0.93(P/P_y)) \quad 0 \leq P/P_y \leq 0.15 \quad (6.14)$$

and,

$$h\sqrt{F_y}/w = 382 (1 - 0.22(P/P_y)) \quad 0.15 \leq P/P_y \leq 1.0 \quad (6.15)$$

This approximation as well as the present web limitations given by Equations 6.12 and 6.13 are also shown in Figure 6.13.

In arriving at the above approximation, point A is located at $P/P_y = 1.0$ and $h\sqrt{F_y}/w = 300$. This value of $h\sqrt{F_y}/w$ is used here so that for pure column action, the web limitations for Class 1, 2, and 3 beam-columns would coincide at a value of $h\sqrt{F_y}/w = 300$. (As explained previously, the value of $h\sqrt{F_y}/w = 325$ for Class 1 sections is due to the sturdier flanges). Point C on Figure 6.13 is located on the vertical axis opposite point D where the initial portion of the curve first deviates from the tangent to the curve at $P/P_y = 0$. Through points A and C, tangents to the curve are drawn and extended to intersect at point B ($P/P_y = 0.15$).

The reason for constructing line BC in this manner is twofold. In the region of low axial loads (corresponding to line CD) the web width-to-thickness term is very sensitive to small changes in the axial load. This is witnessed by the very steep gradient of the initial portion of the curve. Since a value of low axial load would be very difficult to pin-point with any great degree of accuracy (in a practical design case) line BC is constructed to eliminate the effect of this high sensitivity for practical applications. Furthermore, in practical cases, it is very likely that residual axial loads of low magnitudes will be present to some degree even in members

designed for pure bending. This effect is also accounted for by the above construction.

As seen from Figure 6.13, the theoretical method presented herein predicts more liberal web limitations than those presently required for Class 1 sections. For pure beam action at $P/P_y = 0.0$, the present theory indicates a web limitation of $h\sqrt{F_y}/w = 430$ which is about 2 per cent greater than the presently specified value of 420 (Equation 6.13). As P/P_y increases to 0.15, $h\sqrt{F_y}/w$ decreases to 370 and, as P/P_y further increases, the maximum difference between the presently specified value of $h\sqrt{F_y}/w$ and that predicted by the analysis presented herein occurs at $P/P_y = 0.28$. At this point, the presently specified value of $h\sqrt{F_y}/w$ is 255 whereas the theory presented herein predicts a value about 40 per cent higher. As P/P_y increases, this difference decreases and at $P/P_y = 1.0$ the theory presented herein indicates a value about 18 per cent higher than the presently specified value of $h\sqrt{F_y}/w = 255$.

6.4.4 Effects of Residual Stresses

The effects of residual stresses on the local buckling capacities of beam-column sections were investigated for values of $b\sqrt{F_y}/2t = 54, 64$, and 72. Since the effects are similar in all three cases, only one such case will be presented here. For a value of flange slenderness of 54 (corresponding to a Class 1 section) and various values of web slenderness, beam-column interaction curves are shown in Figure 6.12 for $\sigma_{rc} = 0.3\sigma_y$ and in Figure 6.14 for a theoretical value of $\sigma_{rc} = 0$.

The rounded knee portions of the curves in Figure 6.12 are

due to residual stresses which result in a gradual yielding within a cross-section. As shown in Figure 6.14, these rounded knee portions change to an abrupt transition in the absence of residual stresses. As can be seen, a Class 1 beam-column can perform adequately over a range of web slendernesses between 440 and 1000 where the residual stress has a theoretical value of zero. In the presence of a practical value of residual stress of $\sigma_{rc} = 0.3\sigma_y$, on the other hand, Figure 6.12 shows that these web slenderness values are reduced to 325 for pure column action and 800 for pure beam action.

6.4.5 Effects of Strain-hardening Modulus

The effect of varying the strain-hardening modulus on the local buckling capacities of beam-columns was studied for flange slenderness values of 54, 64, and 72. The same three values of strain-hardening modulus used in the study of column and beam local buckling were also used here. For $b\sqrt{F_y}/2t$ values of 72 and 64 and practical values of $h\sqrt{F_y}/w$ between 300 and 800 as used in the interaction diagrams and shown in Figures 6.8 and 6.10, the values of E_{st} investigated had no effect on local buckling capacities. For Class 1 sections ($b\sqrt{F_y}/2t = 54$) and practical values of web slenderness between 325 and 800 (as used in Figure 6.12) the effect of varying the strain-hardening modulus is significant for certain values of $h\sqrt{F_y}/w$.

For the values of strain-hardening modulus considered, Figure 6.15 shows the interaction curves corresponding to $b\sqrt{F_y}/2t = 54$ and values of $h\sqrt{F_y}/w$ of 325, 500 and 800. These three values were chosen as being representative of the range of web slendernesses considered practical for Class 1 sections. When $h\sqrt{F_y}/w = 325$, the

effect of strain-hardening is present over the entire length of the curve. For pure beam action ($P/P_y = 0$), the effect of the strain-hardening modulus is quite significant. As P/P_y increases this effect diminishes and is least significant when pure column action ($P_{cr}/P_y = 1.0$) is approached. As $h\sqrt{F_y}/w$ is increased the significance of strain-hardening (for the values investigated) becomes less noticeable. At $h\sqrt{F_y}/w = 500$ the effect of varying E_{st} is noticeable at the point of pure beam action ($P/P_y = 0$). As P/P_y increases, this effect decreases and is no longer evident for values of P/P_y between 0.5 and the critical load ratio. As $h\sqrt{F_y}/w$ is further increased, the effect of varying the strain-hardening modulus over the range considered also decreases. At $h\sqrt{F_y}/w = 800$ no effect of changing the value of the strain-hardening modulus is evident. As can be seen from Figure 6.15, for the range of values of strain-hardening modulus considered, a Class 1 beam-column section has adequate performance with regard to local buckling capacity.

6.4.6 Effects of Specimen Length

It has been thoroughly demonstrated by several investigators^{2, 3, 6, 16, 26} that critical plate buckling stresses approach relatively high values with decreasing values of aspect ratio (the ratio of the length of a plate in the direction of uniaxial stress to its transverse dimension). At a theoretical aspect ratio equal to zero, the critical buckling stress is infinite and as the aspect ratio increases for a given specimen, the predicted critical buckling stress rapidly decreases. At some point a value of the aspect ratio will be reached above which the predicted critical stress becomes stable. This

behaviour is illustrated in Figure 6.16 for a column having a flange slenderness value of 72 and a web slenderness value of 300. As the length, L , increases from zero, the critical load ratio drops rapidly and reaches a stable value for length values greater than 12. This corresponds to an aspect ratio of 2.4 for the flanges and 1.2 for the web for this particular specimen.

Investigations similar to the above have been carried out for additional columns, beams, and beam-columns of various dimensions. From this analysis it was determined that stable values of critical local buckling stress would be reached for all specimens having minimum aspect ratios of 4 for the flanges and 2 for the webs.

Figure 6.17 summarises the findings of this investigation by showing the length effects on the interaction diagrams of Class 1 beam-columns having web slenderness values of 325, 500, and 800. A Class 1 beam-column was chosen so that the length effect could be evaluated for a range of values of load ratio and moment ratio as well as a range of material conditions from elastic to fully strain-hardened. These include those values that occur: (1) at an elastic or partially yielded stress level ($h\sqrt{F_y}/w = 800$), (2) at an elastic, partially yielded, or a strain-hardened stress level ($h\sqrt{F_y}/w = 500$), and (3) at a strain-hardened stress level ($h\sqrt{F_y}/w = 325$).

Each curve in Figure 6.17 was plotted for values of the length, L , of 15, 20, 25, and 30. These values correspond to flange aspect ratios of 3, 4, 5, and 6, and to web aspect ratios of 1.5, 2.0, 2.5, and 3.0. For all specimens the length effect is negligible in the region for which $M_{cr} > M_p(1-P/P_y)$. This corresponds to the region where complete yielding has occurred and strain-hardening is imminent.

Presumably a negligible effect of the variation of aspect ratios investigated occurs in this region because of the reduced stiffness of the material in the strain-hardening region. In the elastic region (the initially flat portion of the curves corresponding to $h\sqrt{F_y}/w = 500$ and 800) and the partially yielded region (the remaining portion of these curves up to the line $M_{cr} = M_p(1-P/P_y)$), the length effects are noticeable. For all cases considered however, the length effects are negligible for values of length of 20 or greater. A length value of 20 corresponds to a flange aspect ratio of 4 and a web aspect ratio of 2. As a result of this investigation, these aspect ratios were the minimum values used for all specimens in the parametric studies presented herein.

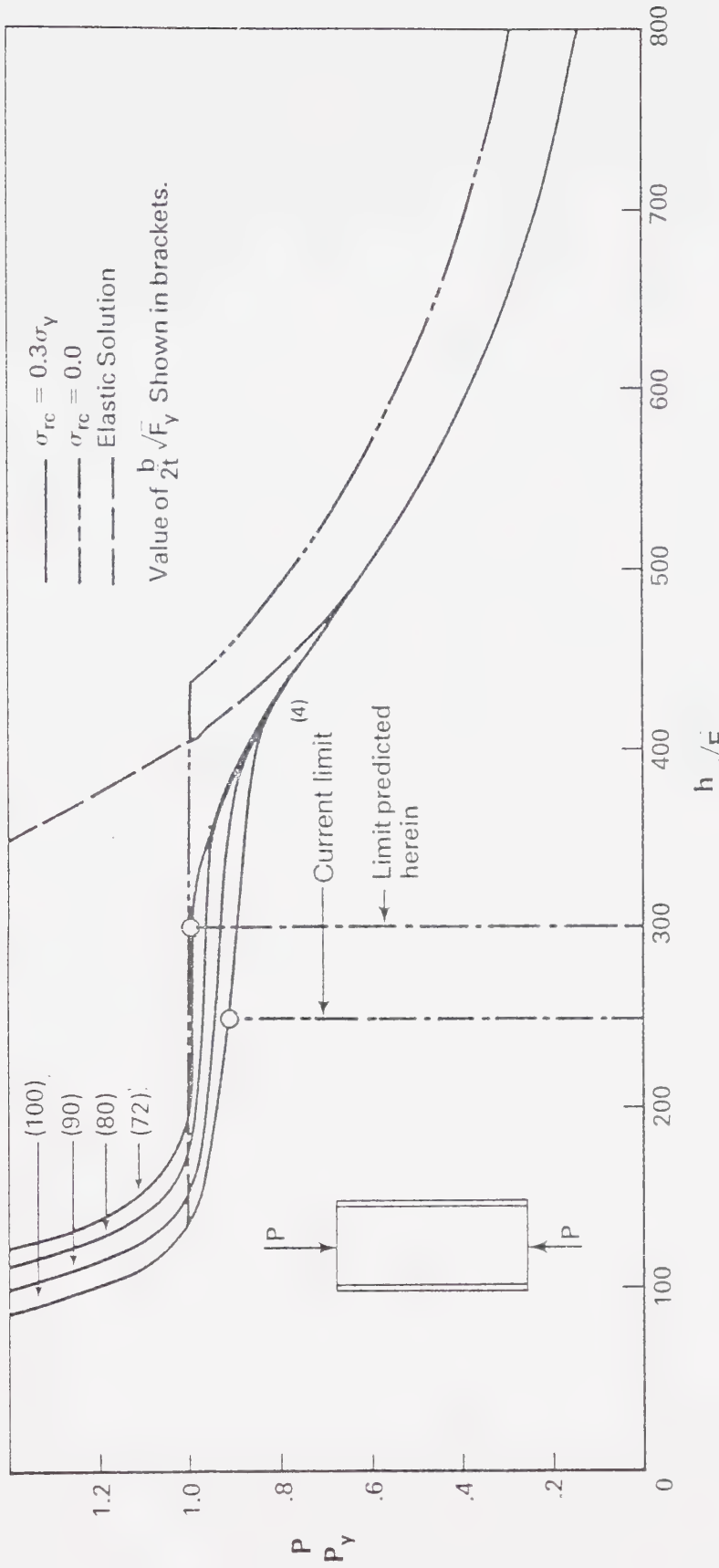


Figure 6.1 Effect of $\frac{h_w}{\sqrt{F_y}}$ on $\frac{P}{P_y}$ for Various Values of $\frac{b}{2t\sqrt{F_y}}$

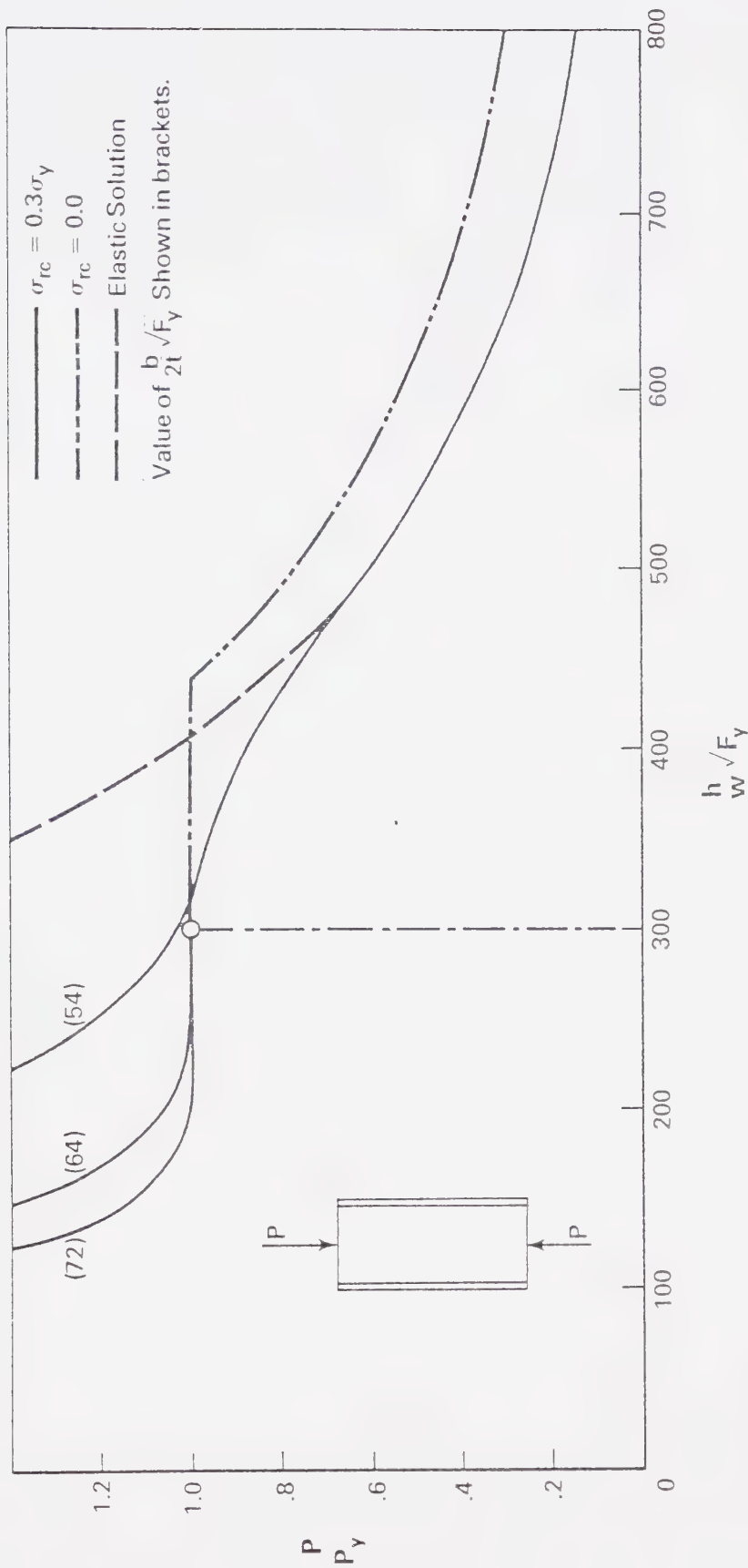


Figure 6.2 Effect of $\frac{h_w}{2t}\sqrt{F_y}$ on $\frac{P}{P_y}$ for $\frac{h_w}{2t}\sqrt{F_y}$ Values of 54, 64, and 72.

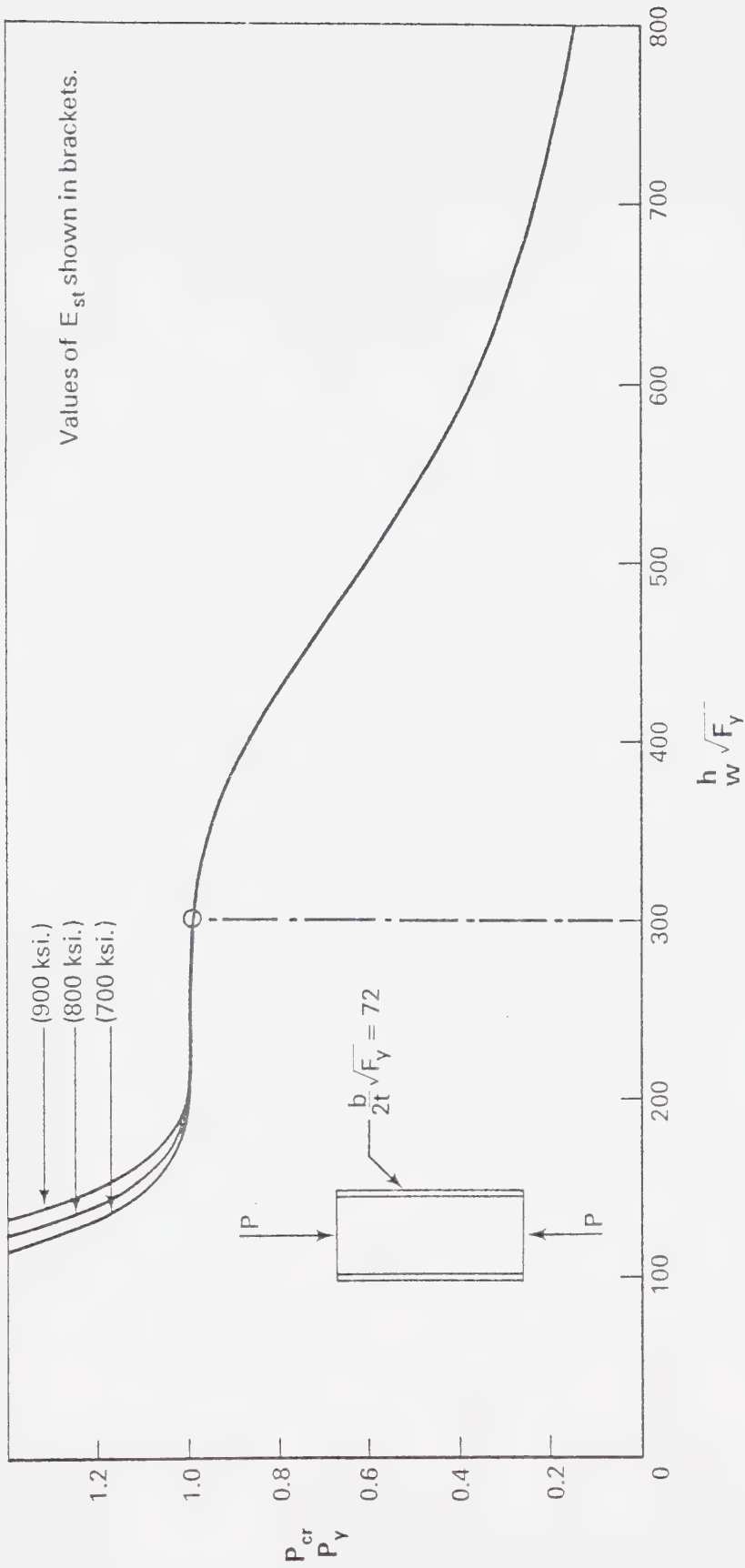


Figure 6.3 $\frac{P_{cr}}{P_y}$ vs. $\frac{h}{w} \sqrt{F_y}$ for Values of $E_{st} = 700, 800$, and 900 ksi.

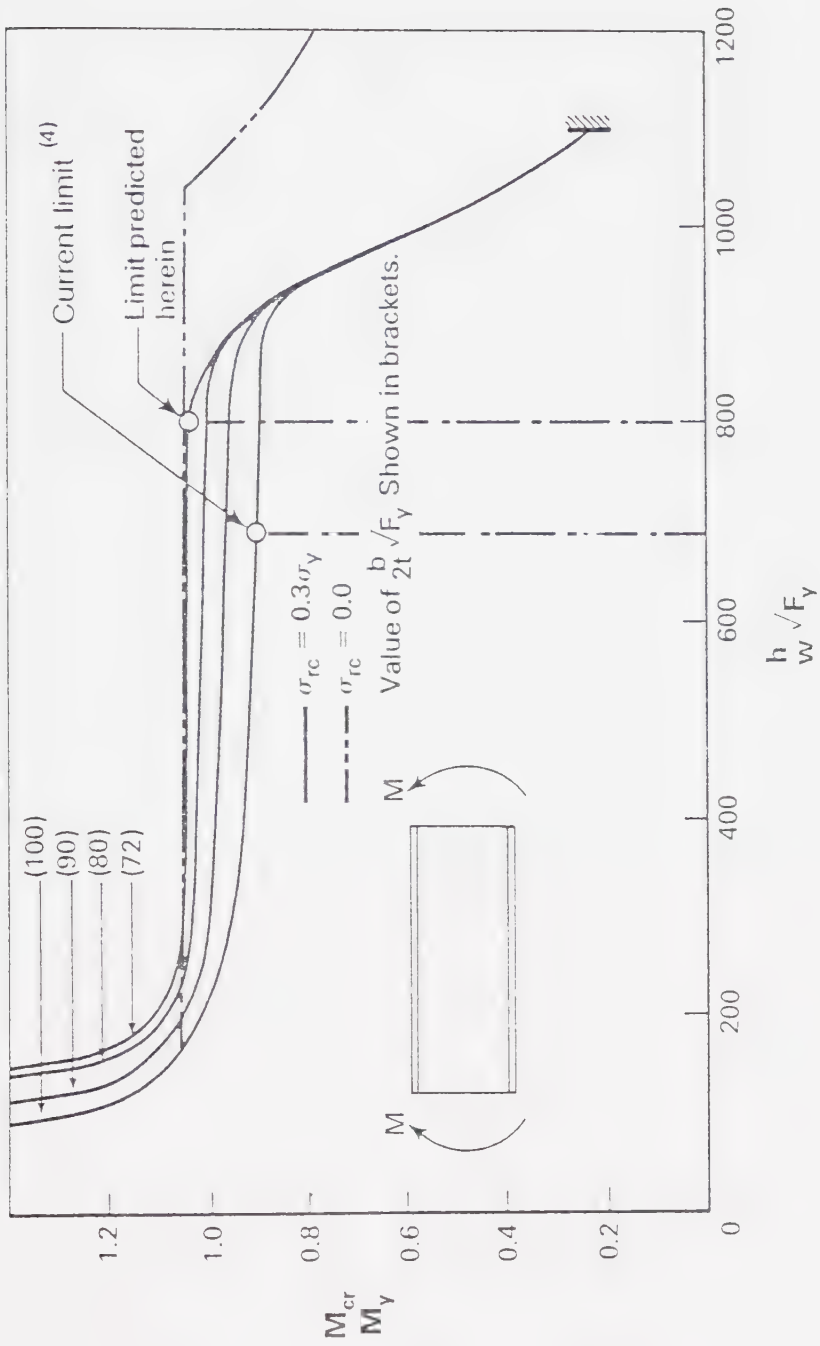


Figure 6.4 Effect of $\frac{h_w}{w} \sqrt{F_y}$ on $\frac{M_{cr}}{M_y}$ for Various Values of $\frac{b}{2t \cdot F_y}$

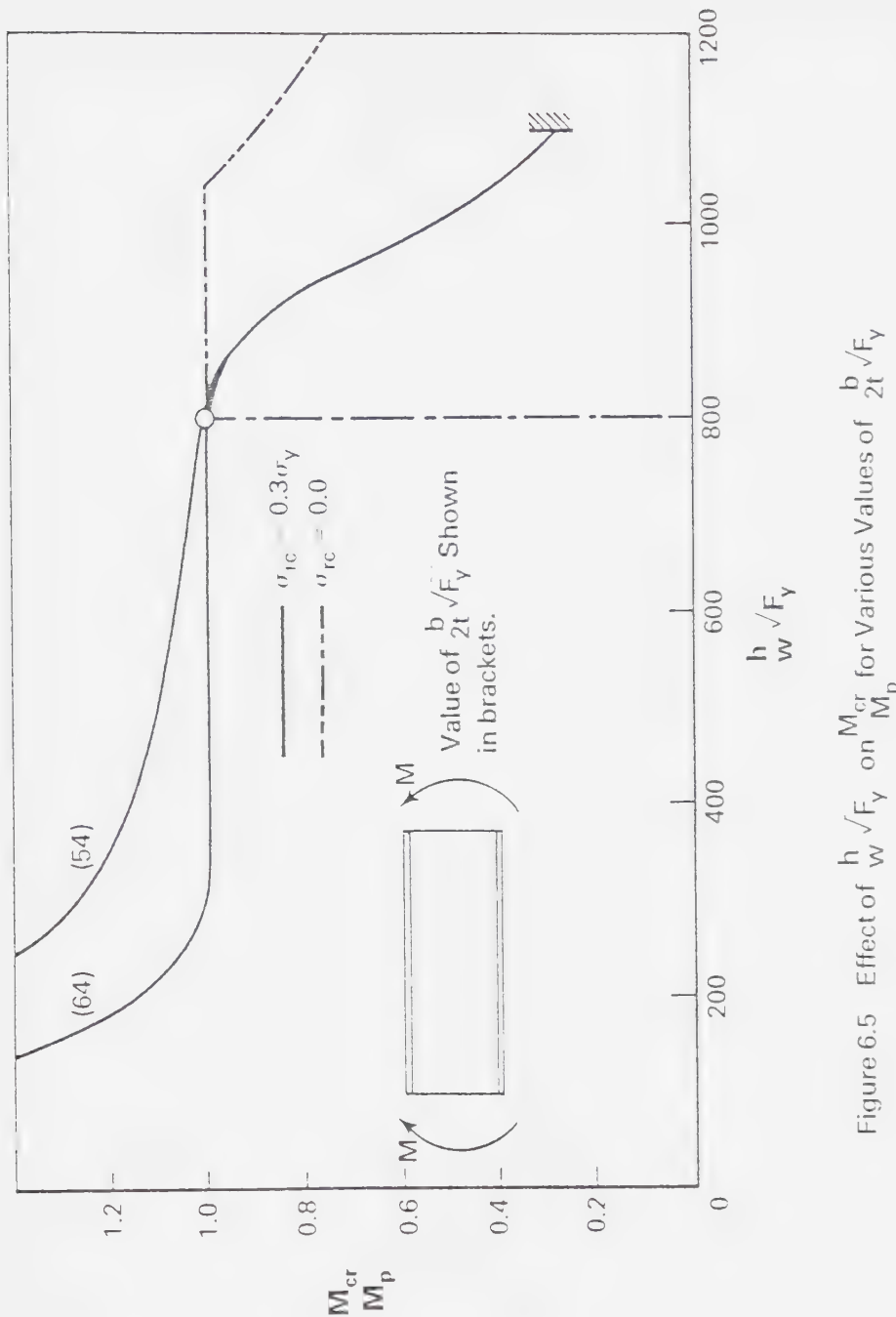


Figure 6.5 Effect of $h_w/\sqrt{F_y}$ on M_{cr}/M_p for Various Values of $b/(2t\sqrt{F_y})$

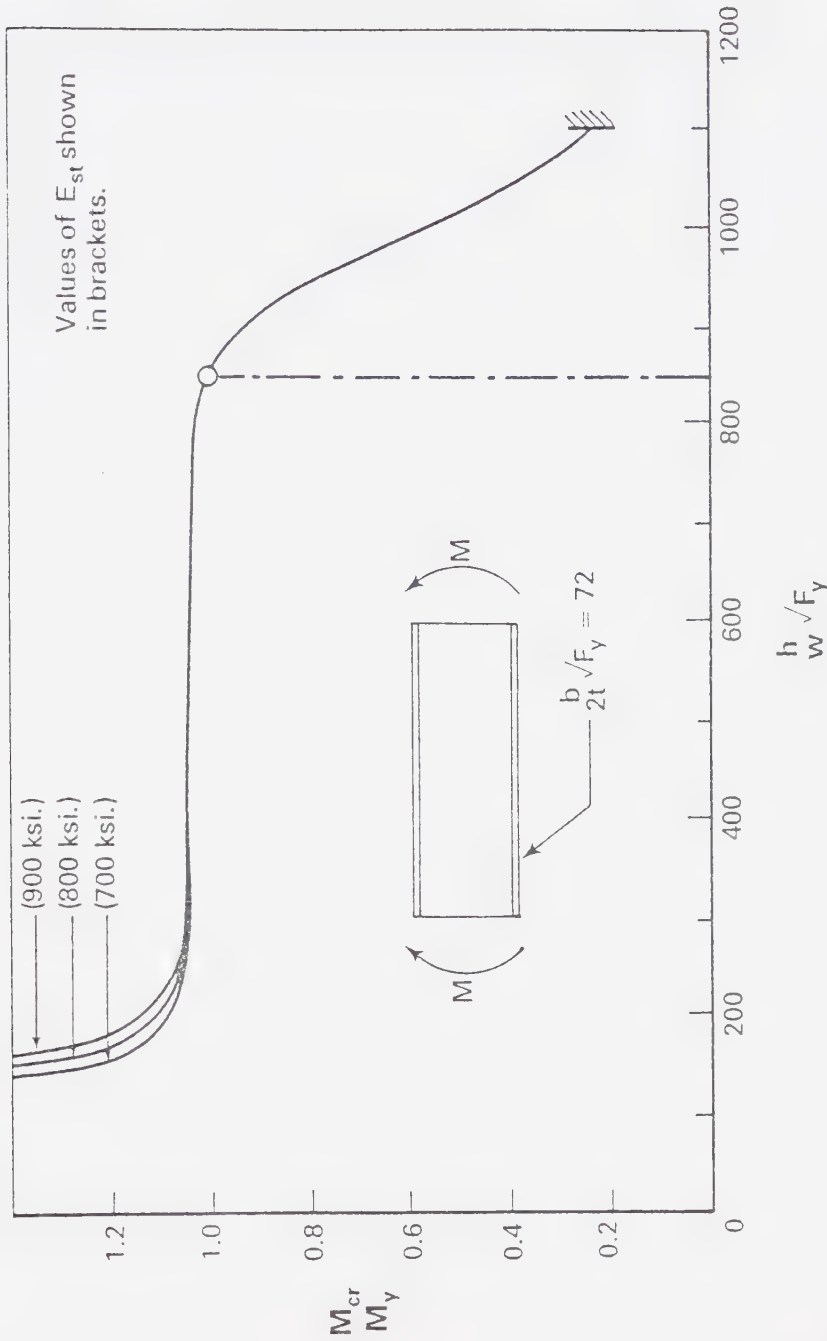


Figure 6.6 M_{cr} vs. $\frac{h_w}{\sqrt{F_y}}$ for Values of $E_{st} = 700, 800$, and 900 ksi.

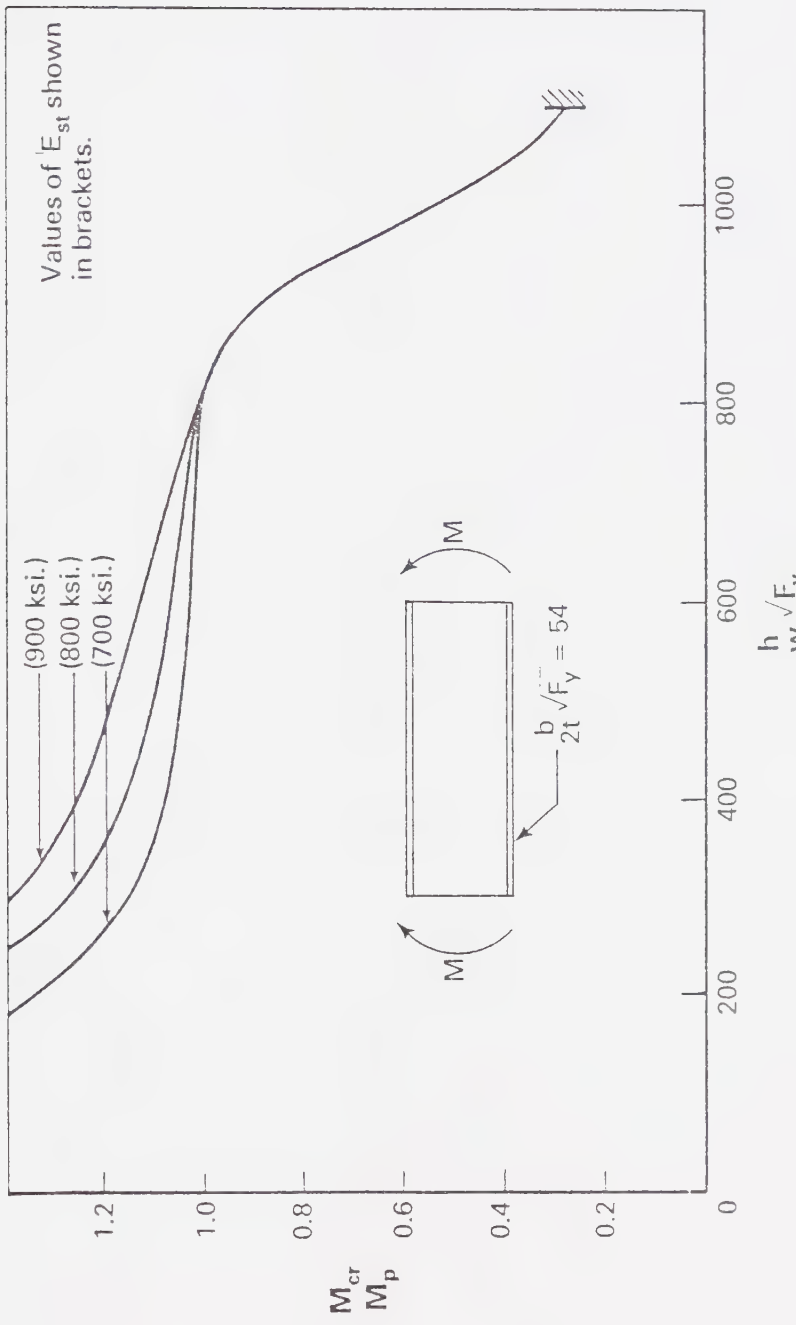


Figure 6.7 $\frac{M_{cr}}{M_p}$ vs. $\frac{h_w}{\sqrt{F_y}}$ for Values of $E_{st} = 700, 800$, and 900 ksi.

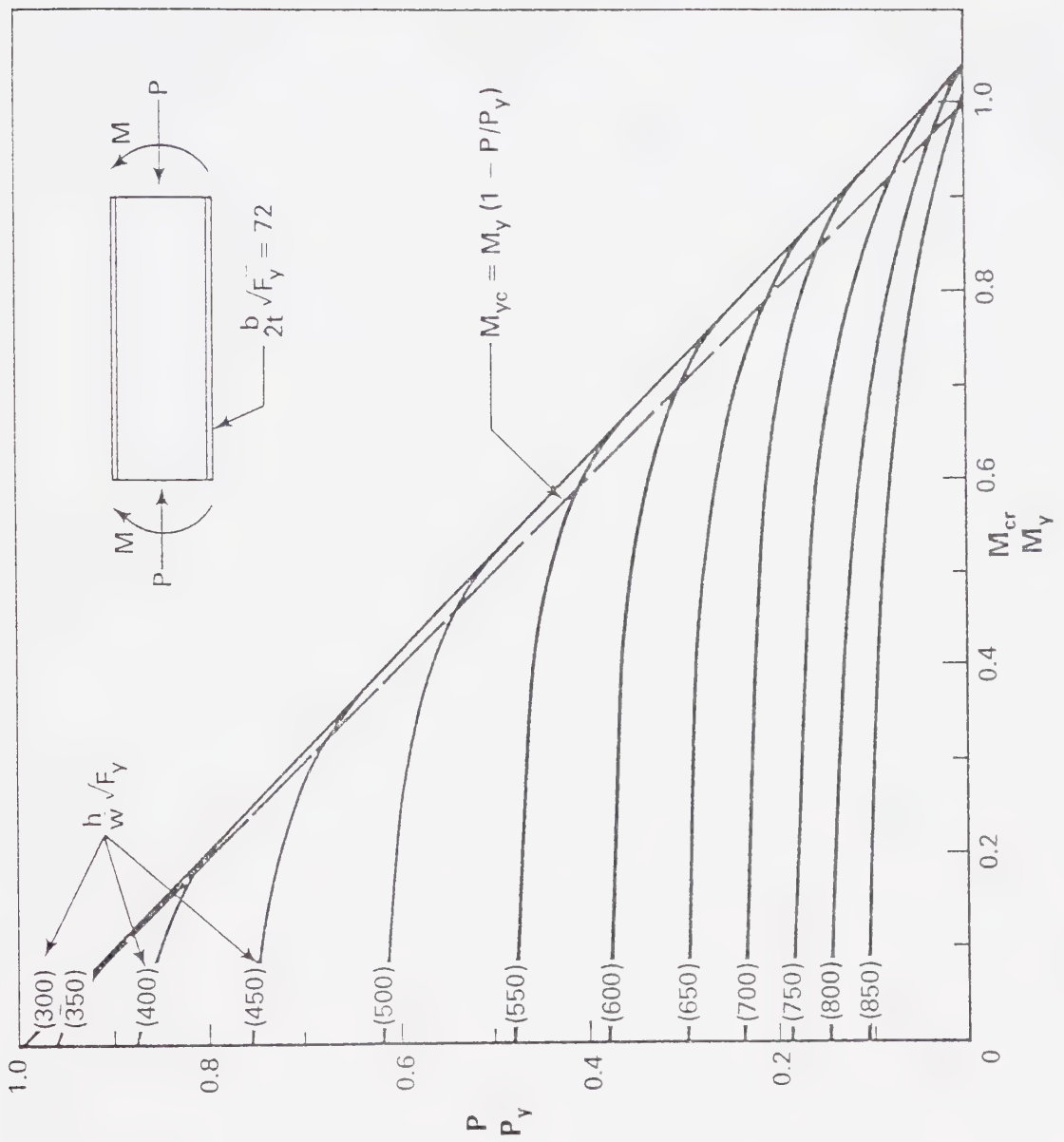


Figure 6.8 Effect of $\frac{P}{P_y}$ on $\frac{M_{cr}}{M_y}$ for Various Values of $\frac{h_w}{\sqrt{F_y}}$

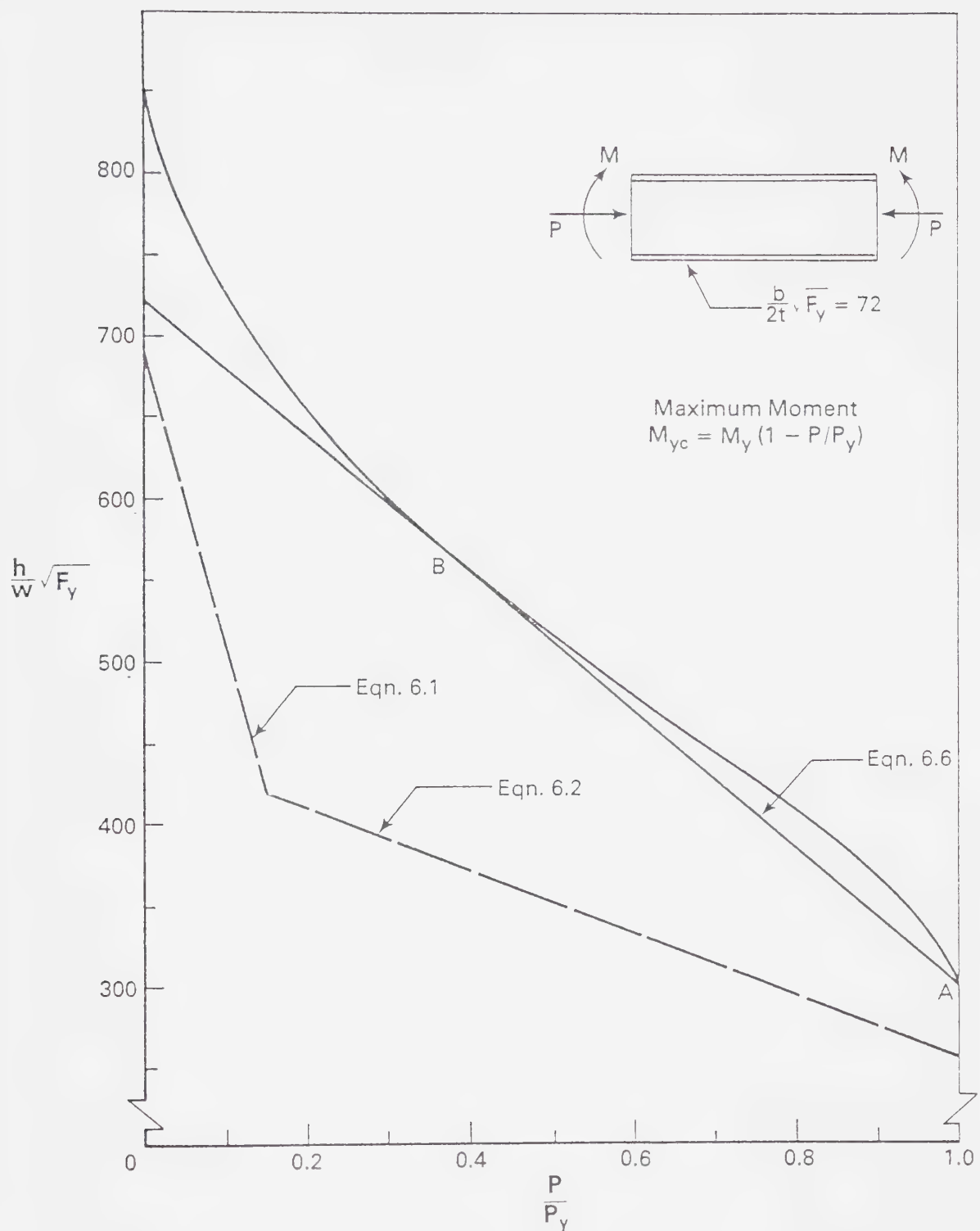


Figure 6.9 $\frac{h}{w} \sqrt{F_y}$ vs. $\frac{P}{P_y}$ for a Class 3 Section

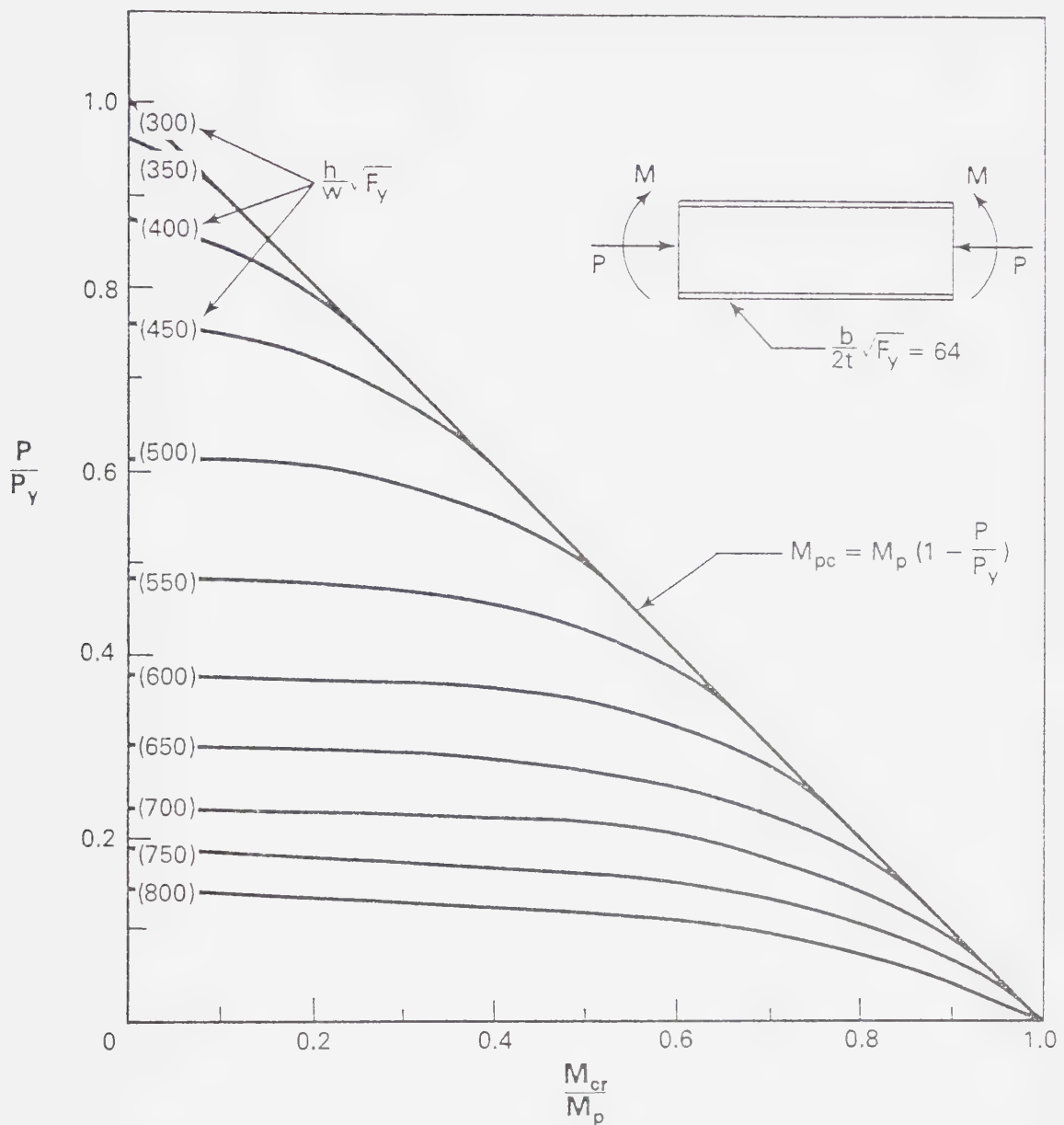


Figure 6.10 Effect of $\frac{P}{P_y}$ on $\frac{M_{cr}}{M_p}$ for Various Values of $\frac{h}{w} \sqrt{F_y}$

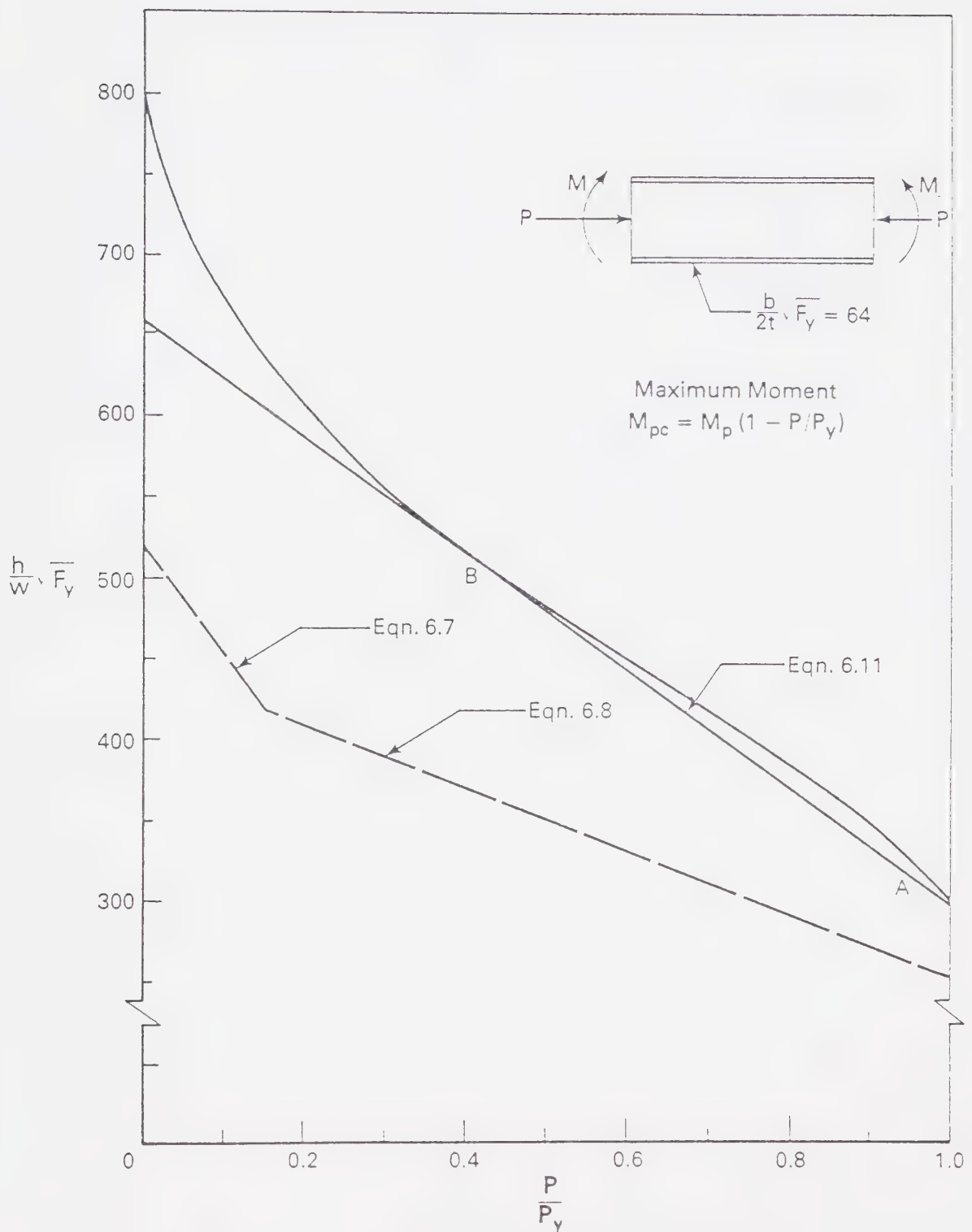


Figure 6.11 $\frac{h}{w} \sqrt{F_y}$ vs. P/P_y for a Class 2 Section

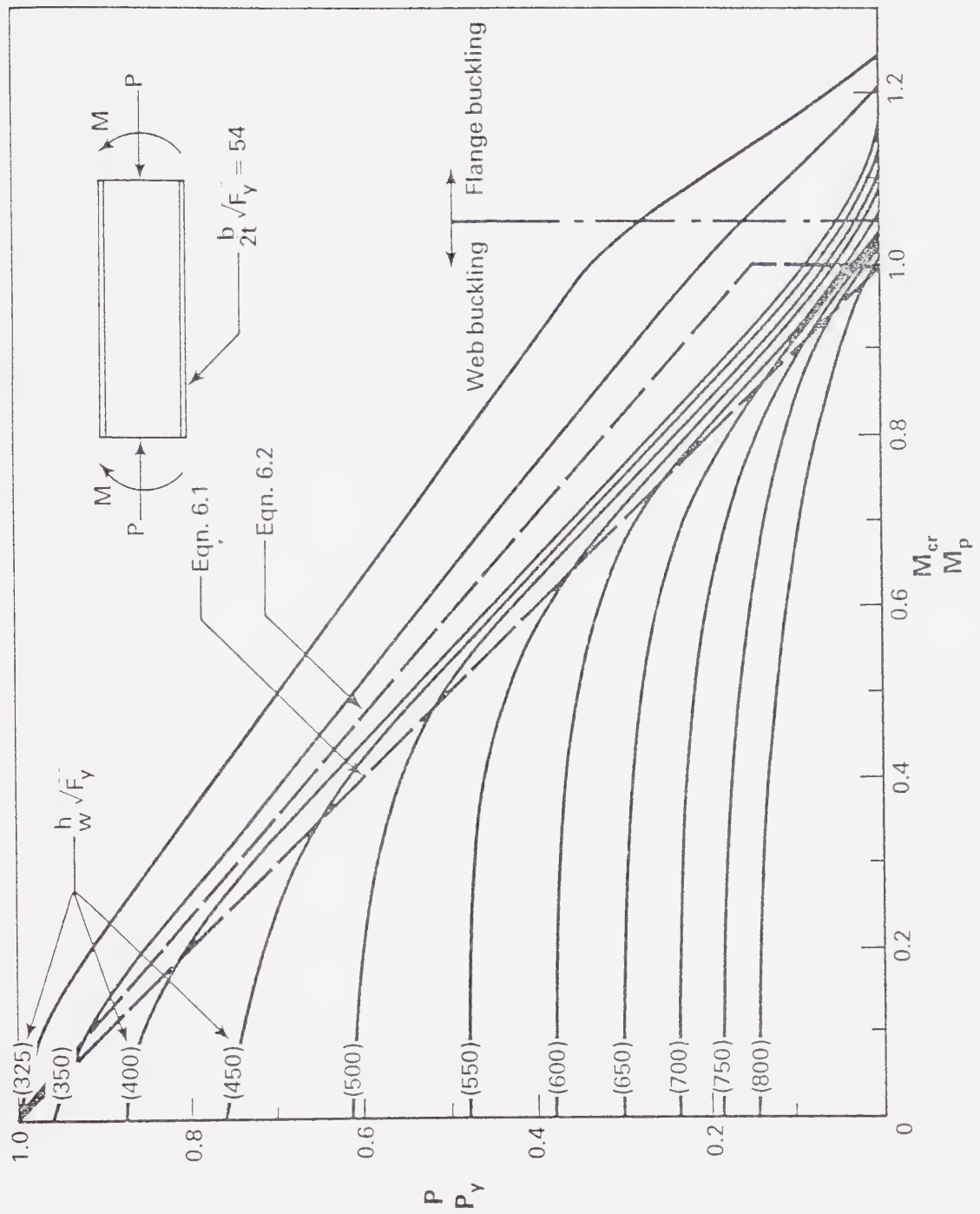


Figure 6.12 Effect of P/P_y on M_{cr}/M_p for Various Values of $h_w/\sqrt{F_y}$

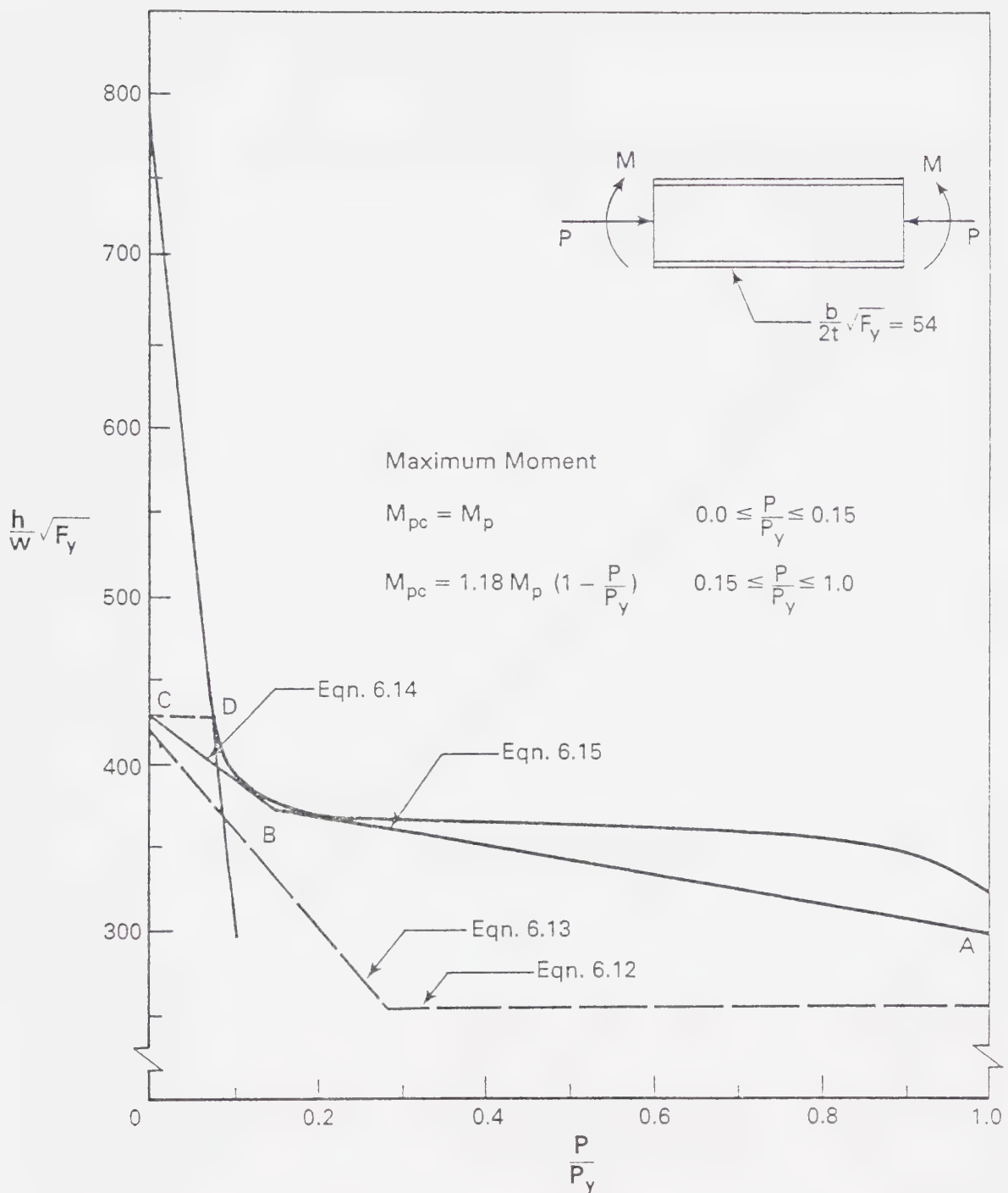


Figure 6.13 $\frac{h}{w} \sqrt{F_y}$ vs. $\frac{P}{P_y}$ for a Class 1 Section

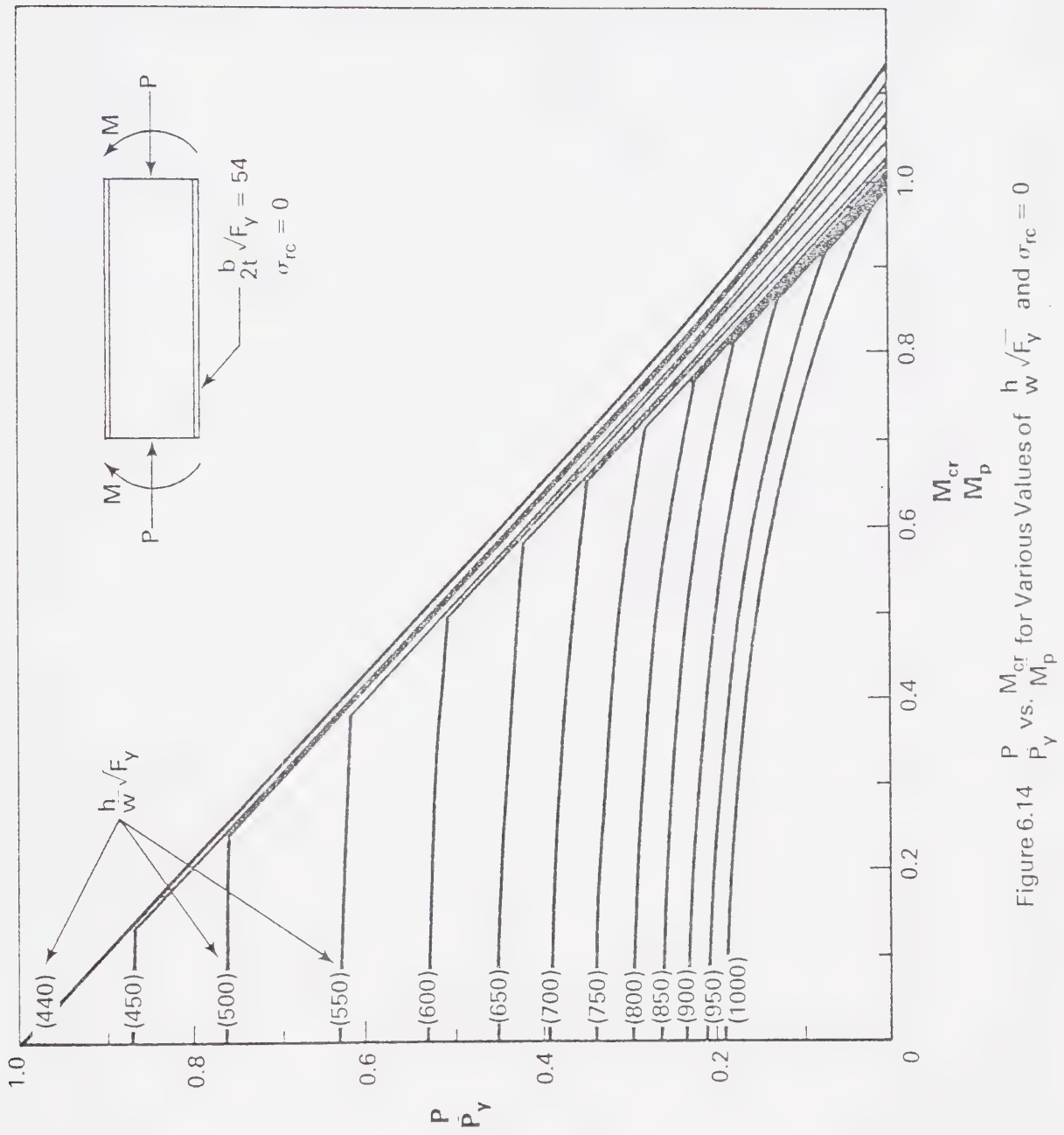


Figure 6.14 $\frac{P}{P_y}$ vs. $\frac{M_{cr}}{M_p}$ for Various Values of $\frac{h_w}{\sqrt{F_y}}$ and $\sigma_{rc} = 0$

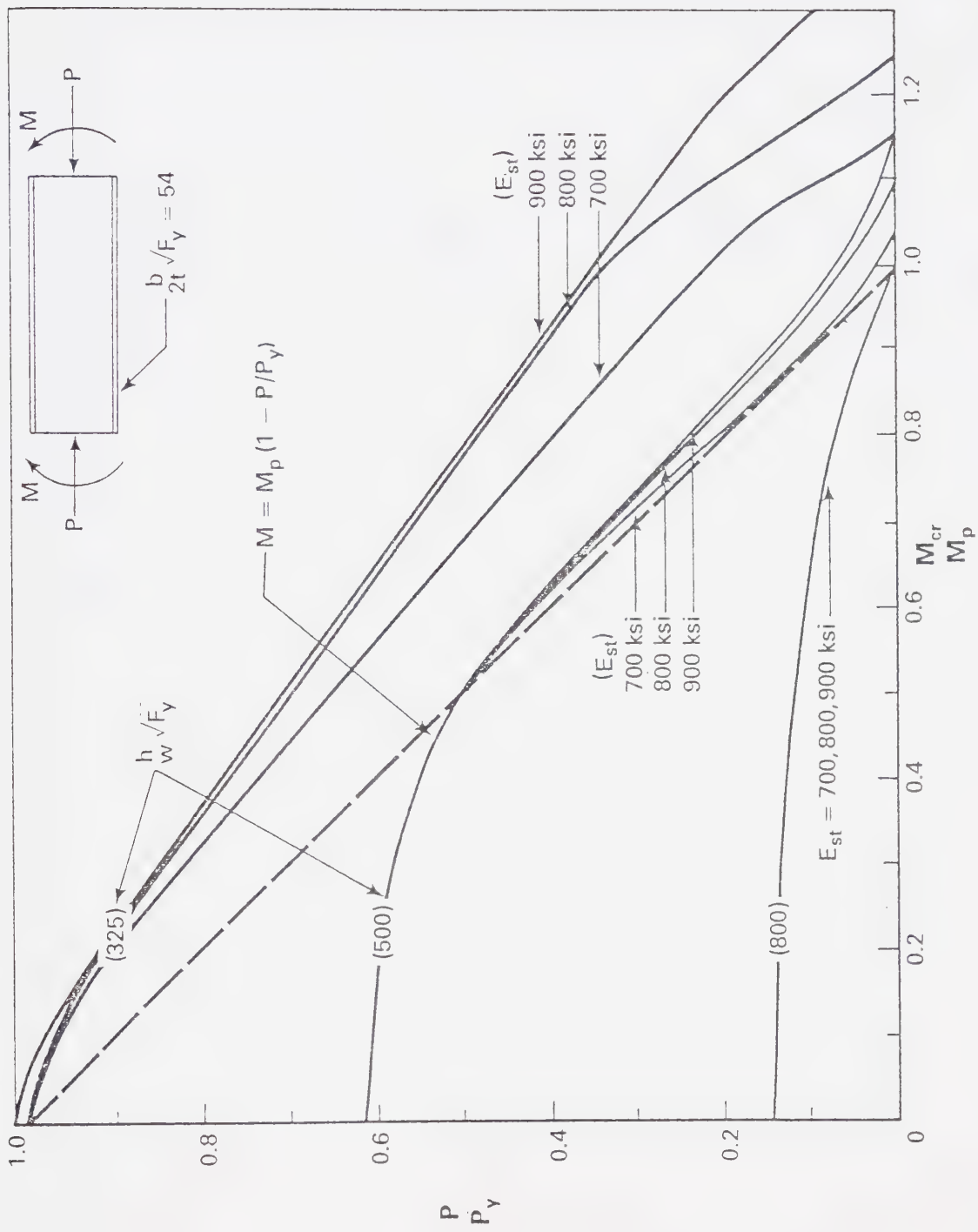


Figure 6.15 Effect of E_{st} on the Interaction of $\frac{P}{P_y}$ and $\frac{M_{cr}}{M_p}$

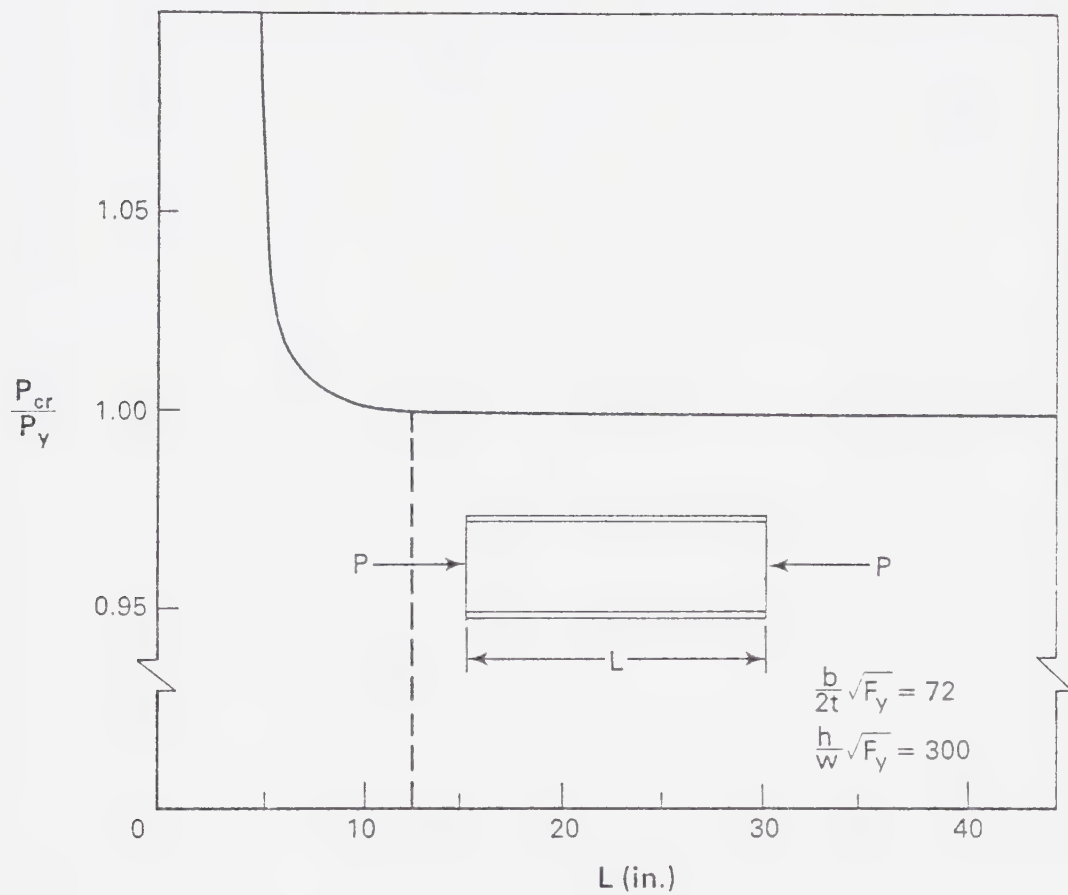


Figure 6.16 Effect of Length on Critical Load Prediction

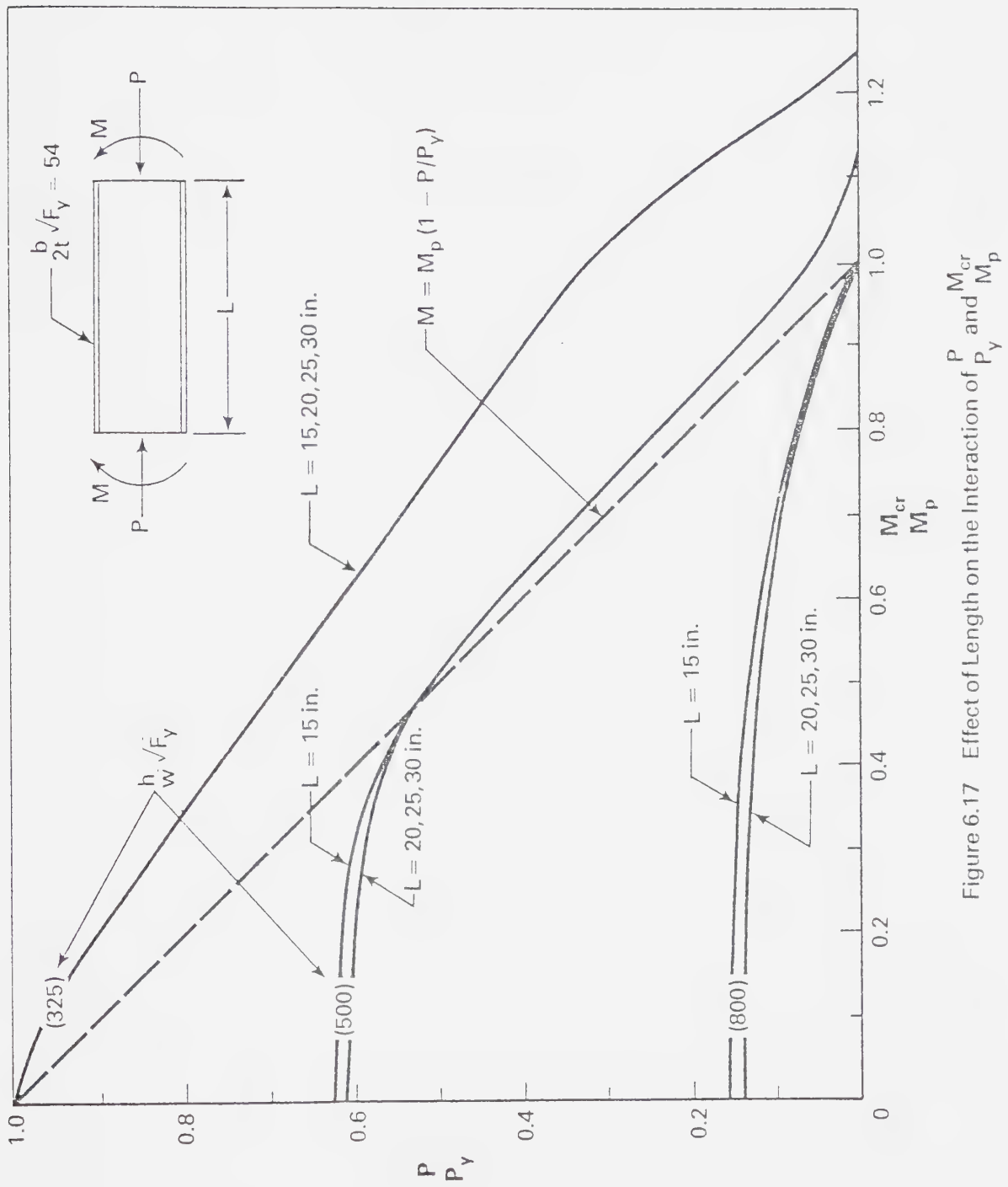


Figure 6.17 Effect of Length on the Interaction of $\frac{P}{P_y}$ and $\frac{M_{cr}}{M_p}$

Chapter 7

SUMMARY AND CONCLUSIONS

7.1 Introduction

The problem of local buckling of flange- and web-plate components of W-shapes subjected to axial compression, flexural compression, and axial and flexural compression combined has been extensively investigated. A review of the available literature in this area has revealed that a few investigators have previously attempted to deal with various aspects of this problem which is complex with respect to the practical difficulties of laboratory testing as well as with respect to theoretical modelling. At the present time, among the more notable contributions in this area are those of Haaijer and Thurlimann⁷, Bleich⁶, Timoshenko^{2,26}, and Kulak^{10,11,12,13}. In all cases, however, the theoretical investigations have been either totally or partially empirical or semi-empirical in nature. Furthermore, only the latter investigator has attempted to include all aspects of the problem in an experimental program for Class 1, 2, and 3 sections subjected to the three types of loading mentioned above. The present investigation is an extension of this work and is primarily an attempt to formulate a sound theoretical basis for predicting both elastic and inelastic local buckling capacities of W shapes. In the following sections the scope of the theory is summarised, the findings are discussed with respect to existing design limitations and suggested modifications are indicated.

7.2 Summary of the Theoretical Method

The theoretical method presented herein has been formulated for the analysis of local buckling capacities of uniform members of W shape cross-sections. These members may be end-loaded in axial compression, flexural compression or combined axial and flexural compression. The flange - web restraint interaction is included directly in the formulation and the ends of a member may be rigidly supported or pinned with respect to plate buckling. The presence of residual stresses is accounted for by including their effects directly in the formulation of the local buckling geometric stiffness matrices of the plate components. Using an eigenvalue matrix iteration technique the elastic local buckling capacity is determined. If this value exceeds the proportional limit, an applied linear strain is gradually incremented above this limit and, at each level, gradual yielding of the section is evaluated and the position of the neutral axis is updated so that equilibrium conditions on the cross-section are satisfied. The member is then analysed for a critical eigenvalue strain. Essentially, when the critical eigenvalue strain is zero, the applied strain corresponds to the critical buckling strain. In this manner, the increase in strains and gradual yielding of a cross-section simulate actual conditions. Because of the flexibility of the shape functions used in the formulation, the method is capable of predicting separate flange or web buckling or a combination of both.

7.3 Summary of Findings

The present theoretical method has been verified by comparison of predicted results with the results of 53 test specimens of various dimensions and subjected to various load combinations.

Additionally, in the elastic range, the method gives results which agree with those predicted using widely acceptable classical methods^{2,6}. A large number of hypothetical beams, columns, and beam-columns for each class of section has also been investigated. As a result of this study the analytical method presented herein indicates that the present code limitation for flanges of Class 3 sections is inadequate. This limitation is based on a purely theoretical torsional analysis of the flange¹. For Class 1 and 2 sections, on the other hand, the analytical method presented herein substantiates the flange slenderness limitations of 54 and 64 which have been well established by experimental investigations. It is clear therefore, that the same theory which substantiates flange slenderness values of 54 and 64 based on experimental results for Class 1 and 2 sections, casts doubt upon the flange slenderness value of 100 based on an approximate torsional analysis of a Class 3 section flange. Assuming the above flange modification as indicated, presently specified web plate width-to-thickness limitations may be increased for columns, beams, and beam-columns.

7.4 Recommendations for Design

As a result of the theoretical investigation presented herein certain modifications of the present code values⁴ of plate width-to-thickness limitations are indicated. These modifications apply to W shapes subjected to axial, flexural, and combined axial and flexural loadings that are uniform along the member lengths. Additionally, certain flange width-to-thickness limitations presently set by the code have been substantiated. These results, as summarised in Figure 7.1, are discussed in the following sections.

7.4.1 Class 1 Sections

The present theory substantiates the use of $b\sqrt{F_y}/2t = 54$ for the flanges of Class 1 sections. It is indicated that the present limitation of $h\sqrt{F_y}/w = 255$ for pure axial loading can be safely increased to 300. For pure flexural loading an increase of $h\sqrt{F_y}/w$ from the present code value of 420 to a value of 430 is indicated. In the intermediate range, where combined axial and flexural loadings occur, the following increases in $h\sqrt{F_y}/w$ are indicated:

$$h\sqrt{F_y}/w = 430 \left(1 - 0.93 \left(\frac{P}{P_y}\right)\right) \quad 0 \leq \frac{P}{P_y} \leq 0.15 \quad (6.14)$$

$$h\sqrt{F_y}/w = 382 \left(1 - 0.22 \left(\frac{P}{P_y}\right)\right) \quad 0.15 \leq \frac{P}{P_y} \leq 1.0 \quad (6.15)$$

For these values the present theoretical method indicates that the following maximum moments reduced for axial load, can be sustained for adequate plastic design behaviour:

$$M_{pc} = M_p \quad 0 \leq \frac{P}{P_y} \leq 0.15 \quad (6.9(a))$$

$$M_{pc} = 1.18 M_p \left(1 - \frac{P}{P_y}\right) \quad 0.15 \leq \frac{P}{P_y} \leq 1.0 \quad (6.9(b))$$

7.4.2 Class 2 Sections

According to the present theoretical method, the value of $b\sqrt{F_y}/2t = 64$, as presently set by the code for Class 2 sections, is adequate with respect to local buckling provided that the maximum reduced moment value is set at:

$$M_{pc} = M_p (1 - P/P_y) \quad (6.10)$$

For pure axial loading it is indicated that the present web limitation of $h\sqrt{F_y}/w = 255$ can be increased to 300. For pure flexural loading the present value of $h\sqrt{F_y}/w = 520$ can be increased to 660. In the intermediate range of combined axial and flexural loading the following increases are indicated:

$$h\sqrt{F_y}/w = 660 (1 - 0.55 (P/P_y)) \quad 0 \leq P/P_y \leq 1.0 \quad (6.11)$$

7.4.3 Class 3 Sections

The present theoretical method indicates that the value of $b\sqrt{F_y}/2t = 100$ for flanges of Class 3 sections is too high. A reduction to a value of 72 is indicated. In the presence of pure axial loads the present value of $h\sqrt{F_y}/w = 255$ can be increased to 300 and, for beams, the present code value of $h\sqrt{F_y}/w = 690$ can be increased to 725. In the intermediate range where combined axial and flexural loadings occur the following increases are indicated:

$$h\sqrt{F_y}/w = 725 (1 - 0.59 (P/P_y)) \quad 0 \leq P/P_y \leq 1.0 \quad (6.6)$$

For these values a maximum moment value of

$$M_{yc} = M_y (1 - P/P_y) \quad (6.5)$$

can be reached in the presence of axial load. The above indicated modifications for Class 1, 2, and 3 sections are summarised in

Figure 7.1.

7.5 Further Recommendations

As a result of the tests performed by Kulak et al^{10,11,12,13}, increases in web limits for Class 2 and 3 sections have recently been implemented by the present code⁴. The theory presented herein indicates that these increases are also justified on a purely theoretical basis. Furthermore, according to this theoretical method, additional increases in web slendernesses are indicated with the reservations that Class 3 flange limits be set at $b\sqrt{F_y}/2t = 72$ and that M_{pc} for Class 2 beam-columns be limited to the value given by Equation 6.10. Increases in web limits for Class 1 sections are also indicated by the theoretical results presented herein.

Before these additional increases are implemented, however, it is suggested that further testing of laboratory specimens be carried out. These tests should be performed in the light of certain implications arising from the present theoretical analysis. The items of particular relevance to test specimens and testing procedure are listed below:

1. End Conditions

As nearly as possible, the end supports of test specimens should approximate simply-supported plate edges with respect to local buckling. For axially loaded members this is not a difficult problem. However, for members that must be subjected to axial and flexural loads combined, it would be necessary to use end-moment connections requiring very rigid support of the plate edges. A solution to this problem

would be to use members sufficiently long so that the effects of rigid edge restraints are reduced. An aspect ratio of at least 4 for webs and flanges is suggested.

2. Lateral Support

To ensure a local buckling mode of failure, adequate lateral support must be provided in order to preclude overall lateral-torsional instability. Lateral supports should be designed so as not to interfere with local buckling. It is suggested that knife-edge lateral supports be placed at web-to-flange junctions if possible.

3. Residual Stresses

If local buckling is expected to occur in the elastic or partially yielded regions, an exact determination of residual stress magnitude and distribution is especially important. In the present correlation of theoretical and test results this information was not available and therefore, typical values had to be assumed. As a result, partially due to this lack of information, discrepancies between theoretical predictions and test results are evident. Future experimental investigations of local buckling should incorporate the exact determination of residual stresses as part of the test program.

4. Material Properties

At the present time there are conflicting opinions^{5,22,24,27,33} as to what values of material properties are applicable in the range of strain between the yield strain and the strain at the onset of strain-hardening. Further investigations in this area

would be desirable. Values of the strain at the onset of strain-hardening as well as values of the strain-hardening modulus were not available for several of the test specimens referred to in the present investigation. Therefore, typical values had to be assumed and this partially contributed to discrepancies between theoretical predictions and test results. In future testing, it is recommended that attempts be made to determine strain-hardening strains and moduli during standard tension coupon tests.

7.6 Conclusions

A sound theoretical analysis similar to a finite strip technique has been developed and verified for the purpose of determining critical local buckling loads for W shape structural members. These members may be end-loaded by axial loads, flexural loads, or axial and flexural loads combined. The method predicts local buckling of flanges and webs in the elastic and inelastic ranges and the interaction of the flanges and web is accounted for in the formulation of the problem. Also, the effects of residual stresses are included directly into the theoretical formulation. The calculations were performed by computer and the theoretical results were verified by comparison with available test results as well as with the predictions of classical analysis for elastic plate buckling.

A wide range of Class 1, 2, and 3 sections of varying dimensions were analysed for axial loadings, flexural loadings, and axial and flexural loadings combined. As a result, interaction diagrams were generated for each class of section and these diagrams were used to determine maximum web limitations for a range of axial loads varying

from zero to the yield load. It was generally indicated that present web limitations are too restrictive and appropriate increases have been suggested. Additionally, it has been suggested that more testing of laboratory specimens be carried out and appropriate recommendations have been made regarding the design of such tests.

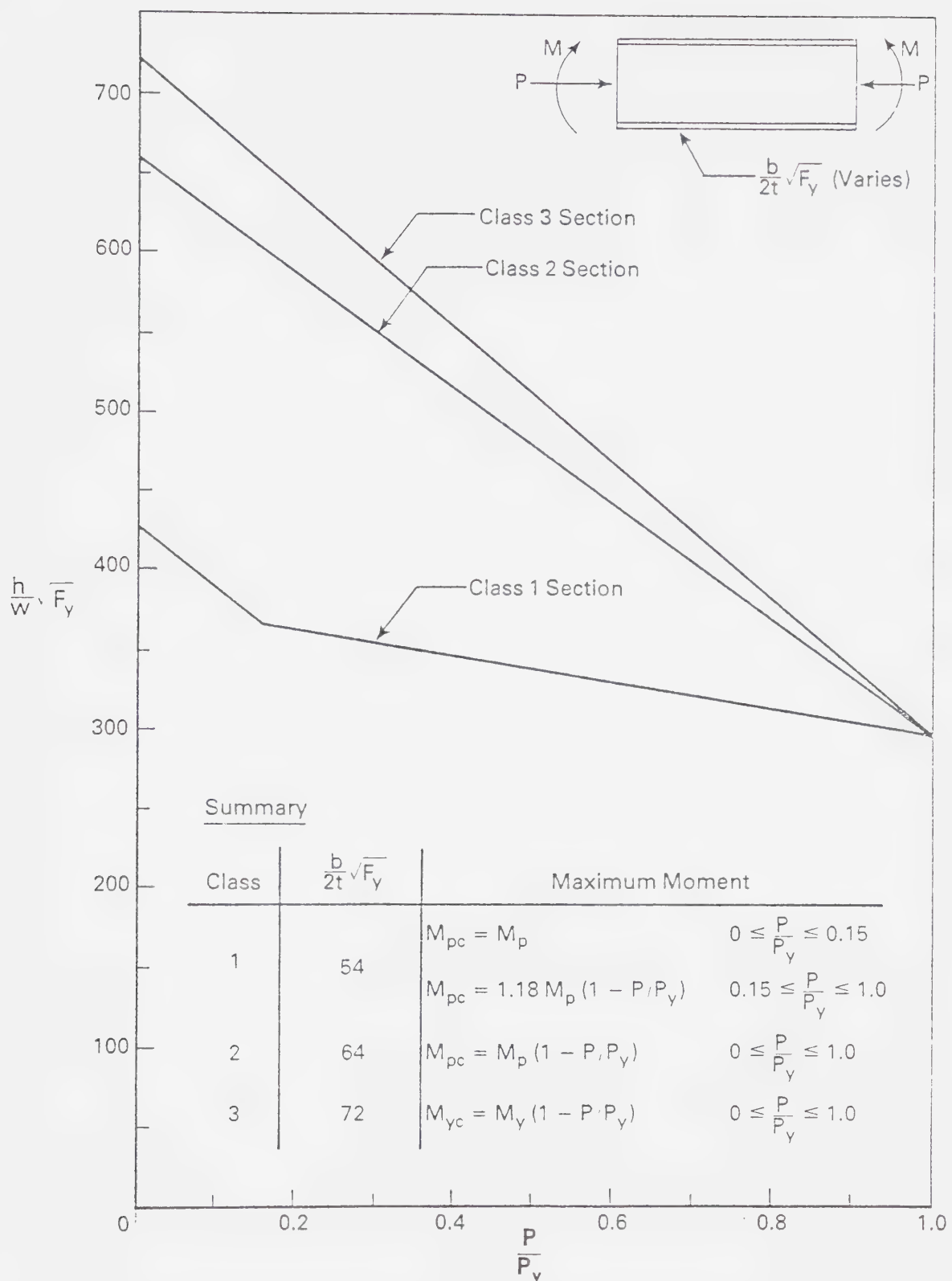


Figure 7.1 Summary of Indicated Modifications

LIST OF REFERENCES

1. Adams, P.F., Krentz, H.A., and Kulak, G.L., "Limit States Design in Structural Steel", Canadian Institute of Steel Construction, Willowdale, Ontario, 1977.
2. Timoshenko, S. and Gere, J., "Theory of Elastic Stability", Second Edition, McGraw-Hill Book Co., Inc., New York, N.Y., 1961.
3. "Guide to Stability Design Criteria for Metal Structures", Third Edition, B.G. Johnston, Editor, John Wiley and Sons, New York, N.Y., 1976.
4. "CSA S 16.1-1974 "Steel Structures for Buildings - Limit States Design", Canadian Standards Association, Rexdale, Ontario, 1975.
5. Galambos, T.V., "Structural Members and Frames", Prentice-Hall, Inc., Englewood Cliffs, N.J., 1968.
6. Bleich, F., "Buckling Strength of Metal Structures", McGraw-Hill Book Co., Inc., New York, N.Y., 1952.
7. Haaijer, G., and Thurlimann, B., "On Inelastic Buckling in Steel", Proceedings, ASCE, Volume 84, No. EM2, April, 1958.
8. Fung, Y.C., "Foundations of Solid Mechanics", Prentice-Hall, Inc., Englewood Cliffs, N.J., 1965.
9. "CSA S16.2-1975 "Steel Structures for Buildings - Working Stress Design", Canadian Standards Association, Rexdale, Ontario, 1975.
10. Holtz, N.M., and Kulak, G.L., "Web Slenderness Limits for Compact Beams", Structural Engineering Report No. 43, Department of Civil Engineering, University of Alberta, March, 1973.
11. Holtz, N.M., and Kulak, G.L., "Web Slenderness Limits of Non-Compact Beams", Structural Engineering Report No. 51, Department of Civil Engineering, University of Alberta, August, 1975.
12. Perlynn, M.J., and Kulak, G.L., "Web Slenderness Limits for Compact Beam-Columns", Structural Engineering Report No. 50, Department of Civil Engineering, University of Alberta, September, 1974.

13. Nash, D.S. and Kulak, G.L., "Web Slenderness Limits for Non-Compact Beam-Columns", Structural Engineering Report No. 53, Department of Civil Engineering, University of Alberta, March 1976.
14. Bryan, G.H., "On the Stability of a Plane Plate under Thrusts in its Own Plane with Applications to the Buckling of the Sides of a Ship", Proceedings of London Mathematical Society, v. 22, pp. 54-67, 1891.
15. Gerard, G., and Becker, H., "Handbook of Structural Stability - Part I: Buckling of Flat Plates", National Advisory Council for Aeronautics, Technical Notes 3781, Washington, D.C., 1957.
16. "Handbook of Structural Stability", Construction Research Council Japan, Corona Publishing Co., Tokyo, Japan, 1971.
17. Ros, M., and Eichinger, A., Reports, 3rd International Congress, Bridge and Structural Engineer, Paris, 1932.
18. Bijlaard, P.P., "Theory and Tests on the Plastic Stability of Plates and Shells", Journal of Aeronautical Science, v. 16, pp. 529-541, September, 1949.
19. Ilyushin, A.A., "Stability of Plates and Shells Beyond the Proportional Limit", National Advisory Council for Aeronautics, Technical Memorandum No. 116, October, 1947.
20. Stowell, E.Z., "A Unified Theory of Plastic Buckling of Columns and Plates", National Advisory Council for Aeronautics, Technical Notes 1556, 1948.
21. Onat, E.T., and Drucker, D.C., "Inelastic Instability and Incremental Theories of Plasticity", Journal of Aeronautical Sciences, Volume 20, p. 181, March, 1953.
22. Handelman, G.H., and Prager, W., "Plastic Buckling of a Rectangular Plate under Edge Thrusts", National Advisory Council for Aeronautics, Technical Note No. 1530, August, 1948.
23. Drucker, D.C., "A Discussion of the Theories of Plasticity", Readers' Forum, Journal of Aeronautical Sciences, Volume 16, No. 9, P. 567, September, 1949.
24. Dubey, R.N., "Bifurcation in Elastic-Plastic Plates", Transactions, CSME, Volume 5, NO. 2, pp. 79-88, 1978-79.
25. Lay, M.G., "Yielding of Uniformly Loaded Steel Members", Journal of the Structural Division, ASCE, Volume 91, No. ST6, Proceedings Paper 4580, December, 1965.

26. Timoshenko, S., "Stability of Webs of Plate Girders", Engineering, Volume 138, p. 207, 1934.
27. Kato, B., "Buckling Strength of Plates in the Plastic Range", Publications, IABSE, Volume 25, pp. 127-141, 1965.
28. Ueda, Y., and Tall, L., "Inelastic Buckling of Plates with Residual Stresses", Publications, IABSE, Volume 27, pp. 211-254, 1967.
29. Paramasivam, P., and Rao, J.K.S., "Buckling of Plates of Abruptly Varying Stiffnesses", Journal of the Structural Division, Proceedings, ASCE, Volume 95, No. ST6, pp. 1313-1337, June, 1969.
30. Sherbourne, A.N., and Korol, R.M., "Post-Buckling of Axially Compressed Plates", Journal of the Structural Division, Proceedings, ASCE, Volume 98, No. ST10, pp. 2223-2234, October, 1972.
31. Crisfield, M.A., "Full Range Analysis of Steel Plates and Stiffened Plating Under Uniaxial Compression", Institute of Civil Engineers, Proceedings, Part 2, Volume 59, pp. 595-624, December, 1975.
32. Przemieniecki, J.S., "Finite Element Structural Analysis of Local Instability" American Institute of Aeronautics and Astronautics Journal, Volume 11, No. 1, January, 1973.
33. Lay, M.G., "Flange Local Buckling in Wide-Flange Shapes", Journal of the Structural Division, Proceedings, ASCE, Volume 91, No. ST6, pp. 95-116, December, 1965.
34. Culver, C.G., and Nasir, G., "Inelastic Flange Buckling of Curved Plate Girders", Journal of the Structural Division, Proceedings, ASCE, Volume 97, No. ST4, pp. 1239-1256, April, 1971.
35. McDermott, J.F., "Local Plastic Buckling of A514 Steel Members" Journal of the Structural Division, Proceedings, ASCE, Volume 95, No. ST9, pp. 1837-1850, September, 1969.
36. Lukey, A.F., and Adams, P.F., "Rotation Capacity of Beams Under Moment Gradient", Journal of the Structural Division, ASCE, Volume 95, No. ST6, June, 1969.
37. Basler, K., and Thurlimann, B., "Strength of Plate Girders in Bending", Journal of the Structural Division, Proceedings, ASCE, Volume 87, No. ST6, pp. 153-181, August, 1961.

38. Croce, A.D., "The Strength of Continuous Welded Girders with Unstiffened Webs", thesis presented at the University of Texas at Austin, Texas in 1970 in partial fulfillment of the requirements for the degree of Master of Science.
39. Rajasekaran, S., and Murray, D.W., "Coupled local Buckling in Wide-Flange Beam Columns", Journal of the Structural Division, ASCE, Volume 99, No. ST6, Proceedings Paper 9774, pp. 1003-1023, June, 1973.
40. Akay, H.V., Johnson, C.P., and Will, K.M., "Lateral and Local Buckling of Beams and Frames", Journal of the Structural Division, ASCE, Volume 103, No. ST9, Proceedings Paper 13226, pp. 1821-1832, September, 1977.
41. Hancock, G.J., "Local, Distortional and Lateral Buckling of I-Beams", Journal of the Structural Division, Proceedings, ASCE, Volume 104, No. ST11, pp. 1787-1798, November, 1978.
42. Plank, R.J., and Wittrick, W.H., "Buckling Under Combined Loading of Thin, Flat-Walled Structures by a Complex Finite Strip Method", International Journal of Numerical Methods in Engineering, Volume 8, No. 2, pp. 323-339, 1974.
43. Goldberg, J.E., Bogdanoff, J.L., and Glauz, W.D., "Lateral and Torsional Buckling of Thin-Walled Beams", Proceedings, IABSE, Volume 24, pp. 91-100, 1964.
44. MacFarland, D.E., Smith, B.L., and Bernhart, W.D., "Analysis of Plates", First Edition, Spartan Books, N.Y., 1972.
45. Lecture Notes, Civil Engineering 664, University of Alberta, 1977, Instructors: Dr. D.W. Murray and Dr. T.M. Hrudey.
46. Chou, P.C., and Pagano, N.J., "Elasticity: Tensor, Dyadic and Engineering Approaches", D. Van Nostrand Company, Inc., Princeton, New Jersey, 1967.
47. Cook, R.D., "Concepts and Applications of Finite Element Analysis", First Edition, John Wiley and Sons, Inc., N.Y., 1974.
48. Clough, R.W., and Penzien, J., "Dynamics of Structures", McGraw-Hill Book Co., N.Y., 1975.
49. Simitses, G.J., "An Introduction to the Elastic Stability of Structures", Prentice-Hall, Inc., Englewood Cliffs, New Jersey, 1976.
50. Bathe, K.J., and Wilson, E.L., "Numerical Methods in Finite Element Analysis", Prentice-Hall, Inc., Englewood Cliffs, New Jersey, 1976.

51. Trahair, N.S., and Kitipornchai, S., "Buckling of Inelastic I-Beams Under Uniform Moment", Journal of the Structural Division, Proceedings, ASCE, Volume 98, No. ST11, pp. 2551-2566, November, 1972.
52. Carskaddan, P.S., "Shear Buckling of Unstiffened Hybrid Beams", Journal of the Structural Division Proceedings Paper 6077, ASCE, Volume 94, No. ST8, pp. 1965-1990, August 1968.
53. Culver, C.G., and Frampton, R.E., "Local Instability of Horizontally Curved Members", Journal of the Structural Division, Proceedings Paper 7079, ASCE, Volume 96, No. ST2, pp. 245-265, February, 1970.
54. Galambos, T.V., and Ravindra, M.K., "Properties of Steel for Use in LRFD", Journal of the Structural Division, Proceedings, ASCE, Volume 104, No. ST9, pp. 1459-1468, September, 1978.
55. Zienkiewicz, O.C., "The Finite Element Method", Third Edition, McGraw-Hill Book Co., Inc., New York, 1977.
56. Kreyszig, E., "Advanced Engineering Mathematics", Second Edition, John Wiley and Sons, Inc., New York, 1967.
57. Yoshida, H., "Lateral Buckling Strength of Plate Girders", Publications, IABSE, Volume 35-11, pp. 163-182, 1975.
58. Yoshida, H., and Imoto, Y., "Inelastic Lateral Buckling of Restrained Beams", Engineering Mechanics Division, ASCE, Volume 99, No. EM2, April, 1973.
59. Thurlimann, B., "New Aspects Concerning Inelastic Instability of Steel Structures", Journal of the Structural Division, Proceedings, ASCE, Volume 86, No. ST1, pp. 99-120.
60. Nash, D.S., Personal Comm., Montreal, June, 1979.
61. McGuire, W., "Steel Structures", Prentice-Hall, Inc., Englewood Cliffs, N.Y., 1968.
62. "Structural Steel Design", First Edition, Lambert Tall, Editor, The Ronald Press Company, New York, 1964.
63. Beedle, L.S., "Plastic Design of Steel Frames", First Edition, John Wiley and Sons, Inc., New York, 1958.
64. Driscoll, G.C., and Beedle, L.S., "The Plastic Behaviour of Structural Members and Frames", The Welding Journal, vol. 36, No. 6, June, 1957.

65. Ketter, R.L., Kaminsky, E.L., and Beedle, L.S., "Plastic Deformation of Wide-Flange Beam-Columns", Transactions, ASCE, vol. 120, 1955.
66. Lay, M.G., and Gimsing, N., "Experimental Studies of the Moment-Thrust-Curvature Relationship", The Welding Journal, Welding Research Supplement, vol. 30, No. 2, February, 1965.
67. Stanley, F.R., "Mechanics of Materials", First Edition, McGraw-Hill Book Co., Inc., New York, N.Y., 1967.
68. Nadai, A., "Theory of Flow and Fracture of Solids", McGraw-Hill Book Co., Inc., New York, N.Y., 1950.
69. Hrudey, T.M., Personal Comm., Edmonton, 1978.
70. Dubey, R.N., and Pindera, M.J., "Effect of Rotation of Principal Axes on Effective Shear Modulus in Elastic-Plastic Solids", Journal of Structural Mechanics, vol. 5, No. 1. 1977.
71. Drucker, D.C., "Introduction to Mechanics of Deformable Solids", McGraw-Hill Book Co., Inc., New York, N.Y., 1967.
72. Lekhnitskii, S.G., "Anisotropic Plates", Gordon and Breach Science Publishers, Second Edition, New York, 1968.
73. Haaijer, G., "Plate Buckling in the Strain-Hardening Range", Journal of the Engineering Mechanics Division, Proceedings, ASCE, vol. 83, No. EM2, April, 1957.

APPENDIX A

DERIVATION OF A PLATE BUCKLING CONDITION

A-1 Introduction

In this section a plate buckling condition is established using the principle of virtual work^{2,8,55}. For a body in equilibrium, the principle states that the work done by an internal equilibrium stress field, σ_{ij} , is equal to the work done by the surface tractions, T_i , when the body is subjected to a virtual displacement field, δu_i . The principle may be expressed as follows:

$$\int_V \sigma_{ij} \delta e_{ij} dV = \int_S T_i \delta u_i dS \quad (A-1)$$

where δe_{ij} is the virtual strain field resulting from a virtual displacement field, δu_i , V refers to the volume, and S refers to the surface area over which surface tractions, T_i , are specified. In this expression, the effects of body forces, F_i , have been neglected.

A-2 Assumptions

In the following derivation it is assumed that:

1. second order strain terms resulting from in-plane displacement components due to buckling are small and may be neglected⁸.
2. at the point of bifurcation of a plate, an in-plane or a buckled equilibrium configuration is possible while

- the system of external forces remains constant,
3. a state of plane stress⁴⁶ exists within the plate,
 4. the plate thickness is small relative to the surface dimensions,
 5. deflections are small relative to the plate thickness,
 6. straight lines perpendicular to the middle surface of an undeformed plate remain straight and perpendicular to the middle surface after buckling,
 7. longitudinal strips of a plate may be elastic or inelastic,
 8. stresses are constant or vary linearly across the thickness of a plate,
 9. stretching of the middle plane of the plate during buckling is small and may be neglected.

A-3 Strain - Displacement Relationships

The strain - displacement relationships in tensor form may be written as follows⁸:

$$e_{ij} = \frac{1}{2} (u_{i,j} + u_{j,i} + u_{k,i} u_{k,j}) \quad (A-2)$$

where i, j, and k cyclically represent the subscripts x, y, and z corresponding to Cartesian coordinates. In this and subsequent expressions, the comma-notation is used to represent differentiation,

and double subscripts indicate summation.¹⁵ Here also, ϵ_{xx} , ϵ_{yy} , and ϵ_{xy} represent strain and displacement components, respectively.

In the present case of plane stress, Equation A-1 may be expanded to the following component equations:

$$\epsilon_{xx} = \nu_{xx} + \frac{1}{2} \nu_{yy} - \nu_{xy}^2 + \nu_x^2 - \nu_y^2 \quad |A-3|$$

$$\epsilon_{yy} = \nu_{yy} + \frac{1}{2} \nu_{xx} - \nu_{xy}^2 - \nu_x^2 + \nu_y^2 \quad |A-4|$$

$$\epsilon_{xy} = \frac{1}{2} \nu_{xy} - \nu_{xx} - \nu_{yy} \nu_{xy} - \nu_x \nu_y \quad |A-5|$$

where ν_x , ν_y , and ν_{xy} represent displacement components in the x -, y -, and xy -coordinate directions, and subscripts xx , yy , and xy indicate differentiation with respect to that particular variable.

According to Assumption II, i.e., strain terms depending on the various displacement fields ν_{xx} , ν_{yy} , ν_{xy} , and ν_{yx} , may be neglected. Second order terms based on ν_{xx} and ν_{yy} result from a buckled configuration and therefore may be retained. Thus, Equations A-3 to A-5 may be rewritten as follows:

$$\epsilon_{xx} = \nu_{xx} + \frac{1}{2} \nu_{yy} \quad |A-3|$$

$$\epsilon_{yy} = \nu_{yy} + \frac{1}{2} \nu_{xx} \quad |A-4|$$

$$\epsilon_{xy} = \frac{1}{2} \nu_{xy} - \nu_{xx} - \nu_{yy} \nu_{xy} \quad |A-5|$$

A-4 Displacement Components

Figure A-1 shows a plate oriented in a 3-dimensional Cartesian coordinate system. The displacement components of a point in the middle plane of the plate during buckling are given as:

$$u = u' \quad (A-9)$$

$$v = v' \quad (A-10)$$

$$w = w \quad (A-11)$$

Figure A-2 shows a portion of a plate before and after buckling in the $x - y$ plane. During buckling, a point P moves tangentially to P' by a distance u' . Due to out-of-plane deflection, P' moves to P'' by a distance equal to w . As a result of rotation of a cross-section of the plate, P'' moves to P''' . Making use of Assumption No. 5 concerning small deflections, and recognizing similar observations for buckling in the $y - z$ plane, the following displacement components are obtained:

$$u = u' - zw, _x \quad (A-12)$$

$$v = v' - zw, _y \quad (A-13)$$

$$w = w \quad (A-14)$$

Using these results in Equations A-6 to A-8, the following strain-displacement relationships are obtained:

$$e_x = u', _x - zw, _{xx} + \frac{1}{2} w^2, _x \quad (A-15)$$

$$e_y = v'_{,y} - zw_{,yy} + \frac{1}{2} w^2_{,y} \quad (A-16)$$

$$e_{xy} = \frac{1}{2}(u'_{,y} + v'_{,x}) - zw_{,xy} + \frac{1}{2} w_x w_{,y} \quad (A-17)$$

A-5 Application of the Principle of Virtual Work

Using Equations A-15 to A-17, the left hand side of Equation A-1, for the case of plane stress, (Assumption No. 3), may be written as follows:

$$\begin{aligned} \int_V \sigma_{ij} \delta e_{ij} dV &= \int_x \int_y \left[N_x \delta u'_{,x} + N_{xy} (\delta u'_{,y} + \delta v'_{,x}) + N_y \delta v'_{,y} \right] dx dy \\ &\quad + \int_x \int_y \left[N_x w_{,x} \delta w_{,x} + N_{xy} (w_{,x} \delta w_{,y} + w_{,y} \delta w_{,x}) \right. \\ &\quad \left. + N_y w_{,y} \delta w_{,y} \right] dx dy + \int_x \int_y \left[M_x \delta w_{,xx} \right. \\ &\quad \left. + 2M_{xy} \delta w_{,xy} + M_y \delta w_{,yy} \right] dx dy \end{aligned} \quad (A-18)$$

In developing this expression, the following relationships were used:

$$\sigma_{ij} \delta e_{ij} = \sigma_x \delta e_x + 2\sigma_{xy} \delta e_{xy} + \sigma_y \delta e_y \quad (A-19)$$

$$\delta e_x = \delta u'_{,x} - z\delta w_{,xx} + w_{,x}\delta w_{,x} \quad (A-20)$$

$$\delta e_y = \delta v'_{,y} - z\delta w_{,yy} + w_{,y}\delta w_{,y} \quad (A-21)$$

$$\begin{aligned} \delta e_{xy} &= \frac{1}{2} (\delta u'_{,y} + \delta v'_{,x}) - z\delta w_{,xy} \\ &\quad + \frac{1}{2} (w_{,x}\delta w_{,y} + w_{,y}\delta w_{,x}) \end{aligned} \quad (A-22)$$

from Equation A-15 to A-17, and,

$$N_x = \int_{-t/2}^{t/2} \sigma_x dy \quad (A-23a)$$

$$N_{xy} = \int_{-t/2}^{t/2} \sigma_{xy} dz \quad (A-23b)$$

$$N_y = \int_{-t/2}^{t/2} \sigma_y dz \quad (A-23c)$$

$$M_x = - \int_{-t/2}^{t/2} \sigma_x z dz \quad (A-24a)$$

$$M_{xy} = - \int_{-t/2}^{t/2} \sigma_{xy} z dz \quad (A-24b)$$

$$M_y = - \int_{-t/2}^{t/2} \sigma_y z dz \quad (A-24c)$$

where N_x , N_{xy} , and, N_y are forces and M_x , M_{xy} , and M_y are moments per unit length of a plate having a thickness, t .

The first integral on the right hand side of expression A-18, may be integrated by parts as follows:

$$\begin{aligned}
& \int_y \left[N_x \delta u' \Big|_0^a + N_{xy} \delta v' \Big|_0^a \right] dy + \int_x \left[N_y \delta v' \Big|_0^b + N_{xy} \delta u' \Big|_0^b \right] dx \\
& - \int_x \int_y \delta u' (N_{x,x} + N_{xy,y}) dx dy - \int_x \int_y \delta v' (N_{y,y} + N_{xy,x}) dx dy
\end{aligned} \tag{A-25}$$

where a and b refer to the length and width of a rectangular plate as shown in Figure A-1. The first two integrals of this expression represent the virtual work done by the applied forces per unit length evaluated at the boundaries of the plate. If body forces are negligible, the conditions of equilibrium^{2,8,46} require that the last two integrals of this expression equal zero. Therefore the first integral on the right hand side of expression A-18 represents the virtual work done by the applied external forces acting through mid-plane displacements.

It is assumed that the strain in the middle plane of a plate at buckling is negligible. Therefore, from Equations A-15 to A-17,

$$u'_{,x} = -\frac{1}{2} w_{,x}^2 \tag{A-26}$$

$$u'_{,y} = -\frac{1}{2} w_{,y}^2 \tag{A-27}$$

$$\frac{1}{2}(u'_{,y} + v'_{,x}) = -\frac{1}{2}w_{,x}w_{,y} \tag{A-28}$$

Substituting these values into the first two integrals of

expression A-25 gives:

$$\int_x \int_y \left[N_x \delta u',_x + N_{xy} (\delta u',_y + \delta v',_x) + N_y \delta v',_y \right] dx dy = \\ - \int_x \int_y \left[N_x w,_x \delta w,_x + N_{xy} (w,_x \delta w,_y + w,_y \delta w,_x) + N_y w,_y \delta w,_y \right] dx dy \quad (A-29)$$

Using this relationship in Equation A-18, the left hand side of Equation A-1 finally reduces to:

$$\int_V \sigma_{ij} \delta e_{ij} dV = \int_x \int_y \left[M_x \delta w,_xx + M_{xy} \delta w,_xy + M_y \delta w,_yy \right] dx dy \quad (A-30)$$

The right hand side of Equation A-1 represents the work done by the surface tractions when the body is subjected to a virtual displacement field. This quantity has already been evaluated in expression A-29 above. Using expressions A-29 and A-30, Equation A-1 finally reduces to:

$$\int_x \int_y \left[M_x \delta w,_xx + 2M_{xy} \delta w,_xy + M_y \delta w,_yy \right] dx dy \\ = - \int_x \int_y \left[N_x w,_x \delta w,_x + N_{xy} (w,_x \delta w,_y + w,_y \delta w,_x) + N_y w,_y \delta w,_y \right] dx dy \quad (A-31)$$

In this equation, the integral on the left hand side represents the strain energy of bending of an equilibrium stress field when a virtual displacement field is superimposed on a buckled configuration. The integral on the right hand side represents the virtual work done by the in-plane stresses acting at the boundaries. In this form, Equation A-31 defines the buckling condition of a plate subjected to in-plane stresses.

In the present analysis, the equilibrium stress field is derived from the general stress-strain relationships for an orthotropic plate. The moments per unit length can be expressed in terms of the plate deflections as follows⁷:

$$M_x = - D_{xx} w_{xx} - D_{xy} w_{yy} \quad (A-32)$$

$$M_y = - D_y w_{yy} - D_{yx} w_{xx} \quad (A-33)$$

$$M_{xy} = - 2G_t I w_{xy} \quad (A-34)$$

where D_x , D_y , D_{xy} , and D_{yx} are plate bending rigidities, G_t is the tangent shear modulus, and I is the moment of inertia per unit length of the plate. These properties are further discussed in Appendix B.

Substituting Equations A-32 to A-34 into Equation A-31, the buckling condition for a uniaxially stressed plate may be expressed as:

$$\begin{aligned}
 & \int_x \int_y (D_{xx} w_{xx} \delta w_{xx} + D_{yy} w_{yy} \delta w_{yy} + D_{xy} w_{yy} \delta w_{xx} + D_{yx} w_{xx} \delta w_{yy} \\
 & + 4G_t I w_{xy} \delta w_{xy}) dx dy - \int_x \int_y N_x w_x \delta w_x dx dy = 0
 \end{aligned} \tag{A-35}$$

A-6 Development of a Matrix Buckling Condition

The first integral of Equation A-35 leads to the bending stiffness matrix of a plate and the second integral results in a geometric stiffness matrix. The subscript, x , refers to integration along the length of a plate, and the subscript, y , refers to integration along its width. In the present analysis, the integration along x is continuous since material properties along the length of a strip of plate under uniaxial stress will be constant. In the transverse direction of a plate however, the uniaxial stress may vary in intensity and therefore certain longitudinal strips may be yielded while others are still elastic or strain-hardened. To account for this, integration in the y direction is done in a piecewise manner and the appropriate material properties for a given strip are incorporated into the integration in a piecewise fashion.

As explained in Chapter 3, a Rayleigh-Ritz technique is applied using a displacement function of the form:

$$w = f\langle\phi\rangle\{\theta\} \tag{A-36}$$

In this expression, f is a function of x only and it describes the buckled shape in the longitudinal direction, $\langle\phi\rangle$ is a row vector of

interpolating functions of y only and $\{\theta\}$ is a column vector of nodal coordinate displacements. Together, $\langle \phi \rangle$ and $\{\theta\}$ define the transverse buckled shape of a plate.

The derivatives and corresponding variations for w are defined as follows:

$$w_{xx} = f_{xx} \langle \phi \rangle \{\theta\} \quad \delta w_{xx} = f_{xx} \langle \phi \rangle \{\delta \theta\} \quad (A-37)$$

$$w_{yy} = f_{yy} \langle \phi \rangle \{\theta\} \quad \delta w_{yy} = f_{yy} \langle \phi \rangle \{\delta \theta\} \quad (A-38)$$

$$w_{xy} = f_x \langle \phi_y \rangle \{\theta\} \quad \delta w_{xy} = f_x \langle \phi_y \rangle \{\delta \theta\} \quad (A-39)$$

$$w_x = f_x \langle \phi \rangle \{\theta\} \quad \delta w_x = f_x \langle \phi \rangle \{\delta \theta\} \quad (A-40)$$

Substituting these expressions into Equation A-35 gives:

$$\begin{aligned} & \langle \delta \theta \rangle \left[F_1 [\Phi_1] + F_2 [\Phi_2] + F_3 [\Phi_3] + F_4 [\Phi_4] \right] \{\theta\} \\ & - \langle \delta \theta \rangle \left[F_5 [\Phi_5] \right] \{\theta\} = 0 \end{aligned} \quad (A-41)$$

where the following relationships have been used:

$$F_1 = D_x \int_x f^2_{xx} dx, \quad (A-42)$$

$$F_2 = D_y \int_x f^2_{yy} dx, \quad (A-43)$$

$$F_3 = 2D_{xy} \int_x f \cdot f,_{xx} dx, \quad (A-44)$$

$$F_4 = 4G_t I \int_x f^2,_{xx} dx, \quad (A-45)$$

$$F_5 = t \int_x f^2,_{xx} dx, \quad (A-46)$$

and,

$$[\Phi_1] = \int_y \{\phi\} \langle \phi \rangle dy \quad (A-47)$$

$$[\Phi_2] = \int_y \{\phi,_{yy}\} \langle \phi,_{yy} \rangle dy \quad (A-48)$$

$$[\Phi_3] = \int_y \left[\{\phi,_{yy}\} \langle \phi \rangle + \{\phi\} \langle \phi,_{yy} \rangle \right] dy \quad (A-49)$$

$$[\Phi_4] = \int_y \{\phi,_{yy}\} \langle \phi,_{yy} \rangle dy \quad (A-50)$$

$$[\Phi_5] = \int_y \sigma_x \{\phi\} \langle \phi \rangle dy \quad (A-51)$$

where, for a plate of constant thickness, t , $N_x = \sigma_x t$ is used.

In Equation A-41, the virtual displacement coordinates are completely arbitrary and therefore the relationship must hold for all values $\langle \delta\theta \rangle$. Therefore the buckling condition defined by Equation A-41 may be written as follows:

$$[K]\{\theta\} - [K_G]\{\theta\} = \{0\} \quad (A-52)$$

where the bending stiffness matrix, $[K]$ is given by:

$$[K] = F_1[\Phi_1] + F_2[\Phi_2] + F_3[\Phi_3] + F_4[\Phi_4] = F_i[\Phi_i] \quad (A-53)$$

where, $i = 1, 2, 3, 4$, and repeated subscripts indicate

summation, and the geometric stiffness matrix, $[K_G]$ is given by:

$$[K_G] = F_5[\Phi_5] \quad (A-54)$$

In Equations A-53 and A-54, the Φ matrices are evaluated by piecewise integration across the width of a plate. The integration is performed for each strip of plate which may be in the elastic, the yielded, or the strain-hardening region. For each such strip, the appropriate bending rigidities, as defined in Appendix B, are used in Equation A-53.

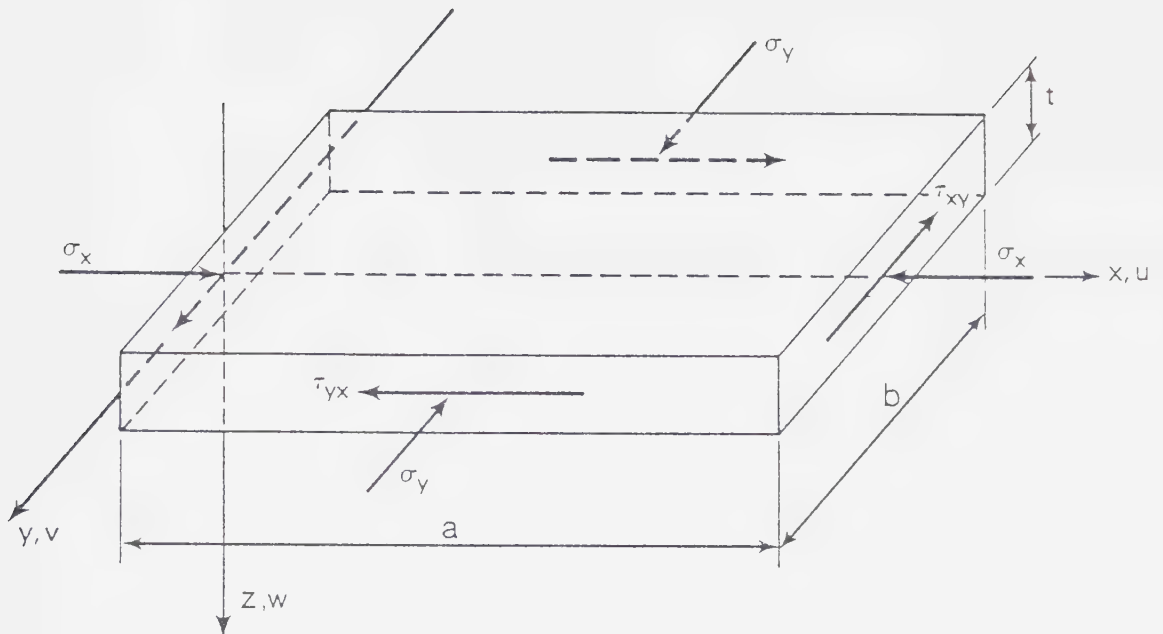


Figure A-1 Rectangular Plate Subjected to Plane Stress

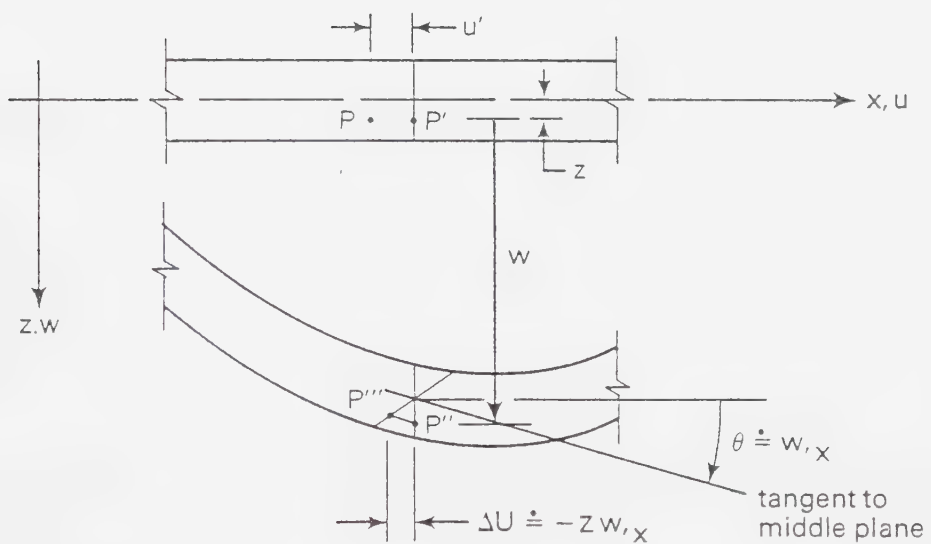


Figure A-2 Plate Buckling in the x-y Plane

APPENDIX B

MATERIAL PROPERTIES

B-1 Introduction

The determination of material properties used in the present study is based on a tangent modulus concept⁵, and therefore, the material properties that determine a critical buckling strain, are those that exist in a plate at the instant before buckling. This concept is considered to give very good correlation between predicted and test results in inelastic buckling of columns^{3,5,6}, and the correlation is further improved with the inclusion of residual stress effects⁵, as in the present study.

B-2 Incremental Stress-Strain Relationships

Figure B-1(a) shows a stress - strain relationship for a strain-hardening material. An increment of total strain, $\Delta\bar{e}$, is assumed to be sufficiently small so that it may be separated into an elastic strain increment and a plastic strain increment⁷¹. Thus,

$$de_{ij} = de_{ij}^{(e)} + de_{ij}^{(p)} \quad (B-1)$$

Elastic strain increments are related to elastic stress increments as follows⁷¹:

$$de_{ij}^{(e)} = \left(\frac{1+\nu}{E}\right)d\sigma_{ij} - \frac{\nu}{E} d\sigma_{kk} \delta_{ij} \quad (B-2)$$

In these relationships, Cartesian tensor notation is used⁴⁶, and

$$\delta_{ij} = 1 \text{ for } i = j, \text{ and}$$

$$\delta_{ij} = 0 \text{ for } i \neq j,$$

and ν and E are Poisson's ratio and Young's modulus respectively⁴⁶.

The relationship between plastic strain increments and corresponding stress increments may be defined for an assumed yield criterion, an associated flow rule, and a work hardening rule^{45,71}. For a material which yields according to von Mises yield criterion^{8,71}, the plastic strain increment tensor coincides with the plastic stress deviator tensor and the following relationship may be used^{45,71}:

$$de_{ij}^{(p)} = S_{ij} d\lambda \quad (B-3)$$

where $d\lambda$ is a positive constant of proportionality and the stress deviator tensor is defined as:

$$S_{ij} = \sigma_{ij} - \frac{c_{kk}}{3} \delta_{ij} \quad (B-4)$$

According to von Mises yield criterion, yielding occurs when the second invariant of the stress deviator tensor reaches a critical value⁷¹. This may be expressed as:

$$J_2 - k^2 = 0 \quad (B-5)$$

where,

$$J_2 = \frac{1}{2} S_{ij} S_{ij} \quad (B-6)$$

and k is a critical constant.

When a work-hardening material is subjected to a uniaxial stress state, σ , Equation B-6 gives:

$$J_2 = \frac{1}{3} \sigma^2 \quad (B-7)$$

or,

$$\bar{\sigma} = \sqrt{3J_2} = \sqrt{\frac{3}{2} S_{ij} S_{ij}} \quad (B-8)$$

where $\bar{\sigma}$ is an effective stress invariant corresponding to an effective plastic strain, $\bar{e}^{(p)}$. In a similar manner, an effective plastic strain increment, $d\bar{e}^{(p)}$ may be obtained. For a uniaxial stress state, Equation B-3 gives:

$$d\bar{e}^{(p)} = \frac{2}{3} \sigma d\lambda \quad (B-9)$$

Equation B-3 may be written as:

$$d\bar{e}_{ij}^{(p)} d\bar{e}_{ij}^{(p)} = S_{ij} S_{ij} d\lambda^2 = \frac{2}{3} \sigma^2 d\lambda^2 \quad (B-10)$$

Combining Equations B-9 and B-10 results in the following effective plastic strain increment:

$$d\bar{e}^{(p)} = \sqrt{\frac{2}{3} d\bar{e}_{ij}^{(p)} d\bar{e}_{ij}^{(p)}} \quad (B-11)$$

Figure B-1(b) shows a plot of the effective stress $\bar{\sigma}$, plotted against effective plastic strain, $\bar{e}^{(p)}$. The slope of this curve is defined as:

$$H' = -\frac{d\bar{\sigma}}{d\bar{e}^{(p)}} . \quad (B-12)$$

It is assumed that for all monotonic loading paths the same $\bar{\sigma} - \bar{e}^{(p)}$ relationship is obtained.

Combining Equations B-8 and B-11 with Equation B-10 gives:

$$d\lambda = \frac{3}{2} \left(\frac{d\bar{e}}{d\bar{\sigma}} \right) \frac{d\bar{\sigma}}{\bar{\sigma}} = \frac{3}{2} \frac{d\bar{\sigma}}{H' \bar{\sigma}} \quad (B-13)$$

where the value H' is defined in Equation B-12. Substituting this value of $d\lambda$ into Equation B-3 gives the following relationship between plastic strain and corresponding stress increments:

$$de_{ij}^{(p)} = \frac{3}{2} \frac{d\bar{\sigma}}{H' \bar{\sigma}} S_{ij} \quad (B-14)$$

Referring to Figure B-1(b), the slope of the effective stress vs. plastic strain curve is given by:

$$H' = \frac{d\bar{\sigma}}{d\bar{e}^{(p)}} = \lim_{\Delta\bar{e} \rightarrow 0} \frac{\Delta\bar{\sigma}}{\Delta\bar{e} - \Delta\bar{\sigma}/E} \quad (B-15)$$

where $\Delta\bar{e}$ is the total effective strain increment, $\Delta\bar{\sigma}$ is the effective stress increment, and E is Young's modulus. In this relationship, $\Delta\bar{\sigma}/E$ is the elastic portion of the total strain increment. Multiplying the numerator and the denominator of Equation B-15 by $E/\Delta e$ and taking the limit gives:

$$H' = \lim_{\Delta\bar{e} \rightarrow 0} \frac{E\Delta\bar{\sigma}/\Delta\bar{e}}{E - \Delta\bar{\sigma}/\Delta\bar{e}} = \frac{E \cdot E_t}{E - E_t} \quad (B-16)$$

where the tangent modulus is defined as:

$$E_t = \frac{d\bar{\sigma}}{d\bar{e}} \quad (B-17)$$

B-4 Stress-Strain Relationships for Plane Stress

In the case of plane stress⁴⁶,

$$\sigma_z = \tau_{zx} = \tau_{yz} = 0 \quad (\text{B-18})$$

and the effective stress for this case may be obtained from Equation B-8 as follows:

$$\bar{\sigma} = \sqrt{\sigma_x^2 + \sigma_y^2 - \sigma_x \sigma_y + 3\tau_{xy}^2}. \quad (\text{B-19})$$

The effective stress increment is obtained from Equation B-19 as:

$$d\bar{\sigma} = \frac{1}{2\bar{\sigma}} \left[(2\sigma_x - \sigma_y)d\sigma_x + (2\sigma_y - \sigma_x)d\sigma_y + 6\tau_{xy}d\tau_{xy} \right] \quad (\text{B-20})$$

In the present analysis a plate element before buckling is in a uniaxial stress state defined by $\sigma_x \neq 0$, $\sigma_y = \tau_{xy} = 0$, and therefore:

$$\bar{\sigma} = \sigma_x \quad (\text{B-21})$$

Immediately after buckling the same element is subjected to a state of plane stress. In applying a tangent modulus theory, only the resulting increment of effective stress is of interest, and it is given by Equation B-20 as:

$$d\bar{\sigma} = d\sigma_x - \frac{1}{2} d\sigma_y \quad (\text{B-22})$$

The corresponding increments in plastic strain are obtained by using these values of $\bar{\sigma}$ and $d\bar{\sigma}$ in Equation B-14 where S_{ij} is the stress deviator tensor for a state of uniaxial stress prior to buckling. The resulting plastic strain increments are:

$$de_x^{(p)} = \frac{d\sigma_x}{H'} - \frac{d\sigma_y}{2H'} \quad (B-23)$$

$$de_y^{(p)} = -\frac{d\sigma_x}{2H'} + \frac{d\sigma_y}{4H'} \quad (B-24)$$

$$de_{xy}^{(p)} = 0 \quad (B-25)$$

Combining Equations B-2, B-23, B-24, and B-25 with Equation B-1, the increments of total strain may be obtained for the strain-hardening region as:

$$de_x = (\frac{1}{E} + \frac{1}{H'})d\sigma_x - (\frac{\nu}{E} + \frac{1}{2H'})d\sigma_y \quad (B-26)$$

$$de_y = -(\frac{\nu}{E} + \frac{1}{2H'})d\sigma_x + (\frac{1}{E} + \frac{1}{4H'})d\sigma_y \quad (B-27)$$

$$de_{xy} = \frac{1+\nu}{E} d\tau_{xy} \quad (B-28)$$

B-5 Stress - Strain Relationships for an Orthotropic Plate

For the general case of a homogeneous elastic body, the generalized stress - strain relationship is given by⁴⁶:

$$\sigma_{ij} = C_{ijkl} e_{kl} \quad (B-29)$$

where C_{ijkl} is a fourth-order tensor representing a total of 81 constants. This number is reduced to 21 independent constants when the symmetry of the stress and strain tensors, and the existence of a potential energy function are considered^{8,46,72}.

If a material is orthotropic and the x, y, and z axes coincide with the principle directions of the material, the following stress-strain relationships apply^{47,72}:

$$e_x = \frac{\sigma_x}{E_x} - \frac{\nu_{yx}\sigma_y}{E_y} - \frac{\nu_{zx}\sigma_z}{E_z} \quad (B-30)$$

$$e_y = -\frac{\nu_{xy}\sigma_x}{E_x} + \frac{\sigma_y}{E_y} - \frac{\nu_{zy}\sigma_z}{E_z} \quad (B-31)$$

$$e_z = -\frac{\nu_{xz}\sigma_x}{E_x} - \frac{\nu_{yz}\sigma_y}{E_y} + \frac{\sigma_z}{E_z} \quad (B-32)$$

$$\gamma_{xy} = \frac{\tau_{xy}}{G_{xy}} \quad (B-33)$$

$$\gamma_{yz} = \frac{\tau_{yz}}{G_{yz}} \quad (B-34)$$

$$\gamma_{zx} = \frac{\tau_{zx}}{G_{zx}} \quad (B-35)$$

where each Poisson ratio, ν_{ij} represents the strain in the j direction

per unit strain in the i direction for $i, j = x, y, z$. The above relationships contain 9 independent material constants and:

$$\frac{v_{yx}}{E_y} = \frac{v_{xy}}{E_x}, \quad \frac{v_{zx}}{E_z} = \frac{v_{xz}}{E_x}, \quad \frac{v_{zy}}{E_z} = \frac{v_{yz}}{E_y} \quad (B-36)$$

Referring to Equations B-30 to B-35, the incremental stress-strain relationships for an orthotropic plate element subjected to a state of plane stress may be written as follows:

$$de_x = \frac{1}{E_x} d\sigma_x - \frac{v_y}{E_y} d\sigma_y \quad (B-37)$$

$$de_y = -\frac{v_x}{E_x} d\sigma_x + \frac{1}{E_y} d\sigma_y \quad (B-38)$$

$$de_{xy} = \frac{1}{2G} d\tau_{xy} \quad (B-39)$$

B-6 Effective Moduli in the Strain Hardening Range

A steel plate subjected to a uniaxial stress yields by the formation of slip bands along preferential shear planes characterised by a dissipation of minimum plastic distortional energy^{67, 68}. For a thin steel plate these shear planes will be normal to the stress axis and inclined with respect to the middle plane of the plate. As a result, in the strain-hardening range, the steel plate will be orthotropic at the instant before buckling.

Based on a tangent modulus theory, the effective moduli in the strain-hardening range may be obtained by comparing Equations B-37

to B-39 with Equations B-26 to B-28⁶⁹. Using the results of this comparison and the value of H' as given by Equation B-16 gives the following effective tangent moduli:

$$E_x = E_t \quad (B-40)$$

$$E_y = \frac{4E \cdot E_t}{3E_t + E} \quad (B-41)$$

$$G_t = G = \frac{E}{2(1+\nu)} \quad (B-42)$$

and the corresponding Poisson's ratios:

$$\nu_x = \frac{(2\nu-1)E_t + E}{2E} \quad (B-43)$$

$$\nu_y = \frac{4\nu_x E}{3E_t + E} \quad (B-44)$$

B-7 Material Properties Used in the Present Analysis

In the elastic range, the tangent modulus is equal to Young's modulus, E , and Equations B-40 to B-44 reduce to:

$$E_x = E_y = E \quad (B-45)$$

$$G_t = G \quad (B-46)$$

$$\nu_x = \nu_y = \nu \quad (B-47)$$

In the yielding range, the tangent modulus $E_t = 0$ and Equations B-40 to B-44 give:

$$E_x = E_y = 0 \quad (B-48)$$

$$G_t = G \quad (B-49)$$

$$\nu_x = 0.5 \quad (B-50)$$

$$\nu_y = 2.0 \quad (B-51)$$

The results given by Equations B-40 to B-44 were originally presented by Handelmann and Prager²². However, since that time it has been well recognized that these values may result in significant error in the prediction of inelastic critical plate buckling stresses. It has further been observed that these discrepancies are mainly due to an over-estimation of the effective shear modulus, G_t , at stresses above the yield^{7,28,33,70}.

For $E = 29,600$ ksi. and $\nu = 0.3$, Equation B-42 gives a value of $G_t = 11,385$ ksi. Using experimental results, Haaijer and Thurlimänn determined that the value of G_t for steel above the yield should be between 2000 and 3000 ksi.⁷, with an actual value selected at 2400 ksi. This 79 per cent reduction in the theoretical value of G_t , which resulted in better correlation with test results, was attributed to the effects of initial imperfections. Independently, Lay³³ disregarded the effects of initial imperfections and, using slip field theory, predicted a value of G of about 3000 ksi. As a result of this work, Lay

presented the following expression for the tangent shear modulus for strain-hardening:

$$G_t = \frac{2G}{1 + \frac{E}{4E_t(1+\nu)}} \quad (B-52)$$

where G is the elastic shear modulus, E is Young's modulus, E_t is the tangent modulus, and ν is Poisson's ratio. For $E = 29,600$ ksi., $G = 11,385$ ksi., $\nu = 0.3$, and $E_t = 800$ ksi., Equation B-51 gives a value of $G_t = 2806$ ksi. In the present study, Equations B-40, B-41, B-43, B-44, and B-51 are used to determine material properties in the inelastic range.

B-8 Plate Bending Rigidities

The plate bending rigidities D_x , D_y , D_{xy} , and D_{yx} were introduced in Appendix A. In terms of the material properties discussed previously the plate bending rigidities may be expressed as follows⁷³.

$$D_x = \frac{E_x I}{1-\nu_{x,y}^2} \quad (B-53)$$

$$D_y = \frac{E_y I}{1-\nu_{x,y}^2} \quad (B-54)$$

$$D_{xy} = \nu_y D_x \quad (B-55)$$

$$D_{yx} = v_x D_y \quad (B-56)$$

where I is the moment of inertia per unit length of a plate.

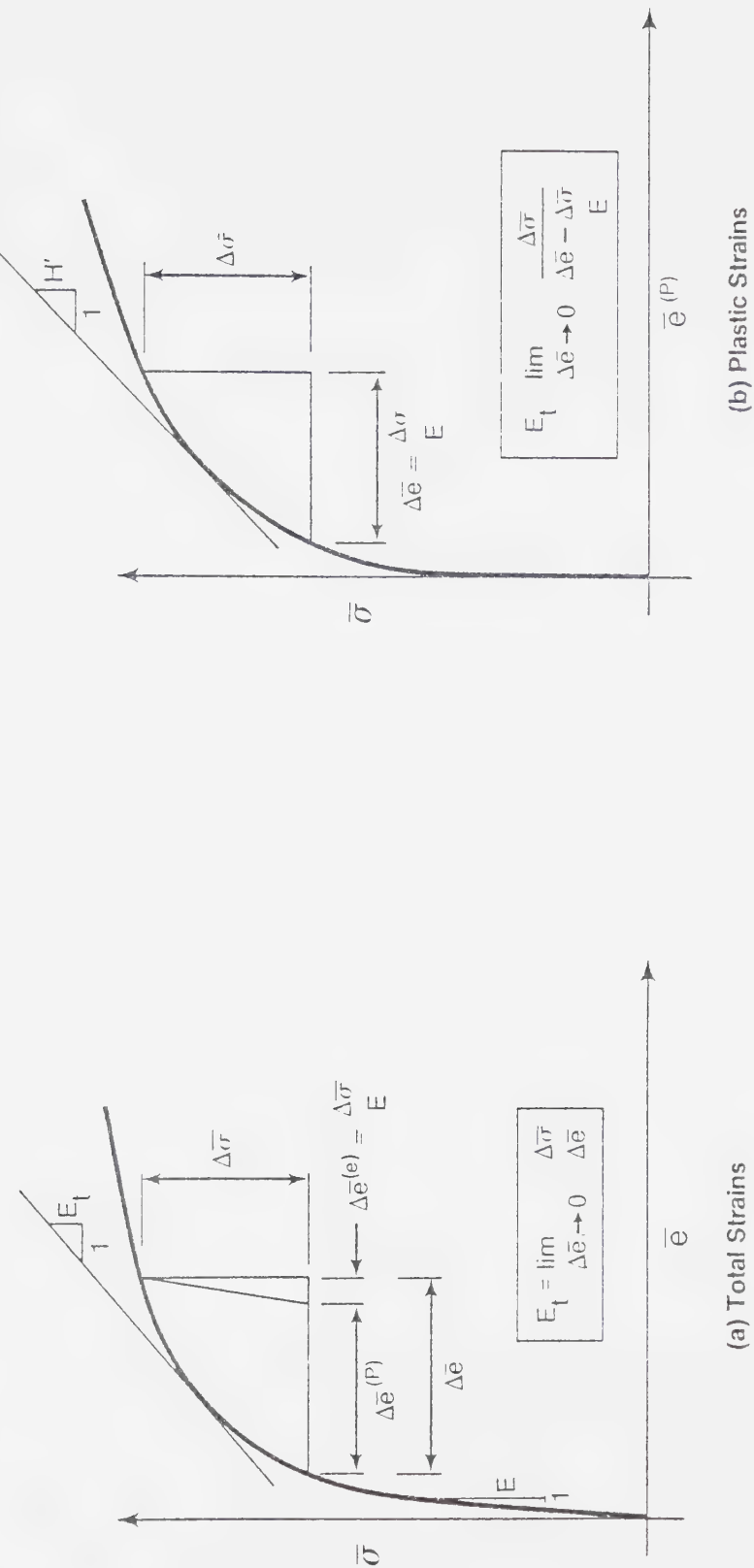


Figure B-1 Effective Stress - Effective Strain Relationships

APPENDIX C

COMPUTER PROGRAM

C.1 Introduction

This appendix contains a listing of the computer program which was developed and used to predict the test results presented in Chapter 5. It was also used in the parametric study presented in Chapter 6. The program consists of one main program and forty-one subroutines. The symbolic names used in the program are defined in the first subroutine in which they are principally used. The purposes of the main program as well as the subroutines are explained by extensive comments placed at the beginning of each. Numerous comments are also used throughout the program to segment and explain blocks of logic. A general outline of the program is given below.

C-2 General Outline

The number of specimens to be analysed, the modulus of elasticity, and Poisson's ratio are read in in the main program. Values indicating the type of cross-section (either a single plate or a W shape configuration) as well as the type of edge supports and the type of loading are also read in. These, as well as the other variables are explained in the comments at the beginning of the program.

The main routine calls one of PLATE1, PLATE2, PLATE3, PLATE4, or PLATE5 depending on the type of problem. PLATE1 and PLATE2 are used to analyse single plate configurations while PLATE3, PLATE4

and PLATE5 apply to W shape configurations used for columns, beams, and beam-columns, respectively. As stated previously, the functions of these subroutines are fully explained by comments inserted at the beginning of each one. Each of the PLATE-series of subroutines reads in additional information necessary for the solution of a problem. Since many aspects of the PLATE-series of subroutines are similar, it will be assumed here (for the purpose of continuing with the general outline of the program) that PLATE5 has been called from the main routine.

PLATE5 analyses a W shape section loaded as a beam-column. At the beginning of this subroutine all subsequent data necessary for the analysis are read in and section properties and residual stress values are calculated. This subroutine, during iteration, must calculate several critical local buckling loads before the correct one is determined. The critical axial load (either elastic or inelastic) is first determined and compared with the applied axial load. If the applied axial load is less than the critical one, the analysis for the critical superimposed bending moment continues (using an iterative technique if inelastic action occurs).

As explained by the comments within the subroutine, each time a critical load is calculated, PLATE5 calls three additional subroutines which calculate tension and compression flange stiffness matrices as well as the web stiffness matrix for an assumed value of strain. A fourth subroutine, ESFORM, is then called. ESFORM formulates the flange and web plate stiffness matrices into a total global stiffness matrix for an assumed number of half wavelengths of m. A matrix iterative subroutine, EIGEN, is then called by ESFORM to

calculate the corresponding eigenpair. This process is continued for values of m incremented by unity until a minimum eigenvalue is obtained. This value is returned to PLATE5 and compared with the previous value and if convergence has not occurred the entire process (beginning with new flange and web stiffness matrices) is repeated.

When this process has converged, the resulting eigenvalue is used to calculate the corresponding critical bending moment in subroutine MCALC. The critical axial load and the critical superimposed bending moment as well as the applied load, deformed configuration during local buckling, and other pertinent data are printed out as illustrated in the sample problems presented in Appendix D.

In subroutines, PLATE1 and PLATE2, since only elastic local buckling stresses are considered, it is necessary to formulate flange and web stiffness matrices only once. Iteration on the number, m , of half wavelengths must still be performed, however. In subroutines, PLATE3 and PLATE4, for columns and beams, respectively, the entire iterative process must be carried out when inelastic local buckling stresses are required.

Listing of
Computer Program


```

452      COMMON /BLK10/HW,TW,BCL,BF1,TF1,BF2,TF2
453      IC=0
454      XMIN=1.0D0
455      C
456      C      BEGIN ITERATION ON THE NUMBER OF HALF WAVELENGTHS
457      C
458      DD 140 M=1,10
459      RM=DFLOAT(M)
460
461      C
462      C      CALCULATE LONGITUDINAL BUCKLING FACTORS, RM1, RM2, RM3,
463      C      RM4, RMS, RM5, RM6, RM7, AND RM8 FOR VARIOUS BOUNDARY
464      C      CONDITIONS
465      C
466      C
467      IF ( ) CLAMP EQ.1) GO TO 10
468      RM1=RM#*4
469      RM2=1.0D0
470      RM3=RM#*2
471      RM4=RM3
472      GO TO 20
473      C
474      C      PERFORM GAUSSIAN INTEGRATION OF BUCKLING FACTORS
475      C      FOR OTHER THAN PINNED ENDS
476      C
477      C
478      10 CALL GOQUAD(M,RM1,RM2,RM3,RM4)
479      20 RM5=RM1
480      RM6=RM2
481      RM7=RM3
482      RM8=RM4
483      IF (ICLAMP.NE.2) GO TO 30
484      CALL GOQUAD(M,RM5,RM6,RM7,RM8)
485      30 IF (ITYPE.LE.2) GO TO 40
486      IF (ITYPE LE 6) GO TO 60
487      IF (ITYPE LE.7) GO TO 80
488      C
489      C
490      C      ASSEMBLE GLOBAL STIFFNESSES FOR FLANGE-TYPE PLATES
491      C
492      40 N=5
493      DO 50 I=1,N
494      DO 50 J=1,N
495      SB(I,J)=RM1*FB1(I,J)+RM2*FB2(I,J)+RM3*FB3(I,J)+RM4*FB4(I,J)
496      SB(J,I)=SB(I,J)
497      SG(I,J)=RM4*FB5(I,J)
498      50 SG(J,I)=SG(I,J)
499      IF (ITYPE EQ.2) SB(5,5)=1.D50
500      GO TO 120
501      C
502      C
503      C      ASSEMBLE GLOBAL STIFFNESSES FOR WEB-TYPE PLATES
504      C
505      60 N=7
506      DO 70 I=1,N
507      DO 70 J=1,N
508      SB(I,J)=RM1*WB1(I,J)+RM2*WB2(I,J)+RM3*WB3(I,J)+RM4*WB4(I,J)
509      SB(J,I)=SB(I,J)
510      SG(I,J)=RM4*WB5(I,J)
511      70 SG(J,I)=SG(I,J)
512      IF (ITYPE EQ.4) SB(1,1)=1.D50
513      IF (ITYPE EQ.5) SB(7,7)=1.D50
514      IF (ITYPE EQ.6) SB(1,1)=1.D50
515      IF (ITYPE EQ.6) SB(7,7)=1.D50
516      GO TO 120
517      C
518      C
519      C      ASSEMBLE GLOBAL STIFFNESSES FOR W-SHAPES.
520      C
521      80 N=15
522      DO 90 I=1,N
523      DO 90 J=1,N
524      SB(J,I)=0.0D0
525      90 SG(J,I)=0.0D0
526      DO 100 I=1,5
527      DO 100 J=1,5
528      SB(I,J)=RM1*FB1(I,J)+RM2*FB2(I,J)+RM3*FB3(I,J)+RM4*FB4(I,J)
529      SB(J,I)=SB(I,J)
530      SG(I,J)=RM4*FB5(I,J)
531      SG(J,I)=SG(I,J)
532      I1=1 TO 10
533      JJ=J+10
534      SB(I1,JJ)=RM1*FT1(I,J)+RM2*FT2(I,J)+RM3*FT3(I,J)+RM4*FT4(I,J)
535      SB(JJ,I1)=SB(I,J)
536      SG(I1,JJ)=RM4*FT5(I,J)
537      100 SG(JJ,I1)=SG(I,J)
538      DO 110 I=1,7
539      DO 110 J=1,7
540      J4=I+4
541      JA=J+4
542      SB(14,J4)=RM5*WB1(I,J)+RM6*WB2(I,J)+RM7*WB3(I,J)+RM8*WB4(I,J)
543      SB(JA,J4)=SB(I,J)
544      SG(14,J4)=RM8*WB5(I,J)
545      SG(JA,J4)=SG(I,J)
546      110 SB(5,5)=SB(5,5)+RM1*FB1(5,5)+RM2*FB2(5,5)+RM3*FB3(5,5)+RM4*FB4(5,5)
547      SB(5,5)=SG(5,5)+RM4*FB5(5,5)
548      SG(5,5)=SG(5,5)+RM4*FB5(5,5)
549      SB(11,11)=SB(11,11)+RM1*FT1(1,1)+RM2*FT2(1,1)+RM3*FT3(1,1)+RM4*FT4
550      A(1,1)
551      SG(11,11)=SG(11,11)+RM4*FT5(1,1)
552      C
553      C
554      C      INVERT THE BENDING STIFFNESS MATRIX (SB INVERSE = SBI)
555      C
556      120 CALL INVERT(N,SB,SBI)
557      C
558      C
559      C      MULTIPLY THE GEOMETRIC STIFFNESS MATRIX BY THE
560      C      BENDING STIFFNESS MATRIX. (ABG = SBI X SG)
561      C
562      CALL MULT(ABG,SBI,SG,N)
563      C
564      C

```



```

678      C
679      C      EVALUATE PARAMETERS ALFB AND ALFBP WHICH INDICATE
680      C      EXTENTS OF YIELDING AND STRAIN HARDENING,
681      C      RESPECTIVELY.
682      C
683      IF (RSTEA.GT.T1) GO TO 20
684      ALFB=0.0D0
685      ALFBP=0.0D0
686      GO TO 70
687      20     IF (RSTEA.GT.T2) GO TO 40
688      IF (AD1.EQ.0.0D0) GO TO 30
689      AN1=RSTEA-T1
690      ALFB=AN1/AD1
691      ALFBP=0.0D0
692      GO TO 70
693      30     ALFB=1.0D0
694      ALFBP=0.0D0
695      GO TO 70
696      40     IF (RSTEA.GT.T3) GO TO 50
697      ALFB=1.0D0
698      ALFBP=0.0D0
699      GO TO 70
700      50     IF (RSTEA.GT.T4) GO TO 60
701      IF (AD1.EQ.0.0D0) GO TO 60
702      AN1=RSTEA-T3
703      ALFBP=AN1/AD1
704      ALFB=1.0D0
705      GO TO 70
706      60     ALFB=1.0D0
707      ALFBP=1.0D0
708      70     CALL FWCALC(BCL,BF1,TF1,E)
709      C
710      C      CALCULATE GEOMETRIC SUBMATRIX COEFFICIENTS, FAC1
711      C      TO FAC6.
712      C
713      C
714      FAC1=(RSTEA+ERTB)*E*FE*STR
715      FAC2=AD1*E*FE*STR
716      FAC3=(YSFB-(T1-RSTEA)*E1)*FE*STR
717      FAC4=AD1*E1*FE*STR
718      FAC5=(YSFB+(ESH-EYBF)*E1-(T2-RSTEA)*E2)*FE*STR
719      FAC6=AD1*E2*FE*STR
720      C
721      C
722      C      FORMULATE STIFFNESS SUBMATRICES FOR ELASTIC REGION.
723      C
724      A=-1.0D0
725      BE=-ALFB
726      IF (DABS(A-B).LT.1.0D-5) GO TO 80
727      CALL PHI(B,A,FI,CB,5,6,11)
728      CALL PHIYY(B,A,FIYY,CB,5,6,7)
729      CALL PHIPHI(B,A,FIIFI,CB,5,6,9)
730      CALL PHIY(B,A,FIY,CB,5,6,9)
731      CALL EPHI(B,A,EFI,CB,5,6,12)
732      DO 80 I=1,5
733      DO 80 J=1,5
734      FB1(I,J)=FA*FI(I,J)
735      FB2(I,J)=FB*FIYY(I,J)
736      FB3(I,J)=FC*FIIFI(I,J)
737      FB4(I,J)=FD*FIY(I,J)
738      80     FB5(I,J)=FAC1*FI(I,J)-FAC2*EFI(I,J)
739      C
740      C
741      C      FORMULATE STIFFNESS SUBMATRICES FOR YIELDED REGION.
742      C
743      80     A=-ALFB
744      B=-ALFBP
745      IF (DABS(A-B).LT.1.0D-5) GO TO 110
746      CALL FWCALC(BCL,BF1,TF1,E1)
747      CALL PHI(B,A,FI,CB,5,6,11)
748      CALL PHIYY(B,A,FIYY,CB,5,6,7)
749      CALL PHIPHI(B,A,FIIFI,CB,5,6,9)
750      CALL PHIY(B,A,FIY,CB,5,6,9)
751      CALL EPHI(B,A,EFI,CB,5,6,12)
752      DO 100 I=1,5
753      DO 100 J=1,5
754      FB1(I,J)=FB1(I,J)+FA*FI(I,J)
755      FB2(I,J)=FB2(I,J)+FB*FIYY(I,J)
756      FB3(I,J)=FB3(I,J)+FC*FIIFI(I,J)
757      FB4(I,J)=FB4(I,J)+FD*FIY(I,J)
758      100    FB5(I,J)=FB5(I,J)-FAC3*FI(I,J)-FAC4*EFI(I,J)
759      C
760      C
761      C      FORMULATE STIFFNESS SUBMATRICES FOR
762      C      STRAIN-HARDENED REGION
763      C
764      110    A=-ALFBP
765      B=0.0D0
766      IF (DAES(A-B).LT.1.0D-5) GO TO 130
767      CALL FWCALC(BCL,BF1,TF1,E2)
768      CALL PHI(B,A,FI,CB,5,6,11)
769      CALL PHIYY(B,A,FIYY,CB,5,6,7)
770      CALL PHIPHI(B,A,FIIFI,CB,5,6,9)
771      CALL PHIY(B,A,FIY,CB,5,6,9)
772      CALL EPHI(B,A,EFI,CB,5,6,12)
773      DO 120 I=1,5
774      DO 120 J=1,5
775      FB1(I,J)=FB1(I,J)+FA*FI(I,J)
776      FB2(I,J)=FB2(I,J)+FB*FIYY(I,J)
777      FB3(I,J)=FB3(I,J)+FC*FIIFI(I,J)
778      FB4(I,J)=FB4(I,J)+FD*FIY(I,J)
779      120    FB5(I,J)=FB5(I,J)-FAC5*FI(I,J)-FAC6*EFI(I,J)
780      130    A=0.0D0
781      B=ALFBP
782      IF (DABS(A-B).LT.1.0D-5) GO TO 150
783      CALL PHI(B,A,FI,CB,5,6,11)
784      CALL PHIYY(B,A,FIYY,CB,5,6,7)
785      CALL PHIPHI(B,A,FIIFI,CB,5,6,9)
786      CALL PHIY(B,A,FIY,CB,5,6,9)
787      CALL EPHI(B,A,EFI,CB,5,6,12)
788      DO 140 I=1,5
789      DO 140 J=1,5
790      FB1(I,J)=FB1(I,J)+FA*FI(I,J)

```



```

791      FB2(I,J)=FB2(I,J)+FB*FIYY(I,J)
792      FB3(I,J)=FB3(I,J)-FC*FIFI(I,J)
793      FB4(I,J)=FB4(I,J)-FD*FIY(I,J)
794      140   FB5(I,J)=FB5(I,J)-FAC5*FI(I,J)+FAC6*EFI(I,J)
795      C
796      C
797      C      FORMULATE STIFFNESS SUBMATRICES FOR YIELDED REGION
798      C
799      150   A=ALFBP
800      B=ALFB
801      IF (DABS(A-B).LT.1.0D-5) GO TO 170
802      CALL FWCALC(BCL,BF1,TF1,E1)
803      CALL PHI(B,A,FI,CB,5,6,11)
804      CALL PHIYY(B,A,FIYY,CB,5,6,7)
805      CALL PHIPH(B,A,FIFI,CB,5,6,9)
806      CALL PHIY(B,A,FIY,CB,5,6,9)
807      CALL EPHI(B,A,EFI,CB,5,6,12)
808      DO 160 I=1,5
809      DO 160 J=1,5
810      FB1(I,J)=FB1(I,J)+FA*FI(I,J)
811      FB2(I,J)=FB2(I,J)+FB*FIYY(I,J)
812      FB3(I,J)=FB3(I,J)-FC*FIFI(I,J)
813      FB4(I,J)=FB4(I,J)+FD*FIY(I,J)
814      160   FB5(I,J)=FB5(I,J)-FAC3*FI(I,J)+FAC4*EFI(I,J)
815      C
816      C
817      C      FORMULATE STIFFNESS SUBMATRICES FOR ELASTIC REGION
818      C
819      170   A=ALFB
820      B=1.0D0
821      IF (DABS(A-B).LT.1.0D-5) GO TO 190
822      CALL FWCALC(BCL,BF1,TF1,E)
823      CALL PHI(B,A,FI,CB,5,6,11)
824      CALL PHIYY(B,A,FIYY,CB,5,6,7)
825      CALL PHIPH(B,A,FIFI,CB,5,6,9)
826      CALL PHIY(B,A,FIY,CB,5,6,9)
827      CALL EPHI(B,A,EFI,CB,5,6,12)
828      DO 180 I=1,5
829      DO 180 J=1,5
830      FB1(I,J)=FB1(I,J)+FA*FI(I,J)
831      FB2(I,J)=FB2(I,J)+FB*FIYY(I,J)
832      FB3(I,J)=FB3(I,J)-FC*FIFI(I,J)
833      FB4(I,J)=FB4(I,J)+FD*FIY(I,J)
834      180   FB5(I,J)=FB5(I,J)-FAC1*FI(I,J)+FAC2*EFI(I,J)
835      190   TF1=SAVE
836      RETURN
837      C
838      C
839      C      PERFORM SUBMATRIX FORMULATION FOR THE CASE WHEN
840      C      THE LOWER (TENSION) FLANGE IS IN COMPRESSION
841      C      INITIALISE STRAIN LIMITS T1, T2, T3, T4 AND
842      C      INTEGRATION LIMITS ALFT AND ALFP
843      C
844      200   T1=EYBF-ERCB
845      T2=EYBF+ERTB
846      T3=ESH-ERCB
847      T4=ESH+ERTB
848      ADEN=ERCB+ERTB
849      IF (EARST.GT.T1) GO TO 210
850      ALFT=1.0D0
851      ALFP=1.0D0
852      GO TO 260
853      210   IF (EARST.GT.T2) GO TO 230
854      IF (ADEN.EQ.0.0D0) GO TO 220
855      DNUM=T2-EARST
856      ALFT=DNUM/ADEN
857      ALFP=1.0D0
858      GO TO 260
859      220   ALFT=0.0D0
860      ALFP=1.0D0
861      GO TO 260
862      230   IF (EARST.GT.T3) GO TO 240
863      ALFT=0.0D0
864      ALFP=1.0D0
865      GO TO 260
866      240   IF (EARST.GT.T4) GO TO 250
867      IF (ADEN.EQ.0.0D0) GO TO 250
868      DNUM=T4-EARST
869      ALFP=DNUM/ADEN
870      ALFT=0.0D0
871      GO TO 260
872      250   ALFP=0.0D0
873      ALFT=0.0D0
874      C
875      C
876      C      CALCULATE GEOMETRIC SUBMATRIX COEFFICIENTS, FAC1
877      C      TO FAC6
878      C
879      260   CALL FWCALC(BCL,BF1,TF1,E2)
880      FAC1=(YSFB-(ESH-EYBF)*E1+(EARST-T4)*E2)*FE*STR
881      FAC2=FADEN*E2*FE*STR
882      FAC3=(YSFB-(EARST-T2)*E1)*FE*STR
883      FAC4=FADEN*E1*FE*STR
884      FAC5=(RSTEA+ERTB)*E*FE*STR
885      FAC6=FADEN*E*FE*STR
886      C
887      C
888      C      FORMULATE STIFFNESS SUBMATRICES FOR
889      C      STRAIN-HARDENED REGION
890      C
891      A=-1.0D0
892      B=-ALFP
893      IF (DABS(A-B).LT.1.0D-5) GO TO 280
894      CALL PHI(B,A,FI,CB,5,6,11)
895      CALL PHIYY(B,A,FIYY,CB,5,6,7)
896      CALL PHIPH(B,A,FIFI,CB,5,6,9)
897      CALL PHIY(B,A,FIY,CB,5,6,9)
898      CALL EPHI(B,A,EFI,CB,5,6,12)
899      DO 270 I=1,5
900      DO 270 J=1,5
901      FB1(I,J)=FA*FI(I,J)
902      FB2(I,J)=FB*FIYY(I,J)
903      FB3(I,J)=-FC*FIFI(I,J)

```



```

1243      COMMON /BLK2/CB(7,9),FB1(5,5),FB2(5,5),FB3(5,5),FB4(5,5),FB5(5,5)
1244      COMMON /BLK4/FA,FB,FC,FD,FE
1245      COMMON /BLKS/ERTB,ERCM,ERTT,ERCB,ERCT,EYW,EYBF,EYTF
1246      COMMON /BLK10/HW,TW,BCL,BF1,TF1,BF2,TF2
1247      COMMON /BLK11/E1,E2,ESH,YSW,YSFB,YSFT,SRTB,SRCM,SRTT,SRCB,SRCT
1248      C
1249      C
1250      C          INITIALISE THE STIFFNESS SUBMATRICES TO ZERO
1251      C
1252      DO 10 I=1,5
1253      DO 10 J=1,5
1254      FB1(I,J)=0.0D0
1255      FB2(I,J)=0.0D0
1256      FB3(I,J)=0.0D0
1257      FB4(I,J)=0.0D0
1258      FB5(I,J)=0.0D0
1259      C
1260      C
1261      C          ADJUST FLANGE THICKNESS TO ACCOUNT FOR
1262      C          WEB-TO-FLANGE FILLETS
1263      C
1264      TSAVE=TF1
1265      TF1=BF1+TF1/(BF1+2.0D0+TW)
1266      C
1267      C
1268      C          INITIALISE STRAINS AND STRAIN LIMITS, T1, T2, T3,
1269      C          T4.
1270      C
1271      STR=1.0D0/ST
1272      T1=EYBF-ERCB
1273      T2=EYBF+ERTB
1274      T3=ESH-ERCB
1275      T4=ESH+ERTB
1276      C
1277      C
1278      C          EVALUATE PARAMETERS ALFT AND ALFP WHICH INDICATE
1279      C          EXTENTS OF YIELDING AND STRAIN HARDENING,
1280      C          RESPECTIVELY
1281      C
1282      ADEN=ERCB+ERTB
1283      IF (ST.GT.T1) GO TO 20
1284      ALFT=1.0D0
1285      ALFP=1.0D0
1286      GO TO 70
1287      20     IF (ST.GT.T2) GO TO 40
1288      IF (ADEN.EQ.0.0D0) GO TO 30
1289      ANUM=T2-ST
1290      ALFT=ANUM/ADEN
1291      ALFP=1.0D0
1292      GO TO 70
1293      30     ALFT=0.0D0
1294      ALFP=1.0D0
1295      GO TO 70
1296      40     IF (ST.GT.T3) GO TO 50
1297      ALFT=0.0D0
1298      ALFP=1.0D0
1299      GO TO 70
1300      50     IF (ST.GT.T4) GO TO 60
1301      IF (ADEN.EQ.0.0D0) GO TO 60
1302      ANUM=T4-ST
1303      ALFP=ANUM/ADEN
1304      ALFT=0.0D0
1305      GO TO 70
1306      60     ALFP=0.0D0
1307      ALFT=0.0D0
1308      C
1309      C
1310      C          CALCULATE GEOMETRIC SUBMATRIX COEFFICIENTS, FAC1
1311      C          TO FAC6.
1312      C
1313      70     CALL FWCALC(BCL,BF1,TF1,E2)
1314      FAC1=(YSFB+(ESH-EYBF)*E1+(ST-T4)*E2)*FE
1315      FAC2=ADEN*E2*FE
1316      FAC3=(YSFB+(ST-T2)*E1)*FE
1317      FAC4=ADEN*E1*FE
1318      FAC5=(ST-ERTB)*E*FE
1319      FAC6=ADEN*E*FE
1320      C
1321      C
1322      C          FORMULATE STIFFNESS SUBMATRICES FOR
1323      C          STRAIN-HARDENED REGION
1324      C
1325      A=-1.0D0
1326      B=-ALFP
1327      IF (DABS(A-B).LT.1.0D-5) GO TO 90
1328      CALL PH1(B,A,FI,CB,5,6,11)
1329      CALL PH1YY(B,A,FIYY,CB,5,6,7)
1330      CALL PH1PHI(B,A,FIPI,CB,5,6,9)
1331      CALL PH1Y(B,A,FIY,CB,5,6,9)
1332      CALL EPHI(B,A,EFI,CB,5,6,12)
1333      DO 80 I=1,5
1334      DO 80 J=1,5
1335      FB1(I,J)=FAC1*FI(I,J)-FAC2*EF1(I,J)
1336      FB2(I,J)=FB*FIYY(I,J)
1337      FB3(I,J)=FAC4*FIPI(I,J)
1338      FB4(I,J)=FD*FIY(I,J)
1339      FB5(I,J)=FAC1*FI(I,J)-FAC2*EF1(I,J)
1340      C
1341      C
1342      C          FORMULATE STIFFNESS SUBMATRICES FOR YIELDED REGION
1343      C
1344      90     A=-ALFP
1345      B=-ALFT
1346      IF (DABS(A-B).LT.1.0D-5) GO TO 110
1347      CALL FWCALC(BCL,BF1,TF1,E1)
1348      CALL PH1(B,A,FI,CB,5,6,11)
1349      CALL PH1YY(B,A,FIYY,CB,5,6,7)
1350      CALL PH1PHI(B,A,FIPI,CB,5,6,9)
1351      CALL PH1Y(B,A,FIY,CB,5,6,9)
1352      CALL EPHI(B,A,EFI,CB,5,6,12)
1353      DO 100 I=1,5
1354      DO 100 J=1,5
1355      FB1(I,J)=FB1(I,J)+FA*FI(I,J)

```



```

1582      COMMON /BLK8/CT(7,9),FT1(E,E),FT2(E,E),FT3(E,E),FT4(E,E),FT5(E,E)
1583      COMMON /BLK10/RW,TW,BCL,BF1,TF1,BF2,TF2
1584      COMMON /BLK11/E1,E2,ESH,YSW,YSFB,YSFT,SRTC,SRCM,SRTT,SRCB,SRCT
1585
1586      C
1587      C      INITIALISE THE STIFFNESS SUBMATRICES TO ZERO
1588      C
1589      DO 10 I=1,5
1590      DO 10 J=1,5
1591      FT1(I,J)=0.0D0
1592      FT2(I,J)=0.0D0
1593      FT3(I,J)=0.0D0
1594      FT4(I,J)=0.0D0
1595      FT5(I,J)=0.0D0
1596
1597
1598      C      ADJUST FLANGE THICKNESS TO ACCOUNT FOR
1599      C      WEB-TO-FLANGE FILLETS
1600
1601      TSAVE=TF2
1602      TF2=BF2*TF2/(BF2-2.0D0-TW)
1603
1604
1605      C      INITIALISE STRAINS AND STRAIN LIMITS, T1, T2, T3,
1606      C      TA
1607
1608      STEA=ST+EAPP
1609      STR=1.0D0/STEA
1610      T1=EYTF-ERTT
1611      T2=EYTF+ERTT
1612      T3=ESH-ERTT
1613      T4=ESH+ERTT
1614      ADEN=ERTT+ERTT
1615
1616
1617      C      EVALUATE PARAMETERS ALFT AND ALFP WHICH INDICATE
1618      C      EXTENTS OF YIELDING AND STRAIN HARDENING,
1619      C      RESPECTIVELY
1620
1621      IF (STEA.GT.T1) GO TO 20
1622      ALFT=1.0D0
1623      ALFP=1.0D0
1624      GO TO 70
1625      20     IF (STEA.GT.T2) GO TO 40
1626      IF (ADEN.EQ.0.0D0) GO TO 30
1627      ANUM=T2-STEA
1628      ALFT=ANUM/ADEN
1629      ALFP=1.0D0
1630      GO TO 70
1631      30     ALFT=0.0D0
1632      ALFP=1.0D0
1633      GO TO 70
1634      40     IF (STEA.GT.T3) GO TO 50
1635      ALFT=0.0D0
1636      ALFP=1.0D0
1637      GO TO 70
1638      50     IF (STEA.GT.T4) GO TO 60
1639      IF (ADEN.EQ.0.0D0) GO TO 60
1640      ANUM=TA-STEA
1641      ALFP=ANUM/ADEN
1642      ALFT=0.0D0
1643      GO TO 70
1644      60     ALFP=0.0D0
1645      ALFT=0.0D0
1646
1647
1648      C      CALCULATE GEOMETRIC SUBMATRIX COEFFICIENTS, FAC1
1649      C      AND FAC6.
1650
1651      70     CALL FWCALC(BCL,BF2,TF2,E2)
1652      FAC1=(YSFT+(ESH-EYTF)*E1+(STEA-T4)*E2)*FE*STR
1653      FAC2=ADEN*E2*FE*STR
1654      FAC3=(YSFT+(STEA-T2)*E1)*FE*STR
1655      FAC4=ADEN*E1*FE*STR
1656      FAC5=(STEA-ERTT)*E*FE*STR
1657      FAC6=ADEN*E*FE*STR
1658
1659
1660      C      FORMULATE STIFFNESS SUBMATRICES FOR
1661      C      STRAIN-HARDENED REGION.
1662
1663      A=-1.0D0
1664      B=-ALFP
1665      IF (DAES(A-B).LT.-1.0D-5) GO TO 90
1666      CALL PHIB(A,B,FI,CT,5,6,11)
1667      CALL PHIYY(B,A,FIYY,CT,5,6,7)
1668      CALL PHIPHI(B,A,FIFI,CT,5,6,9)
1669      CALL PHIY(B,A,FIY,CT,5,6,9)
1670      CALL EPHI(B,A,EF1,CT,5,6,12)
1671      DO 80 I=1,5
1672      DO 80 J=1,5
1673      FT1(I,J)=FA*FI(I,J)
1674      FT2(I,J)=FR*FIY(I,J)
1675      FT3(I,J)=FC*FIFI(I,J)
1676      FT4(I,J)=FD*FIYY(I,J)
1677      80     FT5(I,J)=FAC1*FI(I,J)-FAC2*EF1(I,J)
1678
1679
1680      C      FORMULATE STIFFNESS SUBMATRICES FOR YIELDED REGION
1681
1682      90     A=-ALFP
1683      B=-ALFT
1684      IF (DAES(A-B).LT.-1.0D-5) GO TO 110
1685      CALL FWCALC(BCL,BF2,TF2,E1)
1686      CALL PHIB(A,FI,CT,5,6,11)
1687      CALL PHIYY(B,A,FIYY,CT,5,6,7)
1688      CALL PHIPHI(B,A,FIFI,CT,5,6,9)
1689      CALL PHIY(B,A,FIY,CT,5,6,9)
1690      CALL EPHI(B,A,EF1,CT,5,6,12)
1691      DO 100 I=1,5
1692      DO 100 J=1,5
1693      FT1(I,J)=FT1(I,J)+FA*FI(I,J)
1694      FT2(I,J)=FT2(I,J)+FR*FIY(I,J)

```



```

1608      DD 10 J=1,5
1609      FT1(I,J)=0.0D0
1610      FT2(I,J)=0.0D0
1611      FT3(I,J)=0.0D0
1612      FT4(I,J)=0.0D0
1613      10  FT5(I,J)=0.0D0
1614      C
1615      C
1616      C      ADJUST FLANGE THICKNESS TO ACCOUNT FOR
1617      C      WEB-TO-FLANGE FILLETS
1618      C
1619      TSAVE=TF2
1620      TF2=BF2+TF2/(BF2-2.0D0*TW)
1621      C
1622      C
1623      C      INITIALISE STRAINS AND STRAIN LIMITS. T1, T2, T3,
1624      C      T4.
1625      C
1626      STR=1.0D0/ST
1627      T1=EYTF-ERCT
1628      T2=EYTF-ERTT
1629      T3=ESH-ERCT
1630      T4=ESH+ERTT
1631      C
1632      C
1633      C      EVALUATE PARAMETERS ALFT AND ALFP WHICH INDICATE
1634      C      EXTENTS OF YIELDING AND STRAIN HARDENING,
1635      C      RESPECTIVELY.
1636      C
1637      ADEN=ERCT+ERTT
1638      IF (ST.GT.T1) GO TO 20
1639      ALFT=1.0D0
1640      ALFP=1.0D0
1641      GO TO 70
1642      20  IF (ST.GT.T2) GO TO 40
1643      IF (ADEN.EQ.0.0D0) GO TO 30
1644      ANUM=T2-ST
1645      ALFT=ANUM/ADEN
1646      ALFP=1.0D0
1647      GO TO 70
1648      30  ALFT=0.0D0
1649      ALFP=1.0D0
1650      GO TO 70
1651      40  IF (ST.GT.T3) GO TO 50
1652      ALFT=0.0D0
1653      ALFP=1.0D0
1654      GO TO 70
1655      50  IF (ST.GT.T4) GO TO 60
1656      IF (ADEN.EQ.0.0D0) GO TO 60
1657      ANUM=T4-ST
1658      ALFP=ANUM/ADEN
1659      ALFT=0.0D0
1660      GO TO 70
1661      60  ALFP=0.0D0
1662      ALFT=0.0D0
1663      C
1664      C
1665      C      CALCULATE GEOMETRIC SUBMATRIX COEFFICIENTS, FAC1
1666      C      AND FAC6.
1667      C
1668      70  CALL FWCALC(BCL,BF2,TF2,E2)
1669      FAC1=(YSFT+(ESH-EYTF)*E1+(ST-T4)*E2)*FE
1670      FAC2=ADEN+E2*FE
1671      FAC3=(YSFT+(ST-T2)*E1)*FE
1672      FAC4=ADEN+E1*FE
1673      FAC5=(ST-ERTT)*E*FE
1674      FAC6=ADEN*E*FE
1675      C
1676      C
1677      C      FORMULATE STIFFNESS SUBMATRICES FOR
1678      C      STRAIN-HARDENED REGION.
1679      C
1680      A=-1.0D0
1681      B=-ALFP
1682      IF (DABS(A-B).LT.1.0D-5) GO TO 80
1683      CALL PHI(B,A,FI,CT,5,6,11)
1684      CALL PHIYY(B,A,FIYY,CT,5,6,7)
1685      CALL PHIPHI(B,A,FIFI,CT,5,6,9)
1686      CALL PHIY(B,A,FIY,CT,5,6,8)
1687      CALL EPHI(B,A,EFI,CT,5,6,12)
1688      DO 80 I=1,5
1689      DO 80 J=1,5
1690      FT1(I,J)=FA*FI(I,J)
1691      FT2(I,J)=FB*FIYY(I,J)
1692      FT3(I,J)=FC*FI(I,J)
1693      FT4(I,J)=FD*FIY(I,J)
1694      FT5(I,J)=FAC1*FI(I,J)-FAC2*EF1(I,J)
1695      C
1696      C
1697      C      FORMULATE STIFFNESS SUBMATRICES FOR YIELDED REGION
1698      C
1699      80  A=-ALFP
1700      B=-ALFT
1701      IF (DABS(A-B).LT.1.0D-5) GO TO 110
1702      CALL FWCALC(BCL,BF2,TF2,E1)
1703      CALL PHI(B,A,FI,CT,5,6,11)
1704      CALL PHIYY(B,A,FIYY,CT,5,6,7)
1705      CALL PHIPHI(B,A,FIFI,CT,5,6,9)
1706      CALL PHIY(B,A,FIY,CT,5,6,8)
1707      CALL EPHI(B,A,EFI,CT,5,6,12)
1708      DO 100 I=1,5
1709      DO 100 J=1,5
1710      FT1(I,J)=FT1(I,J)+FA*FI(I,J)
1711      FT2(I,J)=FT2(I,J)+FB*FIYY(I,J)
1712      FT3(I,J)=FT3(I,J)-FC*FI(I,J)
1713      FT4(I,J)=FT4(I,J)+FD*FIY(I,J)
1714      FT5(I,J)=FT5(I,J)+FAC3*FI(I,J)-FAC4*EF1(I,J)
1715      C
1716      C
1717      C      FORMULATE STIFFNESS SUBMATRICES FOR ELASTIC REGION.
1718      C
1719      110  A=-ALFT
1720      B=0.0D0

```



```

2034      C      WEB - TO - FLANGE FILLETS
2035      C
2036      TSAVE=TF2
2037      TF2=BF2*TF2/(BF2-2.0D0*TW)
2038      C
2039      C      INITIAL SE STRAINS AND STRAIN LIMITS, T1, T2, T3,
2040      C      T4.
2041      C
2042      C
2043      STR=1.0D0/ST
2044      T1=EYTF-ERCT
2045      T2=EYTF+ERTT
2046      T3=ESH-ERCT
2047      T4=ESH+ERTT
2048      C
2049      C
2050      C      EVALUATE PARAMETERS ALFT AND ALFP WHICH INDICATE
2051      C      EXTENTS OF YIELDING AND STRAIN HARDENING,
2052      C      RESPECTIVELY.
2053      C
2054      ADEN=ERCT+ERTT
2055      IF (ST.GT.T1) GO TO 20
2056      ALFT=1.0D0
2057      ALFP=1.0D0
2058      GO TO 70
2059      20      IF (ST.GT.T2) GO TO 40
2060      IF (ADEN.EQ.0.0D0) GO TO 30
2061      ANUM=T2-ST
2062      ALFT=ANUM/ADEN
2063      ALFP=1.0D0
2064      GO TO 70
2065      30      ALFT=0.0D0
2066      ALFP=1.0D0
2067      GO TO 70
2068      40      IF (ST.GT.T3) GO TO 50
2069      ALFT=0.0D0
2070      ALFP=1.0D0
2071      GO TO 70
2072      50      IF (ST.GT.T4) GO TO 60
2073      IF (ADEN.EQ.0.0D0) GO TO 60
2074      ANUM=T4-ST
2075      ALFP=ANUM/ADEN
2076      ALFT=0.0D0
2077      GO TO 70
2078      60      ALFP=0.0D0
2079      ALFT=0.0D0
2080      C
2081      C
2082      C      CALCULATE GEOMETRIC SUBMATRIX COEFFICIENTS, FAC1
2083      C      AND FAC6.
2084      C
2085      70      CALL FWCALC(BCL,BF2,TF2,E2)
2086      FAC1=(YSFT+(ESH-EYTF)*E1+(ST-T4)*E2)*FE
2087      FAC2=ADEN*E2*FE
2088      FAC3=(YSFT+(ST-T2)*E1)*FE
2089      FAC4=(ADEN*E1)*FE
2090      FAC5=(ST-ERTT)*E*FE
2091      FAC6=ADEN*E*FE
2092      C
2093      C
2094      C      FORMULATE STIFFNESS SUBMATRICES FOR
2095      C      STRAIN-HARDENED REGION.
2096      C
2097      A=-1.0D0
2098      B=-ALFP
2099      IF (DABS(A-B).LT.1.0D-5) GO TO 90
2100      CALL PH1(B,A,FI,CT,5,6,11)
2101      CALL PH1YY(B,A,FIYY,CT,5,6,7)
2102      CALL PH1PHI(B,A,FIIFI,CT,5,6,9)
2103      CALL PH1Y(B,A,FIY,CT,5,6,9)
2104      CALL EPH1(B,A,EFI,CT,5,6,12)
2105      DO 80 I=1,5
2106      DO 80 J=1,5
2107      FT1(I,J)=FA*FI(I,J)
2108      FT2(I,J)=FB*FIYY(I,J)
2109      FT3(I,J)=-FC*FIJF1(I,J)
2110      FT4(I,J)=FD*FIY(I,J)
2111      80      FTS(I,J)=FAC1*FI(I,J)-FAC2*EF1(I,J)
2112      C
2113      C
2114      C      FORMULATE STIFFNESS SUBMATRICES FOR YIELDED REGION
2115      C
2116      90      A=-ALFP
2117      B=-ALFT
2118      IF (DABS(A-B).LT.1.0D-5) GO TO 110
2119      CALL FWCALC(ECL,BF2,TF2,E1)
2120      CALL PH1(B,A,FI,CT,5,6,11)
2121      CALL PH1YY(B,A,FIYY,CT,5,6,7)
2122      CALL PH1PHI(B,A,FIIFI,CT,5,6,9)
2123      CALL PH1Y(B,A,FIY,CT,5,6,9)
2124      CALL EPH1(B,A,EFI,CT,5,6,12)
2125      DO 100 I=1,5
2126      DO 100 J=1,5
2127      FT1(I,J)=FT1(I,J)+FA*FI(I,J)
2128      FT2(I,J)=FT2(I,J)+FB*FIYY(I,J)
2129      FT3(I,J)=FT3(I,J)-FC*FIJF1(I,J)
2130      FT4(I,J)=FT4(I,J)+FD*FIY(I,J)
2131      100     FTS(I,J)=FT5(I,J)+FAC3*FI(I,J)-FAC4*EFI(I,J)
2132      C
2133      C
2134      C      FORMULATE STIFFNESS SUBMATRICES FOR ELASTIC REGION.
2135      C
2136      110     A=-ALFT
2137      B=0.0D0
2138      IF (DABS(A-B).LT.1.0D-5) GO TO 130
2139      CALL FWCALC(BCL,BF2,TF2,E)
2140      CALL PH1IE(B,A,FI,CT,5,6,11)
2141      CALL PH1YY(B,A,FIYY,CT,5,6,7)
2142      CALL PH1PHI(B,A,FIIFI,CT,5,6,9)
2143      CALL PH1Y(B,A,FIY,CT,5,6,9)
2144      CALL EPH1(B,A,EFI,CT,5,6,12)
2145      DO 120 I=1,5
2146      DO 120 J=1,5

```



```

2486
2487
2488
2489
2490      INITIALISE THE INVERTED MATRIX
2491
2492      DD 10 J=1,N
2493      DO 10 I=1,N
2494      SB1(I,J)=0.0D0
2495      IF (I.EQ.J) SB1(I,J)=1.0D0
2496      CONTINUE
2497      N1=N-1
2498      DO 70 K=1,N
2499      RP=1.0D0/SB1(K,K)
2500      SB1(J,K)=RP
2501      SB1(J,SB1(K,J))=RP
2502      DO 20 I=1,N
2503      SB1(I,J)=SB1(I,J)-SB1*SB1(I,K)
2504      SB1(I,J)=SB1(I,J)-SB1*J*SB1(I,K)
2505      SE(K,J)=SB1
2506      SB1(K,J)=SB1J
2507      RP=1.0D0/SB1(N,N)
2508      DO 60 J=1,K
2509      SB1(J,SB1(K,J))=RP
2510      DO 50 I=1,N
2511      SB1(I,J)=SB1(I,J)-SB1*J*SB1(I,K)
2512      SB1(I,J)=SB1J
2513      70 CONTINUE
2514      RETURN
2515      END
2516
2517
2518
2519      SUBROUTINE 18
2520
2521
2522
2523
2524      SUBROUTINE MULT
2525
2526      THIS ROUTINE MULTIPLIES TWO MATRICES SBI
2527      AND SG AND RETURNS THE RESULTING MATRIX ABG.
2528
2529
2530      SUBROUTINE MULT(ABG,SBI,SG,N)
2531      IMPLICIT REAL*8(A-H,D-Z)
2532      DIMENSION ABG(15,15),SBI(15,15),SG(15,15)
2533      DO 20 J=1,N
2534      DO 20 I=1,N
2535      SUM=0.0D0
2536      DO 10 K=1,N
2537      10 SUM=SUM+SBI(I,K)*SG(K,J)
2538      20 ABG(I,J)=SUM
2539      RETURN
2540      END
2541
2542
2543
2544      SUBROUTINE 20
2545
2546
2547
2548
2549      SUBROUTINE MCALC
2550
2551      THIS SUBROUTINE CALCULATES THE ELASTIC OR
2552      INELASTIC BENDING MOMENT ON A W-SHAPE WHEN THE
2553      STRAIN DISTRIBUTION ON A CROSS-SECTION IS KNOWN
2554      AND THE SECTION IS SUBJECTED TO A KNOWN AXIAL
2555      STRAIN.
2556
2557      SUBROUTINE MCALC(EB,EAPP,BM,BMY,BMP,BMMP,DNA,RDN)
2558      IMPLICIT REAL*8(A-H,D-Z)
2559      COMMON /BLK1/E,V,NS,ITYPE,LTYPE,INEL,N,ICLAMP,IKIND
2560      COMMON /BLKS/ERTB,ERCM,ERTT,ERCB,ERCT,EYW,EYBF,EYTF
2561      COMMON /BLK6/ERTBAR,YB,YI,AREA,ECC,ALAR,R
2562      COMMON /BLK10/HW,TW,BCL,BF1,TF1,BF2,TF2
2563      COMMON /BLK11/E1,E2,ESH,YSW,YSFB,YSFT,SRTB,SRCM,SRTT,SRCB,SRCT
2564      IF (EAPP.EQ.0.0D0) ALAR=0.0D0
2565
2566
2567
2568      CALCULATE YIELD MOMENT, YM, AND THE REDUCED PLASTIC
2569      MOMENT, PM.
2570
2571      Y1=YB-C 5D0*HW
2572      DT=0.5D0*HW-Y1
2573      DB=0.5D0*HW+Y1
2574      YM1=YSFT*ERTBAR/(DT+0.5D0*TF2)
2575      YM2=YSFB*ERTBAR/(DB+0.5D0*TF1)
2576      YM=DMIN1(YM1,YM2)
2577
2578
2579      DETERMINE THE LOCATION OF THE PLASTIC NEUTRAL AXIS.
2580
2581      F1=YSFB*BF1*TF1
2582      F2=YSFT*BF2*TF2
2583      FW=YSW*TW*HW
2584      PY=F1+F2-FW
2585      P=ALAR*PY
2586      D=HW+C 5D0*(TF1+TF2)
2587      APPY=F1.0D0+ALAR*PY
2588      AMPY=(1.0D0-ALAR)*PY
2589      AMPY1=AMPY-2.0D0*F1
2590      F22:2 0D0*F2
2591      FW2:2 0D0*FW
2592      F12:2 0D0*F1
2593      IF (APPY.GT.0.0D0.AND APPY.LE F22) GO TO 10
2594      IF (AMPY1.GE.0.0D0.AND AMPY1.LT.FW2) GO TO 20
2595      IF (AMPY.GE.0.0D0.AND AMPY.LT.F12) GO TO 30
2596
2597
2598      PLASTIC NEUTRAL AXIS IN TOP (COMPRESSION) FLANGE.

```



```

2599      C
2600    10   DSO=D**2
2601    DN=0.5D0*(P+PY)*TF2/F2
2602    DNSO=DN**2
2603    DMT2SO=(D-TF2)**2
2604    T1SO=TF1**2
2605    CPM1=0.5D0*YSFT*BF2*(DSC-2.0D0*DNSO+DMT2SO)
2606    CPM2=0.5D0*YSW*TW*(DMT2SO-T1SO)
2607    CPM3=0.5D0*YSFB*BF1*T1SO
2608    PM=CPM1+CPM2+CPM3-P*(DB+0.5D0*TF1)
2609    GO TO 40
2610
2611  C
2612  C          PLASTIC NEUTRAL AXIS IN THE WEB
2613
2614  20   DSO=D**2
2615    DC=D-TF1-TF2
2616    PFP:PY-F12-P
2617    DN=TF1+0.5D0*PFP*DC/fw
2618    DNSO=DN**2
2619    DMT2SO=(D-TF2)**2
2620    T1SO=TF1**2
2621    B2T2=BF2*TF2
2622    CPM1=0.5D0*YSFT*B2T2*(2.0D0*D-TF2)
2623    CPM2=0.5D0*YSW*TW*(DMT2SO-2.0D0*DNSO+T1SO)
2624    CPM3=0.5D0*YSFB*BF1*T1SO
2625    PM=CPM1+CPM2+CPM3-P*(DB+0.5D0*TF1)
2626    GO TO 40
2627
2628  C
2629  C          PLASTIC NEUTRAL AXIS IN BOTTOM (TENSION) FLANGE.
2630
2631  30   DSO=D**2
2632    DN=0.5D0*TF1*(PY-P)/F1
2633    DNSO=DN**2
2634    DMT2SO=(D-TF2)**2
2635    T1SO=TF1**2
2636    B2T2=BF2*TF2
2637    CPM1=0.5D0*YSFT*B2T2*(2.0D0*D-TF2)
2638    CPM2=0.5D0*YSW*TW*(DMT2SO-T1SO)
2639    CPM3=0.5D0*YSFB*BF1*(T1SO-2.0D0*DNSO)
2640    PM=CPM1+CPM2+CPM3-P*(DB+0.5D0*TF1)
2641
2642
2643  C          DEFINE STRAINS AND STRAIN LIMITS T1, T2, T3, T4 FOR
2644  C          TOP (COMPRESSION) FLANGE.
2645
2646  40   EAPEB=EB+EAPP
2647    EC=12.0D0*Y1/(2.0D0*Y1-HW))/EB
2648    REB1=R*EB
2649    EARST=EAAPP-REB
2650    RSTEAD=REB-EAPP
2651    T1=EYTF-ERCT
2652    T2=EYTF-ERTT
2653    T3=ESH-ERCT
2654    T4=ESH+ERTT
2655
2656  C
2657  C          CALCULATE TOTAL FORCE IN TOP (COMPRESSION) FLANGE
2658
2659    ADEN=ERCT+ERTT
2660    IF (EAPEB.GT.T1) GO TO 50
2661
2662
2663  C          DEFINE LIMITS OF INTEGRATION ALFT AND ALFP.
2664
2665    ALFT=1.0D0
2666    ALFP=1.0D0
2667    GO TO 100
2668    IF (EAPEB.GT.T2) GO TO 70
2669    IF (ADEN.EQ.0.0D0) GO TO 60
2670    ANUM=T2-EAPEB
2671    ALFT=ANUM/ADEN
2672    IF (ALFT.GT.1.0D0) ALFT=1.0D0
2673    IF (ALFT.LT.0.0D0) ALFT=0.0D0
2674    ALFP=1.0D0
2675    GO TO 100
2676    60   ALFT=0.0D0
2677    ALFP=1.0D0
2678    GO TO 100
2679    70   IF (EAPEB.GT.T3) GO TO 80
2680    ALFT=0.0D0
2681    ALFP=1.0D0
2682    GO TO 100
2683    80   IF (EAPEB.GT.T4) GO TO 90
2684    IF (ADEN.EQ.0.0D0) GO TO 90
2685    ANUM=T4-EAPEB
2686    ALFP=ANUM/ADEN
2687    IF (ALFP.GT.1.0D0) ALFP=1.0D0
2688    IF (ALFP.LT.0.0D0) ALFP=0.0D0
2689    ALFT=0.0D0
2690    GO TO 100
2691    90   ALFP=0.0D0
2692    ALFT=0.0D0
2693
2694
2695  C          ELASTIC RANGE.
2696
2697  100  A1=0.5D0*BF2*TF2*ALFT
2698    A2=2.0D0*(EAPEB-ERTT)=E
2699    A3=ADEN*E*ALFT
2700    F21=A1*(A2+A3)
2701
2702
2703  C          YIELDED RANGE
2704
2705    A1=0.5D0*BF2*TF2*(ALFP-ALFT)
2706    A2=2.0D0*(YSFT+(EAPEB-T2)=E1)
2707    A3=ADEN*E1*(ALFP+ALFT)
2708    F22=A1*(A2+A3)
2709
2710
2711  C          STRAIN-HARDENED REGION.

```



```

2712      C
2713      A1=0.5D0*BF2*TF2*(1.0D0-ALFP)
2714      A2=2.0D0*(-YSFT+(ESH-EYTF)*E1+(EAPEB-T4)*E2)
2715      A3=ADEN+E2*(1.0D0+ALFP)
2716      F23=A1*(A2+A3)
2717      F2=F21+F22+F23
2718      C
2719      C
2720      C      CALCULATE TOTAL FORCE IN BOTTOM (TENSION) FLANGE.
2721      C      IF THIS FLANGE IS IN COMPRESSION GO TO THE NEXT
2722      C      PART OF THE ROUTINE, OTHERWISE CONTINUE
2723      C
2724      IF (EARST.GT.0.0D0) GO TO 170
2725      C
2726      C      INITIALISE STRAIN LIMITS FOR BOTTOM (TENSION)
2727      C      FLANGE (T1, T2, T3, T4)
2728      C
2729      T1=EYBF-ERTB
2730      T2=EYBF-ERCB
2731      T3=ESH-ERTB
2732      T4=ESH+ERCB
2733      AD1=ERTB+ERCB
2734
2735      C
2736      C
2737      C      DEFINE LIMITS OF INTEGRATION, ALFB AND ALFBP
2738      C
2739      IF (RSTEA.GT.T1) GO TO 110
2740      ALFB=0.0D0
2741      ALFBP=0.0D0
2742      GO TO 160
2743      110  IF (RSTEA.GT.T2) GO TO 130
2744      IF (AD1.EQ.0.0D0) GO TO 120
2745      AN1=RSTEA-T1
2746      ALFB=AN1/AD1
2747      IF (ALFB.GT.1.0D0) ALFB=1.0D0
2748      IF (ALFB.LT.0.0D0) ALFB=0.0D0
2749      ALFBP=0.0D0
2750      GO TO 160
2751      120  ALFB=1.0D0
2752      ALFBP=0.0D0
2753      GO TO 160
2754      130  IF (RSTEA.GT.T3) GO TO 140
2755      ALFB=1.0D0
2756      ALFBP=0.0D0
2757      GO TO 160
2758      140  IF (RSTEA.GT.T4) GO TO 150
2759      IF (AD1.EQ.0.0D0) GO TO 150
2760      AN1=RSTEA-T3
2761      ALFBP=AN1/AD1
2762      IF (ALFBP.GT.1.0D0) ALFBP=1.0D0
2763      IF (ALFBP.LT.0.0D0) ALFBP=0.0D0
2764      ALFB=1.0D0
2765      GO TO 160
2766      150  ALFB=1.0D0
2767      ALFBP=1.0D0
2768      C
2769      C      STRAIN-HARDENED REGION.
2770
2771      160  A1=0.5D0*BF1*TF1*ALFBP
2772      A2=2.0D0*(-YSFB-(ESH-EYBF)*E1+(T3-RSTEA)*E2)
2773      A3=AD1+E2*ALFBP
2774      F11=A1*(A2+A3)
2775
2776      C
2777      C
2778      C      YIELDED RANGE.
2779      C
2780      A1=0.5D0*BF1*TF1*(ALFB-ALFBP)
2781      A2=2.0D0*(-YSFB+(T1-RSTEA)*E1)
2782      A3=AD1+E1*(ALFB+ALFBP)
2783      F12=A1*(A2+A3)
2784
2785      C
2786      C      ELASTIC RANGE.
2787      C
2788      A1=0.5D0*BF1*TF1*(1.0D0-ALFB)
2789      A2=2.0D0*(EARST-ERTB)*E
2790      A3=AD1+E*(1.0D0+ALFB)
2791      F13=A1*(A2+A3)
2792      F1=F13+F12+F11
2793      GO TO 240
2794
2795
2796      C      CALCULATE TOTAL FORCE WHEN BOTTOM (TENSION) FLANGE
2797      C      IS IN COMPRESSION INITIALISE STRAIN LIMITS T1, T2,
2798      C      T3, T4.
2799
2800      170  T1=EYBF-ERTB
2801      T2=EYBF-ERCB
2802      T3=ESH-ERCB
2803      T4=ESH+ERTB
2804
2805
2806      C      DEFINE LIMITS OF INTEGRATION, ALFT AND ALFP
2807      C
2808      ADEN=ERCB+ERTB
2809      IF (EARST.GT.T1) GO TO 180
2810      ALFT=1.0D0
2811      ALFP=1.0D0
2812      GO TO 230
2813      180  IF (EARST.GT.T2) GO TO 200
2814      IF (ADEN.EQ.0.0D0) GO TO 180
2815      ANUM=T2-EARST
2816      ALFT=ANUM/ADEN
2817      IF (ALFT.GT.1.0D0) ALFT=1.0D0
2818      IF (ALFT.LT.0.0D0) ALFT=0.0D0
2819      ALFP=1.0D0
2820      GO TO 230
2821      190  ALFT=0.0D0
2822      ALFP=1.0D0
2823      GO TO 230
2824      IF (EARST.GT.T3) GO TO 210

```



```

2825      ALFT=0.000
2826      ALFP=1.000
2827      GO TO 230
2228      21C      IF (EARST GT T4) GO TO 220
2229      IF (ADEN EQ 0.000) GO TO 220
2830      ANUM=T4-EARST
2831      ALFP=ANUM/ADEN
2832      IF (ALFP.GT.1.000) ALFP=1.000
2833      IF (ALFP.LT.0.000) ALFP=0.000
2834      ALFT=0.000
2835      GO TO 230
2836      220      ALFP=0.000
2837      ALFT=0.000
2838      C
2839      C
2840      C      ELASTIC REGION
2841      C
2842      230      A1=0.500*BF1*TF1=ALFT
2843      A2=2.000*(EARST-ERTB)=E
2844      A3=ADEN=E*ALFT
2845      F11=A1*(A2+A3)
2846      C
2847      C
2848      C      YIELDED REGION.
2849      C
2850      A1=C 5D0*BF1*TF1=(ALFP-ALFT)
2851      A2=2.000*(YSFB+(EARST-T2)*E1)
2852      A3=ADEN=E1*(ALFP+ALFT)
2853      F12=A1*(A2+A3)
2854      C
2855      C
2856      C      STRAIN-HARDENED REGION.
2857      C
2858      A1=C 5D0*BF1*TF1=(1.000-ALFP)
2859      A2=2.000*(YSFB+(ESH-EYBF)*E1+(EARST-T4)*E2)
2860      A3=ADEN=E2*(1.000+ALFP)
2861      F13=A1*(A2+A3)
2862      F1=F11+F12+F13
2863      C
2864      C
2865      C      CALCULATE BENDING MOMENT FROM LOWER (TENSION)
2866      C      PORTION OF WEB. DEFINE LIMITS OF INTEGRATION T1,
2867      C      T2, T3, T4, TS, T6.
2868      C
2869      240      T1=ERCM+EC
2870      T2=EYW-ERTB
2871      T3=ESH-ERTB
2872      T4=EYW+ERTT
2873      T5=ESH+ERTT
2874      T6=T1+EAPP
2875      C
2876      C
2877      C      DEFINE LIMITS OF INTEGRATION BET1, BETP1, BET3,
2878      C      BETP3.
2879      C
2880      AD1=REB+T1-ERTB
2881      AD2=EB-T1-ERTT
2882      IF (T6.GT.EYW) GO TO 250
2883      BET3=0.000
2884      BETP3=0.000
2885      GO TO 290
2886      250      IF (T6.GT.ESH) GO TO 270
2887      IF (AD1 EQ 0.000) GO TO 260
2888      BET3=(T6-EYW)/AD1
2889      IF (BET3 GT 1.000) BET3=1.000
2890      IF (BET3 LT 0.000) BET3=0.000
2891      BETP3=0.000
2892      GO TO 290
2893      260      BET3=1.000
2894      BETP3=0.000
2895      GO TO 290
2896      270      IF (AD1.EQ.0.000) GO TO 280
2897      BET3=(T6-EYW)/AD1
2898      BETP3=(T6-ESH)/AD1
2899      IF (BET3 GT 1.000) BET3=1.000
2900      IF (BET3 LT 0.000) BET3=0.000
2901      IF (BETP3.GT.1.000) BETP3=1.000
2902      IF (BETP3.LT.0.000) BETP3=0.000
2903      GO TO 290
2904      280      BET3=1.000
2905      BETP3=1.000
2906      290      IF (RSTEA GT T2) GO TO 300
2907      BET1=1.000
2908      BETP1=1.000
2909      GO TO 340
2910      300      IF (RSTEA GT T3) GO TO 320
2911      IF (AD1.EQ.0.000) GO TO 310
2912      BET1=(T6+EYW)/AD1
2913      IF (BET1 GT 1.000) BET1=1.000
2914      IF (BET1.LT.0.000) BET1=0.000
2915      BETP1=1.000
2916      GO TO 340
2917      310      BET1=1.000
2918      BETP1=1.000
2919      GO TO 340
2920      320      IF (AD1.EQ.0.000) GO TO 330
2921      BET1=(T6+EYW)/AD1
2922      BETP1=(T6+ESH)/AD1
2923      IF (BET1.GT.1.000) BET1=1.000
2924      IF (BET1.LT.0.000) BET1=0.000
2925      IF (BETP1.GT.1.000) BETP1=1.000
2926      IF (BETP1.LT.0.000) BETP1=0.000
2927      GO TO 340
2928      330      BET1=1.000
2929      BETP1=1.000
2930      C
2931      C
2932      C      CALCULATE MOMENT FROM LOWER
2933      C      STRAIN-HARDENING REGION
2934      C
2935      340      B1=TW*HW=.2/24.000
2936      B2=3.000*(YSW-(ESH-EYW)*E1+(T6+ESH)*E2)
2937      B3=BETP1*BETP1-1.000

```



```

2938      B4=2.0D0*(REB+T1+ERTB)*E2*(1.0D0-BETP1**3)
2939      WM1=B1*(B2+B3+B4)
2940      C
2941      C      CALCULATE MOMENT FROM YIELDED REGION.
2942      C
2943      C      B2=3.0D0*(-YSW+(TE+EYW)*E1)*(BET1**2-BETP1**2)
2944      C      B3=2.0D0*(REB+T1+ERTB)*E1*(BET1**3-BETP1**3)
2945      C      WM2=B1*(B2+B3)
2946      C
2947      C
2948      C      CALCULATE MOMENT FROM ELASTIC REGION.
2949      C
2950      C      B2=3.0D0*T6*E*(BET3**2-BET1**2)
2951      C      B3=2.0D0*(REB+ERTB+T1)*E*(BET3**3-BET1**3)
2952      C      WM3=B1*(B2+B3)
2953      C
2954      C
2955      C      CALCULATE MOMENT FROM UPPER YIELD REGION.
2956      C
2957      C      B2=3.0D0*(YSW+(T6-EYW)*E1)*(BETP3**2-BET3**2)
2958      C      B3=2.0D0*(REB+ERTB+T1)*E1*(BETP3**3-BET3**3)
2959      C      WM4=B1*(B2+B3)
2960      C
2961      C
2962      C      CALCULATE MOMENT FROM UPPER
2963      C      STRAIN-HARDENED REGION
2964      C
2965      C      B2=3.0D0*(YSW+(ESH-EYW)*E1+(T6-ESH)*E2)*(-BETP3**2)
2966      C      B3=2.0D0*(REB+ERTB+T1)*E2*BETP3**3
2967      C      WM5=B1*(B2+B3)
2968      C
2969      C
2970      C      CALCULATE MOMENT FROM TOP HALF (COMPRESSION)
2971      C      REGION OF WEB
2972      C
2973      C      CASE I - MIDDLE OF WEB ELASTIC.
2974      C      CASE II - MIDDLE OF WEB YIELDED.
2975      C      CASE III - MIDDLE OF WEB STRAIN-HARDENED.
2976      C
2977      C
2978      IF (T6.GT.EYW) GO TO 400
2979      IF (EAPEB.GT.T4) GO TO 350
2980      C
2981      C      CASE I
2982      C
2983      C      DEFINE LIMITS OF INTEGRATION BET2 AND BETP2.
2984      C
2985      C
2986      C
2987      BET2=1.0D0
2988      BETP2=1.0D0
2989      GO TO 350
2990      IF (EAPEB.GT.T5) GO TO 370
2991      IF (AD2.EQ.0.0D0) GO TO 360
2992      BET2=(EYW-T6)/AD2
2993      IF (BET2.GT.1.0D0) BET2=1.0D0
2994      IF (BET2.LT.0.0D0) BET2=0.0D0
2995      BETP2=1.0D0
2996      GO TO 390
2997      BET2=0.0D0
2998      BETP2=1.0D0
2999      GO TO 390
3000      IF (AD2.EQ.0.0D0) GO TO 380
3001      BET2=(EYW-T6)/AD2
3002      BETP2=(ESH-T6)/AD2
3003      IF (BET2.GT.1.0D0) BET2=1.0D0
3004      IF (BET2.LT.0.0D0) BET2=0.0D0
3005      IF (BETP2.GT.1.0D0) BETP2=1.0D0
3006      IF (BETP2.LT.0.0D0) BETP2=0.0D0
3007      GO TO 390
3008      380      BET2=0.0D0
3009      BETP2=0.0D0
3010      C
3011      C
3012      C      CALCULATE MOMENT FROM ELASTIC REGION
3013      C
3014      390      B1=TW*HW**2/2/4.0D0
3015      B2=3.0D0*TE*E*BET2**2
3016      B3=2.0D0*(EB-ERTT-T1)*E*E*BET2**3
3017      WM6=B1*(B2+B3)
3018      C
3019      C
3020      C      CALCULATE MOMENT FROM YIELDED REGION.
3021      C
3022      B2=3.0D0*(YSW+(TE-EYW)*E1)*(BETP2**2-BET2**2)
3023      B3=2.0D0*(EB-ERTT-T1)*E1*(BETP2**3-BET2**3)
3024      WM7=B1*(B2+B3)
3025      C
3026      C
3027      C      CALCULATE MOMENT FROM STRAIN-HARDENED REGION
3028      C
3029      B2=3.0D0*(YSW+(ESH-EYW)*E1+(T6-ESH)*E2)*(1.0D0-BETP2**2)
3030      B3=2.0D0*(EB-ERTT-T1)*E2*(1.0D0-BETP2**3)
3031      WM8=B1*(B2+B3)
3032      GO TO 510
3033      400      IF (T6.GT.ESH) GO TO 460
3034      C
3035      C      CASE II
3036      C
3037      C      DEFINE LIMITS OF INTEGRATION BET2 AND BETP2
3038      C
3039      IF (EAPEB.GT.T4) GO TO 420
3040      IF (AD2.EQ.0.0D0) GO TO 410
3041      BET2=(EYW-T6)/AD2
3042      IF (BET2.GT.1.0D0) BET2=1.0D0
3043      IF (BET2.LT.0.0D0) BET2=0.0D0
3044      BETP2=1.0D0
3045      GO TO 450
3046      410      BET2=1.0D0
3047      BETP2=1.0D0
3048      GO TO 450
3049      420      IF (EAPEB.GT.T5) GO TO 430
3050      BET2=1.0D0

```



```

3616      CALL FBFDRM
3617      CALL FTDRM
3618      CALL WBFDRM
3619      CALL ESFDRM(EIGV,MM1,XVEC,&80)
3620      EIGV=EIGV+E
3621      T1=EYTF-ERCT
3622      T2=EYBF-ERCB
3623      T3=EYW-ERCM
3624      TM=DMIN1(T1,T2,T3)
3625      C
3626      C
3627      C      IF SECTION BUCKLES ELASTICALLY OR IF INELASTIC
3628      C      ANALYSIS NOT REQUIRED WRITE RESULTS FOR ELASTIC
3629      C      BUCKLING. OTHERWISE PROCEED WITH INELASTIC ANALYSIS
3630      C
3631      CRST=EIGV/E
3632      IF (CRST.LE.TM) GO TO 70
3633      IF (INEL.EQ.0) GO TO 70
3634      NSTOP=0
3635      EA1:TM
3636      EA2:EA1
3637      C
3638      C
3639      C      CALCULATE EIGENVALUE FOR FIRST ASSUMED STRAIN (EA1)
3640      C
3641      CALL FBINAX(EA1)
3642      CALL FTINAX(EA1)
3643      CALL WBINAX(EA1)
3644      CALL ESFDRM(S1,MM1,XVEC,&80)
3645      S1=S1-1.0D0
3646      IF (S1.LT.0.0D0) GO TO 24
3647      GO TO 26
3648      NSTOP=NSTOP+1
3649      IF (NSTOP.GT.20) GO TO 115
3650      EA1=0.5D0*EA1
3651      GO TO 22
3652      NSTOP=0
3653      EA2=2.0*EA2
3654      NSTOP=NSTOP+1
3655      IF (NSTOP.GT.20) GO TO 110
3656      C
3657      C
3658      C      CALCULATE EIGENVALUE FOR SECOND ASSUMED STRAIN
3659      C      (EA2)
3660      C
3661      CALL FBINAX(EA2)
3662      CALL FTINAX(EA2)
3663      CALL WBINAX(EA2)
3664      CALL ESFDRM(S2,MM1,XVEC,&80)
3665      S2=S2-1.0D0
3666      IF (S2.GE.0.0D0) GO TO 40
3667      NCOUNT=0
3668      GO TO 50
3669      EA1:EA2
3670      S1=S2
3671      GO TO 30
3672      C
3673      C
3674      C      BEGIN ITERATION USING METHOD OF BISECTION.
3675      C      NOTE: S3 IS THE EIGENVALUE STRAIN CALCULATED FOR A
3676      C      SECTION HAVING AN ASSUMED STRAIN (EA2). CONVERGENCE
3677      C      IS REACHED PERFECTLY WHEN S3=EA3 (I.E. S3-EA3=0.0)
3678      C
3679      EA3=0.5D0*(EA1+EA2)
3680      CALL FBINAX(EA3)
3681      CALL FTINAX(EA3)
3682      CALL WBINAX(EA3)
3683      CALL ESFDRM(S3,MM1,XVEC,&80)
3684      S3=S3-EA3
3685      NCOUNT=NCOUNT+1
3686      DS1=DABS(EA3-EA1)/EA1
3687      DS2=DABS(EA3-EA2)/EA2
3688      C
3689      C      CHECK CONVERGENCE.
3690      C
3691      C
3692      TL=0.001D0
3693      IF (DS1.LT.TL.OR.DS2.LT.TL) GO TO 50
3694      IF (NCOUNT.GT.50) GO TO 100
3695      S13=S1*S3
3696      IF (S13.LT.0.0D0) GO TO 60
3697      EA1:EA3
3698      S1=S3
3699      GO TO 50
3700      EA2:EA3
3701      S2=S3
3702      GO TO 50
3703      C
3704      C      CALCULATION OF CRITICAL LOAD AND PLATE SLENDERNESS
3705      C      FOR ELASTIC CASES.
3706      C
3707      CALL PSCALC(CRST,P,PPY,SAVE)
3708      SB1=0.5D0*BF1/TF1
3709      SE2=0.5D0*BF2/TF2
3710      SW1=(HW-0.5D0*(TF1+TF2))/TW
3711      SB1C=SE1*DSORT1(YSF1)
3712      SB2C=SE2*DSORT1(YSF2)
3713      SW1C=SW1*DSORT1(YSW1)
3714      WRITE(6,250) P,PPY,SAVE,SB1,SB2,SW1,SB1C,SB2C,SW1C
3715      WAVE=BCL/MM1
3716      WRITE(6,220) EIGV,WAVE
3717      WRITE(6,220) XVEC(12,MM1),XVEC(14,MM1),XVEC(13,MM1),XVEC(11,MM1),
3718      &XVEC(15,MM1),XVEC(11,MM1),XVEC(10,MM1),XVEC(9,MM1),XVEC(8,MM1),
3719      &XVEC(7,MM1),XVEC(5,MM1),XVEC(6,MM1),XVEC(1,MM1),XVEC(3,MM1),XVEC(2,
3720      &8,MM1),XVEC(5,MM1),XVEC(4,MM1)
3721      RETURN
3722      C
3723      C
3724      C
3725      C      CALCULATION OF CRITICAL AXIAL LOAD AND PLATE
3726      C      SLENDERNESSES FOR INELASTIC CASES
3727      C
3728      CALL PSCALC(EA3,P,PPY,SAVE)

```



```

3729      SB1=0  SDO=BF1/TF1
3730      SB2=0  SDO=BF2/TF2
3731      SW1=(HW-0  SDO+(TF1+TF2))/TW
3732      SB1C=SB1+DSORT(YSFB)
3733      SB2C=SB2+DSORT(YSFT)
3734      SW1CFSW1+DSORT(YSW)
3735      C
3736      C      WRITE DUT RESULTS.
3737      C
3738      C      WRITE [6,250] P,PPY,SAVE,SB1,SB2,SW1,SB1C,SB2C,SW1C
3739      C      WAVE=BCL/MM1
3740      C      WRITE [6,230] EA3,WAVE
3741      C      WRITE [6,240] XVEC(12,MM1),XVEC(14,MM1),XVEC(13,MM1),XVEC(11,MM1),
3742      &XVEC(15,MM1),XVEC(11,MM1),XVEC(10,MM1),XVEC(9,MM1),XVEC(8,MM1),
3743      &XVEC(7,MM1),XVEC(5,MM1),XVEC(6,MM1),XVEC(1,MM1),XVEC(3,MM1),XVEC(2
3744      &,MM1),XVEC(4,MM1)
3745      C      RETURN
3746      100     WRITE [6,260]
3747      C      STOP
3748      115     WRITE [6,270]
3749      C      RETURN
3750      110     WRITE [6,280]
3751      C      RETURN
3752      C
3753      C
3754      C      FFORMAT STATEMENTS.
3755      C
3756      120     FFORMAT [3F12.6]
3757      130     FFORMAT ['0',10X,'ELASTIC ANALYSIS.']
3758      140     FFORMAT ['0',10X,'INELASTIC ANALYSIS.']
3759      150     FFORMAT ['0',10X,'YIELD MODULUS           ',F8.4,' KSI//'
3760      &80',10X,'STRAIN HARDENING MODULUS          ',F8.4,' KSI//''0',10X,'
3761      &TRAIN HARDENING STRAIN            ',F8.5)
3762      150     FFORMAT ['0',10X,'AREA OF CROSS-SECTION        ',F8.4,' SQ.IN
3763      &8/'0',10X,'DISTANCE TO CENTROID//',10X,'FROM CENTER OF BOTTOM FL
3764      &ANGE           ',F8.4,' INCHES//''0',10X,'CENTROIDAL MOMENT OF INERTIA
3765      &8   ',F8.4,' INCHES ')
3766      170     FFORMAT [F8.4]
3767      180     FFORMAT [7F8.5]
3768      190     FFORMAT ['1//',10X,'WIDE FLANGE SECTION',I3//''0',10X,'SUBJECTED TO
3769      &AXIAL LOAD ONLY.']
3770      200     FFORMAT ['0//',0',10X,'LENGTH OF WIDE FLANGE           ',F8.4,' IN
3771      &CHES//',0',10X,'WEB DEPTH             ',F8.5,' INCHES//'
3772      &'0',10X,'WEB THICKNESS          ',F8.5,' INCHES//''0',
3773      &810X,'BOTTOM FLANGE WIDTH       ',F8.5,' INCHES//''0',10X,'B
3774      &OTTOM FLANGE THICKNESS        ',F8.5,' INCHES//''0',10X,'TOP FLA
3775      &GE WIDTH           ',F8.5,' INCHES//''0',10X,'TOP FLANGE TH
3776      &ICKNESS           ',F8.5,' INCHES')
3777      210     FFORMAT ['0',10X,'WEB YIELD STRESS           ',F8.4,' KSI//'
3778      &80',10X,'BOTTOM FLANGE YIELD STRESS      ',F8.4,' KSI//''0',10X,'T
3779      &OP FLANGE YIELD STRESS         ',F8.4,' KSI//''0',10X,'RES. TENS
3780      &8 STRAIN (BDTT)           ',F8.5,' IN/IN//''0',10X,'RES. COMP. STRAIN
3781      &8 [MID. WEB]           ',F8.5,' IN/IN//''0',10X,'RES. TENS. STRAIN (TOP)
3782      &8   ',F8.5,' IN/IN//''0',10X,'RES. COMP. STRAIN (BOT)
3783      &8   ',F8.5,' IN/IN//''0',10X,'RES. COMP. STRAIN (TOP)
3784      &8   ',F8.5,' IN/IN//''0',10X,'RES. COMP. STRAIN (TOP)
3785      &8   ',F8.5,' IN/IN//''0',10X,'RES. COMP. STRAIN (TOP)
3786      220     FFORMAT ['1//',10X,T8,'CRITICAL STRESS ',F10 E,' KSI//''0',T8,'HA
3787      &LF WAVELENGTH ',F8.4//''')
3788      230     FFORMAT ['1//',10X,T8,'CRITICAL STRAIN ',F10 E//''0',T8,'HALF WAVE
3789      &LENGTH ',F8.4//''')
3790      240     FFORMAT ['1//',T8,'V =',F8.5,T27,'V = 0.00000',T46,'V =',F8.5//T8,'V
3791      &=',F8.5,T27,'V =',F8.5,T46,'V =',F8.5//''0',T13,'V =',F8.5//T8,'V
3792      &=',F8.5//T27,'V =',F8.5//T46,'V =',F8.5//''0',T13,'V =',F8.5//T8,'V
3793      &=',F8.5//T27,'V =',F8.5//T31,'V =',F8.5//T31,'V =',F8.5//T8,'V
3794      &=',F8.5//T31,'V =',F8.5//T31,'V =',F8.5//T31,'V =',F8.5//T8,'V
3795      &=',F8.5//T31,'V =',F8.5//T31,'V =',F8.5//T31,'V =',F8.5//T8,'V
3796      &=',F8.5//T31,'V =',F8.5//T31,'V =',F8.5//T31,'V =',F8.5//T8,'V
3797      &=',F8.5//T31,'V =',F8.5//T31,'V =',F8.5//T31,'V =',F8.5//T8,'V
3798      &=',F8.5//T31,'V =',F8.5//T31,'V =',F8.5//T31,'V =',F8.5//T8,'V
3799      &=',F8.5//T31,'V =',F8.5//T31,'V =',F8.5//T31,'V =',F8.5//T8,'V
3800      &=',F8.5//T31,'V =',F8.5//T31,'V =',F8.5//T31,'V =',F8.5//T8,'V
3801      &=',F8.5//T31,'V =',F8.5//T31,'V =',F8.5//T31,'V =',F8.5//T8,'V
3802      &=',F8.5//T31,'V =',F8.5//T31,'V =',F8.5//T31,'V =',F8.5//T8,'V
3803      &=',F8.5//T31,'V =',F8.5//T31,'V =',F8.5//T31,'V =',F8.5//T8,'V
3804      &=',F8.5//T31,'V =',F8.5//T31,'V =',F8.5//T31,'V =',F8.5//T8,'V
3805      &=',F8.5//T31,'V =',F8.5//T31,'V =',F8.5//T31,'V =',F8.5//T8,'V
3806      &=',F8.5//T31,'V =',F8.5//T31,'V =',F8.5//T31,'V =',F8.5//T8,'V
3807      260     FFORMAT ['//',10X,'CONVERGENCE FAILURE IN SUBROUTINE PLATE3 IN 50
3808      &ITERATIONS ')
3809      270     FFORMAT (' ',5X,'S1 FAILED TO BECOME NEGATIVE IN PLATE3 IN 20 ITERA
3810      &TIONS')
3811      280     FFORMAT (' ',5X,'S2 FAILED TO BECOME NEGATIVE IN PLATE3 IN 20 ITERA
3812      &TIONS')
3813      END
3814      CCCCCCCCCCCCCCCCCCCCCCCCCCCCCCCCCCCCCCCCCCCCCCCCCCCCCCCCCCCCCCCCCCCCCCCCC
3815      C
3816      C
3817      C      SUBROUTINE 28
3818      C
3819      C
3820      CCCCCCCCCCCCCCCCCCCCCCCCCCCCCCCCCCCCCCCCCCCCCCCCCCCCCCCCCCCCCCCCCCCCCCCCC
3821      C
3822      C
3823      C      SUBROUTINE PLATE4
3824      C
3825      C      THIS SUBROUTINE CALCULATES THE CRITICAL
3826      C      STRESS, CRITICAL BENDING MOMENT, AND BUCKLED
3827      C      CONFIGURATION FOR LOCAL BUCKLING OF W-SHAPES
3828      C      IN THE ELASTIC AND INELASTIC RANGES. RESIDUAL
3829      C      STRAINS AND END CONDITIONS MAY BE VARIED.
3830      CCCCCCCCCCCCCCCCCCCCCCCCCCCCCCCCCCCCCCCCCCCCCCCCCCCCCCCCCCCCCCCCCCCCCCCCC
3831      C      SUBROUTINE PLATE4
3832      C      IMPLICIT REAL*8(A-H,D-Z)
3833      C      DIMENSION XVEC(15,20)
3834      C      COMMON /BLK1/E,V,NS,ITYPE,LTYPE,INEL,N,ICLAMP,IKIND
3835      C      COMMON /BLK2/CB17,9),FB1(5,5),FB2(5,5),FB3(5,5),FB4(5,5),FB5(5,5)
3836      C      COMMON /BLK5/ERTBAR,Y,E,ERCB,ERTT,ERCB,ERT,YW,EYBF,EYTF
3837      C      COMMON /BLK8/CT17,9),FT1(5,5),FT2(5,5),FT3(5,5),FT4(5,5),FT5(5,5)
3838      C      COMMON /BLK9/CW17,9),WB1(7,7),WB2(7,7),WB3(7,7),WB4(7,7),WB5(7,7)
3839      C      COMMON /BLK10/HW,TW,BCL,TF1,BF1,TF2
3840      C      COMMON /BLK11/E1,E2,ESH,YSW,YSFT,SRBT,SRCH,SRRT,SRCB,SRCT
3841      C

```



```

3842      C
3843      C
3844      C      READ IN INPUT DATA.
3845      C
3846      C      READ (5,150) YSW,YSFB,YSFT,CAM1,CAM2,CAM3
3847      C      READ (5,150) BCL,HW,TW,BF1,TF1,BF2,TF2
3848      C      READ (5,120) E1,E2,ESH
3849      C
3850      C      CALCULATE SHAPE FUNCTION COEFFICIENT MATRICES
3851      C
3852      C      CALL COEFB(BF1)
3853      C      CALL COEFT(BF2)
3854      C      CALL COEFW
3855      C
3856      C
3857      C      CALCULATE THE FOLLOWING
3858      C
3859      C      EYW = YIELD STRAIN IN THE WEB
3860      C      EYBF = YIELD STRAIN IN THE BOTTOM FLANGE
3861      C      EYTF = YIELD STRAIN IN THE TOP FLANGE
3862      C      AREA = CROSS-SECTIONAL AREA
3863      C      ERTB = RESIDUAL TENSILE STRAIN AT WEB BOTTOM
3864      C      ERCH = RESIDUAL COMPRESSIVE STRAIN AT WEB
3865      C      MIDDLE
3866      C      ERTT = RESIDUAL COMPRESSIVE STRAIN AT WEB
3867      C      TOP
3868      C      ERCB = RESIDUAL COMPRESSIVE STRAIN AT BOTTOM
3869      C      FLANGE
3870      C      ERCT = RESIDUAL COMPRESSIVE STRAIN AT TOP
3871      C      FLANGE
3872      C      YB = DISTANCE TO CENTROID FROM BOTTOM OF
3873      C      SECTION
3874      C      ERTBAR = MOMENT OF INERTIA
3875      C      Y1 = DISTANCE TO THE CENTROID FROM
3876      C      MID-HEIGHT
3877      C      R = RATIO OF STRAIN IN COMPRESSION
3878      C      FLANGE/TENSION FLANGE (BENDING)
3879      C
3880      C      EYW=YSW/E
3881      C      EYBF=YSFB/E
3882      C      EYTF=YSFT/E
3883      C      AF1:=BF1*TF1
3884      C      AF2:=BF2*TF2
3885      C      LFS:=AF1+AF2
3886      C      AW:=HW*TW
3887      C      AREA:=AFS+AW
3888      C      ERTB:=CAM1*EYW
3889      C      ERCH:=CAM2*EYW
3890      C      ERTT:=CAM3*EYW
3891      C      FA1:=AW/(12*ODO*AF1)
3892      C      FA2:=AW/(12*ODO*AF2)
3893      C      SER:=6*ODO*EPCM
3894      C      FERT:=5*ODO*ERTT
3895      C      FERB:=5*ODO*ERTB
3896      C      EPCB:=ERTB-FA1*(SER-ERTT-FERB)
3897      C      ERCT:=ERTT-FA2*(SER-FERT-ERTB)
3898      C      SRTB:=ERTB+E
3899      C      SRCM:=EPCM+E
3900      C      SRTT:=ERTT+E
3901      C      SRCB:=ERCB+E
3902      C      SRCT:=ERCT+E
3903      C      YB:=(O_SDO*AW+AF2)*HW/AREA
3904      C      EPT1:=TW*HW*3/12*ODO
3905      C      EPT2:=BF2*TF2**3/12*ODO
3906      C      ERT3:=BF1*TF1**3/12*ODO
3907      C      ERT4:=LFS*HW*HW*O_25DO
3908      C      ERTIA:=ERT1+ERT2+ERT3+ERT4
3909      C      Y1:=YB+HW/2*ODO
3910      C      ERTBAR:=ERTIA+AREA=Y1**2
3911      C      PDEN:=O_SDO*HW-Y1
3912      C      IF (RDEN.EQ.0.ODO) GO TO 10
3913      C      RNUM:=O_SDO*HW+Y1
3914      C      R=RNUM/RDEN
3915      C      GO TO 20
3916      10      R=1.ODO
3917      C
3918      C      END CHECK INPUT DATA.
3919      C
3920      C
3921      20      WRITE (5,150) NS
3922      C      IF (INEL.EQ.0) WRITE (5,130)
3923      C      IF (INEL.EQ.1) WRITE (5,140)
3924      C      WRITE (5,200) BCL,HW,TW,BF1,TF1,BF2,TF2
3925      C      WRITE (5,150) AREA,YB,ERTBAR
3926      C      WRITE (5,210) YSW,YSFB,YSFT,SRTB,SRCH,SRTT,SRCB,SRCT
3927      C      WRITE (5,170) E1,E2,ESH
3928      C
3929      C
3930      C      CALCULATE ELASTIC CRITICAL STRESS
3931      C
3932      C      CALL FBFDRM
3933      C      CALL FFTDRM
3934      C      CALL WBFDRM
3935      C      CALL ESFDRM(EIGV,MM1,XVEC,80)
3936      C      E1GY:=EIGV/E
3937      C      CRST:=EIGV/E
3938      C      CRST1:=P*CRST
3939      C      ECF:=2*ODO*11/(2*ODO*Y1*HW))+CRST
3940      C      T1:=EYTF-ERCT
3941      C      T2:=EYBF-ERTB
3942      C      T3:=EYW-ERCH
3943      C      T4:=EYW-ERTB
3944      C      T5:=EYW+ERTT
3945      C
3946      C
3947      C      IF SECTION BUCKLES ELASTICALLY OR IF INELASTIC
3948      C      ANALYSIS IS NOT REQUIRED WRITE OUT RESULTS AND
3949      C      RETURN TO MAIN SUBROUTINE FOR NEXT SPECIMEN
3950      C      OTHERWISE CONTINUE WITH INELASTIC ANALYSIS
3951      C
3952      C      TM1=DMIN1(T1,T3,T5)
3953      C      TM2=DMIN1(T2,T4)
3954      C      IF (CRST LE TM1 AND CRST1 LE TM2 AND EC LE T3) GO TO 70

```



```

3955      IF (INEL.EQ.0) GO TO 70
3956      C
3957      C
3958      C      ASSUME A VALUE OF STRAIN, EA1, AND CALCULATE THE
3959      E      CORRESPONDING EIGENVALUE STRAIN, S1, SUCH THAT
3960      E      S1-EA1 > 0. SUBROUTINE SATEQ RESTORES EQUILIBRIUM
3961      C      TO THE SECTION
3962      C
3963      NSTOP=0
3964      EA1=DMIN1(TM1,TM2)
3965      22      EA2=EA1
3966      CALL SATEQ(EA1,0.0D0,0.0D0)
3967      CALL FBINBE(EA1)
3968      CALL FTINBE(EA1)
3969      CALL WBINBE(EA1)
3970      CALL ESFDRM(S1,MM1,XVEC,80)
3971      S1=S1-1.0D0
3972      IF (S1.LT.0.0D0) GO TO 24
3973      GO TO 26
3974      24      NSTOP=NSTOP+1
3975      IF (NSTOP.GT.20) GO TO 105
3976      EA1=0.5D0*EA1
3977      GO TO 22
3978      26      NSTOP=0
3979      C
3980      C
3981      C      DETERMINE A VALUE OF STRAIN, EA2, SUCH THAT
3982      C      S2-EA2 < C
3983      C
3984      30      EA2=1.2D0*EA1+AA*EA2
3985      CALL SATEQ(EA2,0.0D0,0.0D0)
3986      NSTOP=NSTOP+1
3987      IF (NSTOP.GT.20) GO TO 110
3988      CALL FBINBE(EA2)
3989      CALL FTINBE(EA2)
3990      CALL WBINBE(EA2)
3991      CALL ESFDRM(S2,MM1,XVEC,80)
3992      S2=S2-1.0D0
3993      IF (S2.GE.0.0D0) GO TO 40
3994      NCOUNT=0
3995      GO TO 50
3996      40      EA1=EA2
3997      S1=S2
3998      GO TO 30
3999      C
4000      C
4001      C      DETERMINE EA3 BY THE METHOD OF BISECTION AND USE
4002      E      SATEQ TO FIND THE EQUILIBRIUM LOCATION OF THE
4003      C      NEUTRAL AXIS FOR THIS VALUE OF STRAIN. CALCULATE
4004      E      THE CORRESPONDING EIGENVALUE, S3, AND CHECK TO SEE
4005      C      IF S3-EA3 IS LESS THAN OR EQUAL TO THE TOLERANCE,
4006      E      TL.
4007      E
4008      50      EA3=0.5D0*(EA1+EA2)
4009      CALL SATEQ(EA3,0.0D0,0.0D0)
4010      CALL FBINBE(EA3)
4011      CALL FTINBE(EA3)
4012      CALL WBINBE(EA3)
4013      CALL ESFDRM(S3,MM1,XVEC,80)
4014      S3=S3-EA3
4015      NCOUNT=NCOUNT+1
4016      DS1=DABS((EA1-EA3)/EA1)
4017      DS2=DAES((EA2-EA3)/EA2)
4018      C
4019      C
4020      C      IF CONVERGENCE HAS BEEN REACHED WRITE OUT RESULTS
4021      C      OTHERWISE CONTINUE ITERATIONS UP TO A MAXIMUM OF
4022      C      50. IF CONVERGENCE ISNOT REACHED WRITE OUT MESSAGE
4023      C      AND RETURN FOR A NEW SPECIMEN.
4024      C
4025      TL=0.0D1D0
4026      IF (DS1.LT.TL OR DS2.LT.TL) GO TO 90
4027      IF (NCOUNT.GT.50) GO TO 100
4028      S13=S1+S3
4029      IF (S13.LT.0.0D0) GO TO 60
4030      EA1=EA3
4031      S1:S3
4032      GO TO 50
4033      60      EA2=EA3
4034      S2:S3
4035      GO TO 50
4036      C
4037      C
4038      C      CALCULATE PLATE SLENDERNESSES (ELASTIC CASE)
4039      C
4040      70      SB1=0.5D0*BF1/TF1
4041      SB2=0.5D0*BF2/TF2
4042      SW1=(HW-C*5D0*(TF1+TF2))/TW
4043      SB1C=SB1*DSORT(YSFB)
4044      SB2C=SB2*DSORT(YSFB)
4045      SW1C=SW1*DSORT(YSW)
4046      C
4047      C
4048      C      CALCULATE CRITICAL BENDING MOMENT (ELASTIC CASE)
4049      C
4050      CALL MCALC(CRST,0.0D0,BM,BMY,BMP,BMMP,DNA,RDNA)
4051      C
4052      C
4053      C      WRITE OUT RESULTS (ELASTIC CASE)
4054      C
4055      WRITE (6,260) BM,BMY,BMMP,DNA,RDNA,SB1,SB2,SW1,SB1C,SB2C,SW1C
4056      WAVE=BCL/MM1
4057      WRITE (6,220) EIGV,WAVE
4058      WRITE (6,240) XVEC(12,MM1),XVEC(14,MM1),XVEC(13,MM1),XVEC(11,MM1),
4059      8XVEC(15,MM1),XVEC(11,MM1),XVEC(10,MM1),XVEC(9,MM1),XVEC(8,MM1),
4060      8XVEC(7,MM1),XVEC(5,MM1),XVEC(6,MM1),XVEC(1,MM1),XVEC(3,MM1),XVEC(2
4061      8,MM1),XVEC(5,MM1),XVEC(4,MM1)
4062      RETURN
4063      C
4064      C
4065      C      CALCULATE PLATE SLENDERNESSES (INELASTIC CASE)
4066      C
4067      80      SB1=0.5D0*BF1/TF1

```



```

4 181      IMPLICIT REAL*8(A-H,O-Z)
4 182      DIMENSION XVEC(15,20)
4 183      COMMON /BLK1/E,V,NS,ITYPE,INEL,N,ICLAMP,IKIND
4 184      COMMON /BLK2/CB(7,9),FB1(5,5),FB2(5,5),FB3(5,5),FB4(5,5),FB5(5,5)
4 185      COMMON /BLK5/ERCB,ERCM,ERT,EERT,ERCT,EYW,EYBF,EYTF
4 186      COMMON /BLK6/ERTBAR,YB,Y1,AREA,ECC,ALAR,R
4 187      COMMON /BLK8/CT(7,9),FT1(5,5),FT2(5,5),FT3(5,5),FT4(5,5),FT5(5,5)
4 188      COMMON /BLK9/CW(7,9),WB1(7,7),WB2(7,7),WB3(7,7),WB4(7,7),WB5(7,7)
4 189      COMMON /BLK10/HW,TW,BCL,BF1,TF1,BF2,TF2
4 190      COMMON /BLK11/E1,E2,ESH,YSW,YSFB,YSFT,SRTB,SRCM,SRTT,SRCE,SRCT
4 191      C
4 192      C
4 193      C      READ IN PLATE DIMENSIONS AND MATERIAL PROPERTIES
4 194      C
4 195      10     READ (5,310) YSW,YSFB,YSFT,GAM1,GAM2,GAM3
4 196      READ (5,320) BCL,HW,TW,BF1,TF1,BF2,TF2
4 197      READ (5,290) E1,E2,ESH
4 198      C
4 199      C
4 200      C      FORMULATE MATRICES OF COEFFICIENTS OF SHAPE
4 201      C      FUNCTIONS
4 202      C
4 203      CALL COEFT(BF1)
4 204      CALL COEFT(BF2)
4 205      CALL COEFT
4 206      ICASE=1
4 207      C
4 208      C
4 209      C      CALCULATE THE FOLLOWING
4 210      C
4 211      EYW    = YIELD STRAIN IN THE WEB
4 212      EYBF   = YIELD STRAIN IN THE BOTTOM FLANGE
4 213      EYTF   = YIELD STRAIN IN THE TOP FLANGE
4 214      AREA   = CROSS-SECTIONAL AREA
4 215      ERTB   = RESIDUAL TENSILE STRAIN AT WEB BOTTOM
4 216      ERCM   = RESIDUAL COMPRESSIVE STRAIN AT WEB
4 217      MIDDLE
4 218      ERTT   = RESIDUAL COMPRESSIVE STRAIN AT WEB
4 219      TOP
4 220      ERCB   = RESIDUAL COMPRESSIVE STRAIN AT BOTTOM
4 221      FLANGE
4 222      ERCT   = RESIDUAL COMPRESSIVE STRAIN AT TOP
4 223      FLANGE
4 224      YB    = DISTANCE TO CENTROID FROM BOTTOM OF
4 225      SECTION
4 226      ERTBAR = MOMENT OF INERTIA
4 227      Y1    = DISTANCE TO THE CENTROID FROM
4 228      MID-HEIGHT
4 229      R     = RATIO OF STRAIN IN COMPRESSION
4 230      FLANGE/TENSION FLANGE (BENDING)
4 231      C
4 232      AF1=BF1*TF1
4 233      AF2=BF2*TF2
4 234      AFS=AF1+AF2
4 235      AW=HW-TW
4 236      AREA=AFS*AW
4 237      EYW=YSW/E
4 238      EYBF=YSFB/E
4 239      EYTF=YSFT/E
4 240      ERTB=GAM1=EYW
4 241      ERCM=GAM2=EYW
4 242      ERTT=GAM3=EYW
4 243      FA1=AW/(12.0D0*AF1)
4 244      FA2=AW/(12.0D0*AF2)
4 245      SER=6.0D0*ERCM
4 246      FERT=5.0D0*ERTT
4 247      FERB=5.0D0*ERTB
4 248      ERCB=ERTB-FA1*(SER-ERTT-FERB)
4 249      ERCT=ERTT-FA2*(SER-FERT-ERTB)
4 250      SRTB=ERTT*E
4 251      SRCM=ERCM*E
4 252      SRTT=ERTT*E
4 253      SRCE=ERCB*E
4 254      SRCT=ERCT*E
4 255      YB=(O_SDO*AW+AF2)*HW/AREA
4 256      ERT1=TW*HW**3/12.0D0
4 257      ERT2=BF2*TF2**3/12.0D0
4 258      ERT3=BF1*TF1**3/12.0D0
4 259      ERT4=AFS*HW**HW**25D0
4 260      ERTIA=ERT1+ERT2+ERT3+ERT4
4 261      Y1=YB-HW/2.0D0
4 262      ERTBAR=ERTIA*AREA*Y1**2
4 263      RDEN=O_SDO*HW*Y1
4 264      IF (RDEN.EQ.0.0D0) GO TO 20
4 265      RNUM=O_SDO*HW*Y1
4 266      R=RNUM/RDEN
4 267      GO TO 30
4 268      20     R=1.0D0
4 269      30     READ (5,300) ALAR
4 270      AX1=YSFT*AF2
4 271      AX2=YSFB*AF1
4 272      AX3=YSW*AW
4 273      AXLD=ALAR*(AX1+AX2+AX3)
4 274      C
4 275      C      ECHO CHECK INPUT DATA
4 276      C
4 277      C
4 278      IF (INEL.EQ.1) WRITE (6,390) NS
4 279      IF (INEL.EQ.0) WRITE (6,320) NS,AXLD
4 280      IF (INEL.EQ.0) WRITE (6,400)
4 281      IF (INEL.EQ.1) WRITE (6,410)
4 282      WRITE (6,340) ALAR
4 283      WRITE (6,420) BCL,HW,TW,BF1,TF1,BF2,TF2
4 284      WRITE (6,450) AREA,YB,ERTBAR
4 285      WRITE (6,430) YSW,YSFB,YSFT,SRTB,SRCM,SRTT,SRCE,SRCT
4 286      WRITE (6,440) E1,E2,ESH
4 287      IF (INEL.EQ.1) GO TO 50
4 288      LKEEP=LTYPE
4 289      C
4 290      C      CALCULATE ELASTIC CRITICAL AXIAL LOAD
4 291      C
4 292      C
4 293      C

```



```

294      CALL FBFORM
295      CALL FTFORM
296      CALL WBFORM
297      CALL ESFORM(EIGV,MM1,XVEC,.8210)
298      EIGV=E;GY=E
299      CRSTI=EIGV/E
300      APPS=AXL0/AREA
301
302      IF (APPS GE EIGV) GO TO 40
303      LTYPE=LKEEP
304      CALL FBFORM
305      CALL FTFORM
306      CALL WBFORM
307      CALL ESFORM(EIGV,MM1,XVEC,.8210)
308      EIGV=EIGV/E
309      CRSTI=EIGV/E
310      AXAR=AXL0/AREA
311      EAPP=AXAR/E
312
313      CALCULATE PLATE SLENDERNESSES
314
315      SB1=C SDO*BF1/TF1
316      SB2=C SDO*BF2/TF2
317      SW1=(HW-C SDO*(TF1+TF2))/TW
318      SB1C=SB1*DSORT(VSF)
319      SB2C=SB2*DSORT(VSF)
320      SW1C=SW1*DSORT(YSW)
321
322      CALCULATE BENDING MOMENT AND WRITE OUT RESULTS FOR
323      AXIAL BUCKLING
324
325      CALL MCALC(CRSTI,EAPP,BM,BMY,BMP,BMMP,DNA,RDNA)
326      WRITE (6,520) BM,BMY,BMP,BMMP,DNA,RDNA,SB1,SB2,SW1,SB1C,SB2C,SW1C
327      WAVE=BCL/MM1
328
329      WRITE (6,470) EIGV,AXAR,WAVE
330      WRITE (6,520) XVEC(12,MM1),XVEC(14,MM1),XVEC(13,MM1),XVEC(11,MM1),
331      &XVEC(15,MM1),XVEC(11,MM1),XVEC(10,MM1),XVEC(9,MM1),XVEC(8,MM1),
332      &XVEC(7,MM1),XVEC(5,MM1),XVEC(6,MM1),XVEC(1,MM1),XVEC(3,MM1),XVEC(2
333      &8,MM1),XVEC(5,MM1),XVEC(4,MM1)
334      RETURN
335      WAVE=BCL/MM1
336
337      CALCULATE PLATE SLENDERNESSES
338
339      SB1=C SDO*BF1/TF1
340      SB2=C SDO*BF2/TF2
341      SW1=(HW-C SDO*(TF1+TF2))/TW
342      SB1C=SB1*DSORT(VSF)
343      SB2C=SB2*DSORT(VSF)
344      SW1C=SW1*DSORT(YSW)
345
346      WRITE OUT RESULTS FOR ELASTIC BUCKLING DUE TO AXIAL
347      PLUS BENDING STRESSES AND RETURN TO MAIN PROGRAM
348
349      CALL PSCALE(CRST,P,PPY,SAVE)
350      WRITE (6,540) P,PPY,SAVE,SB1,SB2,SW1,SB1C,SB2C,SW1C
351      WRITE (6,460) APPS,EIGV,WAVE
352      WRITE (6,520) XVEC(12,MM1),XVEC(14,MM1),XVEC(13,MM1),XVEC(11,MM1),
353      &XVEC(15,MM1),XVEC(11,MM1),XVEC(10,MM1),XVEC(9,MM1),XVEC(8,MM1),
354      &XVEC(7,MM1),XVEC(5,MM1),XVEC(6,MM1),XVEC(1,MM1),XVEC(3,MM1),XVEC(2
355      &8,MM1),XVEC(5,MM1),XVEC(4,MM1)
356      RETURN
357
358      CALCULATE CRITICAL AXIAL LOAD FOR INELASTIC
359      ANALYSIS SEE PLATE3 FOR STEPS
360
361      LKEEP=LTYPE
362      LTYPE=1
363      T1=ENTF-ERCY
364      T2=ENF-BPCB
365      T3=EVW-ERCM
366      TM=DMIN(T1,T2,T3)
367      CALL FBFORM
368      CALL FTFORM
369      CALL WBFORM
370      CALL ESFORM(EIGV,MM1,XVEC,.8240)
371      EIGV=EIGV/E
372      CRSTI=EIGV/E
373      IF (CRST.LE.TM) GO TO 100
374      NSTOP=0
375      EA1=TM
376      EA2=EA1
377      CALL FBINAX(EA1)
378      CALL FTINAX(EA1)
379      CALL WBINAX(EA1)
380      CALL ESFORM(S1,MM1,XVEC,.8240)
381      S1FS=1 ODO
382      IF (S1.LT.0 ODO) GO TO 54
383      GO TO 56
384      NSTOP=NSTOP+1
385      IF (NSTOP.GT.20) GO TO 285
386      EA1=C SDO*EA1
387      GO TO 52
388      NSTOP=0
389      EA2=1 200*EA1+44*EA2
390      NSTOP=NSTOP+1
391      IF (NSTOP.GT.20) GO TO 270
392      CALL FBINAX(EA2)
393      CALL FTINAX(EA2)
394      CALL WBINAX(EA2)
395      CALL ESFORM(S2,MM1,XVEC,.8240)
396      S2FS=1 ODO
397      IF (S2.GE.0 ODO) GO TO 70

```



```

4407      NCOUNT=0
4408      GO TO 80
4409      70   EA1=EA2
4410      S1=S2
4411      GO TO 60
4412      60   EA3=0.5D0*(EA1+EA2)
4413      CALL FBINAX(EA3)
4414      CALL FTINAX(EA3)
4415      CALL WBINAX(EA3)
4416      CALL ESFORM(S3,MM1,XVEC,&240)
4417      S3=S3-1.0D0
4418      NCOUNT=NCOUNT+1
4419      DS1=DABS((EA1-EA2)/EA1)
4420      DS2=DABS((EA2-EA3)/EA2)
4421      TLFO=0.01D0
4422      IF (DS1 LT TL OR DS2 LT TL) GO TO 110
4423      IF (NCOUNT GT 50) GO TO 200
4424      S13=S1*S3
4425      IF (S13 LT.0.0D0) GO TO 90
4426      EA1=EA2
4427      S1=S3
4428      GO TO 80
4429      80   EA2=EA3
4430      S2=S3
4431      GO TO 80
4432      100  STRAIN=CRST
4433      GO TO 120
4434      110  STRAIN=EA3
4435      120  CALL PSCALC(STRAIN,P,PPY,SAVE)
4436      SB1=0.5D0*BF1/TF1
4437      SB2=0.5D0*BF2/TF2
4438      SW1=(HW-O.5D0*(TF1+TF2))/TW
4439      SB1C=SB1*D_SORT(YSFB)
4440      SB2C=SB2*D_SORT(YSFT)
4441      SW1C=SW1*D_SORT(YSW)
4442      WRITE (6,540) P,PPY,SAVE,SB1,SB2,SW1,SB1C,SB2C,SW1C
4443      WAVE=BCL/MM1
4444      WRITE (6,510) STRAIN,WAVE
4445      WRITE (6,520) XVEC(12,MM1),XVEC(14,MM1),XVEC(13,MM1),XVEC(11,MM1),
4446      &XVEC(15,MM1),XVEC(11,MM1),XVEC(10,MM1),XVEC(9,MM1),XVEC(8,MM1),
4447      &XVEC(7,MM1),XVEC(5,MM1),XVEC(6,MM1),XVEC(1,MM1),XVEC(3,MM1),XVEC(2
4448      &,MM1),XVEC(5,MM1),XVEC(4,MM1)
4449      C
4450      C
4451      C      IF THE APPLIED AXIAL LOAD IS GREATER THAN THE
4452      C      CRITICAL AXIAL LOAD, WRITE OUT MESSAGE. OTHERWISE
4453      C      CONTINUE
4454      C
4455      130  IF (AXLO GE P) GO TO 230
4456      WRITE (6,350) ICASE,AXLO
4457      WRITE (6,340) ALAR
4458      C
4459      C
4460      C      DETERMINE THE STRAIN CORRESPONDING TO THE APPLIED
4461      C      AXIAL LOAD
4462      C
4463      PBODY=TM*E*AREA
4464      IF (AXLO LE PBODY) GO TO 140
4465      CALL GETST(AXLO,EAPP,&210)
4466      GO TO 150
4467      140  EAPP=AXLD/AREA/E
4468      150  LTYPE=LKEEP
4469      WRITE (6,360) STRAIN,EAPP
4470      C
4471      C
4472      C      BEGIN CALCULATION OF CRITICAL BENDING STRAIN.
4473      C      ASSUME INITIAL STRAIN, ESB1, AND RESTORE
4474      C      EQUILIBRIUM TO THE SECTION USING SUBROUTINE SATEO
4475      C      CALCULATE THE CORRESPONDING EIGENVALUE STRAIN SAB1
4476      C      (IDEALLY EQUAL TO ESB1+EAPP, WHERE EAPP IS THE
4477      C      APPLIED AXIAL STRAIN).
4478      C
4479      NSTOP=0
4480      ESB1=0.1D0*(STRAIN-EAPP)
4481      152  ESB2=ESB1
4482      CALL SATEO(ESB1,EAPP,AXLO)
4483      CALL FBINAB(ESB1,EAPP)
4484      CALL FTINAB(ESB1,EAPP)
4485      CALL WBINAB(ESB1,EAPP)
4486      CALL ESFORM(SAB1,MM1,XVEC,&240)
4487      SAB1=SAB1-ESB1-EAPP
4488      IF (SAB1 LT.0.0D0) GO TO 154
4489      GO TO 156
4490      154  NSTOP=NSTOP+1
4491      IF (NSTOP GT 20) GO TO 255
4492      ESE1=0.5D0*ESB1
4493      156  NSTOP=0
4494      160  ESB2=1.2D0*ESB1+AA*ESB2
4495      CALL SATEO(ESB2,EAPP,AXLD)
4496      NSTOP=NSTOP+1
4497      IF (NSTOP GT 20) GO TO 260
4498      C
4499      C
4500      C      DETERMINE THE VALUE OF ESB2 SUCH THAT
4501      C      SAB2-ESB2-EAPP < 0
4502      C
4503      CALL FBINAB(ESB2,EAPP)
4504      CALL FTINAB(ESB2,EAPP)
4505      CALL WBINAB(ESB2,EAPP)
4506      CALL ESFORM(SAB2,MM1,XVEC,&240)
4507      SAB2=SAB2-ESB2-EAPP
4508      IF (SAB2 GE.0.0D0) GO TO 170
4509      NCOUNT=0
4510      GO TO 180
4511      170  ESB1=ESB2
4512      SAB1=SAB2
4513      GO TO 180
4514      180  ESB3=0.5D0*(ESE1+ESB2)
4515      C
4516      C
4517      C      DETERMINE ESB3 BY THE METHOD OF BISECTION AND
4518      C      CONTINUE ITERATIONS UP TO A MAXIMUM OF 50
4519      C      CONVERGENCE IS REACHED WHEN SAB3-EAB3-EAPP IS CLOSE

```



```

4520 C ENOUGH TO ZERO
4521 C
4522 CALL SATEO(ESE3,EAPP,AXLD)
4523 CALL FBINAB(ESE2,EAPP)
4524 CALL FTINAB(ESE2,EAPP)
4525 CALL WBINAB(ESE3,EAPP)
4526 CALL ESFORM(SAE3,MM1,XVEC,8240)
4527 SAB3=SAB3-ESB3-EAPP
4528 NCOUNT=NCOUNT+1
4529 DS1=DABS((ESE3-ESB1)/ESB1)
4530 DS2=DABS((ESB2-ESB3)/ESB2)
4531 TL=0.001D0
4532 IF (DS1.LT.TL .OR. DS2.LT.TL) GO TO 220
4533 IF (NCOUNT.GT.50) GO TO 250
4534 SAB13=SAB1*SAB3
4535 IF (SAB13.LT.0.0D0) GO TO 190
4536 ESB1=ESB3
4537 SAB1=SAB3
4538 GO TO 180
4539 180 ESB2=ESB3
4540 SAB2=SAB3
4541 GO TO 180
4542 200 WRITE (E,480)
4543 210 RETURN
4544 C
4545 C
4546 C CALCULATE PLATE SLENDERNESSES
4547 C
4548 220 SB1=0.5D0*BF1/TF1
4549 SB2=0.5D0*BF2/TF2
4550 SW1=(HW-0.5D0*(TF1+TF2))/TW
4551 SB1C=SB1*DSORT(YSF)
4552 SB2C=SB2*DSORT(YFT)
4553 SW1C=SW1*DSORT(YSW)
4554 C
4555 C
4556 C CALCULATE CRITICAL BENDING MOMENT CORRESPONDING TO
4557 C CRITICAL STRAIN, ESE3, AND WRITE OUT RESULTS
4558 C
4559 CALL MCALC(ESE3,EAPP,BM,BMY,BMP,BMMP,DNA,RDNA)
4560 WRITE (E,520) BM,BMY,BMP,BMMP,DNA,RDNA,SB1,SB2,SW1,SB1C,SB2C,SW1C
4561 WAVE=BCL/MM1
4562 RATIO=ESB3/YTF
4563 WRITE (E,370) RATIO
4564 WRITE (E,510) ESB3,WAVE
4565 WRITE (E,520) XVEC(12,MM1),XVEC(14,MM1),XVEC(13,MM1),XVEC(11,MM1),
4566 &XVEC(15,MM1),XVEC(11,MM1),XVEC(10,MM1),XVEC(9,MM1),XVEC(8,MM1),
4567 &XVEC(7,MM1),XVEC(1,MM1),XVEC(6,MM1),XVEC(1,MM1),XVEC(3,MM1),XVEC(2,
4568 &,MM1),XVEC(5,MM1),XVEC(4,MM1)
4569 GO TO 240
4570 230 WRITE (E,380) ICASE,AXLD
4571 WRITE (E,340) ALAR
4572 WRITE (E,490)
4573 C
4574 C
4575 C READ IN NEXT VALUE OF ALAR = P/PY WHERE P IS THE
4576 C APPLIED AXIAL LOAD AND PY IS THE YIELD LOAD
4577 C CONTINUE WITH CALCULATIONS OF CRITICAL BENDING
4578 C STRESS FOR THIS AXIAL LOAD.
4579 C
4580 240 READ (5,300) ALAR
4581 ICASE=ICASE+1
4582 ALAR1=0.0D0
4583 ALAR2=1.0D0
4584 IF (ALAR.LT.ALAR2) RETURN
4585 IF (ALAR.LT.ALAR1) GO TO 10
4586 AXLD=ALAR*(AX1+AX2+AX3)
4587 IF (AXLD.GE.P) GO TO 230
4588 GO TO 130
4589 250 WRITE (E,500)
4590 RETURN
4591 260 WRITE (E,560)
4592 STOP
4593 270 WRITE (E,550)
4594 STOP
4595 255 WRITE (E,580)
4596 STOP
4597 265 WRITE (E,570)
4598 STOP
4599 C
4600 C
4601 C FORMAT STATEMENTS
4602 C
4603 280 FORMAT (3F12.6)
4604 300 FORMAT (F12.6)
4605 310 FORMAT (6F12.6)
4606 320 FORMAT (7F10.6)
4607 330 FORMAT ('1'//11X,10X,'WIDE FLANGE SECTION 12'//C 10X,'SUBJECT'
4608 BED TO AN APPLIED AXIAL LOAD OF',F10.4,' KIPS PLUS BENDING ')
4609 340 FORMAT ('0'//C 10X,'P(APLIED)')/P(YIELD)
4610 350 FORMAT ('1'//11X,10X,'BEAM COLUMN CASE NO.',I3//O',10X,'SUBJECT'
4611 &D TO AN APPLIED AXIAL LOAD OF',F12.6,' KIPS PLUS BENDING ')
4612 360 FORMAT ('0',10X,'CRITICAL AXIAL STRAIN',F12.8//O',10X
4613 &,'APPLIED AXIAL STRAIN',F12.8)
4614 370 FORMAT ('0',10X,'CRIT. BEND. STRAIN/YIELD STRAIN',F9.5)
4615 380 FORMAT ('0'//11X,10X,'BEAM-COLUMN CASE NO.',I3//O',10X,'SUBJECT'
4616 &D TO AN APPLIED AXIAL LOAD OF',F12.6,' KIPS PLUS BENDING ')
4617 390 FORMAT ('1'//11X,10X,'WIDE FLANGE SECTION 13'//O',10X,'CALCULAT'
4618 &ION OF CRITICAL AXIAL LOAD ')
4619 400 FORMAT ('0',10X,'ELASTIC ANALYSIS.')
4620 410 FORMAT ('0',10X,'INELASTIC ANALYSIS.')
4621 420 FORMAT ('0'//O',10X,'LENGTH OF WIDE FLANGE',F8.4,'INCHES'
4622 &C',10X,'WEB DEPTH',F8.5,'INCHES',F8.4,'INCHES'
4623 &O',10X,'WEB THICKNESS',F8.5,'INCHES',F8.4,'INCHES'
4624 &10X,'BOTTOM FLANGE WIDTH',F8.5,'INCHES',F8.4,'INCHES'
4625 &DTOM FLANGE THICKNESS',F8.5,'INCHES',F8.4,'INCHES'
4626 &NGE WIDTH',F8.5,'INCHES',F8.4,'INCHES'
4627 &ICKNESS',F8.5,'INCHES')
4628 430 FORMAT ('0',10X,'WEB YIELD STRESS',F9.4,'KSI',F9.4,'KSI')//'
4629 &O',10X,'BOTTOM FLANGE YIELD STRESS',F9.4,'KSI',F9.4,'KSI')//'
4630 &OP FLANGE YIELD STRESS',F9.4,'KSI',F9.4,'KSI')//'
4631 &TRESS (BDOT.)',F9.5,'KSI',F9.5,'KSI')//'
4632 &IMD WEB)',F9.5,'KSI',F9.5,'KSI')//'
4633 &OP TENS STRESS',F9.5,'KSI',F9.5,'KSI')//'
4634 &IMD TENS STRESS',F9.5,'KSI',F9.5,'KSI')//'
4635 &OP COMP STRESS',F9.5,'KSI',F9.5,'KSI')//'
4636 &IMD RES TENS STRESS (TOP)',F9.5,'KSI',F9.5,'KSI')//'

```



```

4633      8   F9.5, ' KSI // '0', 10X, 'RES COMP STRESS [BOTT] '
4634      8   FS.5, ' KSI // '0', 10X, 'RES COMP STRESS [TOP] ' F9.5, /
4635      & KSI '
4636 460  FORMAT ['0', 10X, 'YIELD MODULUS          F9.4, ' KSI // '
4637  & 0', 10X, 'STRAIN HARDENING MODULUS        F9.4, ' KSI // '0', 10X, 'S
4638  & TRAIN HARDENING STRAIN           F9.5)
4639 450  FORMAT ['0', 10X, 'AREA OF CROSS-SECTION      F9.4, ' SQ.IN
4640  & /'0', 10X, 'DISTANCE TO CENTROID// '0', 10X, 'FROM CENTER OF BOTTOM FL
4641  & ANGE      F9.4, ' INCHES// '0', 10X, 'CENTROIDAL MOMENT OF INERTIA
4642  & =', F9.4, ' INCHES ')
4643 460  FORMAT ['1//0//', TB, 'APPLIED AXIAL STRESS F12.6, ' KSI // '0',
4644  & TB, 'CRITICAL STRESS F12.6, ' KSI // '0', TB, 'HALF WAVELENGTH F8.4
4645 470  FORMAT ['1//-'// '0', TB, 'CRITICAL ELASTIC BENDING STRESS OF', F12.6,
4646  & ' KSI // ', TB, 'WITH AN APPLIED AXIAL STRESS OF', F8.4, ' KSI // '0', 78
4647 480  FORMAT [' ', 10X, 'SUBROUTINE PLATES FAILS IN 50 ITERATIONS TO FIND
4648  & CRITICAL INELASTIC AXIAL LOAD PRIOR TO FINDING CRITICAL BENDING MO
4649  & MENT ')
4650 480  FORMAT ['--', 10X, ' BEAM COLUMN BUCKLES UNDER THE APPLIED AXIAL LOAD
4651  & ')
4652 500  FORMAT [' ', 10X, ' SUBROUTINE PLATES FAILS TO CONVERGE TO CRITICAL BEND
4653  & ING STRAIN IN 50 ITERATIONS.')
4654 510  FORMAT ['1//-'// '0', TB, 'CRITICAL STRAIN F10.6 // 0', TB, 'HALF WAVE
4655  & LENGTH F8.4 // ')
4656 520  FORMAT ['--', TB, 'V =', F8.5, T27, 'V =', F8.5, T27, 'V = 0.00000', T46, 'V =',
4657  & F8.5/TB, 'V =', F8.5, T27, 'V =', F8.5/TB, 'V = 0.00000', T13, 'V =',
4658  & F8.5/TB, 'V =', F8.5, T27, 'V =', F8.5/TB, 'V = 0.00000', T31, 'V =',
4659  & F8.5/TB, 'V =', F8.5, T27, 'V =', F8.5/TB, 'V = 0.00000', T31, 'V =',
4660  & F8.5/TB, 'V =', F8.5, T27, 'V =', F8.5/TB, 'V = 0.00000', T31, 'V =',
4661  & F8.5/TB, 'V =', F8.5, T27, 'V =', F8.5/TB, 'V = 0.00000', T31, 'V =',
4662  & F8.5/TB, 'V =', F8.5, T27, 'V =', F8.5/TB, 'V = 0.00000', T31, 'V =',
4663  & F8.5/TB, 'V =', F8.5, T27, 'V =', F8.5/TB, 'V = 0.00000', T31, 'V =',
4664  & F8.5/TB, 'V =', F8.5, T27, 'V =', F8.5/TB, 'V = 0.00000', T31, 'V =',
4665  & F8.5/TB, 'V =', F8.5, T27, 'V =', F8.5/TB, 'V = 0.00000', T31, 'V =',
4666  & F8.5/TB, 'V =', F8.5, T27, 'V =', F8.5/TB, 'V = 0.00000', T31, 'V =',
4667 530  FORMAT ['0', 10X, 'CRITICAL BENDING MOMENT          F8.2, ' KIP-IN
4668  & /'0', 10X, 'CRITICAL BENDING MOMENT          F8.5/+', 10X, '-----'
4669  & /'0', 10X, 'YIELD MOMENT                  F8.5/+', 10X, '-----'
4670  & /'0', 10X, 'CRITICAL BENDING MOMENT          F8.5/+', 10X, 'RED. PLAST
4671  & /'0', 10X, 'CRITICAL BENDING MOMENT          F8.5/+', 10X, '-----'
4672  & /'0', 10X, 'CRITICAL BENDING MOMENT          F8.5/+', 10X, 'PLA
4673  & STIC MOMENT
4674  & /'0', 10X, 'DISTANCE TO THE NEUTRAL AXIS
4675  & /'0', 10X, 'FRDM CENTER OF COMPRESSION FLANGE F8.4, ' INCHES'
4676  & /'0', 10X, 'RDNA                      F8.4//0', 10X, 'BOTTOM
4677  & FLANGE SLENDERNESS RATIO F8.4//0', 10X, 'TOP FLANGE SLENDERNESS
4678  & RATIO          F8.4//0', 10X, 'WEB SLENDERNESS RATIO
4679  & F8.4//0', 10X, 'CODE SLENDERNESS RATIO - BDTDM F8.4//0', 10X, 'CO
4680  & DDE SLENDERNESS RATIO - TOP F8.4//0', 10X, 'CODE SLENDERNESS R
4681  &ATIO - WEB F8.4)
4682 540  FORMAT ['0', 10X, 'AXIAL LOAD AT BUCKLING          F8.2, ' KIPS//'
4683  & /'0', 10X, '(AXIAL LOAD)/(YIELD LOAD)          F8.4//0', 10X, 'AVERAGE
4684  & STRESS AT BUCKLING          F8.4, ' KSI//0', 10X, 'BDTDM FLANGE SL
4685  & ENDERNESS RATIO          F8.4//0', 10X, 'TOP FLANGE SLENDERNESS RATIO
4686  & F8.4//0', 10X, 'WEB SLENDERNESS RATIO          F8.4//0', 10X
4687  & , 'CODE SLENDERNESS RATIO - BDTDM F8.4//0', 10X, 'CODE SLENDERNE
4688  &SS RATIO - TOP F8.4//0', 10X, 'CODE SLENDERNESS RATIO - WEE
4689  & F8.4)
4690 550  FORMAT (' ', 5X, 'S2 FAILED TO BECOME NEGATIVE IN 20 ITERATIONS IN P
4691  & LATES')
4692 560  FORMAT (' ', 5X, 'SAB2 FAILED TO BECOME NEGATIVE IN PLATE 5 IN 20 IT
4693  & ERATIONS')
4694 570  FORMAT (' ', 5X, 'S1 FAILED TO BECOME NEGATIVE IN 20 ITERATIONS IN P
4695  & LATES')
4696 580  FORMAT (' ', 5X, 'SAB1 FAILED TO BECOME NEGATIVE IN PLATE 5 IN 20 IT
4697  & ERATIONS')
4698  END
4699  CCCCCCCCCCCCCCCCCCCCCCCCCCCCCCCCCCCCCCCCCCCCCCCCCCCCCCCCCCCCCCCCCCCCC
4700  C
4701  C
4702  C
4703  C
4704  C
4705  CCCCCCCCCCCCCCCCCCCCCCCCCCCCCCCCCCCCCCCCCCCCCCCCCCCCCCCCCCCCCCCCC
4706  C
4707  C
4708  C
4709  C
4710  C
4711  C
4712  C
4713  C
4714  C
4715  CCCCCCCCCCCCCCCCCCCCCCCCCCCCCCCCCCCCCCCCCCCCCCCCCCCCCCCCCCCCCCCCC
4716  C
4717  C
4718  C
4719  C
4720  C
4721  C
4722  C
4723  C
4724  C
4725  C
4726  C
4727  C
4728  C
4729  C
4730  C
4731  C
4732  C
4733  C
4734  C
4735  C
4736  C
4737  C
4738  C
4739  C
4740  C
4741  C
4742 10  C
4743  C
4744  C
4745  C

```



```

4746      ALFP=1.000
4747      GO TO 60
4748      20      ALFT=0.000
4749      ALFP=1.000
4750      GO TO 60
4751      30      IF (AXST GT .T3) GO TO 40
4752      ALFT=0.000
4753      ALFP=1.000
4754      GO TO 60
4755      40      IF (AXST GT .T4) GO TO 50
4756      IF (ADEN EQ 0.000) GO TO 50
4757      ANUM=T4-AXST
4758      ALFP=ANUM/ADEN
4759      ALFT=0.000
4760      GO TO 60
4761      50      ALFP=0.000
4762      ALFT=0.000
4763      C
4764      C
4765      C      CALCULATE FORCES IN BOTTOM FLANGE FOR ELASTIC,
4766      C      YIELDING, AND STRAIN-HARDENING REGIONS.
4767      C
4768      60      A1=0.500*BF1*TF1*ALFT
4769      A2=2.000*(AXST-ERTB)*E
4770      A3=ADEN*E+ALFT
4771      F11=A1*(A2+A3)
4772      A1=0.500*BF1*TF1*(ALFP-ALFT)
4773      A2=2.000*(YSFE+(AXST-T2)*E1)
4774      A3=ADEN*E*(ALFP+ALFT)
4775      F12=A1*(A2+A3)
4776      A1=0.500*BF1*(1.000-ALFP)
4777      A2=2.000*(YSFB*(ESH-EYBF)*E1+(AXST-T4)*E2)
4778      A3=ADEN*E2*(1.000+ALFP)
4779      F13=A1*(A2+A3)
4780      F1=F11+F12+F13
4781      C
4782      C
4783      C      DEFINE STRAIN LIMITS AND LIMITS OF INTEGRATION FOR
4784      C      THE TOP COMPRESSION FLANGE.
4785      C
4786      T1=EYTF-ERCT
4787      T2=EYTF+ERTT
4788      T3=ESH-ERCT
4789      T4=ESH+ERTT
4790      ADEN=EPCF+ERTT
4791      IF (AXST GT .T1) GO TO 70
4792      ALFT=1.000
4793      ALFP=1.000
4794      GO TO 120
4795      70      IF (AXST GT T2) GO TO 90
4796      IF (ADEN EQ 0.000) GO TO 80
4797      ANUM=T2-AXST
4798      ALFT=ANUM/ADEN
4799      ALFP=1.000
4800      GO TO 120
4801      80      ALFT=0.000
4802      ALFP=1.000
4803      GO TO 120
4804      90      IF (AXST GT T3) GO TO 100
4805      ALFT=0.000
4806      ALFP=1.000
4807      GO TO 120
4808      100     IF (AXST GT .T4) GO TO 110
4809      IF (ADEN EQ 0.000) GO TO 110
4810      ANUM=T4-AXST
4811      ALFP=ANUM/ADEN
4812      ALFT=0.000
4813      GO TO 120
4814      110     ALFP=0.000
4815      ALFT=0.000
4816      C
4817      C
4818      C      CALCULATE FORCES IN TOP COMPRESSION FLANGE FOR
4819      C      ELASTIC, YIELDING, AND STRAIN-HARDENING REGIONS.
4820      C
4821      120     A1=0.500*BF2*TF2*ALFT
4822      A2=2.000*(AXST-ERTT)*E
4823      A3=ADEN*E+ALFT
4824      F21=A1*(A2+A3)
4825      A1=0.500*BF2*TF2*(ALFP-ALFT)
4826      A2=2.000*(YSFT+(AXST-T2)*E1)
4827      A3=ADEN*E1*(ALFP+ALFT)
4828      F22=A1*(A2+A3)
4829      A1=0.500*BF2*TF2*(1.000-ALFP)
4830      A2=2.000*(YSFT+(ESH-EYTF)*E1+(AXST-T4)*E2)
4831      A3=ADEN*E2*(1.000+ALFP)
4832      F23=A1*(A2+A3)
4833      F2=F21+F22+F23
4834      C
4835      C
4836      C      DEFINE STRAIN LIMITS AND LIMITS OF INTEGRATION FOR
4837      C      THE WEB FORCES.
4838      C
4839      T1=EYW-EPGM
4840      T2=EYW+EKTB
4841      T3=ESH-EPGM
4842      T4=ESH+ERTB
4843      T5=EYW+ERTT
4844      T6=ESH+ERTT
4845      AD1=ERTB+ERCM
4846      AD2=ERTT+ERCM
4847      IF (AXST GT .T1) GO TO 130
4848      BETB=0.000
4849      BETBP=0.000
4850      GO TO 180
4851      130     IF (AXST GT T2) GO TO 150
4852      IF (AD1 EQ 0.000) GO TO 140
4853      AN1=AXST-T1
4854      BETB=AN1/AD1
4855      BETBP=0.000
4856      GO TO 180
4857      140     BETB=1.000
4858      BETBP=0.000

```



```

5085      GO TO 110
5086      70   IF (RSTEA GT T3) GO TO 90
5087      IF (AD1 EQ 0 ODO) GO TO BC
5088      BET1=(T6+EYW)/AD1
5089      BETP1=1.ODO
5090      GO TO 110
5091      80   BET1=1.ODO
5092      BETP1=1.ODO
5093      GO TO 110
5094      90   IF (AD1 EQ 0 ODO) GO TO 100
5095      BET1=(T6+EYW)/AD1
5096      BETP1=(T6+ESH)/AD1
5097      GO TO 110
5098      100  BET1=1.ODO
5099      BETP1=1.ODO
5100      110  CALL FWCALC(BCL,HW,TW,E2)
5101      C
5102      C
5103      C           INTEGRATION OVER LOWER HALF OF WEB
5104      C
5105      C           CALCULATE COEFFICIENTS OF GEOMETRIC STIFFNESS
5106      C           SUBMATRICES
5107      C
5108      FAC1=(YSW+(ESH-EYW)*E1-(ESH+T6)*E2)*FE*STR
5109      FAC2=(RST+T1-ERTB)*E2*FE*STR
5110      FAC3=(YSW-(EYW+T6)*E1)*FE*STR
5111      FAC4=AD1*E1*FE*STR
5112      FAC5=T6*E*FE*STR
5113      FACE=AD1*E*FE*STR
5114      FAC7=(YSW+(T6-EYW)*E1)*FE*STR
5115      FAC6=(YSW+(ESH-EYW)*E1+(T6-ESH)*E2)*FE*STR
5116      C
5117      C
5118      C           INTEGRATE STIFFNESS SUBMATRICES OVER
5119      C           STRAIN-HARDENED REGION OF THE WEB
5120      C
5121      A=-1.ODO
5122      B=-BETP1
5123      IF (DABS(A-B).LT.1.OD-5) GO TO 130
5124      CALL PHI(B,A,FI),CW,7,9,17)
5125      CALL PHIYY(B,A,FIYY,CW,7,9,13)
5126      CALL PHIPHI(B,A,FIPI,CW,7,9,15)
5127      CALL PHIY(B,A,FIY,CW,7,9,15)
5128      CALL EPHI(B,A,EFI,CW,7,9,18)
5129      DO 120 I=1,7
5130      DO 120 J=1,7
5131      WB1(I,J)=FA*FI(I,J)
5132      WB2(I,J)=FB*FIYY(I,J)
5133      WB3(I,J)=FC*FIPI(I,J)
5134      WB4(I,J)=FD*FIY(I,J)
5135      120   WB5(I,J)=FAC1*FI(I,J)+FAC2*EF1(I,J)
5136      130   A=-BETP1
5137      B=-BET1
5138      IF (DABS(A-B).LT.1.OD-5) GO TO 150
5139      CALL FWCALC(BCL,HW,TW,E1)
5140      CALL PHI(B,A,FI),CW,7,9,17)
5141      CALL PHIYY(B,A,FIYY,CW,7,9,13)
5142      CALL PHIPHI(B,A,FIPI,CW,7,9,15)
5143      CALL PHIY(B,A,FIY,CW,7,9,15)
5144      CALL EPHI(B,A,EFI,CW,7,9,18)
5145      DO 140 I=1,7
5146      DO 140 J=1,7
5147      WE1(I,J)=WB1(I,J)+FA*FI(I,J)
5148      WE2(I,J)=WB2(I,J)+FB*FIYY(I,J)
5149      WE3(I,J)=WB3(I,J)-FC*FIPI(I,J)
5150      WE4(I,J)=WB4(I,J)+FD*FIY(I,J)
5151      140   WB5(I,J)=WB5(I,J)-FAC3*FI(I,J)+FAC4*EF1(I,J)
5152      C
5153      C
5154      C           INTEGRATE STIFFNESS SUBMATRICES OVER ELASTIC REGION
5155      C           OF THE WEB
5156      C
5157      150   A=-BET1
5158      B=-BET3
5159      IF (DABS(A-B).LT.1.OD-5) GO TO 170
5160      CALL FWCALC(BCL,HW,TW,E)
5161      CALL PHI(B,A,FI),CW,7,9,17)
5162      CALL PHIYY(B,A,FIYY,CW,7,9,13)
5163      CALL PHIPHI(B,A,FIPI,CW,7,9,15)
5164      CALL PHIY(B,A,FIY,CW,7,9,15)
5165      CALL EPHI(B,A,EFI,CW,7,9,18)
5166      DO 160 I=1,7
5167      DO 160 J=1,7
5168      WB1(I,J)=WB1(I,J)+FA*FI(I,J)
5169      WB2(I,J)=WB2(I,J)+FB*FIYY(I,J)
5170      WB3(I,J)=WB3(I,J)-FC*FIPI(I,J)
5171      WB4(I,J)=WB4(I,J)+FD*FIY(I,J)
5172      160   WB5(I,J)=WB5(I,J)+FAC5*FI(I,J)+FAC6*EF1(I,J)
5173      C
5174      C
5175      C           INTEGRATE STIFFNESS SUBMATRICES OVER YIELDED REGION
5176      C           OF THE WEB
5177      C
5178      170   A=-BET3
5179      B=-BETP3
5180      IF (DABS(A-B).LT.1.OD-5) GO TO 190
5181      CALL FWCALC(BCL,HW,TW,E1)
5182      CALL PHI(B,A,FI),CW,7,9,17)
5183      CALL PHIYY(B,A,FIYY,CW,7,9,13)
5184      CALL PHIPHI(B,A,FIPI,CW,7,9,15)
5185      CALL PHIY(B,A,FIY,CW,7,9,15)
5186      CALL EPHI(B,A,EFI,CW,7,9,18)
5187      DO 180 I=1,7
5188      DO 180 J=1,7
5189      WB1(I,J)=WB1(I,J)+FA*FI(I,J)
5190      WB2(I,J)=WB2(I,J)+FB*FIYY(I,J)
5191      WB3(I,J)=WB3(I,J)-FC*FIPI(I,J)
5192      WB4(I,J)=WB4(I,J)+FD*FIY(I,J)
5193      180   WB5(I,J)=WB5(I,J)+FAC7*FI(I,J)+FAC4*EF1(I,J)
5194      C
5195      C
5196      C           INTEGRATE STIFFNESS SUBMATRICES OVER
5197      C           STRAIN-HARDENED REGION OF THE WEB

```



```

5198      C
5199      190  A=-BETP3
5200      B=0.0D0
5201      IF (DABS(A-B).LT.1.0D-5) GO TO 210
5202      CALL FWCALC(BCL,HW,TW,E2)
5203      CALL PHI(B,A,FI,CW,7,9,17)
5204      CALL PHIY(B,A,FIYY,CW,7,9,13)
5205      CALL PHIPHI(B,A,FIFI,CW,7,9,15)
5206      CALL PHIY(B,A,FIY,CW,7,9,15)
5207      CALL EPHI(B,A,EFI,CW,7,9,18)
5208      DO 200 I=1,7
5209      DO 200 J=1,7
5210      WB1(I,J)=WB1(I,J)+FA*FI(I,J)
5211      WB2(I,J)=WB2(I,J)+FB*FIYY(I,J)
5212      WB3(I,J)=WB3(I,J)+FC*FIFI(I,J)
5213      WB4(I,J)=WB4(I,J)+FD*FIY(I,J)
5214      WB5(I,J)=WB5(I,J)+FAC8*FI(I,J)+FAC2*EFI(I,J)
5215      C
5216      C
5217      C      SET LIMITS OF INTEGRATION FOR TOP HALF OF WEB FOR
5218      C      ELASTIC, YIELDED, AND STRAIN HARDENED REGIONS.
5219      C
5220      C      CASE I - MIDDLE ELASTIC
5221      C
5222      210  IF (TE.GT.EYW) GO TO 330
5223      IF (STEAL.GT.T4) GO TO 220
5224      BETZ=1.0D0
5225      BETP2=1.0D0
5226      GO TO 260
5227      220  IF (STEAL.GT.T5) GO TO 240
5228      IF (AD2.EQ.0.0D0) GO TO 230
5229      BETZ=(EYW-T6)/AD2
5230      BETP2=1.0D0
5231      GO TO 260
5232      230  BETZ=0.0D0
5233      BETP2=1.0D0
5234      GO TO 260
5235      240  IF (AD2.EQ.0.0D0) GO TO 250
5236      BETZ=(EYW-T6)/AD2
5237      BETP2=(ESH-T6)/AD2
5238      GO TO 260
5239      250  BETZ=0.0D0
5240      BETP2=0.0D0
5241      C
5242      C
5243      C      CALCULATE FACTORS FOR MULTIPLYING GEOMETRIC
5244      C      STIFFNESS SUBMATRICES
5245      C
5246      260  CALL FWCALC(BCL,HW,TW,E)
5247      FAC1=T6*E*FE*STR
5248      FAC2=AD2*E*FE*STR
5249      FAC3=(YSW-(T6-EYW))*E1)*FE*STR
5250      FAC4=AD2*E1*FE*STR
5251      FAC5=(YSW-(ESH-EYW))*E1+(T6-ESH)*E2)*FE*STR
5252      FAC6=AD2*E2*FE*STR
5253      C
5254      C
5255      C      INTEGRATE STIFFNESS SUBMATRICES OVER ELASTIC REGION
5256      C      OF THE WEB
5257      C
5258      A=0.0D0
5259      B=BETZ
5260      IF (DABS(A-B).LT.1.0D-5) GO TO 280
5261      CALL PHI(B,A,FI,CW,7,9,17)
5262      CALL PHIY(B,A,FIYY,CW,7,9,13)
5263      CALL PHIPHI(B,A,FIFI,CW,7,9,15)
5264      CALL PHIY(B,A,FIY,CW,7,9,15)
5265      CALL EPHI(B,A,EFI,CW,7,9,18)
5266      DO 270 I=1,7
5267      DO 270 J=1,7
5268      WB1(I,J)=WB1(I,J)+FA*FI(I,J)
5269      WB2(I,J)=WB2(I,J)+FB*FIYY(I,J)
5270      WB3(I,J)=WB3(I,J)+FC*FIFI(I,J)
5271      WB4(I,J)=WB4(I,J)+FD*FIY(I,J)
5272      270  WB5(I,J)=WB5(I,J)+FAC1*FI(I,J)+FAC2*EFI(I,J)
5273      C
5274      C
5275      C      INTEGRATE STIFFNESS SUBMATRICES OVER ELASTIC REGION
5276      C      OF THE WEB
5277      C
5278      280  A=BETZ
5279      B=BETP2
5280      IF (DABS(A-B).LT.1.0D-5) GO TO 300
5281      CALL FWCALC(BCL,HW,TW,E1)
5282      CALL PHI(B,A,FI,CW,7,9,17)
5283      CALL PHIY(B,A,FIYY,CW,7,9,13)
5284      CALL PHIPHI(B,A,FIFI,CW,7,9,15)
5285      CALL PHIY(B,A,FIY,CW,7,9,15)
5286      CALL EPHI(B,A,EFI,CW,7,9,18)
5287      DO 290 I=1,7
5288      DO 290 J=1,7
5289      WB1(I,J)=WB1(I,J)+FA*FI(I,J)
5290      WB2(I,J)=WB2(I,J)+FB*FIYY(I,J)
5291      WB3(I,J)=WB3(I,J)+FC*FIFI(I,J)
5292      WB4(I,J)=WB4(I,J)+FD*FIY(I,J)
5293      290  WB5(I,J)=WB5(I,J)+FAC3*FI(I,J)+FAC4*EFI(I,J)
5294      C
5295      C
5296      C      INTEGRATE STIFFNESS SUBMATRICES OVER
5297      C      STRAIN-HARDENED REGION OF THE WEB
5298      C
5299      300  A=BETP2
5300      B=1.0D0
5301      IF (DABS(A-B).LT.1.0D-5) GO TO 320
5302      CALL FWCALC(BCL,HW,TW,E2)
5303      CALL PHI(B,A,FI,CW,7,9,17)
5304      CALL PHIY(B,A,FIYY,CW,7,9,13)
5305      CALL PHIPHI(B,A,FIFI,CW,7,9,15)
5306      CALL PHIY(B,A,FIY,CW,7,9,15)
5307      CALL EPHI(B,A,EFI,CW,7,9,18)
5308      DO 310 I=1,7
5309      DO 310 J=1,7
5310      WB1(I,J)=WB1(I,J)+FA*FI(I,J)

```



```

5311      WB2(I,J)=WB2(I,J)+FB*FIYY(I,J)
5312      WB3(I,J)=WB3(I,J)-FC*FIFI(I,J)
5313      WB4(I,J)=WB4(I,J)+FD*FIY(I,J)
5314      WB5(I,J)=WB5(I,J)+FAC5*FI(I,J)+FAC6*EFI(I,J)
5315      TW=TSAVE
5316      RETURN
5317
5318      C
5319      C      SET LIMITS OF INTEGRATION FOR TOP HALF OF WEB FOR
5320      C      ELASTIC, YIELDED, AND STRAIN HARDENED REGIONS
5321
5322      C      CASE II - MIDDLE YIELDED
5323
5324      330 IF (T6 GT ESH) GO TO 450
5325      IF (STEA.GT.T4) GO TO 350
5326      IF (AD2.EQ.0.0DC) GO TO 340
5327      BET2=(EYW-T6)/AD2
5328      BETP2=1.0D0
5329      DO TO 380
5330      340 BETP2=1.0D0
5331      BETP2=1.0D0
5332      DO TO 380
5333      350 IF (STEA.GT.T5) GO TO 360
5334      BET2=1.0D0
5335      BETP2=1.0D0
5336      DO TO 380
5337      360 IF (AD2.EQ.0.0DC) GO TO 370
5338      BETP2=(ESH-T6)/AD2
5339      BET2=BETP2
5340      DO TO 380
5341      370 BETP2=1.0D0
5342      BET2=BETP2
5343
5344      C
5345      C      CALCULATE FACTORS FOR MULTIPLYING GEOMETRIC
5346      C      STIFFNESS SUBMATRICES
5347
5348      380 CALL FWCALC(BCL,HW,TW,E1)
5349      FAC1=(YSW-(T6-EYW)*E1)*FE*STR
5350      FAC2=AD2+E1*FE*STR
5351      FAC3=T6*E*FE*STR
5352      FAC4=AD2*E*FE*STR
5353      FAC5=(YSW-(ESH-EYW)*E1+(T6-ESH)*E2)*FE*STR
5354      FAC6=AD2*E2*FE*STR
5355
5356      C
5357      C      INTEGRATE STIFFNESS SUBMATRICES OVER ELASTIC REGION
5358      C      OF THE WEB
5359
5360      A=0.0DC
5361      B=BET2
5362      IF (DABS(A-B).LT.1.0D-5) GO TO 400
5363      CALL PHI(B,A,FI,CW,7,9,17)
5364      CALL PHIYY(B,A,FIYY,CW,7,9,13)
5365      CALL PHIPHI(B,A,FIFI,CW,7,9,15)
5366      CALL PHIY(B,A,FIY,CW,7,9,15)
5367      CALL EPHI(B,A,EFI,CW,7,9,16)
5368      DO 390 I=1,7
5369      DO 390 J=1,7
5370      WB1(I,J)=WB1(I,J)+FA*FI(I,J)
5371      WB2(I,J)=WB2(I,J)+FB*FIYY(I,J)
5372      WB3(I,J)=WB3(I,J)-FC*FIFI(I,J)
5373      WB4(I,J)=WB4(I,J)+FD*FIY(I,J)
5374      390 WB5(I,J)=WB5(I,J)+FAC2*FI(I,J)
5375
5376
5377      C      INTEGRATE STIFFNESS SUBMATRICES OVER ELASTIC REGION
5378      C      OF THE WEB
5379
5380      400 A=BET2
5381      B=BETP2
5382      IF (DABS(A-B).LT.1.0D-5) GO TO 420
5383      CALL FWCALC(BCL,HW,TW,E)
5384      CALL PHI(B,A,FI,CW,7,9,17)
5385      CALL PHIYY(B,A,FIYY,CW,7,9,13)
5386      CALL PHIPHI(B,A,FIFI,CW,7,9,15)
5387      CALL PHIY(B,A,FIY,CW,7,9,15)
5388      CALL EPHI(B,A,EFI,CW,7,9,16)
5389      DO 410 I=1,7
5390      DO 410 J=1,7
5391      WB1(I,J)=WB1(I,J)+FA*FI(I,J)
5392      WB2(I,J)=WB2(I,J)+FB*FIYY(I,J)
5393      WB3(I,J)=WB3(I,J)-FC*FIFI(I,J)
5394      WB4(I,J)=WB4(I,J)+FD*FIY(I,J)
5395      410 WB5(I,J)=WB5(I,J)+FAC3*FI(I,J)+FAC4*EFI(I,J)
5396
5397
5398      C      INTEGRATE STIFFNESS SUBMATRICES OVER
5399      C      STRAIN-HARDENED REGION OF THE WEB
5400
5401      420 A=BETP2
5402      B=1.0D0
5403      IF (DABS(A-B).LT.1.0D-5) GO TO 440
5404      CALL FWCALC(BCL,HW,TW,E2)
5405      CALL PHI(B,A,FI,CW,7,9,17)
5406      CALL PHIYY(B,A,FIYY,CW,7,9,13)
5407      CALL PHIPHI(B,A,FIFI,CW,7,9,15)
5408      CALL PHIY(B,A,FIY,CW,7,9,15)
5409      CALL EPHI(B,A,EFI,CW,7,9,16)
5410      DO 430 I=1,7
5411      DO 430 J=1,7
5412      WB1(I,J)=WB1(I,J)+FA*FI(I,J)
5413      WB2(I,J)=WB2(I,J)+FB*FIYY(I,J)
5414      WB3(I,J)=WB3(I,J)-FC*FIFI(I,J)
5415      WB4(I,J)=WB4(I,J)+FD*FIY(I,J)
5416      430 WB5(I,J)=WB5(I,J)+FAC5*FI(I,J)+FAC6*EFI(I,J)
5417      440 TW=TSAVE
5418      RETURN
5419
5420
5421      C      SET LIMITS OF INTEGRATION FOR TOP HALF OF WEB FOR
5422      C      ELASTIC, YIELDED, AND STRAIN HARDENED REGIONS
5423

```



```

C CASE II - MIDDLE STRAIN-HARDENED
C
450 IF (STEA.GT.T4) GO TO 470
451 IF (AD2.EQ.0.0D0) GO TO 480
452 BETZ2=(EWY-T6)/AD2
453 BETP2=(ESH-T6)/AD2
454 GO TO 480
455
460 BETZ2=1.0D0
461 BETP2=1.0D0
462 GO TO 480
463
470 IF (STEA.GT.T5) GO TO 480
471 IF (AD2.EQ.0.0D0) GO TO 480
472 BETZ2=1.0D0
473 BETP2=(ESH-T6)/AD2
474 GO TO 480
475
480 BETZ2=1.0D0
481 BETP2=1.0D0
482
C
5443      CALCULATE FACTORS FOR MULTIPLYING GEOMETRIC
5444      STIFFNESS SUBMATRICES.
5445
5446      CALL FWCALC(BCL,HW,TW,E2)
5447      FAC1=(YSW*(ESH-EYW)*E1+(T6-ESH)*E2)=FE=STR
5448      FAC2=AD2*E2*FE=STR
5449      FAC3=(YSW*(T6-EYW)*E1)=FE=STR
5450      FAC4=AD2*E1*FE=STR
5451      FAC5=T6*FE=STR
5452      FAC6=AD2*E=FE=STR
5453
5454
5455      INTEGRATE STIFFNESS SUBMATRICES OVER
5456      STRAIN-HARDENED REGION OF THE WEB.
5457
5458      A=0.0D0
5459      B=BETP2
5460      IF (DABS(A-B).LT.1.0D-5) GO TO 510
5461      CALL PHI(B,A,FI,CW,7,9,17)
5462      CALL PHIYY(B,A,FIYY,CW,7,9,13)
5463      CALL PHIPHI(B,A,FIFI,CW,7,9,15)
5464      CALL PHIY(B,A,FIY,CW,7,9,15)
5465      CALL EPHI(B,A,EFI,CW,7,9,18)
5466      DO 500 I=1,7
5467      DO 500 J=1,7
5468      WB1(I,J)=WB1(I,J)+FA=FI(I,J)
5469      WB2(I,J)=WB2(I,J)+FB=FIYY(I,J)
5470      WB3(I,J)=WB3(I,J)-FC=FIFI(I,J)
5471      WB4(I,J)=WB4(I,J)+FD=FIY(I,J)
5472      WB5(I,J)=WB5(I,J)+FAC1*FI(I,J)+FAC2*EFI(I,J)
5473
5474
5475      INTEGRATE STIFFNESS SUBMATRICES OVER ELASTIC REGION
5476      OF THE WEB
5477
5478      S10=A=BETP2
5479      B=BETZ
5480      IF (DABS(A-B).LT.1.0D-5) GO TO 530
5481      CALL FWCALC(BCL,HW,TW,E1)
5482      CALL PHI(B,A,FI,CW,7,9,17)
5483      CALL PHIYY(B,A,FIYY,CW,7,9,13)
5484      CALL PHIPHI(B,A,FIFI,CW,7,9,15)
5485      CALL PHIY(B,A,FIY,CW,7,9,15)
5486      CALL EPHI(B,A,EFI,CW,7,9,18)
5487      DO 520 I=1,7
5488      DO 520 J=1,7
5489      WB1(I,J)=WB1(I,J)+FA=FI(I,J)
5490      WB2(I,J)=WB2(I,J)+FB=FIYY(I,J)
5491      WB3(I,J)=WB3(I,J)-FC=FIFI(I,J)
5492      WB4(I,J)=WB4(I,J)+FD=FIY(I,J)
5493      WB5(I,J)=WB5(I,J)+FAC3*FI(I,J)+FAC4*EFI(I,J)
5494
5495
5496      INTEGRATE STIFFNESS SUBMATRICES OVER ELASTIC REGION
5497      OF THE WEB.
5498
5499      S30=A=BETZ
5500      B=1.0D0
5501      IF (DABS(A-B).LT.1.0D-5) GO TO 550
5502      CALL FWCALC(BCL,HW,TW,E)
5503      CALL PHI(B,A,FI,CW,7,9,17)
5504      CALL PHIYY(B,A,FIYY,CW,7,9,13)
5505      CALL PHIPHI(B,A,FIFI,CW,7,9,15)
5506      CALL PHIY(B,A,FIY,CW,7,9,15)
5507      CALL EPHI(B,A,EFI,CW,7,9,18)
5508      DO 540 I=1,7
5509      DO 540 J=1,7
5510      WB1(I,J)=WB1(I,J)+FA=FI(I,J)
5511      WB2(I,J)=WB2(I,J)+FB=FIYY(I,J)
5512      WB3(I,J)=WB3(I,J)-FC=FIFI(I,J)
5513      WB4(I,J)=WB4(I,J)+FD=FIY(I,J)
5514      WB5(I,J)=WB5(I,J)+FAC5*FI(I,J)+FAC6*EFI(I,J)
5515
5516      TW=TSAVE
5517      RETURN
5518      END
5519
5520
5521      C
5522      C
5523      C
5524      C
5525      C
5526      C
5527      C
5528      THIS ROUTINE FORMULATES STIFFNESS
5529      SUBMATRICES FOR THE WEB WHEN THE SPECIMEN IS
5530      SUBJECTED TO AXIAL STRESSES.
5531
5532      C
5533      C
5534      C
5535      IMPLICIT REAL*8(A-H,O-Z)
5536      DIMENSION F1(7,7),FIY(7,7),FIFI(7,7),FIY(7,7),EFI(7,7)
5537      COMMON /BLK1/E,V,NS,ITYPE,LTYPE,INEL,N,ICLAMP,IKIND

```



```

5537      COMMON /BLK4/FA,FB,FC,FD,FE
5538      COMMON /BLKS/ERTB,ERCM,ERTT,ERCB,ERCT,EYW,EYBF,EYTF
5539      COMMON /BLKB/CW(7,9),WB1(7,7),WB2(7,7),WB3(7,7),WB4(7,7),WB5(7,7)
5540      COMMON /BLK10/HW,TW,BCL,BF1,TF1,BF2,TF2
5541      COMMON /BLK11/E1,E2,ESH,YSW,YSBF,YSTF,SRTB,SRCH,SRRT,SRCB,SRCT
5542      C
5543      C      INITIALISE STIFFNESS SUBMATRICES TO ZERO
5544      C
5545      C      DO 10 I=1,7
5546      C      DO 10 J=I,7
5547      C      WB1(I,J)=0.0D0
5548      C      WB2(I,J)=0.0D0
5549      C      WB3(I,J)=0.0D0
5550      C      WB4(I,J)=0.0D0
5551      C      WB5(I,J)=0.0D0
5552      10
5553      C
5554      C
5555      C      CALCULATE STRAINS AND STRAIN LIMITS
5556      C
5557      STR=1.0D0/ST
5558      TSAVE=TW
5559      TW=2.0D0*TW=HW/(2.0D0*HW-TF1-TF2-2.0D0*TW)
5560      T1=EYW-ERCM
5561      T2=EYW+ERTB
5562      T3=ESH-ERCM
5563      T4=ESH+ERTB
5564      T5=EYW+ERTT
5565      T6=ESH+ERTT
5566      AD1=ERTB+ERCM
5567      AD2=ERTB+ERCM
5568      C
5569      C
5570      C      SET LIMITS OF INTEGRATION FOR ELASTIC, YIELDED, AND
5571      C      STRAIN-HARDENED PORTIONS OF PLATE IN LOWER HALF OF
5572      C      WEB
5573      C
5574      IF (ST.GT.T1) GO TO 20
5575      BETB=0.0D0
5576      BETBP=0.0D0
5577      GO TO 70
5578      20
5579      IF (ST.GT.T2) GO TO 40
5580      IF (AD1.EQ.0.0D0) GO TO 30
5581      AN1=ST-T1
5582      BETB=AN1/AD1
5583      BETBP=0.0D0
5584      GO TO 70
5585      30
5586      BETB=1.0D0
5587      BETBP=0.0D0
5588      GO TO 70
5589      40
5590      IF (ST.GT.T3) GO TO 50
5591      IF (AD1.EQ.0.0D0) GO TO 60
5592      IF (AD1.EQ.0.0D0) GO TO 60
5593      AN1=ST-T3
5594      BETB=1.0D0
5595      BETBP=AN1/AD1
5596      GO TO 70
5597      60
5598      BETB=1.0D0
5599      BETBP=1.0D0
5600      70
5601      IF (ST.GT.T1) GO TO 80
5602      BETT=0.0D0
5603      BETTP=0.0D0
5604      GO TO 130
5605      80
5606      IF (ST.GT.T5) GO TO 100
5607      IF (AD2.EQ.0.0D0) GO TO 90
5608      AN2=ST-T1
5609      BETT=AN2/AD2
5610      BETTP=0.0D0
5611      GO TO 130
5612      90
5613      BETT=1.0D0
5614      BETTP=0.0D0
5615      GO TO 130
5616      100
5617      IF (ST.GT.T3) GO TO 110
5618      IF (AD2.EQ.0.0D0) GO TO 120
5619      BETT=1.0D0
5620      AN2=ST-T3
5621      BETTP=AN2/AD2
5622      GO TO 130
5623      120
5624      BETT=1.0D0
5625      BETTP=1.0D0
5626      130
5627      CALL FWCALC(BCL,HW,TW,E)
5628      C
5629      C      CALCULATE FACTORS FOR MULTIPLYING GEOMETRIC
5630      C      STIFFNESS SUBMATRICES
5631      C
5632      FAC1=(ST+ERCM)*E*FE
5633      FAC2=AD1*E*FE
5634      FAC3=(YSW*(ST-T1)*E1)*FE
5635      FAC4=AD1*E1*FE
5636      FAC5=(YSW*(ESH-EYW)*E1+(ST-T3)*E2)*FE
5637      FAC6=AD1*E2*FE
5638      FAC7=AD2*E2*FE
5639      FAC8=AD2*E1*FE
5640      FAC9=AD2*E*FE
5641      C
5642      C      INTEGRATE STIFFNESS SUBMATRICES OVER ELASTIC REGION
5643      C      OF THE WEB
5644      C
5645      A=-1.0D0
5646      B=BETB
5647      IF (DABS(A-B).LT.1.0D-5) GO TO 150
5648      CALL PHI(E,A,F1,CW,7,9,17)
5649      CALL PHIY(B,A,FIYY,CW,7,9,13)
      CALL PHIPHI(B,A,FIFI,CW,7,9,15)

```



```

5763          SUBROUTINE 34
5764
5765
5766
5767
5768
5769          SUBROUTINE WBINBE
5770
5771          THIS ROUTINE FORMULATES THE STIFFNESS
5772          SUBMATRICES WB1, WB2, WB3, WB4 AND WBS FOR THE
5773          WEB IN THE INELASTIC AND STRAIN-HARDENING RANGES
5774          WHEN THE SPECIMEN IS SUBJECTED TO BENDING
5775          STRESSES.
5776
5777
5778          SUBROUTINE WBINBE(IST)
5779          IMPLICIT REAL*8(A-H,O-Z)
5780          DIMENSION FI(7,7),FIYY(7,7),FIFI(7,7),FIY(7,7),EF1(7,7)
5781          COMMON /BLK1/E,V,NS,ITYPE,LTYPE,INEL,N,JCLAMP,JKIND
5782          COMMON /BLK4/F,F,B,F,C,F,D,F,E
5783          COMMON /BLK5/ERTB,ERCM,ERTT,ERCB,ERCT,EYW,EYBF,EYTF
5784          COMMON /BLK6/ERTBAR,YB,YI,AREA,ECC,ALAR,R
5785          COMMON /BLK9/CW(7,9),WB1(7,7),WB2(7,7),WB3(7,7),WB4(7,7),WB5(7,7)
5786          COMMON /BLK10/HW,TW,BCL,BF1,TF1,BF2,TF2
5787          COMMON /BLK11/E1,E2,ESH,YSW,YSFB,SRTB,SRCH,SRRT,SRCB,SRCT
5788
5789
5790          INITIALISE STIFFNESS SUBMATRICES TO ZERO
5791
5792          DO 10 I=1,7
5793          DO 10 J=1,7
5794          WB1(I,J)=0.0D0
5795          WB2(I,J)=0.0D0
5796          WB3(I,J)=0.0D0
5797          WB4(I,J)=0.0D0
5798          10   WBS(I,J)=0.0D0
5799
5800
5801          CALCULATE STRAINS AND STRAIN LIMITS.
5802
5803          STR=1.0D0/ST
5804          RST=RST
5805          TSAVE=TW
5806          TW=2.0D0*TW/(2.0D0*HW-TF1-TF2-2.0D0*TW)
5807          EC=[2.0D0*Y1/(2.0D0*Y1+HW)]*ST
5808          T1=ERCM+EC
5809          T2=EYW-ERTB
5810          T3=ESH-ERTB
5811          T4=EYW+ERTT
5812          TS=ESH+ERTT
5813          AD1=RST+T1+ERTB
5814          AD2=ST-T1-ERTT
5815
5816
5817          SET LIMITS OF INTEGRATION FOR ELASTIC, YIELDED, AND
5818          STRAIN-HARDEDNED PORTIONS OF PLATE IN LOWER HALF OF
5819          WEB.
5820
5821          IF (T1.GT.EYW) GO TO 20
5822          BET3=0.0D0
5823          BETP3=0.0D0
5824          GO TO 60
5825          20   IF (T1.GT.ESH) GO TO 40
5826          IF (AD1.EQ.0.0D0) GO TO 30
5827          BET3=[T1-EYW]/AD1
5828          BETP3=0.0D0
5829          GO TO 60
5830          30   BET3=1.0D0
5831          BETP3=0.0D0
5832          GO TO 60
5833          40   IF (AD1.EQ.0.0D0) GO TO 50
5834          BET3=[T1-EYW]/AD1
5835          BETP3=[T1-ESH]/AD1
5836          GO TO 60
5837          50   BET3=1.0D0
5838          BETP3=1.0D0
5839          60   IF (RST.GT.T2) GO TO 70
5840          BET1=1.0D0
5841          BETP1=1.0D0
5842          GO TO 110
5843          70   IF (RST.GT.T3) GO TO 90
5844          IF (AD1.EQ.0.0D0) GO TO 80
5845          BET1=[T1+EYW]/AD1
5846          BETP1=1.0D0
5847          GO TO 110
5848          80   BET1=1.0D0
5849          BETP1=1.0D0
5850          GO TO 110
5851          90   IF (AD1.EQ.0.0D0) GO TO 100
5852          BET1=[T1+EYW]/AD1
5853          BETP1=[T1+ESH]/AD1
5854          GO TO 110
5855          100  BET1=1.0D0
5856          BETP1=1.0D0
5857          110  CALL FWEALC(BCL,HW,TW,E2)
5858
5859
5860          INTEGRATION OVER LOWER HALF OF WEB
5861
5862          CALCULATE FACTORS FOR MULTIPLYING GEOMETRIC
5863          STIFFNESS SUBMATRICES.
5864
5865          FAC1=[YSW+(ESH-EYW)*E1-(ESH+T1)*E2]*FE
5866          FAC2=[RST+T1+ERTB]*E2*FE
5867          FAC3=[YSW-(EYW+T1)*E1]*FE
5868          FAC4=AD1*E1*FE
5869          FAC5=T1*E*FE
5870          FAC6=AD1*E*FE
5871          FAC7=(YSW+(T1-EYW)*E1)*FE
5872          FAC8=(YSW+(ESH-EYW)*E1+(T1-ESH)*E2)*FE
5873          A=1.0D0
5874          B=BETP1
5875          IF [DABS(A-B).LT.1.0D-5] GO TO 130

```



```

5876      CALL PHI(B,A,FI,CW,7,9,17)
5877      CALL PHIYY(B,A,FIYY,CW,7,9,13)
5878      CALL PHIPHI(B,A,FIFI,CW,7,9,15)
5879      CALL PHIY(B,A,FIY,CW,7,9,15)
5880      CALL EPHI(B,A,EFI,CW,7,9,18)
5881      DO 120 I=1,7
5882      DO 120 J=1,7
5883      WB1(I,J)=FA*FI(I,J)
5884      WB2(I,J)=FB*FIYY(I,J)
5885      WB3(I,J)=FC*FIFI(I,J)
5886      WB4(I,J)=FD*FIY(I,J)
5887      120  WB5(I,J)=-FAC1*FI(I,J)+FAC2*EFI(I,J)
5888      C
5889      C
5890      C      INTEGRATE STIFFNESS SUBMATRICES OVER
5891      C      STRAIN-HARDENED REGION OF THE WEB
5892      C
5893      130  AF=BETP1
5894      BF=BET1
5895      IF (DABS(A-B).LT.1.0D-5) GO TO 150
5896      CALL FWCALC(BCL,HW,TW,E1)
5897      CALL PHI(B,A,FI,CW,7,9,17)
5898      CALL PHIYY(B,A,FIYY,CW,7,9,13)
5899      CALL PHIPHI(B,A,FIFI,CW,7,9,15)
5900      CALL PHIY(B,A,FIY,CW,7,9,15)
5901      CALL EPHI(B,A,EFI,CW,7,9,18)
5902      DO 140 I=1,7
5903      DO 140 J=1,7
5904      WB1(I,J)=WB1(I,J)+FA*FI(I,J)
5905      WB2(I,J)=WB2(I,J)+FB*FIYY(I,J)
5906      WB3(I,J)=WB3(I,J)-FC*FIFI(I,J)
5907      WB4(I,J)=WB4(I,J)+FD*FIY(I,J)
5908      140  WB5(I,J)=WB5(I,J)-FAC3*FI(I,J)+FAC4*EFI(I,J)
5909      C
5910      C
5911      C      INTEGRATE STIFFNESS SUBMATRICES OVER ELASTIC REGION
5912      C      OF THE WEB.
5913      C
5914      150  AF=BET1
5915      BF=BET3
5916      IF (DABS(A-B).LT.1.0D-5) GO TO 170
5917      CALL FWCALC(BCL,HW,TW,E)
5918      CALL PHI(B,A,FI,CW,7,9,17)
5919      CALL PHIYY(B,A,FIYY,CW,7,9,13)
5920      CALL PHIPHI(B,A,FIFI,CW,7,9,15)
5921      CALL PHIY(B,A,FIY,CW,7,9,15)
5922      CALL EPHI(B,A,EFI,CW,7,9,18)
5923      DO 160 I=1,7
5924      DO 160 J=1,7
5925      WB1(I,J)=WB1(I,J)+FA*FI(I,J)
5926      WB2(I,J)=WB2(I,J)+FB*FIYY(I,J)
5927      WB3(I,J)=WB3(I,J)-FC*FIFI(I,J)
5928      WB4(I,J)=WB4(I,J)+FD*FIY(I,J)
5929      160  WB5(I,J)=WB5(I,J)+FAC5*FI(I,J)+FAC6*EFI(I,J)
5930      C
5931      C
5932      C      INTEGRATE STIFFNESS SUBMATRICES OVER YIELDED REGION
5933      C      OF THE WEB.
5934      C
5935      170  AF=BET3
5936      BF=BETP2
5937      IF (DABS(A-B).LT.1.0D-5) GO TO 190
5938      CALL FWCALC(BCL,HW,TW,E1)
5939      CALL PHI(B,A,FI,CW,7,9,17)
5940      CALL PHIYY(B,A,FIYY,CW,7,9,13)
5941      CALL PHIPHI(B,A,FIFI,CW,7,9,15)
5942      CALL PHIY(B,A,FIY,CW,7,9,15)
5943      CALL EPHI(B,A,EFI,CW,7,9,18)
5944      DO 180 I=1,7
5945      DO 180 J=1,7
5946      WB1(I,J)=WB1(I,J)+FA*FI(I,J)
5947      WB2(I,J)=WB2(I,J)+FB*FIYY(I,J)
5948      WB3(I,J)=WB3(I,J)-FC*FIFI(I,J)
5949      WB4(I,J)=WB4(I,J)+FD*FIY(I,J)
5950      180  WB5(I,J)=WB5(I,J)+FAC7*FI(I,J)+FAC4*EFI(I,J)
5951      C
5952      C
5953      C      INTEGRATE STIFFNESS SUBMATRICES OVER
5954      C      STRAIN-HARDENED REGION OF THE WEB
5955      C
5956      190  AF=BETP3
5957      BF=ODO
5958      IF (DABS(A-B).LT.1.0D-5) GO TO 210
5959      CALL FWCALC(BCL,HW,TW,E2)
5960      CALL PHI(B,A,FI,CW,7,9,17)
5961      CALL PHIYY(B,A,FIYY,CW,7,9,13)
5962      CALL PHIPHI(B,A,FIFI,CW,7,9,15)
5963      CALL PHIY(B,A,FIY,CW,7,9,15)
5964      CALL EPHI(B,A,EFI,CW,7,9,18)
5965      DO 200 I=1,7
5966      DO 200 J=1,7
5967      WB1(I,J)=WB1(I,J)+FA*FI(I,J)
5968      WB2(I,J)=WB2(I,J)+FB*FIYY(I,J)
5969      WB3(I,J)=WB3(I,J)-FC*FIFI(I,J)
5970      WB4(I,J)=WB4(I,J)+FD*FIY(I,J)
5971      200  WB5(I,J)=WB5(I,J)+FAC8*FI(I,J)+FAC2*EFI(I,J)
5972      C
5973      C
5974      C      SET LIMITS OF INTEGRATION FOR TOP HALF OF WEB FOR
5975      C      ELASTIC, YIELDED, AND STRAIN HARDENED REGIONS
5976      C
5977      C      CASE I - MIDDLE ELASTIC
5978
5979      210  IF (T1.GT.EYW) GO TO 330
5980      IF (ST.GT.T4) GO TO 220
5981      BET2=1.0D0
5982      BETP2=1.0D0
5983      GO TO 260
5984      220  IF (ST.GT.T5) GO TO 240
5985      IF (AD2.EQ.0.0D0) GO TO 230
5986      BET2=(EYW-T1)/AD2
5987      BETP2=1.0D0
5988      GO TO 260

```



```

5905      230  BET2=0.0D0
5906      BETP2=1.0D0
5907      GO TO 260
5908      240  IF (AD2 EQ.0.0D0) GO TO 250
5909      BET2=(EWY-T1)/AD2
5910      BETP2=(ESH-T1)/AD2
5911      GO TO 260
5912      250  BET2=0.0D0
5913      BETP2=0.0D0
5914      C
5915      C      CALCULATE FACTORS FOR MULTIPLYING GEOMETRIC
5916      STIFFNESS SUBMATRICES
5917      C
5918      260  CALL FWCALC(BCL,HW,TW,E)
5919      FAC1=T1*E*FE
5920      FAC2=AD2*E*FE
5921      FAC3=(YSW*(T1-EYW)*E1)*FE
5922      FAC4=AD2*E1*FE
5923      FAC5=(YSW*(ESH-EYW)*E1+(T1-ESH)*E2)*FE
5924      FACE=AD2*E2*FE
5925      C
5926      C      INTEGRATE STIFFNESS SUBMATRICES OVER ELASTIC REGION
5927      OF THE WEB.
5928      C
5929      A=0.0D0
5930      B=BET2
5931      IF (DABS(A-B).LT.1.0D-5) GO TO 280
5932      CALL PH1(B,A,FI,CW,7.9,17)
5933      CALL PHIYY(B,A,FIYY,CW,7.9,13)
5934      CALL PHIPH(B,A,FIIFI,CW,7.9,15)
5935      CALL PHIY(B,A,FIY,CW,7.9,15)
5936      CALL EPHI(B,A,EFI,CW,7.9,16)
5937      DD 270 I=1,7
5938      DD 270 J=1,7
5939      WB1(I,J)=WB1(I,J)+FA*FI(I,J)
5940      WB2(I,J)=WB2(I,J)+FB*FIYY(I,J)
5941      WB3(I,J)=WB3(I,J)-FC*FIIFI(I,J)
5942      WB4(I,J)=WB4(I,J)+FD*FIY(I,J)
5943      WB5(I,J)=WB5(I,J)+FAC1*FI(I,J)+FAC2*EFI(I,J)
5944      C
5945      C      INTEGRATE STIFFNESS SUBMATRICES OVER ELASTIC REGION
5946      OF THE WEB.
5947      C
5948      280  A=BET2
5949      B=BETP2
5950      IF (DABS(A-B).LT.1.0D-5) GO TO 300
5951      CALL FWCALC(BCL,HW,TW,E1)
5952      CALL PH1(B,A,FI,CW,7.9,17)
5953      CALL PHIYY(B,A,FIYY,CW,7.9,13)
5954      CALL PHIPH(B,A,FIIFI,CW,7.9,15)
5955      CALL PHIY(B,A,FIY,CW,7.9,15)
5956      CALL EPHI(B,A,EFI,CW,7.9,16)
5957      DD 290 I=1,7
5958      DD 290 J=1,7
5959      WB1(I,J)=WB1(I,J)+FA*FI(I,J)
5960      WB2(I,J)=WB2(I,J)+FB*FIYY(I,J)
5961      WB3(I,J)=WB3(I,J)-FC*FIIFI(I,J)
5962      WB4(I,J)=WB4(I,J)+FD*FIY(I,J)
5963      WB5(I,J)=WB5(I,J)+FAC3*FI(I,J)+FAC4*EFI(I,J)
5964      C
5965      C      INTEGRATE STIFFNESS SUBMATRICES OVER
5966      STRAIN-HARDENED REGION OF THE WEB.
5967      C
5968      300  A=BETP2
5969      B=1.0D0
5970      IF (DABS(A-B).LT.1.0D-5) GO TO 320
5971      CALL FWCALC(BCL,HW,TW,E2)
5972      CALL PH1(B,A,FI,CW,7.9,17)
5973      CALL PHIYY(B,A,FIYY,CW,7.9,13)
5974      CALL PHIPH(B,A,FIIFI,CW,7.9,15)
5975      CALL PHIY(B,A,FIY,CW,7.9,15)
5976      CALL EPHI(B,A,EFI,CW,7.9,16)
5977      DD 310 I=1,7
5978      DD 310 J=1,7
5979      WB1(I,J)=WB1(I,J)+FA*FI(I,J)
5980      WB2(I,J)=WB2(I,J)+FB*FIYY(I,J)
5981      WB3(I,J)=WB3(I,J)-FC*FIIFI(I,J)
5982      WB4(I,J)=WB4(I,J)+FD*FIY(I,J)
5983      WB5(I,J)=WB5(I,J)+FAC5*FI(I,J)+FAC6*EFI(I,J)
5984      310
5985      320  TW=TSAYE
5986      RETURN
5987      C
5988      C      SET LIMITS OF INTEGRATION FOR TOP HALF OF WEB FOR
5989      ELASTIC, YIELDED, AND STRAIN-HARDENED REGIONS
5990      C
5991      C      CASE II - MIDDLE YIELDED
5992      C
5993      330  IF (T1.GT.ESH) GO TO 450
5994      IF (ST.GT.T4) GO TO 350
5995      IF (AD2.EQ.0.0D0) GO TO 340
5996      BET2=(EWY-T1)/AD2
5997      BETP2=1.0D0
5998      GO TO 380
5999      340  BET2=1.0D0
6000      BETP2=1.0D0
6001      GO TO 380
6002      350  IF (ST.GT.T5) GO TO 360
6003      BET2=1.0D0
6004      BETP2=1.0D0
6005      GO TO 380
6006      360  IF (AD2.EQ.0.0D0) GO TO 370
6007      BETP2=ESH-T1/AD2
6008      BET2=BETP2
6009      GO TO 380
6010      370  BETP2=1.0D0
6011      BET2=BETP2
6012      C
6013      C

```



```

61C2      C      CALCULATE FACTORS FOR MULTIPLYING GEOMETRIC
61C3      C      STIFFNESS SUBMATRICES
61C4      C
61C5      380    CALL FWCALC(BCL,HW,TW,E1)
61C6      FAC1=(YSW*(T1-EYW)*E1)*FE*STR
61C7      FAC2=AD2*E1*FE*STR
61C8      FAC3=T1*E*FE*STR
61C9      FAC4=AD2*E*FE*STR
61C10     FAC5=(YSW*(ESH-EYW)*E1+(T1-ESH)*E2)*FE*STR
61C11     FAC6=AD2*E2*FE*STR
61C12     C
61C13     C
61C14     C      INTEGRATE STIFFNESS SUBMATRICES OVER ELASTIC REGION
61C15     C      OF THE WEB
61C16     C
61C17     A=0 ODO
61C18     B=BET2
61C19     IF (DABS(A-B).LT.1.0D-5) GO TO 400
61C20     CALL PHI(B,A,FI,CW,7,9,17)
61C21     CALL PHIY(B,A,FIYY,CW,7,9,13)
61C22     CALL PHIPHI(B,A,FIPI,CW,7,9,15)
61C23     CALL PHIY(B,A,FIY,CW,7,9,15)
61C24     CALL EPHI(B,A,EFI,CW,7,9,16)
61C25     DO 390 I=1,7
61C26     DO 390 J=1,7
61C27     WB1(I,J)=WB1(I,J)+FA*FI(I,J)
61C28     WB2(I,J)=WB2(I,J)+FB*FIYY(I,J)
61C29     WB3(I,J)=WB3(I,J)-FD*FIPI(I,J)
61C30     WB4(I,J)=WB4(I,J)+FD*FIY(I,J)
61C31     390   WB5(I,J)=WB5(I,J)+FAC1*FI(I,J)+FAC2*EFI(I,J)
61C32     C
61C33     C
61C34     C      INTEGRATE STIFFNESS SUBMATRICES OVER ELASTIC REGION
61C35     C      OF THE WEB
61C36     C
61C37     400   A=BET2
61C38     B=BETP2
61C39     IF (DABS(A-B).LT.1.0D-5) GO TO 420
61C40     CALL FWCALC(BCL,HW,TW,E)
61C41     CALL PHI(B,A,FI,CW,7,9,17)
61C42     CALL PHIY(B,A,FIYY,CW,7,9,13)
61C43     CALL PHIPHI(B,A,FIPI,CW,7,9,15)
61C44     CALL PHIY(B,A,FIY,CW,7,9,15)
61C45     CALL EPHI(B,A,EFI,CW,7,9,16)
61C46     DO 410 I=1,7
61C47     DO 410 J=1,7
61C48     WB1(I,J)=WB1(I,J)+FA*FI(I,J)
61C49     WB2(I,J)=WB2(I,J)+FB*FIYY(I,J)
61C50     WB3(I,J)=WB3(I,J)-FC*FIPI(I,J)
61C51     WB4(I,J)=WB4(I,J)+FD*FIY(I,J)
61C52     410   WB5(I,J)=WB5(I,J)+FAC3*FI(I,J)+FAC4*EFI(I,J)
61C53     C
61C54     C
61C55     C      INTEGRATE STIFFNESS SUBMATRICES OVER
61C56     C      STRAIN-HARDENED REGION OF THE WEB
61C57     C
61C58     420   A=BETP2
61C59     B:1 ODO
61C60     IF (DABS(A-B).LT.1.0D-5) GO TO 440
61C61     CALL FWCALC(BCL,HW,TW,E2)
61C62     CALL PHI(B,A,FI,CW,7,9,17)
61C63     CALL PHIY(B,A,FIYY,CW,7,9,13)
61C64     CALL PHIPHI(B,A,FIPI,CW,7,9,15)
61C65     CALL PHIY(B,A,FIY,CW,7,9,15)
61C66     CALL EPHI(B,A,EFI,CW,7,9,16)
61C67     DO 430 I=1,7
61C68     DO 430 J=1,7
61C69     WB1(I,J)=WB1(I,J)+FA*FI(I,J)
61C70     WB2(I,J)=WB2(I,J)+FB*FIYY(I,J)
61C71     WB3(I,J)=WB3(I,J)-FC*FIPI(I,J)
61C72     WB4(I,J)=WB4(I,J)+FD*FIY(I,J)
61C73     430   WB5(I,J)=WB5(I,J)+FAC5*FI(I,J)+FAC6*EFI(I,J)
61C74     440   TW=TSAVE
61C75     RETURN
61C76     C
61C77     C
61C78     C      SET LIMITS OF INTEGRATION FOR TOP HALF OF WEB FOR
61C79     C      ELASTIC, YIELDED, AND STRAIN HARDENED REGIONS
61C80     C
61C81     C      CASE II - MIDDLE STRAIN-HARDENED
61C82     C
61C83     450   IF (ST.GT.T4) GO TO 470
61C84     IF (AD2.EQ.0.0D0) GO TO 460
61C85     BET2=(EYW-T1)/AD2
61C86     BETP2=(ESH-T1)/AD2
61C87     GO TO 490
61C88     460   BET2=1.0D0
61C89     BETP2=1.0D0
61C90     GO TO 490
61C91     470   IF (ST.GT.T5) GO TO 480
61C92     IF (AD2.EQ.0.0D0) GO TO 480
61C93     BET2=1.0D0
61C94     BETP2=(ESH-T1)/AD2
61C95     GO TO 490
61C96     480   BET2=1.0D0
61C97     BETP2=1.0D0
61C98     C
61C99     C
62C00     C      CALCULATE FACTORS FOR MULTIPLYING GEOMETRIC
62C01     C      STIFFNESS SUBMATRICES
62C02     C
62C03     490   CALL FWCALC(BCL,HW,TW,E2)
62C04     FAC1=(YSW*(ESH-EYW)*E1-(T1-ESH)*E2)*FE*STR
62C05     FAC2=AD2*E2*FE*STR
62C06     FAC3=(YSW*(T1-EYW)*E1)*FE*STR
62C07     FAC4=AD2*E1*FE*STR
62C08     FAC5=T1*FE*STR
62C09     FAC6=AD2*E*FE*STR
62C10     C
62C11     C
62C12     C      INTEGRATE STIFFNESS SUBMATRICES OVER
62C13     C      STRAIN-HARDENED REGION OF THE WEB
62C14     C

```



```

6780      C      REB = BENDING STRAIN IN THE TENSION FLANGE
6781
6782      C
6783      EC=(2.0DO*Y1/(2.0DO*Y1-HW))*ESB
6784      EAPEB=ESB+EAPP
6785      EB=ESB
6786      REB=R*ESB
6787      EARST=EAPP-REB
6788      RSTEAE=REB-EAPP
6789      T1=EYTF-ERTC
6790      T2=EYTF+ERTT
6791      T3=ESH-ERTC
6792      T4=ESH+ERTT
6793      ADEN=ERTC+ERTT
6794      IF (EAPEB.GT.T1) GO TO 10
6795      ALFT=1.0D0
6796      ALFP=1.0D0
6797      GO TO 60
6798      10     IF (EAPEB.GT.T2) GO TO 30
6799      IF (ADEN EQ 0.0D0) GO TO 20
6800      ANUM=T2-EAPEB
6801      IF (ALFT.GT.1.0D0) ALFT=1.0D0
6802      IF (ALFT.LT.0.0D0) ALFT=0.0D0
6803      ALFP=1.0D0
6804      GO TO 60
6805      20     ALFT=0.0D0
6806      ALFP=1.0D0
6807      GO TO 60
6808      30     IF (EAPEB GT T3) GO TO 40
6809      ALFT=0.0D0
6810      ALFP=1.0D0
6811      GO TO 60
6812      40     IF (EAPEB GT T4) GO TO 50
6813      IF (ADEN EQ 0.0D0) GO TO 50
6814      ANUM=T4-EAPEB
6815      ALFP=ANUM/ADEN
6816      IF (ALFP.GT.1.0D0) ALFP=1.0D0
6817      IF (ALFP.LT.0.0D0) ALFP=0.0D0
6818      ALFT=0.0D0
6819      GO TO 60
6820      50     ALFP=0.0D0
6821      ALFT=0.0D0
6822      C
6823      C
6824      C      EVALUATE FORCES IN THE COMPRESSION FLANGE
6825      C
6826      60     A1=0.5D0*BF2*TF2*ALFT
6827      A2=2.0D0*(EAPEB-ERTT)*E
6828      A3=ADEN*E=ALFT
6829      F21=A1*(A2+A3)
6830      A1=0.5D0*BF2*TF2*(ALFP+ALFT)
6831      A2=2.0D0*(YSFT+(EAPEB-T2)*E1)
6832      A3=ADEN*E1*(ALFP+ALFT)
6833      F22=A1*(A2+A3)
6834      A1=0.5D0*BF2*TF2*(1.0D0-ALFP)
6835      A2=2.0D0*(YSFT+(ESH-EYTF)*E1+(EAPEB-T4)*E2)
6836      A3=ADEN*E2*(1.0D0+ALFP)
6837      F23=A1*(A2+A3)
6838      F2=F21+F22+F23
6839      IF (EARST.GT.0.0D0) GO TO 130
6840      T1=EYBF-ERTB
6841      T2=EYBF+ERC8
6842      T3=ESH-ERTB
6843      T4=ESH+ERC8
6844      AD1=ERTB+ERC8
6845      IF (RSTEAE.GT.T1) GO TO 70
6846      ALFB=0.0D0
6847      ALFBP=0.0D0
6848      GO TO 120
6849      70     IF (RSTEAE GT T2) GO TO 90
6850      IF (AD1 EQ 0.0D0) GO TO 80
6851      AN1=RSTEAE-T1
6852      ALFB=AN1/AD1
6853      IF (ALFB.GT.1.0D0) ALFB=1.0D0
6854      IF (ALFB.LT.0.0D0) ALFB=0.0D0
6855      ALFBP=0.0D0
6856      GO TO 120
6857      80     ALFB=1.0D0
6858      ALFBP=0.0D0
6859      GO TO 120
6860      90     IF (RSTEAE GT T3) GO TO 100
6861      ALFB=1.0D0
6862      ALFBP=0.0D0
6863      GO TO 120
6864      100    IF (RSTEAE GT T4) GO TO 110
6865      IF (AD1 EQ 0.0D0) GO TO 110
6866      AN1=RSTEAE-T3
6867      ALFBP=AN1/AD1
6868      IF (ALFBP.GT.1.0D0) ALFBP=1.0D0
6869      IF (ALFBP.LT.0.0D0) ALFBP=0.0D0
6870      ALFB=1.0D0
6871      GO TO 120
6872      110    ALFB=1.0D0
6873      ALFBP=1.0D0
6874      C
6875      C
6876      C      EVALUATE FORCES IN TENSION FLANGE WHEN FLANGE IS
6877      C      IN TENSION
6878      C
6879      120    A1=0.5D0*BF1*TF1*ALFBP
6880      A2=2.0D0*(-YSFB-(ESH-EYBF)*E1+(T3-RSTEAE)*E2)
6881      A3=AD1*E2*ALFBP
6882      F11=A1*(A2+A3)
6883      A1=0.5D0*BF1*TF1*(ALFB-ALFBP)
6884      A2=2.0D0*(-YSFB+(T1-RSTEAE)*E1)
6885      A3=AD1*E1*(ALFB+ALFBP)
6886      F12=A1*(A2+A3)
6887      A1=0.5D0*BF1*TF1*(1.0D0-ALFB)
6888      A2=2.0D0*(EARST-ERTB)*E
6889      A3=AD1*E*(1.0D0+ALFB)
6890      F13=A1*(A2+A3)
6891      F1=F13+F12+F11
6892      GO TO 200

```



```

6893      130   T1=EYBF-ERCB
6894      T2=EYBF-ERTB
6295      T3=ESH-ERCB
6896      T4=ESH+ERTB
6897      ADEN=ERCB+ERTE
6898      IF (EARST.GT.T1) GO TO 140
6899      ALFT=1.0D0
6900      ALFP=1.0D0
6901      GO TO 190
6902      140   IF (EARST.GT.T2) GO TO 160
6903      IF (ADEN.EQ.0.0D0) GO TO 150
6904      ANUM=T2-EARST
6905      ALFT=ANUM/ADEN
6806      IF (ALFT.GT.1.0D0) ALFT=1.0D0
6907      IF (ALFT.LT.0.0D0) ALFT=0.0D0
6908      ALFP=1.0D0
6909      GO TO 190
6910      150   ALFT=0.0D0
6911      ALFP=1.0D0
6912      GO TO 190
6913      160   IF (EARST.GT.T3) GO TO 170
6814      ALFT=0.0D0
6915      ALFP=1.0D0
6816      GO TO 190
6917      170   IF (EARST.GT.T4) GO TO 180
6918      IF (ADEN.EQ.0.0D0) GO TO 160
6919      ANUM=T4-EARST
6920      ALFP=ANUM/ADEN
6921      IF (ALFP.GT.1.0D0) ALFP=1.0D0
6922      IF (ALFP.LT.0.0D0) ALFP=0.0D0
6923      ALFT=0.0D0
6924      GO TO 190
6925      180   ALFP=0.0D0
6926      ALFT=0.0D0
6927      C
6928      C
6929      C      EVALUATE FORCES IN TENSION FLANGE WHEN FLANGE IS IN
6930      C      COMPRESSION
6931      C
6932      190   A1=0.5D0*BF1*TF1*ALFT
6933      A2=2.0D0*(EARST-ERTB)=E
6934      A3=ADEN*E=ALFT
6935      F11=A1*(A2+A3)
6936      A1=0.5D0*BF1*TF1*(ALFP-ALFT)
6937      A2=2.0D0*(YSFB+(EARST-T2)=E1)
6938      A3=ADEN*E1=(ALFP+ALFT)
6939      F12=A1*(A2+A3)
6940      A1=0.5D0*BF1*TF1*(1.0D0-ALFP)
6941      A2=2.0D0*(YSFB*(ESH-EYBF)=E1+(EARST-T4)=E2)
6942      A3=ADEN*E2*(1.0D0+ALFP)
6943      F13=A1*(A2+A3)
6944      F1=F11+F12+F13
6945      200   T1=ERCM+EC
6946      T2=EYW-ERTB
6947      T3=ESH-ERTB
6948      T4=EYW+ERTT
6949      TS=ESH+ERTT
6950      T6=T1+EAPP
6951      AD1=REB+T1+ERTB
6952      AD2=EB-T1)-ERTT
6953      IF (T6.GT.EYW) GO TO 210
6954      BET2=0.0D0
6955      BETP3=0.0D0
6956      GO TO 250
6957      210   IF (T6.GT.ESH) GO TO 230
6958      IF (AD1.EQ.0.0D0) GO TO 220
6959      BET3=(T6-EYW)/AD1
6960      IF (BET3.GT.1.0D0) BET3=1.0D0
6961      IF (BET3.LT.0.0D0) BET3=0.0D0
6962      BETP3=0.0D0
6963      GO TO 250
6964      220   BET3=1.0D0
6965      BETP3=0.0D0
6966      GO TO 250
6967      230   IF (AD1.EQ.0.0D0) GO TO 240
6968      BET3=(T6-EYW)/AD1
6969      BETP3=(T6-ESH)/AD1
6970      IF (BET3.GT.1.0D0) BET3=1.0D0
6971      IF (BET3.LT.0.0D0) BET3=0.0D0
6972      IF (BETP3.GT.1.0D0) BETP3=1.0D0
6973      IF (BETP3.LT.0.0D0) BETP3=0.0D0
6974      GO TO 250
6975      240   BET3=1.0D0
6976      BETP3=1.0D0
6977      250   IF (RSTEA.GT.T2) GO TO 260
6978      BET1=1.0D0
6979      BETP1=1.0D0
6980      GO TO 300
6981      260   IF (RSTEA.GT.T3) GO TO 280
6982      IF (AD1.EQ.0.0D0) GO TO 270
6983      BET1=(T6-EYW)/AD1
6984      IF (BET1.GT.1.0D0) BET1=1.0D0
6985      IF (BET1.LT.0.0D0) BET1=0.0D0
6986      BETP1=1.0D0
6987      GO TO 300
6988      270   BET1=1.0D0
6989      BETP1=1.0D0
6990      GO TO 300
6991      280   IF (AD1.EQ.0.0D0) GO TO 290
6992      BET1=(T6-EYW)/AD1
6993      BETP1=(T6-ESH)/AD1
6994      IF (BET1.GT.1.0D0) BET1=1.0D0
6995      IF (BET1.LT.0.0D0) BET1=0.0D0
6996      IF (BETP1.GT.1.0D0) BETP1=1.0D0
6997      IF (BETP1.LT.0.0D0) BETP1=0.0D0
6998      GO TO 300
6999      290   BET1=1.0D0
7000      BETP1=1.0D0
7001      C
7002      C
7003      C      EVALUATE FORCES IN LOWER HALF OF WEB
7004      C
7005      300   B1=0.25D0*HW*TW*(1.0D0-BETP1)

```



```

7006      B2=2.0D0*(-YSW-(ESH-EYW)*E1+(ESH+T6)*E2)
7007      B3=(REB+T1*ERTB)*E2*(1.0D0+BETP1)
7008      FW1=B1*(B2+B3)
7009      B1=0.25D0*HW*TW*(BETP1-BET1)
7010      B2=2.0D0*(-YSW+(EYW+T6)*E1)
7011      B3=(REB+T1*ERTB)*E1*(BETP1+BET1)
7012      FW2=B1*(B2+B3)
7013      B1=0.25D0*HW*TW*(BET1-BET3)
7014      B2=2.0D0*T6*E
7015      B3=(REB+T1*ERTB)*E=(BET1+BET3)
7016      FW3=B1*(B2+B3)
7017      B1=0.25D0*HW*TW*(BET3-BETP3)
7018      B2=2.0D0*(YSW+(T6-EYW)*E1)
7019      B3=(REB+T1*ERTB)*E1*(BET3+BETP3)
7020      FW4=B1*(B2+B3)
7021      B1=0.25D0*TW*HW*BETP3
7022      B2=2.0D0*(YSW+(ESH-EYW)*E1+(T6-ESH)*E2)
7023      B3=(REB+T1*ERTB)*E2*BETP3
7024      FW5=B1*(B2+B3)
7025      IF (T6.GT.EYW) GO TO 360
7026      IF (EAPEB.GT.T4) GO TO 310
7027      BET2=1.0D0
7028      BETP2=1.0D0
7029      GO TO 350
7030      310 IF (EAPEB.GT.T5) GO TO 330
7031      IF (AD2.EQ.0.0D0) GO TO 320
7032      BET2=(EYW-T6)/AD2
7033      IF (BET2.GT.1.0D0) BET2=1.0D0
7034      IF (BET2.LT.0.0D0) BET2=0.0D0
7035      BETP2=1.0D0
7036      GO TO 350
7037      320 BET2=0.0D0
7038      BETP2=1.0D0
7039      GO TO 350
7040      330 IF (AD2.EQ.0.0D0) GO TO 340
7041      BET2=(EYW-T6)/AD2
7042      BETP2=(ESH-T6)/AD2
7043      IF (BET2.GT.1.0D0) BET2=1.0D0
7044      IF (BET2.LT.0.0D0) BET2=0.0D0
7045      IF (BETP2.GT.1.0D0) BETP2=1.0D0
7046      IF (BETP2.LT.0.0D0) BETP2=0.0D0
7047      GO TO 350
7048      340 BET2=0.0D0
7049      BETP2=0.0D0
7050      C
7051      C
7052      C      EVALUATE FORCES IN UPPER HALF OF WEB WHEN MIDDLE OF
7053      C      WEB IS STILL ELASTIC.
7054      C
7055      350 B1=0.25D0*HW*TW*BET2
7056      B2=2.0D0*T6*E
7057      B3=(ESB-T1*ERTT)*E*BET2
7058      FW6=B1*(B2+B3)
7059      B1=0.25D0*HW*TW*(BETP2-BET2)
7060      B2=2.0D0*(YSW+(T6-EYW)*E1)
7061      B3=(ESB-T1*ERTT)*E1*(BETP2+BET2)
7062      FW7=B1*(B2+B3)
7063      B1=0.25D0*HW*TW*(1.0D0-BETP2)
7064      B2=2.0D0*(YSW+(ESH-EYW)*E1+(T6-ESH)*E2)
7065      B3=(ESB-T1*ERTT)*E2*(1.0D0+BETP2)
7066      FW8=B1*(B2+B3)
7067      GO TO 470
7068      360 IF (T6.GT.ESH) GO TO 420
7069      IF (EAPEB.GT.T4) GO TO 380
7070      IF (AD2.EQ.0.0D0) GO TO 370
7071      BET2=(EYW-T6)/AD2
7072      IF (BET2.GT.1.0D0) BET2=1.0D0
7073      IF (BET2.LT.0.0D0) BET2=0.0D0
7074      BETP2=1.0D0
7075      GO TO 410
7076      370 BET2=1.0D0
7077      BETP2=1.0D0
7078      GO TO 410
7079      380 IF (EAPEB.GT.T5) GO TO 390
7080      BET2=1.0D0
7081      BETP2=1.0D0
7082      GO TO 410
7083      390 IF (AD2.EQ.0.0D0) GO TO 400
7084      BETP2=(ESH-T6)/AD2
7085      IF (BETP2.GT.1.0D0) BETP2=1.0D0
7086      IF (BETP2.LT.0.0D0) BETP2=0.0D0
7087      BET2=BETP2
7088      GO TO 410
7089      400 BETP2=1.0D0
7090      BET2=BETP2
7091      C
7092      C
7093      C      EVALUATE FORCES IN UPPER HALF OF WEB WHEN MIDDLE OF
7094      C      WEB IS YIELDED.
7095      C
7096      410 B1=0.25D0*HW*TW*BET2
7097      B2=2.0D0*(YSW+(T6-EYW)*E1)
7098      B3=(ESB-T1*ERTT)*E1*BET2
7099      FW8=B1*(B2+B3)
7100      B1=0.25D0*HW*TW*(BETP2-BET2)
7101      B2=2.0D0*T6*E
7102      B3=(ESB-T1*ERTT)*E=(BETP2+BET2)
7103      FW7=B1*(B2+B3)
7104      B1=0.25D0*HW*TW*(1.0D0-BETP2)
7105      B2=2.0D0*(YSW+(ESH-EYW)*E1+(T6-ESH)*E2)
7106      B3=(ESB-T1*ERTT)*E2*(1.0D0+BETP2)
7107      FW8=B1*(B2+B3)
7108      GO TO 470
7109      420 IF (EAPEB.GT.T4) GO TO 440
7110      IF (AD2.EQ.0.0D0) GO TO 430
7111      BET2=(EYW-T6)/AD2
7112      BETP2=(ESH-T6)/AD2
7113      IF (BET2.GT.1.0D0) BET2=1.0D0
7114      IF (BET2.LT.0.0D0) BET2=0.0D0
7115      IF (BETP2.GT.1.0D0) BETP2=1.0D0
7116      IF (BETP2.LT.0.0D0) BETP2=0.0D0
7117      GO TO 460
7118      430 BET2=1.0D0

```



```

7222      Y1=0.5D0*HW-YD3
7223      RDEN=0.5D0*HW-Y1
7224      IF (RDEN EQ 0.0D0) GO TO 80
7225      RNUM=0.5D0*HW+Y1
7226      R=RNUM/RDEN
7227      GO TO 90
7228      80      R#1 ODO
7229      90      CALL FORCE(ESB,EAPP,AXLO,SF3)
7230      NCOUNT=NCOUNT+1
7231      DY1=DABS((YD1-YD3)/YD1)
7232      DY2=DABS((YD2-YD3)/YD2)
7233      C
7234      C
7235      C      WHEN YD3 IS SUCH THAT THE LOCATION Y1 OF THE
7236      C      NEUTRAL AXIS DOES NOT CHANGE BY MORE THAN 1% STOP
7237      C      ITERATION AND RETURN. OTHERWISE CONTINUE WITH THE
7238      C      METHOD OF BISECTION.
7239      C
7240      C
7241      C
7242      C
7243      C
7244      C
7245      C
7246      C
7247      C
7248      C
7249      C
7250      TL=0.01D0
7251      IF ((DY1 LT TL OR DY2 LT TL)) RETURN
7252      IF (NCOUNT GT 50) GO TO 120
7253      SF13:SF1=S傅3
7254      IF (SF13.LT.0.0D0) GO TO 100
7255      YD1=YD3
7256      SF1=S傅3
7257      GO TO 70
7258      100     YD2=YD3
7259      SF2=S傅3
7260      GO TO 70
7261      110     WRITE (6,130)
7262      STOP
7263      120     WRITE (6,140)
7264      STOP
7265      130     FORMAT (' ',5X,'SF2 FAILED TO BECOME NEGATIVE IN 20 ITERATIONS IN
7266      &SUBROUTINE SATEQ')
7267      140     FORMAT (' ',5X,'SUBROUTINE SATEQ FAILED TO CONVERGE IN 50 ITERATIO
7268      &NS ')
7269      END
END OF FILE

```


APPENDIX D

SAMPLE PROBLEMS

D.1 Introduction

The results of two sample problems were obtained using the computer program listed in Appendix C. These results are presented below for the purpose of illustrating the use of the computer program. In sample problem number one a W shape is subjected to pure bending and the critical local buckling moment as well as the buckled configuration are determined (by an inelastic analysis if necessary). In sample problem number two the same W shape is subjected to a given axial load and analysed for the critical superimposed moment which causes local buckling. As part of the output of this problem, the critical axial load causing local buckling as well as the buckled configuration are presented. The superimposed local buckling moment and resulting buckled configuration are also given.

D.2 Example Number 1

The input data for this problem consists of 6 lines (one line per computer card). Referring to the first line of data, the total number of specimens to be analysed is 1, the modulus of elasticity is 29600 (ksi.) and Poisson's ratio is 0.3. The first integer of the second line of input indicates that this is the first specimen in this group to be analysed. The second, third and fourth

digits indicate that the configuration to be analysed is a W shape (ITYPE = 7), the loading is to be pure bending (LTYPE = 2), and an inelastic analysis is to be performed (INEL = 1). The fifth and sixth digits indicate that the ends of the specimen are pinned (ICLAMP = 0), and that an unmodified longitudinal sinewave shape is to be used (IKIND = 0).

In the third line of input, the first three members indicate that the yield stress of the compression flange, web, and tension flange are all 44.0 (ksi.). The last three numbers indicate that the ratio of residual strain to yield strain in the tension zone edge of web, middle of web, and compression zone edge of web are 0.3. In the fourth line there are seven numbers corresponding to the specimen length (20.0 in.), the distance between mid-planes of flanges (10.0 in.), the web thickness (0.25 in.), the width and thickness of the tension flange (10.0 in. and 0.35 in.), and the width and thickness of the compression flange (10.0 in. and 0.35 in.), respectively.

The slope of the yielding portion of the stress-strain curve, the strain-hardening modulus, and the strain at the onset of strain-hardening are given in the fifth line as 800.0 ksi., 800.0 ksi., and 0.02 in./in., respectively. The integer zero in the sixth line is a signal to indicate the end of the data for this particular run.

In the output portion of this problem the data from the input are listed. In addition to these, various geometric properties of the section are listed as well as the critical bending moment, and the ratios of the critical bending moment to the yield and plastic moments. The final page of output shows the critical compression flange

strain and the half wavelength of the longitudinal local buckle. The buckled configuration is shown in the form of values of the displacement coordinates indicated on a computer reproduction of the cross-section shape.

D-3 Example Number 2

In this problem the same W shape section as used in Example Number 1 is analysed here as a beam-column. The input data consists of 8 lines. Lines 1 to 5 are identical to those of the previous problem with the exception that an integer, 3, in the second line is used to indicate that the number is subjected to an axial and flexural load combined. The ratio of applied axial load to the yield load is 0.3 as shown in line 6. Negative unity in line 7 indicates that control is to be returned to the main program and zero in line 8 signals the end of this run.

During the output stage, the input data and various geometric properties of the section are listed. In the first block of output the critical axial load, critical axial strain and buckled configuration of the cross-section are also printed. In the second stage of the solution, the superimposed moment causing local buckling and the corresponding buckled configuration are determined. These, in addition to the ratios of critical moment to yield moment, reduced plastic moment, and plastic moment, form the major part of the second block of output. The remainder of the output is similar to that described previously for Example Number 1.

Example Number 1

1 1,29600.0,0.3
2 1,7,2,1,0,0,
3 44.0,44.0,44.0,0.3,0.3,0.3,
4 20.0,10.0,0.25,10.0,0.35,10.0,0.35,
5 800.0,800.0,0.02
6 0,

Number of specimens to be analysed = 1

Poisson ratio = 0.3000

Elastic modulus = 29600.0 ksi

Critical Bending Moment = 1790.30 Kip-in
Critical Bending Moment = 1.07483
Yield Moment
Critical Bending Moment = 0.99678
Plastic Moment
Distance to the Neutral Axis
From Center of Compression Flange = 5.6912 inches
RDNA = 0.5691 inches
Bottom Flange Slenderness Ratio = 14.2857
Top Flange Slenderness Ratio = 14.2857
Web Slenderness Ratio = 38.6000
Code Slenderness Ratio - Bottom = 94.7607
Code Slenderness Ratio - Top = 94.7607
Code Slenderness Ratio - Web = 256.0434

Critical strain = 0.002079

Half wavelength = 10.0000

$v = -1.00000$
 $v' = 0.26955$

$v = 0.00000$
 $v' = 0.16517$

$v = 1.00000$
 $v' = 0.26955$

	$u = 0.00000$ $u' = 0.16517$ $u'' = 0.10170$	
	$u = -0.14546$ $u' = -0.03173$ $u'' = 0.00636$	
	$u = 0.00000$ $u' = -0.00715$ $u'' = -0.01907$	

$v = 0.03020$
 $v' = -0.00667$

$v = 0.00000$
 $v' = -0.00715$

$v = -0.03020$
 $v' = -0.00667$

Example Number 1

1 1,29600.0,0.3,
2 1,7,3,1,0,0,
3 44.0,44.0,44.0,0.3,0.3,0.3
4 20.0,10.0,0.25,10.0,0.35,10.0,0.35,
5 800.0,800.0,0.02,
6 0.3,
7 -1.0,
8 0,

Number of specimens to be analysed = 1

Poisson ratio = 0.3000

Elastic modulus = 29600.0 ksi

Wide Flange Section 1

Subjected to pure bending.

Inelastic analysis.

Length of Wide Flange	= 20.0000 inches
Web Depth	= 10.00000 inches
Web Thickness	= 0.25000 inches
Bottom Flange Width	= 10.00000 inches
Bottom Flange Thickness	= 0.35000 inches
Top Flange Width	= 10.00000 inches
Top Flange Thickness	= 0.35000 inches
Area of Cross-section	= 9.5000 sq.in.
Distance to Centroid From Center of Bottom Flange	= 5.0000 inches
Centroidal Moment of Inertia	= 195.9048 inches
Web Yield Stress	= 44.0000 Ksi
Bottom Flange Yield Stress	= 44.0000 Ksi
Top Flange Yield Stress	= 44.0000 Ksi
Res. Tens. Strain (bott.)	= 13.2000 in/in
Res. Comp. Strain (Mid. Web)	= 13.20000 in/in
Res. Tens. Strain (Top)	= 13.20000 in/in
Res. Comp. Strain (Bott.)	= 13.20000 in/in
Res. Comp. Strain (Top)	= 13.20000 in/in
Yield Modulus	= 800.0000 Ksi
Strain Hardening Modulus	= 800.00000 Ksi
Strain Hardening Strain	= 0.02000

Wide Flange Section 1

Calculation of critical axial load.

Inelastic analysis.

P(Applied)/P(Yield)	=	0.3000
Length of Wide Flange	=	20.0000 inches
Web Depth	=	10.00000 inches
Web Thickness	=	0.25000 inches
Bottom Flange Width	=	10.00000 inches
Bottom Flange Thickness	=	0.35000 inches
Top Flange Width	=	10.00000 inches
Top Flange Thickness	=	0.35000 inches
Area of Cross-section	=	9.5000 sq.in.
Distance to Centroid From Center of Bottom Flange	=	5.0000 inches
Centroidal Moment of Inertia	=	195.9048 inches
Web Yield Stress	=	44.0000 ksi
Bottom Flange Yield Stress	=	44.0000 ksi
Top Flange Yield Stress	=	44.0000 ksi
Res. Tens. Stress (bott.)	=	13.20000 ksi.
Res. Comp. Stress (Mid. Web)	=	13.20000 ksi.
Res. Tens. Stress (Top)	=	13.20000 ksi.
Res. Comp. Stress (Bott.)	=	13.20000 ksi.
Res. Comp. Stress (Top)	=	13.20000 ksi.
Yield Modulus	=	800.0000 ksi
Strain Hardening Modulus	=	800.0000 ksi

Strain Hardening Strain = 0.02000
Axial Load at Buckling = 390.66 Kips
(Axial Load)/(Yield Load) = 0.9346
Average Stress at Buckling = 41.1220 Ksi
Bottom Flange Slenderness Ratio = 14.2857
Top Flange Slenderness Ratio = 14.2857
Web Slenderness Ratio = 38.6000
Code Slenderness Ratio - Bottom = 94.7607
Code Slenderness Ratio - Top = 94.7607
Code Slenderness Ratio - Web = 256.0434

Critical strain = 0.001509

Half wavelength = 10.0000

v = 1.00000
v' = -0.27582

v = 0.00000
v' = -0.15985

v = -1.00000
v' = -0.27582

	<p>u = 0.00000 u' = -0.15985 u" = -0.03508</p>	
	<p>u = 0.41076 u' = -0.00000 u" = -0.03734</p>	
	<p>u = 0.00000 u' = 0.15985 u" = -0.03508</p>	

v = -1.00000
v' = 0.27582

v = 0.00000
v' = 0.15985

v = 1.00000
v' = 0.27582

Beam Column Case No 1

Subjected to an applied axial load of 125.400000 Kips plus bending.

P(Applied)/P(Yield)	=	0.3000
Critical Axial Strain	=	0.00150891
Applied Axial Strain	=	0.00044595
Critical Bending Moment	=	1163.74 Kip-in
<u>Critical Bending Moment</u> Yield Moment	=	0.69866
<u>Critical Bending Moment</u> Red. Plast. Mom.	=	0.80500
<u>Critical Bending Moment</u> Plastic Moment	=	0.64793
Distance to the Neutral Axis From Center of Compression Flange	=	7.3309 inches
RDNA	=	0.7331
Bottom Flange Slenderness Ratio	=	14.2857
Top Flange Slenderness Ratio	=	14.2857
Web Slenderness Ratio	=	38.6000
Code Slenderness Ratio - Bottom	=	94.7607
Code Slenderness Ratio - Top	=	94.7607
Code Slenderness Ratio - Web	=	256.0434
Crit. Bend. Strain/Yield Strain	=	0.75463

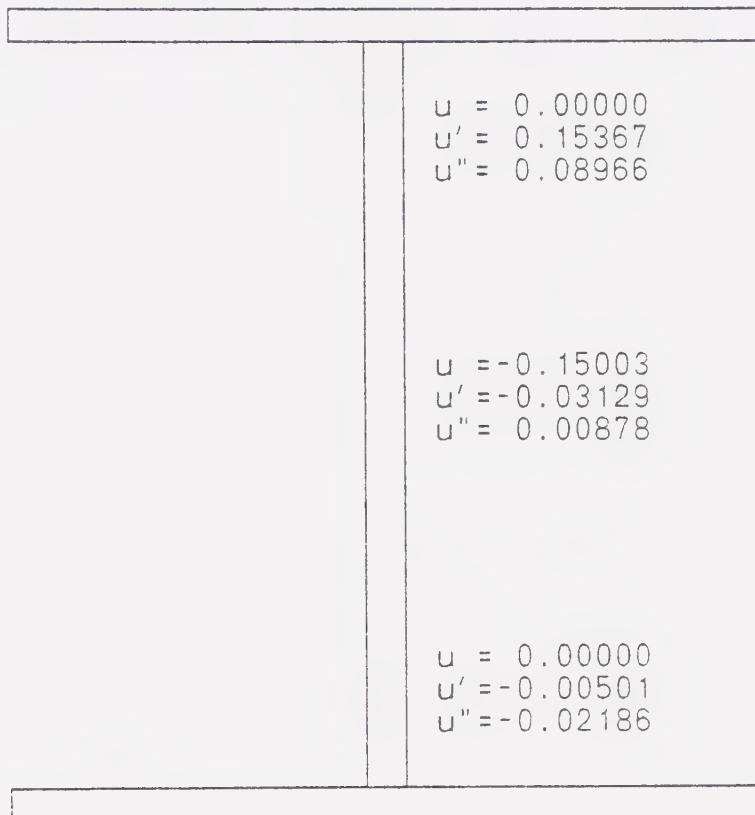
Critical strain = 0.001122

Half wavelength = 10.0000

v = -1.00000
v' = 0.27928

v = 0.00000
v' = 0.15367

v = 1.00000
v' = 0.27928



v = 0.01497
v' = -0.00195

v = 0.00000
v' = -0.00501

v = -0.01497
v' = -0.00195

B30290